

Doctoral thesis

Doctoral theses at NTNU, 2022:222

Christiana Bjørkli

The inside-out of Alzheimer's disease

NTNU
Norwegian University of Science and Technology
Thesis for the Degree of
Philosophiae Doctor
Faculty of Medicine and Health Sciences
Department of Neuromedicine and Movement
Science



Norwegian University of
Science and Technology

Christiana Bjørkli

The inside-out of Alzheimer's disease

Thesis for the Degree of Philosophiae Doctor

Trondheim, August 2022

Norwegian University of Science and Technology
Faculty of Medicine and Health Sciences
Department of Neuromedicine and Movement Science

NTNU

Norwegian University of Science and Technology

Thesis for the Degree of Philosophiae Doctor

Faculty of Medicine and Health Sciences

Department of Neuromedicine and Movement Science

© Christiana Bjørkli

ISBN 978-82-326-6552-5 (printed ver.)

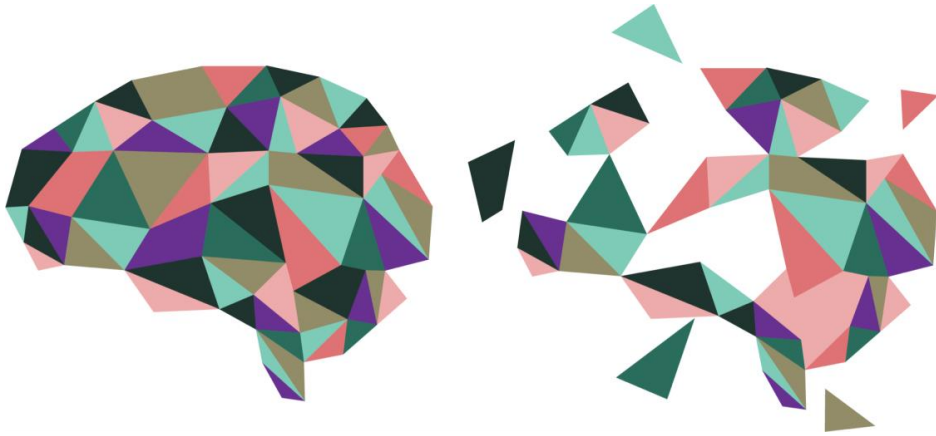
ISBN 978-82-326-5894-7 (electronic ver.)

ISSN 1503-8181 (printed ver.)

ISSN 2703-8084 (online ver.)

Doctoral theses at NTNU, 2022:222

Printed by NTNU Grafisk senter



“The existence of forgetting has never been proved: We only know that some things don't come to mind when we want them.” – Friedrich Nietzsche

© Christiana Bjørkli, figure made in Adobe Illustrator

Sammendrag: Innsiden ut av Alzheimers sykdom

Funnene presentert i denne avhandlingen støtter tidligere resultater som tilsier at et lite område i temporallappene av hjernen (betegnet som lateral entorhinal cortex [LEC] lag II) er et sårbart område for utviklingen av proteiner som skader hjerneceller (nevroner) i tidlig fase av Alzheimers sykdom. Disse skadelige proteinene bygger seg større i løpet av sykdommen, helt fram til de blokkerer kommunikasjonen mellom nevronene, noe som leder til celledød og hukommelsestap. I denne avhandlingen presenterer vi nye funn angående opprinnelsen og mekanismen for spredning av disse skadelige proteinene, og viser at forsøksdyr og molekylære verktøy er avgjørende for å besvare store spørsmål innenfor forskningsfeltet. Jeg håper at arbeidet mitt en dag vil hjelpe til å innlemme funn fra grunnforskningen inn til klinikken og pasienter med Alzheimers sykdom.

Hvert tredje sekund stilles en ny demensdiagnose i verden, og majoriteten av disse er forårsaket av Alzheimers sykdom. Det finnes ingen kur for sykdommen, noe som gjør at hypotesetesting rundt sykdommens begynnelse og spredning, samt utvikling av metoder for tidlig diagnose og behandling, er særdeles viktig. Forskere har gjort store fremskritt med å forstå hvordan sykdommen starter, og vi vet nå at nevroner i LEC lag II er utsatt for tidlig degenerasjon i pasienter som først utvikler mild kognitiv svikt og til slutt Alzheimers demens. I løpet av denne perioden er så mye som halvparten av disse nevronene mistet. Forskere har også kartlagt progresjonen av sykdommen ved bruk av biomarkører for å vurdere nevropatologi i løpet av sykdomsprosessen. På tross av disse fremskrittene har man enda ikke klart å finne hva som må til for å hindre at kognitiv svikt starter i pasienter. En av grunnene til sakte fremgang er at data fra forsøksdyr ikke har vært overførbare til pasienter.

Navn kandidat: Christiana Bjørkli

Institutt: Nevromedisin og bevegelsesvitenskap

Veiledere: Prof. Ioanna Sandvig, Prof., Overlege Axel Sandvig og Prof. Menno P. Witter

Finansieringskilder: Samarbeidsorganet Helse-Midt Norge og Felles Forskningsutvalg for St. Olavs Hospital og Fakultetet for Medisin og Helsevitenskap

*Ovennevnte avhandling er funnet verdig til å forsvares offentlig
for graden PhD i medisin, Doctor Philosophiae.
Disputas finner sted i Auditoriet BS31, Bevegelsesenteret
Mandag 29. august 2022, kl. 12:15*

This doctoral thesis is dedicated to my loving partner Marcus, and our pride and joy, Grogu.



© Christiana Bjørkli

Contents

| | |
|---|------|
| SAMMENDRAG: INNSIDEN UT AV ALZHEIMERS SYKDOM..... | III |
| ACKNOWLEDGEMENTS | VII |
| PREFACE | IX |
| SUMMARY: THE INSIDE-OUT OF ALZHEIMER’S DISEASE | XI |
| ABBREVIATIONS (IN ORDER OF APPEARANCE)..... | XIII |
| LIST OF ARTICLES..... | XV |
| 1. GENERAL INTRODUCTION..... | 1 |
| 1.1. Introduction to Alzheimer’s disease..... | 1 |
| 1.2. Pathology in Alzheimer’s disease | 4 |
| 1.2.1. The role of amyloid- β | 5 |
| 1.2.1.1. Amyloid plaques | 7 |
| 1.2.1.2. Amyloid- β oligomers | 8 |
| 1.2.2. The role of tau..... | 8 |
| 1.3. Neuroanatomy and Alzheimer’s disease | 9 |
| 1.4. The hippocampus and memory in Alzheimer’s disease | 11 |
| 1.5. Biomarkers in Alzheimer’s disease | 12 |
| 1.6. Approaches to attenuate Alzheimer’s disease pathophysiology | 14 |
| 1.6.1. Current treatment of Alzheimer’s disease..... | 14 |
| 1.6.2. Cholinergic enhancers..... | 15 |
| 1.6.3. Reduction of amyloid- β | 15 |
| 1.6.4. Reduction of tau..... | 17 |
| 1.6.5. Increase in cellular clearance..... | 17 |
| 1.7. Mouse models of Alzheimer’s disease | 18 |
| 2. THESIS AIMS AND OBJECTIVES..... | 20 |
| 3. SYNOPSIS OF MAIN METHODS | 22 |
| 3.1. Paper II <i>In Vivo</i> Microdialysis in Mice Captures Changes in Alzheimer’s Disease Cerebrospinal Fluid Biomarkers Consistent with Developing Pathology | 22 |
| 3.2. Paper III Combined Targeting of Pathways Regulating Synaptic Formation and Autophagy Attenuates Alzheimer’s Disease Pathology in Mice | 23 |
| 3.3. Paper IV Overexpression of Human Tau in Lateral Entorhinal Cortex Layer II of 3xTg AD Mice Leads to Tau Deposition and a Shift in Perforant Path Terminals in the Dentate Gyrus..... | 24 |
| 3.4. Paper V Manipulation of Neuronal Activity in the Entorhinal-Hippocampal Circuit Affects Intraneuronal Amyloid- β Levels | 24 |
| 4. SYNOPSIS OF RESULTS | 27 |
| 4.1. Paper II <i>In Vivo</i> Microdialysis in Mice Captures Changes in Alzheimer’s Disease Cerebrospinal Fluid Biomarkers Consistent with Developing Pathology..... | 27 |
| 4.2. Paper III Combined Targeting of Pathways Regulating Synaptic Formation and Autophagy Attenuates Alzheimer’s Disease Pathology in Mice | 27 |
| 4.3. Paper IV Overexpression of Human Tau in Lateral Entorhinal Cortex Layer II of 3xTg AD Mice Leads to Tau Deposition and a Shift in Perforant Path Terminals in the Dentate Gyrus..... | 28 |
| 4.4. Paper V Manipulation of Neuronal Activity in the Entorhinal-Hippocampal Circuit Affects Intraneuronal Amyloid- β Levels | 28 |
| 5. METHODOLOGICAL CONSIDERATIONS..... | 30 |
| 5.1. <i>In vivo</i> microdialysis..... | 30 |
| 5.2. Infusing repurposed drugs using <i>in vivo</i> microdialysis | 31 |
| 5.3. Viral injections of <i>MAPT</i> _{P301L} | 34 |
| 5.4. Designer receptors exclusively activated by designer drugs (DREADDs)..... | 36 |
| 5.5. Context-dependent spatial memory task | 38 |
| 5.6. Tissue processing | 39 |
| 5.7. Animal models of Alzheimer’s disease | 42 |
| 6. GENERAL DISCUSSION..... | 44 |

| | | |
|------|--|----|
| 6.1. | Translational validity of mouse models of Alzheimer’s disease..... | 44 |
| 6.2. | Pharmacologically attenuating amyloid- β and tau pathology | 45 |
| 6.3. | The origin and spread of pathology in Alzheimer’s disease | 46 |
| 6.4. | Future directions..... | 50 |
| 7. | CONCLUDING REMARKS | 52 |
| 8. | REFERENCES | 53 |
| | SUPPLEMENTARY MATERIAL | 71 |
| | PAPERS I – V | 77 |

Acknowledgements

This thesis work was carried out at the Department of Neuromedicine and Movement Science at the Norwegian University of Science and Technology (NTNU), under the supervision of Professors Ioanna Sandvig, Axel Sandvig and Menno P. Witter.

I am deeply grateful to Ioanna and Axel for offering me this opportunity, and for their careful scientific advice and guidance. Thank you both for being supportive and enthusiastic about my ideas and work and allowing me to bring them to life. My thanks also extend to Keiko, for letting her parents invest this time and energy into my scientific endeavors. To my PhD thesis co-supervisor and former master's thesis group leader Menno, thank you for being such a great mentor for the past years, and for sharing your passion and expertise in neuroanatomy. I am also grateful to my coworkers in the Sandvig group for fruitful discussions and sharing of knowledge.

I further would like to thank the co-authors of the papers, in particular Mary Hemler, Nora Cecilie Ebbesen, Joshua Julian, and Rajeev Nair. Mary and Nora, you are both every supervisor's dream and two of these papers would not have been possible to complete without your invaluable help in the lab. Josh, thank you for allowing me to bring your ideas from the drawing board to life with testing contextual memory in mice, and for your great support throughout. Rajeev, thank you for your collaboration on the Tau Propagation project, and trusting me with this important work. I would like to thank Grethe and Bruno for their invaluable expertise in the Witter lab. Thank you Asgeir for inspiring me to continue working within the field, and for your unreserved sharing of expertise.

This process has been exciting, although intense at times, but I am grateful for this experience that has allowed me to grow personally and scientifically. Janelle and Katrine, thanks for being a huge support during my PhD process, both in terms of being my office mates, translating my findings *in vitro*, and as great friends. Karoline and Flo, thanks for inspiring me to become a better scientist and person, and for all your support. I would like to give a special thanks to the staff at the Comparative Medicine Core Facility for supporting all my animal work, and to all the mice that made this work possible. Thank you for your sacrifice (**Figure 1**). Finally, I

would like to thank all my friends and family for the love and support. Thank you Edit for always believing in me and shaping me to who I am today. Especially Marcus and Grogg, without your encouragement and support this thesis would not see the light of day.



Figure 1. A statue in Russia that honors all the laboratory mice that have sacrificed their lives in order to further scientific research. Photo: Stock Photos from SaliVit/Shutterstock.

Preface

Memory has a central role in life: our experiences contribute to making us who we are and give us an identity, a history, a culture. What would we be without our past, without a story to tell, without people to remember? A literal illustration of this can be seen in the last series of self-portraits by William Utermohlen (Fig. 2), who drew a representation of himself at the end-stage of Alzheimer's disease resembling nothing like his first self-portrait. Without memory our existence would be leaky, and although filled with new memories each day, these would flow away, erasing the past and damaging the future.

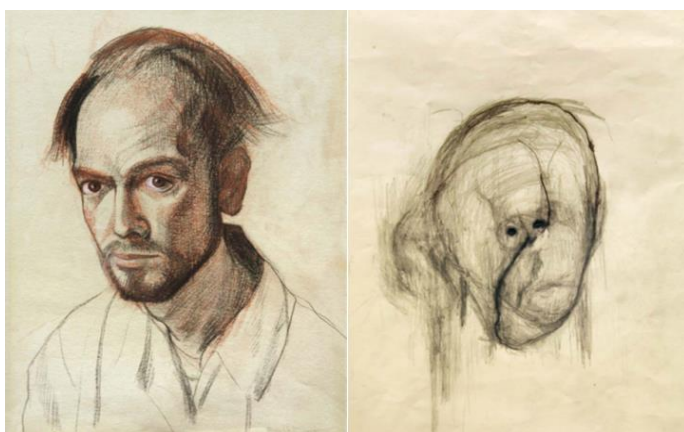


Figure 2. Artist William Utermohlen (1933-2007) was diagnosed with Alzheimer's disease in 1995, but before his death in 2007 he created a heart-wrenching final series of self-portraits over the stages of the disease. The image shows his first and last self-portrait. Left: 1967, Pencil and Conté crayon on paper, 26.5 x 20 cm, Private collection. Right: 2000, Pencil on paper, 40.5 x 33 cm, Estate of the Artist, Paris. Photos from [6], courtesy of Chris Boïcos Fine Arts, Paris. Reproduced with permission.

The American biochemist Gregory Petsko said that «Alzheimer's disease starts when a protein that should be folded up properly misfolds into a kind of demented origami» in his 2008 TED talk titled *The Coming Neurological Epidemic*. This quote inspired the geometric illustration on the inner sleeve of this thesis and has driven my passion to understand the underlying biochemical processes that drive the disease. Ultimately, Alzheimer's disease will become an epidemic as stated by Petsko, as the elderly population is incrementally increasing year by year. Having worked at various dementia facilities to financially support myself during my studies, I have gotten a first-hand experience on the toll this disease puts on families, health personnel, and the patients themselves. Hopefully, some of the research presented here can help unfold the demented origami for future generations.

Christiana Bjørkli, April 2022

Summary: The inside-out of Alzheimer's disease

Every three seconds someone is diagnosed with dementia, and Alzheimer's disease (AD) constitutes most of these cases. In the absence of a cure for AD, testing hypotheses regarding disease onset and spread, and developing methods for early diagnosis and treatment of the disease remain an urgent priority. Researchers have made tremendous strides in research to understand the origin of AD, and we now know that the neurons in lateral entorhinal cortex (LEC) layer II (a small brain region in the temporal lobes) are at selective risk for neurodegeneration in patients going through transition stages to AD (referred to as mild cognitive impairment [MCI]), and during this transition stage as much as half of the cell population is lost. The disease progression in human AD has been well-characterized by biomarker studies to assess pathological hallmarks at various stages of the disease. Biomarkers in AD can be elucidated by cerebrospinal fluid (CSF) analysis (commonly used biomarkers include decreased amyloid- β ($A\beta$)₄₂, increased total tau, and increased phosphorylated tau) or neuroimaging markers of disease, such as positron emission tomography (PET) revealing amyloid plaques and tau pathology. Despite these research efforts, we still do not know how to hinder cognitive decline in patients with AD, and one reason may be the poor translatability between preclinical models and patients.

Before any new hypotheses and treatments can reach the clinic, they first need to be tested in preclinical models using basic research strategies. We therefore need robust preclinical models that can help us achieve improved comparability with the human condition, and thereby improved translatability into the clinic. Here we used a highly clinically comparable rodent model of AD, the 3xTg AD mouse, which contains human genetic mutations recapitulating neuropathology observed in patients. First, we developed and applied our modified microdialysis method for repeated, longitudinal *in vivo* CSF collection and characterized biomarker protein changes in mice along the entire AD disease progression (*Paper II*). We subsequently applied our optimized microdialysis method to administer repurposed drugs aimed at attenuating AD-related $A\beta$ and tau neuropathology (*Paper III*). In another set of experiments, we overexpressed human tau pathology in LEC layer II in mice using a viral vector delivery system, and then monitored tau spread from LEC layer II to its projection targets in the hippocampus (*Paper IV*). Lastly, we chemogenetically silenced

neurons in LEC layer II and monitored the effect on intraneuronal A β levels in LEC and in downstream hippocampus (*paper V*).

Using our modified microdialysis protocol, we found that the concentrations of CSF A β and tau proteins in mouse models of AD are comparable to changes observed along the disease cascade in patients (*Paper II*). Repurposed drugs not only attenuated neuropathology at the molecular, but also at the functional level when administered in combination using our microdialysis protocol at various therapeutic time windows (*Paper III*). Moreover, we found that the presence and spread of tau from LEC layer II to the hippocampus increased with age and was affected by the presence of endogenous tau load (*Paper IV*). We also show a correlation between intraneuronal A β levels and neuronal activity, and that chemogenetic silencing of LEC layer II neurons led to reduced early intraneuronal A β in LEC and in the downstream hippocampus (*Paper V*).

In summary, I have (i) characterized CSF biomarkers along the entire disease cascade in a mouse model of AD and have validated the translational value of this model to patients. (ii) My findings lend support to the application of repurposed drugs to attenuate AD neuropathology at various therapeutic time windows. (iii) I have shown that tau spread from its site of anatomical origin depends upon aging and the pre-existence of tau. (iv) Lastly, I have demonstrated that the activity of LEC layer II neurons affects early intraneuronal A β build-up. In line with previous research, I have shown the vulnerability of EC layer II for developing AD-related neuropathology, obtained insights into the origins and mechanisms of neuropathological spread, and shown that experimental animal models and molecular techniques are invaluable tools for answering fundamental questions within the field. Ultimately, I have aimed to develop a springboard for future integration of basic research findings to the clinic and AD patients.

Abbreviations (in order of appearance)

| | |
|------------------------------|---|
| LEC | Lateral entorhinal cortex |
| MCI | Mild cognitive impairment |
| A β | Amyloid- β |
| PET | Positron emission tomography |
| DREADDs | Designer receptor exclusively activated by designer drugs |
| AD | Alzheimer's disease |
| LEC | Lateral entorhinal cortex |
| CSF | Cerebrospinal fluid |
| NFT | Neurofibrillary tangle |
| BMI | Body mass index |
| TBI | Traumatic brain injury |
| APP | Amyloid precursor protein |
| PSEN | Presenilin |
| APOE | Apolipoprotein E |
| FTLD | Frontotemporal lobar degeneration |
| DS | Down's syndrome |
| BACE1 | β -secretase cleavage enzyme 1 |
| EC | Entorhinal cortex |
| <i>APP_{SWE}</i> | Swedish APP mutation |
| MAPT | Microtubule associated protein tau |
| <i>MAPT_{P301L}</i> | P301L MAPT tau mutation |
| <i>PSEN1_{M146V}</i> | M146V PSEN1 mutation |
| LTP | Long-term potentiation |
| R | Repeats |
| MTL | Medial temporal lobe |
| DG | Dentate gyrus |
| CA | Cornu ammonis |
| MEC | Medial entorhinal cortex |
| MRI | Magnetic resonance imaging |
| t-tau | Total tau |
| p-tau | Phosphorylated tau |

| | |
|-------|---|
| NfL | Neurofilament light |
| NMDA | N-methyl-D-aspartate |
| BBB | Blood-brain barrier |
| ROCK | Rho-associated protein kinase |
| PCP | Planar cell polarity |
| Dkk1 | Dickkopf-1 |
| RNA | Ribonucleic acid |
| UPS | Ubiquitin–proteasome systems |
| LC3 | Microtubule associated protein 1 light-chain 3 |
| AAV | Adeno-associated virus |
| GFP | Green fluorescent protein |
| hM4 | Human M4 muscarinic receptor |
| hM4Di | hM4 inhibitory DREADDs |
| TREM2 | Triggering receptor expressed on myeloid cells 2 |
| FTD | Frontotemporal dementia |
| CBA | Chicken beta actin |
| CMV | Cytomegalovirus |
| CNO | Clozapine-n-oxide |
| DCZ | Deschloroclozapine |
| KOR | Human kappa opioid receptor |
| IP | Intraperitoneal |
| NOR | Novel object recognition |
| IEG | Immediate-early gene |
| pERK | Phosphorylated extra cellular signal-regulated kinase |
| Iba1 | Antibody ionized calcium-binding adapter molecule 1 |
| LAMP1 | Lysosomal-associated membrane protein 1 |
| MAP2 | Microtubule-associated protein 2 |
| DAB | 3, 3'-diaminobenzidine |
| ALS | Amyotrophic lateral sclerosis |
| mTOR | Mechanistic target of rapamycin |
| EDGE | Enhancer-driven gene expression |
| DBS | Deep brain stimulation |

List of articles

Article I

Bridging the Gap Between Fluid Biomarkers for Alzheimer's Disease, Model Systems, and Patients

Christiana Bjorkli, Axel Sandvig and Ioanna Sandvig.

Review, Frontiers in Aging Neuroscience, September 2020, doi: 10.3389/fnagi.2020.00272

Article II

In Vivo Microdialysis in Mice Captures Changes in Alzheimer's Disease Cerebrospinal Fluid Biomarkers Consistent with Developing Pathology

Christiana Bjorkli, Claire Louet, Trude Helen Flo, Mary Hemler, Axel Sandvig and Ioanna Sandvig.

Journal of Alzheimer's disease, September 2021, doi: 10.3233/JAD-210715

Article III

Combined Targeting of Pathways Regulating Synaptic Formation and Autophagy Attenuates Alzheimer's Disease Pathology in Mice

Christiana Bjorkli, Mary Hemler, Joshua B. Julian, Axel Sandvig and Ioanna Sandvig.

Frontiers in Pharmacology, section Neuropharmacology, June 2022, doi: 10.3389/fphar.2022.913971

Article IV

Overexpression of Human Tau in Lateral Entorhinal Cortex Layer II of 3xTg AD Mice Leads to Tau Deposition and a Shift in Perforant Path Terminals in the Dentate Gyrus

Christiana Bjorkli, Rajeev Nair, Menno P. Witter, Axel Sandvig and Ioanna Sandvig.

Manuscript

Article V

Manipulation of Neuronal Activity in the Entorhinal-Hippocampal Circuit Affects Intraneuronal Amyloid- β Levels

Christiana Bjorkli, Nora C. Ebbesen, Joshua B. Julian, Menno P. Witter, Axel Sandvig and Ioanna Sandvig.

Preprint, BioRxiv 2022, doi.org/10.1101/2022.07.05.498797

1. General introduction

1.1. Introduction to Alzheimer's disease

At a psychiatric hospital in Frankfurt, a 51-year-old woman named Auguste Deter sought help because her family had noticed that she had become uncharacteristically jealous of her husband, and soon became forgetful and tended to get lost. In November 1901, she became a patient of Alois Alzheimer [19], who followed her clinical manifestations until her death in 1906. Alzheimer reported the autopsy of Auguste's brain to a conference in Tübingen, Germany, that same year [20]:

"A woman, 51 years old, showed jealousy towards her husband as the first noticeable sign of the disease. Soon a rapidly increasing loss of memory could be noticed. She could not find her way around in her own apartment. She carried objects back and forth and hid them. At times she would think that someone wanted to kill her and would begin shrieking loudly. In the institution her behavior bore the stamp of utter perplexity. . . . Periodically she was totally delirious, dragged her bedding around, called her husband and her daughter, and seemed to have auditory hallucinations."

The autopsy disclosed a generally atrophic brain without large lesions. The large brain vessels were altered by arteriosclerosis (or the thickening/hardening of artery walls). Alzheimer found

". . .peculiar changes of the neurofibrils...(which) are eventually seen clustering together in thick bundles which emerge at the surface of the cell and miliary foci distinguishable by the deposit in the cerebral cortex of a peculiar substance which can be recognized without stain and is, in fact, very refractory to staining."[5] (**Fig. 3**)

Unfortunately for Alzheimer, the audience declined to ask any questions, as they were eager to hear the next lecturer give a presentation on *compulsive masturbation* [21].

Later these changes observed by Alzheimer were referred to as neurofibrillary tangles (NFTs) and amyloid plaques, respectively [22, 23]. Alzheimer did not claim that he had found a new disease [24], rather, he was impressed by the histological

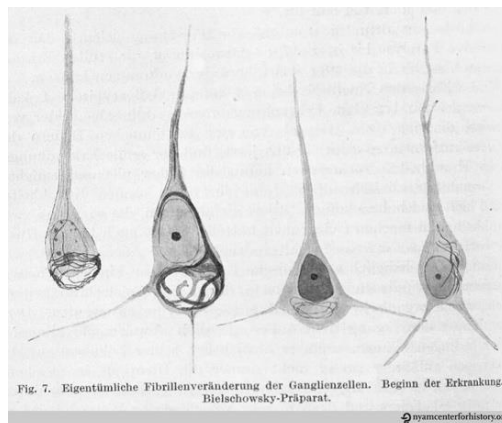


Figure 3. Drawings of histological preparations of Auguste Deter's material, stained by Bielschowsky's technique to demonstrate tau tangles, and their stages [5]. © The New York Academy of Medicine Center for History. Reproduced with permission.

variation of the neuropathological process in Auguste's brain, which he did not yet understand. A year later, his colleague Francesco Bonfiglio (1883–1966) published a second case, and two years later another Italian, Gaetano Perusini (1879–1915), described four cases: two of them were the cases described by Alzheimer and Bonfiglio. They too believed that they had observed an unusual variant of senile dementia. Emil Kraepelin (**Fig. 4**) introduced the term Alzheimer's disease (AD) in the 8th edition of his textbook *Compendium der Psychiatrie* [1] (1910; **Fig. 5**). When a case of AD was first reported in 1907, life expectancy was much shorter than today. A diagnosis of AD was relatively uncommon and limited to demented patients younger than 65 years, and the future devastating impact of the disease



Figure 4. Left to right: Alois Alzheimer and Emil Kraepelin with psychiatrist Robert Gaupp and neuropathologist Franz Nissl, circa 1908 [2]. © Archive for History of Psychiatry, Department of Psychiatry University of Munich. Reproduced with permission.

remained unrecognized until, in a 1976 editorial, Katzman first argued that senile dementia and AD formed a continuum [24, 25].

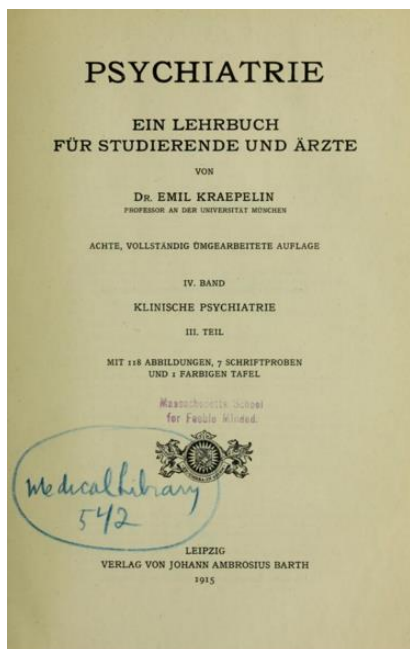


Figure 5. Cover of Emil Kraepelin's 1910 textbook [1]. Screenshot from Google Books.

Today, 100 thousand individuals in Norway are affected by AD, with half of these cases being 65 years or older. After 65 years of age, the prevalence of AD doubles approximately every 5 years [26]. Various health organizations have predicted that by 2050, 13.8 million individuals will have the disease, and to put that into perspective, it would *be the equivalent of filling up Denmark twice with its current population*. Clinically, the disease presents with prominent memory impairment, language difficulties, behavioral disturbances, and functional decline in patients. There are several risk factors for developing AD, including age, sex, family history, low education, increased body mass index (BMI), diabetes, sleep disorders, depression, traumatic brain injury (TBI), smoking, alcohol consumption and hearing loss [27]. However, old age and the presence of disease-predisposing genetic polymorphisms are the most prevalent risk factors.

AD exists in both familial and sporadic forms. Familial – *or early-onset* – forms are caused by mutations in single genes that are inherited in an autosomal-dominant fashion, and account for about 5% of cases [28]. Sporadic – *or late-onset* – forms have a multifactorial etiology, in which some genetic polymorphisms are known to act as predisposing factors [29]. Familial AD is characterized by possessing one or more mutation in the amyloid precursor protein (*APP*) or presenilin (*PSEN*) genes, whereas sporadic AD is partially caused by possession of $\epsilon 4$ allele(s) in the apolipoprotein E (*APOE*) gene, and both AD types are thought to involve inflammation, endosomal, synaptic and lipid metabolism genes. Environmental factors play a larger role in sporadic, compared to familial AD, and include toxins, pollution, heavy metals, trauma, and infectious agents. However, both types of AD lead to gross neurodegeneration (**Fig. 6**), and associated synapse/vascular damage and inflammation. Neurodegeneration is caused by abiotrophic proteinopathy, involving aggregated amyloid- β ($A\beta$) and tau.

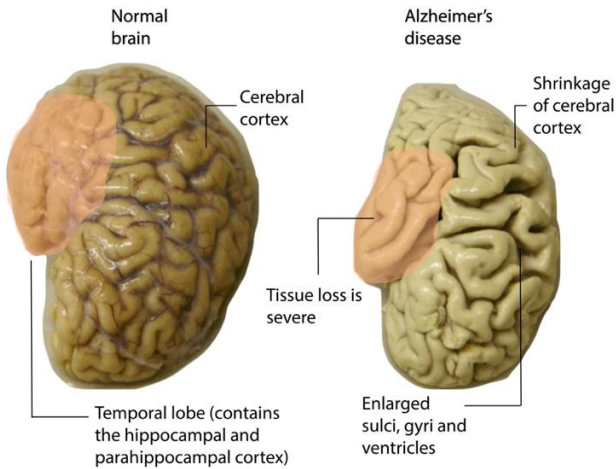


Figure 6. Neurodegeneration in AD. Pathological changes, including those caused by A β and tau pathologies, result in severe synaptic and neuronal dysfunction and loss. At postmortem, the brain of an AD patient may weigh one-third less than the brain of an age-matched, non-demented individual [9]. © Christiana Bjørkli, figure made in Adobe Illustrator.

1.2. Pathology in Alzheimer's disease

A healthy brain contains about 86 billion neurons [30]. One neuron may connect with up to

10,000 other neurons, passing signals via 1000 trillion synaptic connections. For comparison, the latest estimates put *the number of stars in the Milky Way at somewhere between 200 and 400 billion*. AD leads to a gradual and eventual irreversible loss of most of these neurons and synapses. Progressive cortical atrophy is the main gross anatomical correlate of AD and is most prominent in the frontal, parietal, and temporal lobes (**Fig. 6**), with relative sparing of occipital, and primary motor and sensory regions. Atrophy of the hippocampus is prominent and can extend to the amygdala. The ventricles, particularly the temporal horns, are frequently enlarged (**Fig. 6**). Notably, none of these features are specific to AD [31]. Based on Alzheimer's work, we now know that the most remarkable features of AD are the stereotypic patterns by which amyloid plaques and NFTs appear throughout the brain [22], and that toxic, misfolded A β and tau can serve as templates that convert their innocuous counterparts into equivalent pathological forms both *in vitro* [32-35] and *in vivo* [36-40]. Pathological tau is also involved in other diseases like progressive supranuclear palsy, corticobasal degeneration, Pick's disease, frontotemporal degeneration (FTLD), and more [41]. Pathological A β is also seen in cerebral amyloid angiopathy, vascular dementia and Down's syndrome (DS) [42]. AD is unique in the fact that it is *characterized by the misfolding of otherwise unrelated proteins*, A β and tau, causing distinct histopathological changes that converge into the amyloid plaque, which is composed of A β deposits, surrounded by degenerating neurites accumulating tau protein [26].

1.2.1. The role of amyloid- β

The basis of the amyloid cascade hypothesis [43], which forms the backbone of the current understanding of the pathogenesis of AD, is that accumulation of A β is an early event leading to neurodegeneration. A β peptides are composed of various amino-acids and generated through proteolytic cleavage of APP by several enzyme complexes (i.e., secretases; **Fig. 7**). Cleavage by α -secretase and subsequently by the γ -secretase complex forms non-amyloidogenic products of APP. An alternative amyloidogenic pathway, with cleavage of APP first by the β -secretase – or *β -secretase cleavage enzyme 1 (BACE1)* –, and subsequently by the γ -secretase complex, leads to an accumulation of insoluble¹ A β proteins in the brain. APP cleavage through β -secretase and γ -secretase can produce several isoforms of A β , of which the 40 and 42 amino-acid forms are the most prominent [8]. A β ₄₀ is considerably less prone to oligomerization (i.e., the process of aggregating into oligomers from which larger, insoluble fibrils are formed) compared to A β ₄₂, and is regarded as less neurotoxic [44].

Crucially, the exact mechanism of A β toxicity remains elusive. Once released, A β undergoes complex conformational changes, transitioning from small soluble fragments and oligomers into large fibrils, which in turn form amyloid plaques (**Fig. 7**). The toxicity of amyloid plaques has been confirmed and have been found to cause microglial activation within few days of formation [45]. Furthermore, in recent years evidence has accumulated pointing to significant neurotoxicity of A β oligomers, which have much larger surface-to-volume ratio and diffusivity compared to other assembly forms of A β [46]. Moreover, oligomeric forms of A β have been implicated as the critical pathological species in AD [9]. A β can be produced intracellularly [9, 47, 48] or taken up from extracellular compartments through receptor binding and subsequent internalization, which leads to accumulation within lysosomes, endosomes, multivesicular bodies, mitochondria, the endoplasmic reticulum and trans-Golgi network, and the cytosol [9]. A β oligomerization may occur intracellularly, possibly through membrane interactions, and these A β oligomers may cause damage inside cells or spill into the extracellular space [9].

¹ When proteins become misfolded, *they usually expose hydrophobic regions* that form insoluble aggregates.

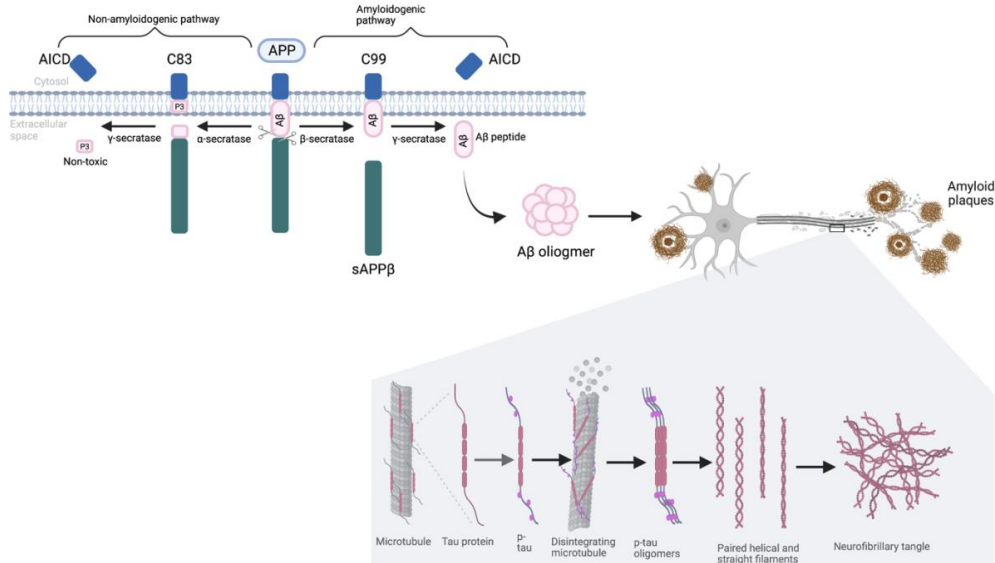


Figure 7. Neuropathological hallmarks in Alzheimer’s disease. Predominantly on the cellular membrane: APP has the characteristic of a cell surface receptor and is expressed in many tissues, in particular in synapses, as a part of normal metabolic processes. Although its primary function remains unclear, APP is believed to be implicated in synaptic formation and repair, signaling, and cell adhesion [8]. As depicted in this figure, the A β region of APP spans the cell membrane. APP is cleaved by α -secretase and β -secretase, both of which release a soluble extracellular fragment (α -sAPP and β -sAPP). Cleavage by β -secretase leaves the A β region attached to the C-terminus fragment (β -CTF), while α -secretase cleavage takes place within the A β region, thereby preventing release of the full-length A β peptide. The α -CTF and β -CTF are subsequently cleaved by γ -secretase in the transmembrane region releasing, respectively, either a harmless p3 fragment or the A β peptide [8]. The physiological roles of the A β converting enzyme 1 (BACE1) and of its homologue BACE2, both of which have β -secretase activity, are less clear, but several non-APP substrates have been identified and BACE1-knockout mice display behavioral and metabolic abnormalities [11, 12]. Notably, several recent studies have demonstrated decreased α -secretase activity and increased β -secretase activity in sporadic AD [12, 13]. In addition to its role in APP processing, the γ -secretase complex is important in the cleavage of Notch, a widely expressed transmembrane protein involved in cell communication [16]. **Predominantly inside axons:** tau is a microtubule-associated protein, whose normal physiological function involves binding tubulin subunits and thereby promoting assembly and stability of microtubules, which is crucial for axonal function and transport of molecular cargo. Tau mutations or dysregulation of kinases/phosphatases leads to tau hyperphosphorylation, and tau translocates from axons to the somatodendritic compartments where it becomes misfolded and aggregated. When hyperphosphorylated, tau becomes less able to bind to tubulin subunits. It has been postulated that the failed interaction of tau with microtubules leads to the latter becoming unstable and consequently disassembling, leading to a collapse in the neuronal transport system [18]. Moreover, in AD, tau aggregates occur intracellularly and may thus trap functional proteins (including tau itself), adding to microtubule destabilization, cellular dysfunction and ultimately neuronal death [18]. Abbreviations; APP: amyloid precursor protein; AICD: amyloid precursor protein intracellular domain; A β : amyloid- β ; sAPP: soluble APP; p-tau: phosphorylated tau. © Christiana Bjørkli, figure created in Biorender.com.

Intraneuronal A β accumulation has been identified in AD patients, transgenic mice, and cultured cells [49-55], has been found to appear prior to extracellular amyloid plaque formation and results in synaptic dysfunction [49, 54, 56-63]. It is still unclear whether intraneuronal A β builds up because of pre-existing A β that remains within the neuron and is not secreted, or whether secreted A β is returned to the neuron by reuptake to form intraneuronal A β pools [64-67]. The release of A β from neurons could potentially occur

wherever APP and the β - and γ -secretases are localized [68]. These results provide direct evidence that neurons can take up extracellular A β , possibly via endocytic processes [69].

In patients with mild cognitive impairment (MCI), intraneuronal A β immunoreactivity has been reported in brain regions that are more prone to the development of early AD pathology, such as the hippocampus and the entorhinal cortex (EC) [50]. Because the accumulation of intraneuronal A β has been shown to precede extracellular amyloid plaque formation [51], and intraneuronal A β levels decrease once amyloid plaques accumulate [59], it has been suggested that the build-up of intraneuronal A β is an early event in the progression of AD. These conclusions are not only limited to patients [51, 59] but are also consistent with results from transgenic mouse models [61, 70-75]. For instance, in a well-utilized model of AD – *the 3xTg AD mouse* –, which overexpresses the Swedish APP gene mutation (*APP_{SWE}*), and the P301L microtubule associated protein tau (*MAPT*) gene mutation (*MAPT_{P301L}*), as well as carrying a knock-in M146V PSEN1 gene mutation (*PSEN1_{M146V}*), intraneuronal A β levels decrease as amyloid plaques begin to accumulate [76].

1.2.1.1. Amyloid plaques

Amyloid plaques, first described by Alzheimer using Bielschowsky silver staining on brain sections from patient Auguste, were determined in the early 1980s to be largely composed of the A β peptide [77, 78]. Neuritic – or ‘dense-core’ –, plaques have a dense center of amyloid surrounded by a halo of silver-positive neurites. Dense-core plaques frequently include neuronal – *neurites and synaptic terminals* – and glial – *reactive astrocytes and activated microglia* – cellular elements [31, 79]. After the sequencing of the peptide (to determine the amino-acids that make up A β) and development of antibodies, it was found that A β also aggregates in ‘diffuse’ plaques of several different morphologies [80-83]. Diffuse plaques are much less dense and consist of non-fibrillary forms of A β [84], are only visible with immunohistochemical techniques, and are hypothesized to represent an early stage in the formation of amyloid plaques. Another distinguishing feature between dense-core and diffuse plaques is that the mitochondria within each differs [85]. From cross-sectional studies of postmortem human brains, it appears that amyloid plaque deposition occurs early in the disease process and proceeds slowly, beginning in the neocortex and progressing through the allocortex, then to the diencephalon, striatum, and basal forebrain cholinergic nuclei,

followed by progression to brainstem nuclei and finally to the cerebellum [23]. Amyloid plaques form within 24 hours, and the effects on surrounding neurites occur within days after amyloid plaque formation [45]. Observations of amyloid plaques appearing in real-time in the brains of mice that overexpress AD-associated *APP* and *PSEN1* mutations with *in vivo* multiphoton imaging surprisingly revealed that individual amyloid plaques come together from soluble A β remarkably rapidly. However, as mentioned previously, A β oligomers have emerged as the most toxic species of A β [86, 87], and this most likely explains why memory impairment or cellular dysfunction cannot be attributed to amyloid plaque formation.

1.2.1.2. Amyloid- β oligomers

How, then, can the relationship between A β and cognitive alterations be understood? The association of amyloid pathology with local synapse loss was largely pioneered in animal and cell culture models. Due to the degeneration of neuropil surrounding dense-core plaques, fibrillar A β was long assumed to be toxic, however studies over the past decade strongly implicate soluble forms of A β as more toxic than fibrils. Elegant experiments by several groups over the late 1990s and 2000s demonstrated that soluble forms of A β cause loss of dendritic spines in cultured neurons, while fibrils and monomers are comparatively innocuous [88, 89]. A series of studies demonstrated that oligomeric A β produced by cultured cells or extracted from human AD brains were toxic to synaptic function, including disrupting long-term potentiation (LTP) in brain slices and impairing cognition when injected into healthy rodents *in vivo* [90-94]. There have also been reports of an association of A β dimers with dementia in human brains [87]. *In vivo* imaging studies of amyloid plaque-bearing mice have revealed a loss of dendritic spines around amyloid plaques due to altered structural plasticity [62, 95, 96]. Removal of soluble A β with topical application of an antibody was shown to result in increased formation of dendritic spines *in vivo* and long-lasting increases in synaptic markers [97, 98], supporting the idea that soluble forms of A β are toxic to synapses. Crucially, A β oligomers instigate tau hyperphosphorylation, which eventually leads to the formation of NFTs [99].

1.2.2. The role of tau

Co-occurring with extracellular A β accumulation, the intracellular build-up of twisted filaments (pre-tangles) – *mainly consisting of abnormally phosphorylated tau protein* –, leads

to accumulations of abnormal tau in dendrites (i.e., neuropil threads) [100] and cell somata of selected neuronal populations (NFTs) [101, 102]. NFTs take a flame-shaped appearance in pyramidal neurons and a globose shape in basket and stellate cells (**Fig. 3**). Tau is a microtubule-binding protein found largely in axons where it serves to stabilize microtubules [103]. During the course of AD, tau is hyperphosphorylated, becomes detached from microtubules, and accumulates in the somatodendritic compartment as paired helical filaments and straight filaments [104-106] (**Fig. 7**). The deposition of NFTs occur in a hierarchical fashion beginning in the superficial lateral EC (LEC) and progressing through the hippocampus, association cortices, and only affecting primary sensory areas in late stages of the disease [22, 107]. The brain density of NFTs directly correlates with the degree of dementia in patients [108].

Abnormal hyperphosphorylation of tau precedes and promotes its self-assembly into paired-helical filaments [109, 110]. As much as ~40% of the abnormally hyperphosphorylated tau is recovered as oligomeric, non-filamentous protein in cytosol of AD brains [109, 111]. Paired-helical filament tau disrupts intracellular compartments that are essential for normal metabolism. Overexpression of tau affects morphology, retards cell growth, and dramatically alters the distribution of various organelles transported by microtubule-dependent motor proteins [112, 113]. Concomitant with the hyperphosphorylation of tau, the axonal transport of the cells is prominently damaged, the outgrowth of axon-like cell processes is inhibited, and typical degenerative profiles of the cells can be observed [114]. Moreover, transgenic mice that overexpress the 4-repeats (R) of human tau protein, – *the R contains microtubule-binding modules* – develop axonal degeneration in specific neurons of the brain [115]. These studies suggest that tau hyperphosphorylation blocks intraneuronal transport.

1.3. Neuroanatomy and Alzheimer’s disease

The structures of the medial temporal lobe (MTL) in the mammalian brain are critical for memory functions that record experience, acquire new facts, and preserve information about life events. Anatomically, these structures include the hippocampus (dentate gyrus [DG], the cornu ammonis fields 1-3 [CA1-3], and the subiculum), and the parahippocampal region (EC, the pre- and parasubiculum, the perirhinal cortex, and the postrhinal cortex). This system undergoes changes during aging in circuits that are highly susceptible to neurodegeneration

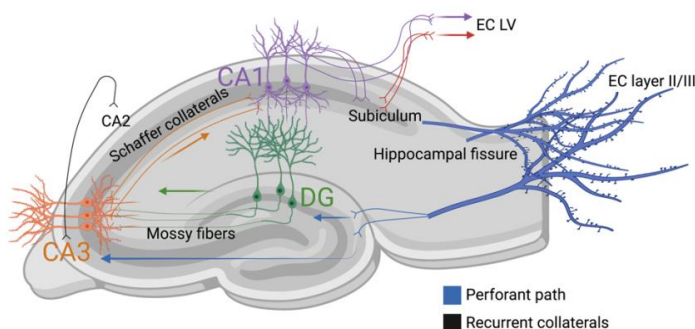
in AD [116, 117]. It has been evident through years of research that by the time of AD diagnosis, marked neuronal loss has already occurred in the EC, the brain's interface between the hippocampus and neocortex. In their classic study, Gómez-Isla and colleagues [118] reported that brains from mild AD patients exhibited more than 50% loss of LEC layer II neurons, while this neuronal population was maintained in healthy-aged brains. Following these findings, stereological investigations have revealed that the number of neurons is largely preserved in the MTL system in humans and other species during healthy aging [119] while significant neuronal loss in EC is evident in the earliest stages of clinically diagnosed AD [120-122].

The EC functions as the nodal point between the cortex and hippocampus [123]. The EC can be subdivided into two distinct functional regions, namely the medial EC (MEC) and LEC. Most neurons in MEC are spatially modulated, and guide egocentric navigation, or – *self-location relative to the geometry of the environment*, and include to date grid cells [124], head-direction cells [125], border cells [126], speed cells [127], aperiodic cells [128], and object-vector cells [129]. Such spatial modulation is absent in LEC, and instead neurons code for odors or objects in context [130-132] or the temporal progression of an event [133, 134].

Like other cortical regions, the EC has six distinguishing layers, of which layers I and IV are relatively free of neurons [135-137]. The principal neurons of the EC, – *i.e., the neurons that are among the main recipients of incoming axons and constitute the major source of entorhinal output* –, are generally pyramidal neurons, or modified versions, such as the so-called fan cells in LEC [135-137]. These neurons mainly utilize glutamate as an excitatory neurotransmitter [136]. The EC projects to the hippocampus with a striking topographical organization, such that projections from the parts of EC closest to the rhinal fissure terminate in the dorsal (posterior in primates) hippocampus, and projections from EC further away from the rhinal fissure terminate in more ventral (anterior in primates) parts of the hippocampus [135, 138].

Principal neurons in superficial layers of EC project to DG, CA1/3 and subiculum of the hippocampus, and this connectivity circuit constitutes the *perforant pathway* (**Fig. 8**). The specific neurons that give rise to the perforant path are closely tied to the pathophysiology

observed in AD [22, 121, 139, 140]. Moreover, *in vivo* diffusion tensor imaging of the perforant path has revealed decreased integrity in older as compared to young adults [141], suggesting a circuit-specific basis for signaling abnormality. Traditionally, the LEC and MEC convey nonspatial 'what' and spatial 'where' information, respectively, into CA1, via both the indirect (or *trisynaptic*) EC layer II → DG → CA3 → CA1 and the direct (or *temporo-ammonic*) EC layer III → CA1 → subiculum pathways – *but see Doan et al. [142] for evidence of LEC as the main parahippocampal multimodal integrative structure.*



1.4. The hippocampus and memory in Alzheimer's disease

Given the notable episodic memory impairments observed early in AD patients, one would expect AD neuropathology to begin in regions mediating this form of memory. The studies of patient H. M. – *or Henry Molaison* –, who

suffered retrograde amnesia following his complete bilateral hippocampal resection [143], established the hippocampus as vital for declarative memory [144], encompassing both episodic and semantic forms. Declarative memory is composed of long-term memory of temporally dated episodes or events – *or episodic memory* –, as well as concepts and facts – *or semantic memory* – that are accessible for conscious recollection [145, 146]. Several behaviors are disrupted when the parahippocampal region is disconnected from the hippocampus [147], such as the association between objects and places and spatial memory [148]. The main hypothesized function of the hippocampus is to bind together multi-modal cortical signals representing a current event into a memory engram, such that a cue presented

at a later stage can trigger the reactivation of the corresponding engram and thereby the episodic memory recall [149].

Different subsets of hippocampal neurons are assigned to encode memories experienced in different contexts [150, 151]. More specifically, DG neurons encoding various memories in one context are not only sparse and distributed but also independent from those encoding memories in a different context [152, 153], and the DG involves a local inhibitory circuit for context-based retrieval [152]. Importantly, animal research has revealed the input from EC layer II to DG and CA3 (part of the *perforant path*) is considered critical for encoding distinct representations of experiences that share overlapping elements with existing memories, commonly referred to as pattern separation [152, 154, 155]. Moreover, impaired pattern separation has been shown to correlate with changes in memory performance coupled to altered function in the DG-CA3 network in older individuals and animal models [156-159]. Aged rats that do not suffer from overt neurodegeneration in the hippocampal region nonetheless have decreased synaptic input from EC layer II onto the hippocampus, with accompanying spatial memory impairments [160]. In line with this, degradation of perforant path connections from EC layer II has been shown in mouse models of AD without accompanying neuronal death [161].

1.5. Biomarkers in Alzheimer's disease

Biomarkers can be objectively measured and evaluated as an indicator of disease state, prognosis, stage, risk, and treatment response. Biomarkers should be reproducible stable and widely available [162]. Magnetic resonance imaging (MRI) and positron emission tomography (PET) can be used to measure amyloid plaque and NFT deposition, brain metabolism and volume. Amyloid PET uses a labeled amyloid tracer, and the cortical standardized uptake ratio is calculated as an index for A β deposits. Certain regions of interest in the brain are determined, and the uptake is compared to a cerebellar reference. This allows objective measurement, with higher sensitivity and specificity than visual inspections of scans. Studies have confirmed the ability of amyloid PET to separate AD patients from control subjects. A β_{42} in cerebrospinal fluid (CSF) and amyloid plaque deposition in the brain are inversely correlated. Low A β_{42} and high total tau (t-tau) and phosphorylated tau (p-tau) in CSF

[163, 164] and/or high retention of amyloid tracer measured with amyloid PET in connection with AD are required as pathophysiological markers according to the latest research criteria.

In the clinic, AD is currently diagnosed using the NIA-AA 2018 criteria, and the disease is defined by underlying pathophysiological processes assessed by biomarkers or by postmortem analyses. Biomarkers are often grouped using the **ATN** system, where **A** covers amyloid plaques, low CSF A β ₄₂ (or low CSF A β ₄₂/A β ₄₀ ratio [165]), amyloid PET [166] and plasma. The CSF concentrations of A β ₄₂ are reduced in patients with AD with respect to controls, probably as a result of increased sequestration into insoluble deposits [167, 168]. This particular biomarker can provide sensitivity and specificity of the disease in 85% of cases [168, 169]. CSF A β ₄₂ levels becomes abnormal in the earliest stages of AD, before amyloid PET and before neurodegeneration starts [170]. The **T** covers aggregated tau, high levels of CSF p-tau [165], tau PET [171] and plasma. The total concentration of tau protein in the CSF is significantly increased in patients with AD with respect to controls already in early stages of the disease [167, 168, 172-174]. However, while it can distinguish patients and controls with sensitivity and specificity above 80%, its role in differential diagnosis is very limited because t-tau is elevated in a wide spectrum of disorders including stroke, multiple sclerosis, and some tumors, in addition to other dementias. On the contrary, high levels of CSF p-tau appears to be a more specific marker of AD [167, 168, 172-175].

The **N** covers neuronal injury and neurodegeneration, measured by structural MRI, PET, high CSF t-tau levels and neurofilament-light (NfL) levels [176]. Autopsy studies have revealed that loss of neurons led to cognitive decline in AD, but also that hippocampal neuronal loss far exceeded hippocampal volume loss [122]. Therefore, *in vivo* assessment of neuronal loss in the hippocampus may serve as a more effective biomarker for disease progression than measures of atrophy. More recently, authors have reported that changes in EC may be a good biomarker to discriminate individuals with MCI from normal control subjects. For instance, studies have shown that a larger degree of atrophy in EC predicts increased disease severity in AD, and that the EC seems to have an obvious advantage of the hippocampus as a biomarker when predicting future conversion to AD in individuals with MCI [177].

1.6. Approaches to attenuate Alzheimer's disease pathophysiology

The mutations leading to familial AD were first discovered in 1991, and subsequently in Auguste's brain material [178]. In the early 2000s, the first drugs aimed at reducing A β came on the market, and a theory of what leads to developing AD was formulated [178]. Subsequently, in 2012, an A β lowering mutation was discovered that dramatically protects against AD, and the first prevention trial against A β was launched [178]. More recently in 2020, tau drug trials have been launched, as well as combination therapy and primary intervention programs [179]. Despite comprehensive research and an immense number of therapeutic trials, there is still no curative treatment for AD. Disease modifying treatments available today are designed to delay symptoms and cognitive decline in symptomatic patients. Acetylcholinesterase inhibitors for mild to moderate AD, and memantine, an N-methyl-D-aspartate (NMDA) receptor antagonist for moderate and severe AD, aim to slow progression and control symptoms by replacing altered neurotransmitters. Meta-analyses show a short-term effect on cognitive function, but no effect on progression of disease [180].

1.6.1. Current treatment of Alzheimer's disease

Therapeutic drugs currently used for AD only bring some degree of symptomatic relief, but no drug has been identified that can effectively block or reverse the process of AD progression, highlighting an urgent need for new therapies. During the last decade all phase III clinical trials focusing on a single target have failed because of adverse effects and the lack of cognitive improvement. Previous research suggests that inhibiting NMDA receptors is beneficial to AD patients [181]. One such NMDA receptor inhibitor is memantine [182, 183]. Prescribed in moderate-to-severe AD and combining acetylcholine inhibitors and memantine led to better cognitive outcomes in patients [184, 185]. Several fluorinated derivatives of memantine have been tested as PET radiotracers for the *in vivo* labelling of NMDA receptors, with ¹⁸F-FENM showing promising *in vitro*- and *in vivo*-binding in mice and monkeys, with good brain accumulation [186, 187].

However, the blood-brain barrier (BBB) remains a major challenge for engaging pharmaceutical drug targets in the brain [188]. Some researchers have developed technologies to shuttle monoclonal antibodies across the barrier [189], and the most recent

drug therapy on the market, Aducanumab², has been found to cross the BBB, as well as binding amyloid plaques, attracting microglia and stimulating phagocytosis of A β ₄₂ [190].

1.6.2. Cholinergic enhancers

The contribution from dysfunction of the cholinergic system to the cognitive symptoms of AD became clear in the early 1980s, soon after the publication of Katzman's editorial, and cholinergic enhancement was among the first treatment options to be explored. As opposed to other approaches such as the administration of acetylcholine precursors and muscarinic agonists, inhibition of acetylcholine degradation was soon found to be a viable route [25, 191-193]. At the time of writing, 3 inhibitors of cholinesterase are available for treatment of AD, namely galantamine, donepezil, and rivastigmine. Galantamine and donepezil selectively inhibit acetylcholinesterase, which is the prominent mechanism of acetylcholine hydrolysis in the brain, while rivastigmine also inhibits butyrylcholinesterase [194-196]. In addition to its effect on acetylcholinesterase, galantamine also acts as an allosterically potentiating ligand of nicotinic receptors, increasing the strength of the residual acetylcholinergic synapses [197]. For cholinesterase inhibitors, there is currently no evidence that they alter A β or tau pathology.

1.6.3. Reduction of amyloid- β

In recent years, the main focus of research on novel pharmacotherapies was based on the amyloid cascade hypothesis of AD, which posits that the A β peptide is chiefly responsible for cognitive impairment and neuronal death. The goal of such treatments is (i) to reduce A β production through the inhibition of β - and γ -secretase enzymes and (ii) to promote dissolution of existing cerebral amyloid plaques [198]. Despite some success in amyloid plaque removal, no therapeutics have succeeded in phase III trials because no cognitive improvement has been demonstrated. One explanation for this may be that the intervention came too late in the disease continuum, often in the early dementia phase, when brain pathology has evolved too far, and the neuronal damage is too great. Patient selection has also often been based on a clinical diagnosis alone, so it has been unclear whether the participants have amyloid pathology or not. Optimizing selection of participants and better

² Aducanumab is not yet authorized for use in the EU at the time of submitting this doctoral thesis.

understanding of the pathophysiological processes of AD are essential to develop novel disease-modifying drugs.

The first immunotherapy approach to be used was active vaccination. Initial findings showed a drastic reduction in the density of amyloid plaques in *APP* transgenic mice [199]. After an uneventful phase I trial, a phase II trial was started on 300 patients with mild AD. Although no major cognitive improvements were found, there was a trend toward slower cognitive decline, especially in patients with a robust antibody response. Unfortunately, the trial had to be interrupted because about 6% of patients developed aseptic meningoenzephalitis [200]. Refined forms of active vaccination are still considered potentially viable, and phase I trials are underway [201]. The majority of efforts have, however, been directed toward passive vaccination. Monoclonal antibodies have been shown to decrease amyloid plaque pathology and to reduce behavioral impairments in transgenic mice [199, 202-204]. At the time of writing, a phase III clinical trial is under way for an antibody, bapineuzumab, which has been shown to bind to both soluble and insoluble A β .

The Wnt – a portmanteau created from the names of two genes, the *Drosophila* **wingless** gene and the murine homologue **integration site 1** gene – signaling pathway influences many aspects of neural development and function. For instance, Wnts are required from neural induction and axis formation to axon guidance and synapse development, and even help modulate synapse activity. There are two Wnt signaling pathways: the canonical pathway – or *Wnt-catenin* –, which promotes synapse and neuronal maintenance, and the non-canonical pathway – or *Wnt-PCP* –, which promotes synaptic disassembly and degradation. Canonical Wnt signaling has been found to be involved in AD development, including synaptic dysfunction, amyloidosis and tauopathy [205, 206]. In *APP* knock-in AD mouse models, a dysregulation of Wnt signaling has been observed, and this down-regulation may be at very early stages of AD (i.e., before the accumulation of amyloid plaques) [207]. This down-regulation effect was more significant in older transgenic mice, and the signaling regulation presented gender differences, where female mice showed more significant down-regulation compared to male mice. Therefore, inhibiting parts of the Wnt signaling pathway may attenuate AD pathology. For instance, Fasudil targets a protein called Rho-associated protein kinase (ROCK) in the Wnt-planar cell polarity (PCP) signaling pathway, effectively derailing the

synaptotoxic cascade of A β production. Previous research has demonstrated that ROCK kinases can induce the processing of APP to the toxic A β ₄₂ peptide and that this can be prevented by ROCK inhibition [208]. Wnt-PCP synaptic signaling is triggered from the increased presence of A β protein, and increased expression of Dickkopf-1 (Dkk1) has been shown in postmortem AD brains [209] and in animal models [210] of A β pathology.

1.6.4. Reduction of tau

The importance of characterizing the early stages of neurodegenerative processes is increasingly clear as decline in brain function and alteration of tau proteins occur prior to major cell loss, suggesting that early stages may be more targetable for therapeutic intervention. There are multiple therapeutic approaches to lower tau levels, including aggregation inhibitors, tau expression inhibitors, modulation of autophagy and proteasomal digestion, and active/passive immunization [211]. There is now consensus that there are early and prolonged cellular changes in tauopathies, including mitochondria function, immune response, intracellular activity, cytoskeletal stability and ribonucleic acid (RNA) metabolism [212]. Mouse models of tauopathy have recapitulated many of these changes, highlighting the potential for screening new therapeutic targets. Many studies that experimentally alter the expression of a single protein have revealed that these pathways are amenable to single-target manipulation for cognitive rescue. However, selective drugs targeting these pathways have not been developed, necessitating the use of broad or semi-selective drugs to narrow potential targets.

1.6.5. Increase in cellular clearance

Autophagy or macroautophagy [213] refers to an evolutionarily conserved process in which intracellular membrane structures sequester proteins and organelles for lysosomal degradation [214]. Autophagy has been found to be impaired in the AD brain [215]. Interestingly, microglia can act as a macrophage-like phagocytic cell in the autophagic pathway and clear away A β [216, 217]. Moreover, A β proteins can cause a blockage in the autophagy-lysosomal pathway [218]. NFTs have also been observed to be degraded by the endo-lysosomal and autophagic pathways [219]. There is a complex interplay between AD and autophagy, as A β may also be generated in the autophagosomes which can then affect its extracellular secretion [220]. *PICALM*, a genetic risk factor for AD, is a clathrin-adaptor

protein that affects autophagy at multiple levels, and *PSEN1* (another genetic risk factor for AD) similarly plays a role in this pathway [220].

The two major pathways involved in tau metabolism under physiological and pathological conditions are autophagy-lysosomal and ubiquitin-proteasome systems (UPS) [221, 222]. For a long time, UPS was considered as a critical route for degradation of proteins such as tau, but recently it has been well-established that tau can be cleared by autophagy [223]. Thereby, autophagy but not the UPS can degrade protein aggregates [222]. However, impairment of both pathways has been described in AD [224, 225]. Hyperphosphorylated tau has been found to co-localize with microtubule associated protein 1 light-chain 3 (LC3)-positive vesicles and with p62 (an autophagic receptor) in neurodegenerative diseases. LC3 is a central protein in macroautophagy [217, 226]. Strong evidence shows that in AD, p62 immunoreactivity is associated with NFTs and is involved in tau degradation. The Ras family of oncoproteins all undergo a posttranslational modification called farnesylation, where a farnesyl transferase takes their C-terminal end with a branched 15-carbon group, then the hydrophobic tail anchors the proteins to intracellular membranes. Without this anchor, Ras protein gets degraded, and this is the result of farnesyl transferase inhibition. One such inhibitor is Lonafarnib, previously approved as a drug for cancer therapy, and such inhibition activates autophagy. This drug is promising for AD research as autophagy directs abnormal tau protein into lysosomes, which degrades tau before it can form NFTs [227].

1.7. Mouse models of Alzheimer's disease

Several mouse models of AD have been generated to better understand the cause and progression of the disease. The amyloid cascade hypothesis of AD argued for A β aggregates being the main culprit for developing the disease in the 1990s. It was therefore of great interest to remove these deposits, but the field was lacking animal models in which such experiments could be performed. This is because researchers could find no evidence of the condition in other organisms besides humans. However, in 1995, a breakthrough occurred, and the creation of transgenic mice carrying a single gene mutation associated with familial AD happened. These PD-APP mice expressed high levels of mutant human *APP* in their brains and developed amyloid plaques and cognitive deficits [228]. Mouse models like this have provided important insights into AD, such as showing that mutations associated with familial

AD favor the production of A β ₄₂ [229]. They have also been invaluable in preclinical testing of drugs, such as in 1999 when an experimental vaccine was able to clear A β from the brains of PD-APP mice [199]. Immunization trials have failed to benefit AD patients, and even in cases where amyloid plaques were cleared from the brain, subjects did not show improved cognitive function. One reason for this could be that mice modelling amyloid pathology do not reflect the entire biology of the disease. In this thesis work, we have used the most complete transgenic mouse model for AD to date, the 3xTg AD model which is characterized by the age-dependent build-up of both amyloid plaques and NFTs [61, 230], and which expresses three human transgenes, namely *APP*_{SWE}, *PS1*_{M146V}, and *MAPT*_{P301L}, expressed under the transcriptional control of the Thy1.2 cassette [231].

2. Thesis aims and objectives

Fundamental goals in AD research include detailed characterization of how the disease progresses and its comparability between experimental models and patients, understanding how the disease initiates, and whether any intervention can halt the wave of toxic protein aggregates before neuronal loss and cognitive impairments occur. Progress has been made within the field using biomarkers to assess pathological hallmarks at various stages of the disease. There has also been an abundance of research on the development of therapies aimed at delaying or halting the progression of AD. Despite this research, all clinical drugs to date (including the recently approved drug Aducanumab) have repeatedly failed to prevent cognitive decline in patients. The poor translational value of experimental models within the field, the relative lack of research focus on the synergy between A β or tau pathology, and challenges in bypassing the BBB, could all be major reasons for the inefficacy of current treatments.

Researchers are also beginning to pinpoint the origin of biochemical events that lead to AD. Yet, the underlying factors for aggregated protein spread in the brain throughout the disease has remained unclear. For instance, there is an inverse spread of amyloid plaques and NFTs in the brain of patients; while amyloid plaques accumulate in the neocortex before appearing in the hippocampus and the parahippocampal region, the appearance of NFTs in the brain follows the opposite sequence. However, recent evidence suggests that unlike extracellular amyloid plaques, intraneuronal A β may emerge early in LEC layer II and may affect intraneuronal A β in downstream hippocampus. The hierarchical pattern of anatomical involvement of A β and tau pathology suggests that AD-related pathology is transmitted from one area of the brain to other regions via anatomical connections.

Thus, the aims and objectives of this thesis have been to:

- 1) Characterize the 3xTg AD mouse model in terms of neuropathology and CSF biomarkers along the disease continuum. We further aimed to provide recommendations for standardized procedures during repeated, longitudinal CSF sample collections to enhance translational validity of preclinical AD models.

- 2) Repurpose already-approved drugs to attenuate AD pathology and to improve cognitive decline.
- 3) Determine the underlying factors that affect neuropathological spread throughout the brain.
- 4) Understand where and how in the brain the disease is initiated.

3. Synopsis of main methods

3.1. Paper II | *In Vivo* Microdialysis in Mice Captures Changes in Alzheimer's Disease Cerebrospinal Fluid Biomarkers Consistent with Developing Pathology

In the first paper, I used 28 awake and freely moving 3xTg AD mice (and two B6129 mice as age-matched controls; **Supplementary Table 1**) to sample A β and tau from CSF using a push-pull microdialysis method modified by our lab. First, the relative recovery – *or concentration of the analyte in the dialysate divided by the concentration in the bulk sample, multiplied by 100* – was calculated to examine the extraction efficiency of the true analyte concentration in extracellular fluid. For *in vitro* experiments, three CSF samples collected by lumbar puncture from healthy human participants was used. Next, four 3xTg AD mice were used to refine microdialysis probe implantation surgery. Implantation surgery was performed to insert microdialysis guide cannulas into the lateral ventricle of mice. After levelling the skull, the stereotaxic coordinates were derived to target the lateral ventricle (A/P -0.1 mm, M/L +1.2 mm, D/V -2.75 mm). Then, using a protocol developed from previous work, intracerebral microdialysis sampling was done once per month, for 10-12 months. We simultaneously sampled A β and tau from the same microdialysis probe in a much larger microdialyte volume than previous *in vivo* collections in mice. Artificial CSF that consisted of NaCl (147 mmol/l), KCl (2.7 mmol/l), CaCl₂ (1.2 mmol/l), and MgCl₂ (0.85 mmol/l) was used to replace the collected CSF from mice. This artificial CSF was mixed with 4 % BSA to increase osmotic pressure of the perfusate to allow for better recovery of A β and tau, and to minimize the chance of microdialyte fluid loss. Following, the MILLIPLEX® MAP human A β and tau magnetic bead panel 4-plex ELISA kit and the Bio-Plex 200 System were used to simultaneously assess the concentrations of A β ₄₀, A β ₄₂, t-tau, and p-tau in CSF samples. Then, immunohistochemical processing was conducted on tissue from implanted and non-implanted transgenic mice. Sections were then scanned using a Mirax-midi scanner, using either reflected fluorescence (for sections stained with a fluorophore) or transmitted white light (for sections stained with Nissl; cresyl violet) as the light source.

3.2. Paper III | Combined Targeting of Pathways Regulating Synaptic Formation and Autophagy Attenuates Alzheimer's Disease Pathology in Mice

In the second paper, thirty 3xTg AD mice and two control B6129 mice (**Supplementary Table 1**) were used to first validate the 3xTg AD mouse for modelling AD neuropathology, then to assess the efficacy of two repurposed drugs on attenuating AD pathology. First, implantation surgery was performed to insert microdialysis guide cannulas into the lateral ventricle of mice. Stereotaxic injections of P301L tau into LEC layer II was done to overexpress tau in this region. Then, push-pull microdialysis was performed for simultaneous infusions of drugs (**Supplementary Table 1**) and CSF sampling from animals for a length of 1-2 weeks. The first drug, Fasudil (a Wnt-PCP inhibitor) in powder form (10 mM) was diluted in sterile saline for a final concentration of 50 mg/kg. The second drug, Lonafarnib (an autophagic inducer) in powder form was dissolved in sterile saline at 60°C to a final concentration of 80 mg/kg. All dosages in ml were calculated using; dosage (mg) / concentration (mg/ml) = dose x ml and were infused at a volume of 60 µl at a rate of 1 µl/min using saline as a control vehicle. In one group of animals ($n = 3$), 0.6 ml of 80 mg/kg Lonafarnib and 50 mg/kg Fasudil were mixed into baby porridge for oral delivery. Next, the MILLIPLEX® MAP human Aβ and tau magnetic bead panel 4-plex ELISA kit and the Bio-Plex 200 System were used to simultaneously assess the concentrations of Aβ₄₀, Aβ₄₂, t-tau, and p-tau in CSF samples. Next, animals were tested in a context-dependent spatial memory task. In this paradigm, mice were initially taught to associate a specific reward location in a square and a circle context. The reward was embedded in one of four cups with ginger-scented bedding. A trial was assessed as correct if the mice dug in the reward location associated with each chamber. If the animals passed the training phase (66.6% correct digging), their contextual memory performance was tested in morph chambers: decagon (circle morph 1), octagon (circle morph 2), hexagon (square morph 1), and a pentagon (square morph 2). If they were able to complete the morph testing, they were tested in a Squirgle chamber on the fifth day. Then, immunohistochemical processing was conducted on tissue, and sections were scanned using a Mirax-midi scanner. Lastly, the number of cells containing intraneuronal Aβ, tau, and amyloid plaques, in dorsal subiculum and LEC of vehicle- and drug-infused 3xTg AD mice (and between infused/non-infused hemispheres of each mouse) was estimated with Ilastik using the Density cell counting workflow. Dorsal subiculum and LEC was delineated using cytoarchitectonic features in sections stained with Nissl, based on The Paxinos & Franklin mouse atlas [232]. Effect size

(Cohen's D) was calculated based on initial experiments between an experimental group infused with Fasudil and a control group infused with a vehicle and the resulting effects on intraneuronal A β -positive neurons in dorsal subiculum.

3.3. Paper IV | Overexpression of Human Tau in Lateral Entorhinal Cortex Layer II of 3xTg AD Mice Leads to Tau Deposition and a Shift in Perforant Path Terminals in the Dentate Gyrus

A total of twenty-four 3xTg AD mice, nine APP/PS1 mice (**Supplementary Table 1**), and eight B6129 mice were used to determine whether age or endogenous presence of human tau affected tau spread from LEC to DG. After levelling the skull, the stereotaxic coordinates were derived to target LEC layer II (+0.5 mm to lambda, ~+4 mm lateral [dependent on animal weight] and ~-3.6 mm ventral from the surface of the brain [dependent on animal weight]), and the hilar region of the DG (A/P: -2 mm, M/L: +1.6 mm, D/V: -2 mm). We used 300-1500 nl of the following adeno-associated viruses (AAVs) for injections into LEC layer II and the hilus: AAV8 green fluorescent protein (GFP)-2a-P301Ltau and AAV8 GFP (**Supplementary Table 1**). The short 2a peptide of the viral vector causes a cleavage that separates GFP and human tau during translation at the ribosome [233]. This results in neurons transduced with the virus (GFP+/MC1+) being able to produce GFP and human tau as individual proteins. Conversely, neurons that receive human tau from cross-neuronal spread express human tau, but no GFP (GFP-/MC1+). The microsyringe was kept in place for 5 minutes prior and after the injection, to minimize potential upward leakage of the viral solution. Metacam was given within 24 hours post-surgery. Animals were sacrificed two months following injections. Then, immunohistochemical processing was conducted on tissue, and sections were scanned using a Mirax-midi scanner. Lastly, the number of cells containing MC1 and GFP in LEC and DG were estimated with Ilastik (**Supplementary Table 1**) using the Density cell counting workflow. LEC and DG were delineated using cytoarchitectonic features in sections stained with Nissl, based on the Paxinos & Franklin mouse atlas [232].

3.4. Paper V | Manipulation of Neuronal Activity in the Entorhinal-Hippocampal Circuit Affects Intraneuronal Amyloid- β Levels

A total of twenty-seven 3xTg AD mice and seventeen B6129 mice (**Supplementary Table 1**) were used to understand where and how intraneuronal A β builds up in the brain. After levelling the skull, the stereotaxic coordinates were derived to target LEC layer II, and we used

500-1000 nl of the following AAVs for injections using a microinjector: AAV8 human M4 muscarinic receptor (hM4) inhibitory DREADD (Di)-mCherry and AAV8 mCherry (**Supplementary Table 1**). The hM4Di is an engineered inhibitory G protein-coupled receptor based on hM4 that causes hyperpolarization in neurons through the G_i pathway. The microsyringe was kept in place for 10 minutes prior and after the injection, to minimize potential upward leakage of the viral solution. Metacam was given within 24 hours post-surgery. Animals were implanted with osmotic minipumps 6-7 days following injections. Mice were implanted with Alzet[®] osmotic minipumps subcutaneously on the flank, slightly posterior to the scapulae. The minipump was primed with DCZ (100 µg/kg), or sterile saline, at 38°C in sterile saline for 48 hours prior to implantation. The intracranial cannula attached to the minipump was implanted into the lateral ventricle, and it was attached to the skull using superglue and dental cement, while the catheter and minipump was secured under the skin with sutures. Analgesics were repeated within 24 hours post-surgery. Animals were implanted with minipumps for 2-3 weeks. Next, animals were tested in a context-dependent spatial memory paradigm. Then, immunohistochemical processing was conducted on tissue, and sections were scanned using a Mirax-midi scanner. Lastly, the number of cells containing intraneuronal Aβ and in LEC and hippocampus (DG, dorsal/ventral subiculum and CA1) were estimated with Ilastik (**Supplementary Table 1**). LEC and hippocampus were delineated using cytoarchitectonic features in sections stained with Nissl, based on the Paxinos & Franklin mouse atlas [232], described in more detail below.

In the rostro-caudal axis of the mouse brain, the first appearance of the hippocampus is CA3 and DG and moving more caudal the CA1 and CA2 appear. CA1 has smaller and more densely packed cells compared to CA2 and CA3, and the pyramidal cell layer of CA2 is thicker than in CA1 and CA3. Moving more caudal, the first part of the dorsal subiculum appears, and can be delineated by a wider pyramidal cell layer compared to the bordering CA1. More caudal again, the ventral subiculum appears, and as this region merges, the stratum radiatum cell layer of the CA1 disappears and cells from the pyramidal cell layer merge and overlap with those of ventral subiculum. The rostral beginning of LEC is considered to appear at approximately the same level as the ventral hippocampus. The dorsal regions of LEC borders with perirhinal cortex at rostral levels, and can be differentiated based on its much larger, and partially 'out of place' layer II cells. More caudal, LEC can be separated from postrhinal cortex using the

same criterion. The ventral regions of LEC borders the piriform cortex and is easily separated since the latter only has three layers. More caudo-medial, the LEC borders the amygdaloentorhinal transition area, and since the latter is a nucleus, it is easily differentiated based on its circular formation of neurons. More caudal the LEC generally occupies more of the dorsoventral extent of the hemisphere, and eventually comes to border MEC roughly as the cortical amygdaloid nucleus disappears. At the caudal end of the hemisphere, LEC disappears and MEC emerges.

4. Synopsis of results

4.1. Paper II | *In Vivo* Microdialysis in Mice Captures Changes in Alzheimer's Disease Cerebrospinal Fluid Biomarkers Consistent with Developing Pathology

Our modified push-pull microdialysis method enabled novel longitudinal, simultaneous sampling of two large proteins, namely A β and tau, and their phosphorylated forms. Here we showed that A β and tau concentrations change with age and pathological deposition in 3xTg AD mice. We demonstrated that not only could we successfully follow the pathophysiological alterations in relevant CSF biomarkers along the AD disease cascade in a preclinical model, but also that these changes reflected ones observed in AD patients. Compared to cut-off levels of CSF biomarkers in patients, the highest mean A β_{42} levels were observed in mice that were 10 months-old (940 pg/ml) and are comparable to the cut-off level at 1026 pg/ml in patients. The highest mean t-tau levels were observed in 9 month-old mice (1199 pg/ml), and were much higher than the cut-off level at 238 pg/ml in patients, and the highest mean p-tau levels at 9 months-of-age (14 pg/ml) was lower than the cut-off level at 22 pg/ml in patients. In line with previous research, we found that a slower flow rate resulted in better recovery of analytes within the microdialyte. Although our method allowed for the recovery of A β_{40} , A β_{42} , p-tau, and t-tau, the recovery rates for A β were low, with slightly higher recovery for tau proteins.

4.2. Paper III | Combined Targeting of Pathways Regulating Synaptic Formation and Autophagy Attenuates Alzheimer's Disease Pathology in Mice

Here we repurposed two FDA-approved drugs, Fasudil and Lonafarnib, both targeting independent biochemical cascades that halted the development of AD pathology. Treatment with Fasudil reduced early intraneuronal A β , the number and size of amyloid plaques in dorsal subiculum, and CSF A β_{40-42} and p-tau levels. Lonafarnib infusions, on the other hand, did not affect intraneuronal A β but rather reduced early non-fibrillar forms of tau after AAV-tau injections into LEC layer II. Treatment with Lonafarnib also reduced the number of amyloid plaques, but unexpectedly increased their size in dorsal subiculum, and only effectively decreased CSF A β_{40} and t-tau levels. Both drugs affected dense-core amyloid plaques that are associated with microglial activation, and subsequent neurodegeneration and cognitive decline in patients. We found that novel combinatorial administration of these drugs

effectively reduced early intraneuronal A β in younger mice, led to reduced CSF A β ₄₀ and p- and t-tau levels, and improved context-dependent spatial memory. This type of pattern completion dependent behavior is thought to depend on the normal function of the hippocampus, a region that is compromised during early phases of the disease.

4.3. Paper IV | Overexpression of Human Tau in Lateral Entorhinal Cortex Layer II of 3xTg AD Mice Leads to Tau Deposition and a Shift in Perforant Path Terminals in the Dentate Gyrus

After overexpression of human tau in LEC layer II of 3xTg AD mice, tau recipient neurons were unexpectedly observed in hilar mossy cells, and not in granule cells which receive unidirectional projections from LEC layer II. Our AAV-tau injections into LEC layer II of young mice induced tau pathology which is otherwise absent in 3xTg AD mice. Moreover, we observed an apparent shift of perforant path terminals in the molecular layer of DG following AAV-tau injections. After overexpressing tau in LEC layer II of young 3xTg AD mice, we observed GFP-positive fibers from donor neurons in the outer molecular layer of DG, whereas in older 3xTg AD mice (18-months-old), we observed these fibers in the inner molecular layer of DG. In line with previous findings, we found an age-associated increase in tau recipient neurons in the hilar region of DG, and further show that endogenous tau load affected the transfer of tau from LEC to DG, as AAV-tau injections in LEC layer II in mice without a human tau mutation (APP/PS1 and B6129) did not result in spreading. This is in line with findings of intracellular tau seeds causing aggregation of native tau proteins and eventually spread.

4.4. Paper V | Manipulation of Neuronal Activity in the Entorhinal-Hippocampal Circuit Affects Intraneuronal Amyloid- β Levels

Here we successfully silenced LEC layer II neuronal activity in mice after targeted hM4D_i-injections followed by intraventricular DCZ infusions. Successful silencing was verified by the expression of mCherry and hM4 and subsequent reduction of cFos in LEC layer II neurons. We also verified LEC layer II neuronal silencing by observing context-dependent spatial memory deficits in mice, indicating a functional role of LEC layer II neurons in cognitive functions known to be impaired in human AD. Moreover, chronic inhibition of LEC layer II caused a reduction of early intraneuronal A β within LEC neurons. Critically, chronic LEC layer II neuronal silencing also caused a reduction of intraneuronal A β deposition in hippocampal subregions CA1 and subiculum, suggesting that activity levels in LEC affect intraneuronal A β in

downstream HPC. The first subregion of the HPC that displayed reduced intraneuronal A β levels after LEC layer II silencing was the subiculum. Together, these results suggest that intraneuronal A β build-up in LEC layer II and its perforant path terminals is regulated by neuronal activity.

5. Methodological considerations

5.1. *In vivo* microdialysis

Microdialysis sampling relies on diffusion of analytes across a semi-permeable dialysis membrane [234]. Molecules have kinetic energy which leads to motion, and this motion is the basis of diffusion of molecules along concentration gradients. Diffusion is a passive process that occurs without the need for specific reactions with other molecules. Moreover, the diffusion rate across the microdialysis membrane is dependent upon several factors, including concentration gradient, molecular size, membrane surface area and temperature. Larger molecules that can pass through the semi-permeable membrane pores have a low rate of migration across the microdialysis membrane. This lower recovery is due to larger molecules moving with a slower velocity; the larger molecules do not collide or meet with the membrane as frequently as smaller molecules. The microdialysis perfusate needs to be similar in its tonicity to the fluid surrounding the probe to prevent significant shifts of water across the microdialysis membrane.

The recovery of proteins reflects the concentration in the dialysate of the substance or molecules of interest in relation to the true concentration surrounding the microdialysis probe. A high recovery means that the concentration in the dialysate is close to the true concentration in the interstitial fluid of the brain (**Fig. 9**). Recovery in microdialysis is dependent upon many factors, such as perfusion flow rate, diffusion rate, and the probe used (molecular weight cut-off, diameter, and length of the membrane). To establish high recovery, a long membrane, with an optimal pore size and a low perfusion rate needs to be used. Also, there might be some trauma caused to the tissue after microdialysis guide cannula implantation and probe insertion, which may potentially influence analyses of CSF samples. Therefore, an equilibrium period is needed prior to CSF sample collection. Histochemical analyses have revealed that severe gliosis around implanted devices such as microdialysis cannulas takes place at about 4 days after the surgery [235-237]. Reports suggest that a complete recovery of physiological functions occurs at the earliest at 5-7 days after the implantation surgery [238]. Therefore, we always waited one week after surgeries before starting sampling procedures.

This method is advantageous over other CSF sampling techniques as it enables serial sampling that follows the dynamic, temporal alterations of a target molecule without necessitating the collection of biopsy samples or animal sacrifice [239-242]. Importantly, each subject can serve as their own intrinsic control to reduce inter-animal variability and the number of animals used in experiments. One limitation of this method, however, is detection of large molecules due to adsorption in tubing and the dialysis membrane, as well as low concentration of analytes in the target tissue [243]. Despite this, the method serves as a valuable tool for measuring CSF AD biomarkers. Validated biomarkers in CSF include reduction in the level of $A\beta_{42}$, increased t-tau and p-tau₁₈₁. A combination of these three biomarkers increases the diagnostic validity for sporadic AD compared to healthy controls with a combined sensitivity

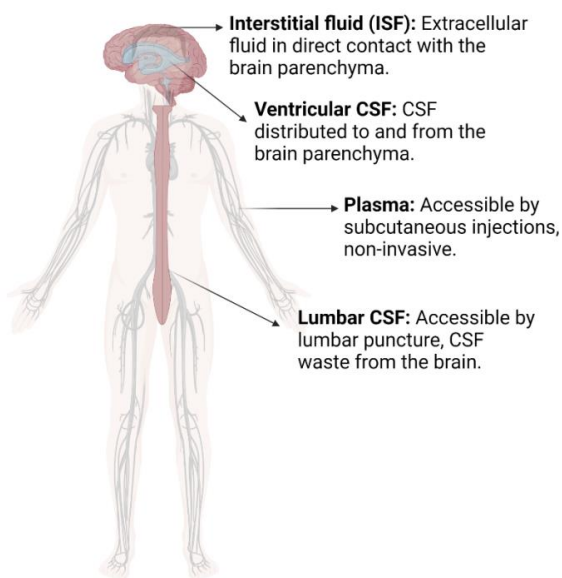


Figure 9. Areas and methods for CSF and plasma biomarker collection. Interstitial fluid (ISF) cannot be collected in living patients, highlighting the importance of using preclinical models in proteomic biomarker research. CSF can be collected from the ventricles of the brain and lumbar region of the spinal cord. A non-invasive method for biomarker collection is blood sampling and proteomic analyses of plasma. However, no blood-based biomarker is currently used for diagnosis in AD. Abbreviations; CSF: cerebrospinal fluid; ISF: interstitial fluid; AD: Alzheimer’s disease. © Christiana Bjørkli, figure created in Biorender.com.

of >95%, and specificity of >85%.

5.2. Infusing repurposed drugs using *in vivo* microdialysis

Most drugs directed towards the brain parenchyma are unable to cross the tightly regulated BBB, leading to increased dosages of drugs and off-target binding. Drug distribution into the CSF is a function of drug transport across the choroid plexus, which forms the blood-CSF barrier, and not drug transport across the BBB, which is situated at the microvascular endothelium of the brain [3]. Drugs injected into the CSF undergo rapid efflux to the blood compartment

via bulk flow. Drug penetration into the brain parenchyma from the CSF is limited by diffusion, and drug concentrations decrease exponentially relative to the CSF concentration. The blood-CSF barrier is relatively leaky compared to the BBB, and water-soluble substances that do not

cross the BBB are able to cross the blood-CSF barrier and enter CSF at a rate inversely related to molecular weight [244]. Moreover, the volume of the CSF ranges from 35 μ l in the mouse to over 100 ml in humans, and the rate of production of CSF ranges from 0.32 μ l/min in mice to 350 μ l/min in humans (**Table 1**). Consequently, CSF turnover across species is fairly constant. The CSF flows from the ventricles over the surface of the brain parenchyma and is absorbed into the superior sagittal sinus of the systemic venous circulation via passage across valves in the arachnoid villi [245]. Brain pulsation resulting from cardiac beats can favor dissemination of CSF between parenchymal arterial and venous perivascular spaces [246].

Table 1. CSF volume and turnover in mice, monkeys, and humans.

| Species | CSF production (μ l/min) | CSF volume | CSF turnover | |
|---------|-------------------------------|------------|--------------|---------------|
| | | | Percent/min | Turnover time |
| Mouse | 0.32 | 35 μ l | 0.89 | 1.8 hours |
| Monkey | 41 | 13 μ l | 0.22 | 5.2 hours |
| Human | 350 | 100 ml | 0.38 | 4.8 hours |

Turnover time = (CSF volume)/(CSF production). Table adapted from [3].

Diffusion is constant in small or large animals, but the brain size varies widely. The brain volume in mice, monkeys, and humans is approximately 0.5 ml, 100 ml, and 1400 ml, respectively [3]. The diffusion distances thus increase proportionately, as illustrated in representative coronal sections of the brain of the mouse, monkey, and human shown in **Fig. 10**. The diameter of the brain is 10 mm, 40 mm, and 140 mm in the mouse, monkey, and

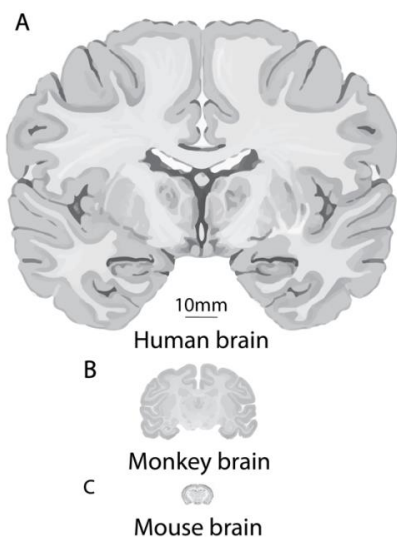


Figure 10. Relative diffusion diameter of each species. Coronal sections, shown to scale, of the human brain (140 mm wide, A), monkey brain (40 mm wide, B), and mouse brain (10 mm wide, C). Scale bar = 10 mm. Figure adapted from [3]. © Christiana Bjørkli, figure created in Biorender.com.

humans, respectively. Diffusion of drugs through 2 mm of brain may be significant in the mouse brain, but is small for the human brain, which has a width of 140 mm. The primary mechanism by which a drug in CSF distributes into the brain parenchyma is diffusion from the CSF into the

brain tissue, and this diffusion rate decreases with distance [247]. The distance traversed by the drug over time would be very small if the CSF

compartment was static without flow. However, this compartment is not static and turns over the entire volume every 2 hours in the mouse brain, and every 5 hours in the human brain (**Table 1**).

Despite the tremendous research efforts that have been put into the development of BBB-penetrating drugs, the success rate in this field is still disappointing. There is contrary evidence in the literature regarding CSF as a conduit to the brain parenchyma, and whether a drug injected into the CSF distributes into deep brain tissue. Some research suggests that drugs injected into CSF have been found to preferentially distribute to the blood rather than the brain [3]. However, researchers [248] have infused horseradish peroxidase – a 40 kDa enzyme – into the lateral ventricle of mice, and found that there was a distribution of 0.2 and 1 mm after 10 and 90 min, respectively, in the periaqueductal gray, which connects the third and fourth ventricles. This is the same distance predicted based on free diffusion and suggests that drugs infused into the CSF have the potential to reach deep brain tissue.

In our experiments, we targeted two biochemical pathways in the hopes of attenuating AD pathology. First, we targeted the non-canonical (i.e., Wnt-PCP) pathway, and along with its canonical (i.e., Wnt-catenin) counterpart, these pathways will provide a balanced maintenance of synapses in a healthy individual, but in an AD brain the Wnt-PCP pathway is overactive and leads to synaptic loss, most likely mediated by a protein called Dkk1 [206, 249]. Fasudil (**Supplementary Table 1**), currently approved as a treatment for cerebral vasospasm, targets a protein called ROCK in the Wnt-PCP signaling pathway, effectively derailing the synaptotoxic cascade of A β production. Previous research has demonstrated that ROCK kinases can induce the processing of APP to the toxic A β ₄₂ peptide and that this can be prevented by ROCK inhibition [250]. Wnt-PCP synaptic signaling is triggered from the increased presence of A β protein, and increased expression of Dkk1 has been shown in postmortem AD brains and in animal models of A β pathology [210, 249].

Second, we targeted the autophagic pathway with the aim of attenuating AD pathology. One way of activating the autophagic pathway is to inhibit the posttranslational modification of proteins by the addition of a farnesyl group (i.e., farnesylation). The Ras family of oncoproteins (i.e., cell proliferation proteins) all undergo farnesylation, and therefore this

pathway is being investigated as a potential target for anti-cancer drugs. One farnesylation inhibitor is Lonafarnib (**Supplementary Table 1**), which is currently approved for cancer therapy. The autophagic system is of special interest in the field since it directs abnormal tau protein into lysosomes, which then degrades tau before it can form NFTs [251]. While an excess of autophagosomes and other autophagic vacuoles is frequently observed in the neocortex of AD brains [252], it is unclear whether autophagy impairment is a contributor or consequence of tauopathy [253, 254]. Activating autophagy is now becoming a prominent candidate as a potential therapeutic target for AD, with animal and cellular models showing that autophagy activators can reduce the levels of misfolded and aggregation proteins, prevent the spread of tau, and reduce neuronal loss [251, 255, 256].

5.3. Viral injections of *MAPT*_{P301L}

The different AAV serotypes display different affinity and transduction to different subtypes of neurons, and it is therefore prudent to conduct pilot and titration testing of new viral vectors. The most used viral serotypes³ within the field are 1, 2, 5, 6, 8, and 9 [257]. The different viral serotypes have also been shown to spread differently in the brain parenchyma. For instance, serotypes 1-4 display limited spread whereas serotypes 5-9 diffuse more readily throughout larger brain structures [257]. There are several advantages and limitations to using viral vector delivery systems for manipulation of cell populations/brain regions. Advantages include high level of protein expression, the possibility of combining several fluorophores, the virus filling whole neurons or subcellular compartments, achieving cell-type specificity, and using it in combination with transgenic mouse lines. Limitations include high costs, laborious preliminary studies used to establish titer, and cytotoxicity in the long-term. A limitation that is specific to pressure viral injections is that it is difficult to avoid leakage of the virus during retraction of the microsyringe.

A recent advancement with AAVs is the possibility of expressing more than one protein in the same virus by insertion of a cleavage protein, such as 2A [258]. In *Paper IV*, we used a viral construct (**Fig. 11**) that separated GFP and human tau (*MAPT*_{P301L}) by 2A self-cleavage during gene translation (**Supplementary Table 1**). Transduction of GFP allowed us to determine

³ The viral serotype is the capsid that encloses the protein that the virus shall transduce.

starter cells – or “donor” cells –, that were first transfected after injection. *MAPT*_{P301L} causes a dramatic increase in the tendency of 4R versions of tau to aggregate and subsequently form β -sheets. This aggregation causes the 4R domain that normally binds microtubules to start binding other tau proteins instead [259]. This mutation does not seem to cause tau proteins to trigger their own hyperphosphorylation, but rather it makes tau more vulnerable to becoming phosphorylated by the already-existing ensemble and levels of kinases [260]. This mutation is considered to be fully penetrant in terms of developing frontotemporal dementia (FTD). Aside from the frontal lobe, it also leads to neurodegeneration in the lateral temporal lobe and contrasts with another FTD-causing *MAPT*-mutation, the *N279K* gene mutation [261]. This latter mutation causes neurodegeneration in the medial temporal lobe and is thus more like tauopathy observed in AD.

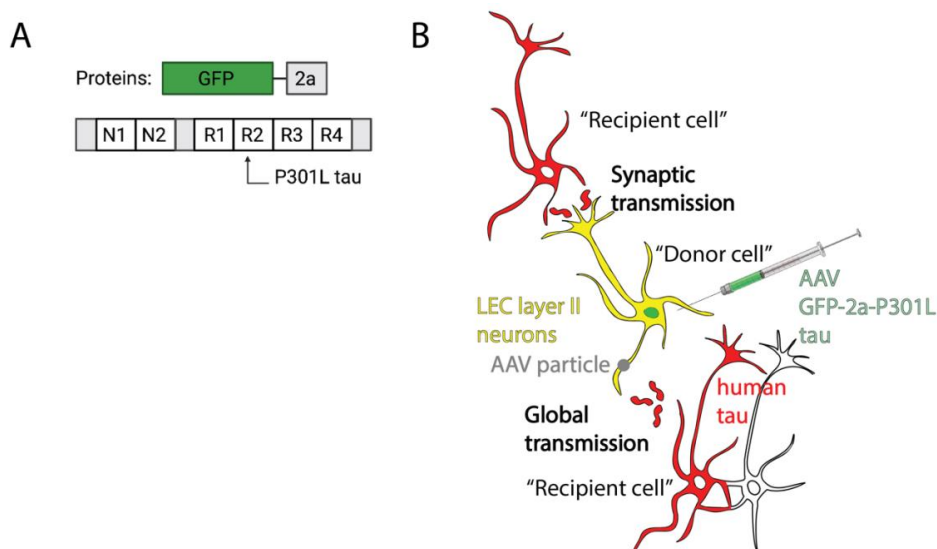


Figure 11. The AAV8 GFP-2a-P301Ltau construct. **A)** The short 2A peptide causes a cleavage that separates GFP and P301L tau (human tau) during translation at the ribosome. **B)** This results in neurons transduced with the virus (GFP+/tau+) being able to produce GFP and human tau as individual proteins. Conversely, neurons that receive human tau from cross-neuronal spread have human tau, but no GFP (GFP-/tau+). Abbreviations; GFP: green fluorescent protein; AAV: adeno-associated virus; LEC: lateral entorhinal cortex. Figure adapted from [7]. © Christiana Bjørkli, figure made in Adobe Illustrator.

While tau gene delivery supplemented with 2A self-cleaving peptides has emerged as an attractive tool in differentiating donor and recipient neurons while monitoring intraneuronal tau transfer, the specificity of the technique is still unclear [262]. In *Paper IV*, we show that GFP and human tau was not separated by 2A peptide cleavage as expected [7, 233], although previous work have also observed cross-neuronal spread of GFP when using this viral tool [7]. Neuronal specificity could have been enhanced in our experiments by using other promoters

than chicken beta actin (CBA) or the cytomegalovirus (CMV), or by using the Cre/loxP binary system to drive tau expression in for instance reelin-expressing LEC layer II neurons. Moreover, for successful modelling of tau pathology by viral overexpression, small and precise injections volumes of tau that is truly restricted to the target area needs to be done. Pressure injections of a large volume in the brain parenchyma can be problematic since it may cause off-targeting of neurons that are irrelevant to the circuit of interest. Co-injection of neuronal tracers could be advantageous when monitoring tau spread from one anatomical region to another.

5.4. Designer receptors exclusively activated by designer drugs (DREADDs)

Chemogenetics take advantage of chemical ligands to modulate genetically engineered receptors. DREADDs are based on engineered muscarinic acetylcholine receptors that have lost their affinity to the endogenous ligand acetylcholine and gained affinity to a designer ligand, most commonly clozapine-n-oxide (CNO). However, one major limitation of CNO is that it does not cross the BBB in mice to any large extent, and maybe even more troubling, are the findings of CNO metabolizing into Clozapine – *a potent antipsychotic drug used to treat schizophrenia* –, which crosses the BBB with high efficiency [263]. This complicates the

use of CNO to activate DREADDs, since it could lead to numerous off-target effects and dubious readouts of cellular activity and behavior. In our experiments we circumvented all of these limitations by using the novel DREADD ligand deschloroclozapine (DCZ; **Fig. 12; Supplementary Table 1**) [264]. DCZ represents the most potent, selective, metabolically stable, and fast-

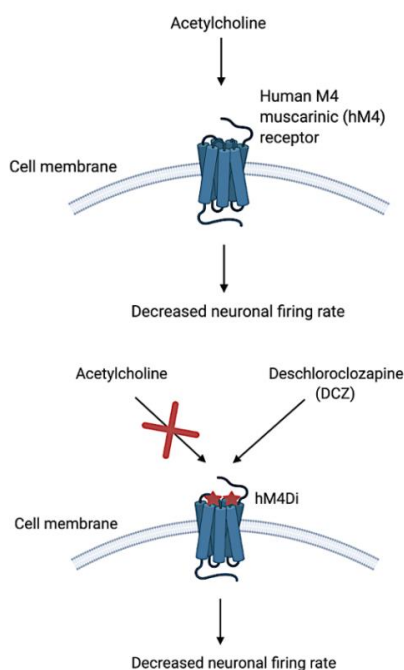


Figure 12. Mechanism of action for inhibitory DREADDs. Human M4 muscarinic (hM4) receptor normally has affinity to the endogenous ligand acetylcholine. hM4 inhibitory DREADDs (hM4Di) is an engineered hM4 receptor that has lost its affinity to acetylcholine and has instead gained affinity to a designer ligand (such as DCZ). DCZ binding to the hM4Di, decreases cAMP signaling, increases MAPK signaling, and activates G-protein inwardly-rectifying potassium channels. This leads to potassium efflux and hyperpolarization. Abbreviations; DREADDs: designer receptors exclusively activated by designer drugs; DCZ: deschloroclozapine; cAMP: cyclic adenosine monophosphate; MAPK: mitogen-activated protein kinase. © Christiana Bjørkli, figure created in Biorender.com.

acting DREADD agonist with utility in mice and non-human primates to date.

There are several different approaches to targeting DREADD expression to a specific cell population using a viral vector delivery system. First, the physical targeting of the viral infusion into the brain gives spatial specificity but low cell-type specificity. However, cell-type specificity can be increased by tailoring the plasmid constructs delivered to the cell via AAVs, for instance by using a CaMKII promoter (like we did in *Paper V*; **Supplementary Table 1**), to drive expression of the chemogenetic receptor in excitatory cells only. However, promoter-driven systems may not always be tight, and leakiness to undesired cell populations may be an issue [257]. Researchers have induced behavioral deficits by intramuscular injections of DCZ in hM4D_i-expressing monkeys [264]. hM4D_i and KORD – *a modified form of the human kappa opioid receptor (KOR)* –, appear to silence neuronal activity via two mechanisms: (i) induction of hyperphosphorylation of Gβ/γ-mediated activation of G protein inwardly rectifying potassium channels [265, 266] and (ii) inhibition of the presynaptic release of neurotransmitters [266, 267]. Early pilot experiments using AAV hM4D_i-mCherry with the serotype 2/1 resulted in transfected fibers rather than somata. Although hM4D_i is fused to a fluorescent tag in this virus, the fusion may undergo lysis, and this could explain a diffused expression of mCherry. Based on the aforementioned challenge and that silencing by hM4D_i occurs presynaptically – *and we wanted intraneuronal hM4 receptor expression akin to previous studies* [268] –, we changed the viral serotype of the virus from 1/2 to 8.

There are various strategies for longitudinally “activating” chemogenetic receptors, and most commonly this includes intraperitoneal (IP) injections of CNO or compound 21 [269]. Osmotic minipumps that can be implanted on the flank of the animal offer a way of longitudinally and continuously infusing a DREADD agonist [270], without inoculation. These minipumps can steadily release a systemic dose of chemicals for up to 6 weeks, whereas more traditional methods like IP injections usually activate chemogenetic receptors for 60 minutes [271]. Osmotic minipumps rely on osmotic pressure which displaces the chemical from the pump at a controlled, predetermined rate. These minipumps can also be attached to a catheter for intracerebral infusion as we did in *Paper V*, rather than relying on diffuse osmotic spread from the implantation site. However, by longitudinally inhibiting LEC layer II, the multitude of

physiological functions performed by this brain region was impaired, and this needs to be considered when interpreting our results from *Paper V*.

5.5. Context-dependent spatial memory task

Lesion and observational studies have demonstrated that the hippocampus and EC are necessary for contextual memory formation [272, 273]. Studies have recently emerged that show context-specific signals in the hippocampal-entorhinal network during the execution of spatial memory tasks [274]. Spatial context might be represented in the hippocampus through the activity of place cells that fire whenever a navigator occupies particular environmental locations [275]. When context is altered, place cells undergo a process known as re-mapping, in which all place cells shift their relative firing fields to new locations or stop firing altogether [276, 277]. Re-mapping might be driven by entorhinal inputs to the hippocampus [278, 279]. The EC contains several types of place-modulated neurons, including grid cells that fire whenever a navigator occupies a hexagonal lattice of environmental locations [280]. Coincident with place cells re-mapping across different contexts, grid cells coherently shift and rotate their firing fields, a process known as grid re-alignment [279, 281].

Memory functions of the hippocampus include the process of pattern separation and pattern completion. Pattern separation performed by the DG of the hippocampus [282-284] is thought to support our ability to avoid confusion between similar episodic memories by transforming interchangeable cortical input patterns of neural activity into dissimilar output patterns before their long-term storage in other parts of the hippocampus [285]. Pattern completion by the CA3 region of the hippocampus enables episodic memories to be formed and stored in the same region, as well as retrieval of a whole representation to be initiated by a recall cue [286]. Attractor dynamics can explain both why hippocampal neurons react coherently following sufficiently large changes to the environment (i.e., discrete attractors) and how hippocampal firing patterns move more smoothly from one representation to the next as an animal travels through space (i.e., continuous attractors) [287]. Evidence in favor of such attractor dynamic processes in the hippocampus come from experiments using progressive morphs of environmental geometry between two different spatial contexts [288, 289]. In *Papers III* and *V* we used a context-dependent spatial memory task in which boundary geometry was morphed between two familiar contexts and found improved performance in

the morphed settings after drug treatment, suggestive of improved attractor-like performance.

In this context-dependent spatial memory task, mice were first trained to associate a specific reward location, out of four, in a square and circle context. If they passed the training phase, mice were tested in probe trials (i.e., without rewards) in progressive morphs of environmental geometry: a decagon (circle morph 1), an octagon (circle morph 2), a hexagon (square morph 1), and a pentagon (square morph 2). If mice were able to associate the progressive morphs with the previously learned reward location of the square and the circle, they were tested in an ambiguous half-square half-circle context – *the “Squircle”* – on the fifth day. Since the Squircle equally resembles the square and a circle context, a trial was considered correct if mice were digging in either the circle- or square-related reward location. Thus, to remember the reward location in each context, mice needed to learn the appropriate location-context associations throughout training. These contexts were made in-house using Lego to get the correct geometrical proportions of each context as well as simplifying disinfection between trials.

A question remains regarding which steps of this behavioral paradigm taps into the retrieval, encoding, or the consolidation stage of contextual memory. Simply translating the steps of this experiment conducted in humans [274] would suggest that the training phase acts as the retrieval, the morph stage act as the encoding, and the context-dependent spatial memory task acts as the consolidation of contextual memory. Another widely used behavioral paradigm that assesses the integrity of the LEC is the novel object recognition (NOR) task [290]. However, the NOR task fails to assess the relationship between objects and context and is therefore not an appropriate paradigm to assess the role of the hippocampal-entorhinal circuit in contextual memory.

5.6. Tissue processing

In these experiments a variety of histological and immunohistochemical staining procedures have been conducted. See **Supplementary Table 1** for key resources used in *Papers II-V*. For visualization of cytoarchitecture (and RNA), Nissl staining has been used. The NeuN antibody was used to identify neurons, whereas DAPI was used as a counterstain for general DNA

labelling. For labelling fan cells in LEC layer II (and verifying viral injection location), we used an antibody against reelin. We labelled for activation of immediate-early genes (IEGs) to observe general protein translation and activation of neurons by our behavioral task [291, 292].; an antibody against cFos has been used for observing somatic markers, whereas an antibody against Arc has been used as an indicator for dendritic markers. However, a potential constraint of IEG expression is that we cannot infer a causal relationship between behavior and the neural activity detected by this method [293]. Another limitation of IEGs in terms of our experiments is that research suggests decreased expression of for instance cFos in the hippocampus of AD mouse models [294]. Therefore, we also used an antibody against phosphorylated extra cellular signal-regulated kinase (pERK) as a measure of increased neural activity in these experiments.

In these experiments, we used specialized antibodies for visualization of developing tau pathology. First, we used the HT7 antibody for visualization of endogenous human MAPT [295] in the 3xTg AD mouse model. This antibody recognizes human tau between residues 159 and 163 and does not cross-react with murine tau. We used this antibody to differentiate between endogenous and injected human tau in mice in *Paper IV*. Tau pathology in AD first involves the somatodendritic accumulation of conformationally altered, non-fibrillar tau, which is recognized by the MC1 antibody [296, 297]. The MC1 antibody was developed and donated to us by the late Peter Davies. It has also been shown that the conformational change recognized by MC1 may precede the aggregation of tau into filaments and the resultant neurofibrillary degeneration seen in AD [296]. The AT8 antibody recognizes phosphorylated paired helical filament tau [298] at serine 202 and threonine 205 and displays no cross-reactivity with unphosphorylated tau. However, many publications within the field equate tau phosphorylation with aggregation, and this is probably not correct [299]. A staining procedure that is specific to NFTs is Gallyas-silver staining [300, 301], which dye NFTs and associated glial inclusions.

Despite numerous publications in a range of animal models indicating that A β may accumulate intracellularly, the acceptance of this concept has been slow and controversial, mainly due to technical issues [9]. One of these technical issues relate to antibody cross-reactivity, as it is possible that A β -specific antibodies may also recognize full-length APP or its

other derivatives [9]. Another issue relates to pre-treatment steps in immunohistochemical protocols. For instance, two groups have demonstrated that the heating protocol (microwave antigen retrieval or hydrated autoclaving) markedly enhanced intraneuronal A β immunoreactivity, whereas formic acid exposure, a common pre-treatment step in A β immunostaining, is not optimal for visualization [302, 303]. Because of the above-mentioned technical issues, we have used conformation-specific A β antibodies and heat-induced antigen retrieval on all tissue. The anti-oligomer A11 antibody recognizes A β oligomers but not pre-fibrillar oligomers or monomers [304]. This antibody also reacts with soluble A β_{40-42} oligomers but does not react with soluble low molecular weight or fibrillar A β_{40} . We also used an antibody specific to A β_{42} in our experiments. Cytosolic labeling of the McSA1 antibody, which recognizes A β_{38-42} [304], was used as a generic marker for the presence of intraneuronal A β .

To visualize amyloid plaques, we used the above-mentioned McSA1 antibody as well as the anti-amyloid fibrils OC antibody which recognizes epitopes common to many amyloid fibrils and fibrillar oligomers, but not pre-fibrillar oligomers or monomers [304]. Thereby, our antibodies provided good coverage of the pre-plaque aggregation steps of A β , including pre-oligomeric A β_{42} , A β pre-fibrils (anti-oligomer A11) and A β protofibrils (anti-amyloid fibrils OC). To verify surrounding neuroinflammation we stained with the microglial-specific antibodies; ionized calcium-binding adapter molecule 1 (Iba1) and TREM2. To verify lysosomal activation after infusions of Lonafarnib in *Paper III* we used a lysosomal-associated membrane protein 1 (LAMP1) antibody and observed its co-localization with amyloid plaques visualized by the anti-amyloid fibrils OC antibody. To distinguish dense-core from diffuse amyloid plaques in *Paper III* we used an antibody against microtubule-associated protein 2 (MAP2) [305] with 3, 3'-diaminobenzidine (DAB) as a chromogen.

The proteins transduced by viral vectors in *Papers IV* and *V* were visualized by GFP or mCherry. To enhance visualization of infected cells, antibodies against these two fluorescent tags were used. We encountered some issues when staining against mCherry, and endogenous expression of this fluorescent tag was very poor. Tissue fixation-time might play a significant role in the expression of red fluorophores, as we have observed strong mCherry expression in live cells but poor expression after fixation in both cell cultures and mouse brain tissue in

our group (data not shown). In future studies we opt to fix brain tissue in the matter of hours rather than 24 hours to enhance mCherry expression.

5.7. Animal models of Alzheimer's disease

Although they are not always the best species for mimicking human disease, transgenic mice are still undoubtedly the most popular and extensively used animal models for studying AD. The studies carried out in animal models have yielded invaluable information on the pathogenesis and pathophysiology of AD including, for instance, novel insights into the molecular mechanisms underlying the pathological aggregation of pivotal proteins, the underlying pathways that lead to neuronal damage, the contribution of genetic risk factors and the role of neuroinflammation in neurodegeneration. Yet, these models appear to have only partially contributed to shed light on the actual mechanisms triggering the disease, thus preventing true translation into new therapies, diagnosis, and prevention. Although an impressive amount of knowledge has been gained from the use of animal models, it has to date only marginally enriched research into therapeutic avenues.

One of the main reasons for the lack of true translation between animal models and the clinic is the number of confounding factors that needs to be kept in mind when trying to model AD. These complex elements include genetics – *such as mutations, risk-associated common variants of sporadic AD, and epigenetics* –, environmental factors – *such as toxins, diet, stress, social interactions, and infections* –, and aging factors – *such as metabolic changes, hormones, genomic instability, and accumulation of damaging insults*. Most of the currently used models are not able to recreate the complexity of the human disease since they usually address these elements individually. Also, current models most commonly only address familial versions of AD. In our experiments, we have addressed the first element of genetics in a comparable manner to human disease. The 3xTg AD mouse model harbors three human gene mutations, in the *APP*, *PSEN1* and *MAPT* genes, which result in amyloid plaques and NFTs like that seen in patients. However, it's important to note that these gene mutations often result in a much higher expression of aggregated proteins than that seen in the human brain. Likewise, AD patients do not overexpress *APP* or *PSEN1* [306], and the overexpression of these mutant genes may cause problems unrelated to AD in mice, such as displaying cognitive deficits before amyloid pathology starts. Also, the *MAPT* mutation in this mouse model results in FTD

and not AD in patients. Moreover, there are only 4R tau in mice, whereas in humans 6R tau is expressed. The spatiotemporal spread of A β is similar in the mouse model to that seen in patients, with depositions in neocortex before appearance and hippocampus. On the other hand, the spatiotemporal spread of tau pathology mimics that of FTD patients, and therefore human tau was overexpressed in the brain region of emergence in our mouse model in *Paper IV*. Overall, however, this mouse model allowed us to investigate what is hypothesized to be the core of AD pathology; the interplay between aggregated A β and tau.

Addressing the second element for the complex interplay of factors leading to AD, the role of environment has been attempted to be modeled in the current experiments. For instance, the value of environmental enrichment has played a major role here [307]. This includes mice housed in groups without being isolated for long periods of time, as well as enrichment toys in their cages during experiments. We have also adopted the principle of the 3Rs, by reducing the number of animals in experiments due to statistical power estimations [308] and reusing animals in experiments, where possible.

Addressing the third complex element on ageing, AD mice may be a better model of the early preclinical stages of the disease than the later dementia stages [309]. This is because the lifespan of a mouse ranges between 2 to 2.5 years, whereas the age of onset of sporadic AD usually occurs after 60 years of age. This difference could explain why drugs that are successful in treating mice do not work in patients, seeing as they are being administered too late in the disease continuum. However, this short lifespan is advantageous to researchers as they can study *most of the disease process* during this short timeframe instead of a lifetime in patients. Studying *most of the disease process* poses a major limitation of current mouse models of the disease, as they do not display neurodegeneration, the suspected sole culprit for the manifestation of clinical symptoms in patients. This limitation in disease modelling could be due to more resilient neurons in mouse models, but the more likely scenario is that due to their short lifespan they are unable to completely mimic the disease. Many of these mouse models, including the 3xTg AD model used here, display cognitive decline prior to pathological development, which suggests that early pre-aggregates of proteins play a major role in the behavioral expression of this disease.

6. General discussion

In *Paper I*, we reviewed the urgent need for progress within the AD biomarker field to be able to translate markers across animal models and clinical populations. We found that not all pathological hallmarks seen in patients can be translated to preclinical models, and therefore one needs to be aware of pertinent differences when comparing AD research across species and bridging findings into the clinic. In *Paper II* we show that our modified push-pull microdialysis method enables longitudinal, simultaneous sampling of A β and tau and their phosphorylated forms. Moreover, we show that the concentrations of A β and tau change with age and pathological deposition in the brains of 3xTg AD mice, and that these levels are comparable to those observed in human AD patients. In *Paper III* we found that Fasudil – a *Wnt-PCP inhibitor* – reduced intraneuronal A β as well as the number and size of amyloid plaques in hippocampus. Lonafarnib – an *autophagic inductor* –, on the other hand, reduced conformation-specific tau in LEC following human tau overexpression, and the number of amyloid plaques in hippocampus. Lastly, we found that combinatorial treatment of both drugs effectively reduced intraneuronal A β in hippocampus and improved cognitive performance in mice. In *Paper IV* we show that tau injections in LEC layer II results in tau spread to the hilus in DG and the manifestation of tau pathology which is otherwise absent in 3xTg AD mice. Moreover, we found an age-associated increase in tau spread, and that the presence of endogenous human tau was necessary this spread. In *Paper V*, we successfully silenced LEC layer II neuronal activity in 3xTg AD mice, verified by reduced cFos expression and context-dependent spatial memory deficits. Neuronal silencing of LEC layer II reduced early intraneuronal A β within LEC neurons, suggesting that A β may originate in this brain region and affect A β levels in downstream hippocampus. The first hippocampal subregion to show reduced levels of intraneuronal A β after LEC layer II neuronal silencing was the subiculum.

6.1. Translational validity of mouse models of Alzheimer's disease

Despite the rise in incidence of AD, it has been over a decade since a new drug treatment has been introduced to the market. One reason is that researchers have struggled with the lack of translatability of preclinical studies to the clinic. One aspect that has come under heavy scrutiny is whether the mouse is an appropriate model for a complex human disease such as AD. There are approximately 160 AD-related mouse models described on Alzforum, including

APP, *PSEN1-2* mice and *APP* knock-ins to model amyloid plaque pathology, and mice with FTD mutations and human tau mice to model tau pathology. Current mouse models of AD have incorporated well-known early onset AD mutations on a single genetic background – *C57BL/6J* –, which does not model human genetic diversity. Moreover, transgenic mice have been invaluable but generally offer aggressive phenotypes or are missing key consequences of tauopathy, such as neuronal loss [310]. Studies suggest that mice are resistant to developing NFTs even with heavy amyloid plaque load due to the lack of TREM2 loss-of-function variants [311, 312].

Since AD transgenic mice mostly model early onset familial mechanisms of the disease, their relevance to biomarkers observed in sporadic AD patients has been debatable. In forms of FTD caused by *MAPT* mutations in patients (and which causes tau pathology in 3xTg AD mice), CSF tau levels usually do not increase [313]. In *Paper II*, however, we provided evidence of similarities between the temporal span of CSF biomarkers between the 3xTg AD mouse model and AD patients. Not only did we find that CSF tau increased during the span of AD, but also that the highest CSF tau levels coincided with the highest CSF A β levels, giving support to findings of these two proteins working in concert in AD pathophysiology. In *Paper III*, we characterized our own 3xTg AD mouse colony to select timepoints for treatment with Fasudil and Lonafarnib. We found that genetic drift with phenotypic effects occurred in our mouse colony, but that this mouse model presents as a valid translational tool for studying AD-related neuropathology. Of note, experimental models of disease do not necessarily have to recapitulate the entire disease process since the main point is to reduce complexity to better understand the underpinning mechanisms of the disease.

6.2. Pharmacologically attenuating amyloid- β and tau pathology

Although the pathogenesis of AD is now partially understood, effective treatment strategies for delay or prevention of AD remain to be developed. However, the recent positive results of the antibody Aducanumab have re-energized the field. Despite removing amyloid plaques, treatment with the antibody does not improve cognitive decline, and therefore there is a great need to identify treatments that can improve this facet of AD symptoms. One such possible intervention is ROCK, a serine/threonine kinase regulated by the small GTPase RhoA, which was pharmacologically regulated in experiments in *Paper III*. The ROCK signaling

pathway is involved in regulating cell migration, proliferation, and survival, and has been found to be related to developing AD [314]. Moreover, ROCK induction can promote a neuroinflammatory response by activating microglia and astrocytes. In line with this, ROCK activation increases A β production, and Fasudil, a ROCK inhibitor, has been shown to reduce A β [315-317] by reducing A β -induced neuronal damage [249, 317] and neuroinflammation [315, 316]. Our results following Fasudil infusions in *Paper III* are in line with these previous reports of its efficacy in reducing A β levels.

Activating biological clean-up systems has recently gained attraction as a method for attenuating AD pathophysiology and was therefore another pathway we pharmacologically regulated in *Paper III*. It has been demonstrated that a dysfunctional autophagic system contributes to AD progression [318]. Our results following Lonafarnib infusions in *Paper III* are in line with previous results of its efficacy to reduce AD-related neuropathology. However, combinatorial treatment of both drugs in *Paper III* attenuated AD-related pathology at the functional, as well as at the molecular level. In line with this, pharmacological inhibition of ROCK2 has been shown to promote translocation of APP and BACE1 to lysosomes [319], and several studies indicate that inhibition of ROCKs can induce autophagy [320, 321]. Based on the beneficial effect of Fasudil on neuronal plasticity and survival, it is currently being used in clinical trials for the treatment of amyotrophic lateral sclerosis (ALS) [322]. A regulator of autophagy, mechanistic target of rapamycin (mTOR) phosphorylation, has been found to be increased in MCI and AD patients [323]. It has also been shown that an increase in mTOR signaling activity could suppress autophagic processes, leading to a failure to clear tau aggregates in vulnerable neurons [324]. Lonafarnib, a farnesyltransferase and mTOR signaling inhibitor [325], can induce autophagy through activation of lysosomes, prevent the formation of tau aggregation, and attenuate behavioral dysfunction in FTD mice [251].

6.3. The origin and spread of pathology in Alzheimer's disease

The prion-like propagation hypothesis [326] argues that aggregates of misfolded A β and tau proteins can propagate similarly to infectious, misfolded prions. This implies that pathological seeds – *i.e.*, *misfolded proteins* – are secreted into the extracellular space by an infected neuron and subsequently absorbed by a nearby, recipient neuron [327, 328]. Once the pathological seed is taken up by a neuron, it can infect healthy, intraneuronal A β and tau

monomers, thus facilitating pathological aggregation and the progression of the disease [329]. This idea has been supported by findings demonstrating that both A β and tau pathology can be induced *in vitro* and *in vivo* by injecting pathological seeds from postmortem AD brains into healthy rodent brains or rat neuronal cultures [330-334]. However, although prions, A β and tau proteins share similarities in their propagation mechanisms, prion-like mechanisms cannot account for all aspects of the spread of the disease as neither A β nor tau proteins are contagious like prions [335, 336]. Instead, emerging evidence suggests that aggregated proteins may be transmitted in a cell-to-cell manner, – or *transsynaptically* –, whereby tau propagates via the synapse in an anterograde fashion.

The transsynaptic hypothesis was initially proposed based on studies using bigenic neurospint-tTA⁴-tau mice [37, 38], generated by crossing a tTA-EC line and the Tg(tetO-tau_{P301L})4510 responder line. Aggregated tau in this mouse model was expressed predominantly in the superficial MEC and the pre/parasubiculum, and it took several months for somatodendritic tau – *i.e., where hyperphosphorylated tau accumulates after detaching from axonal microtubules* –, to transfer along the direct projection pathway to the granular cell layer of DG. Interestingly, removal of endogenous murine tau in these mice did not affect tau transfer from MEC to granule cells [337], suggesting that late-onset tau pathology in DG was a consequence of transsynaptic propagation of tau and not due to prion-like mechanisms. This is in line with our findings in *Paper IV* of murine tau present in APP/PS1 and B6129 mice not affecting tau spread from LEC to DG.

A contemporary hypothesis states that tau spreads transsynaptically [36, 338-340] (**Fig. 13**), however, whether this extends to A β *in vivo* has remained unresolved. If the spread of A β and tau is dependent on synaptic connectivity, this may help explain the spatiotemporal progression commonly seen in AD patients. For instance, data from *in vivo* studies in humans and rodents have provided evidence that pathological tau can spread through neuronal projection pathways that resemble functional brain networks [37, 38, 341-343], and that tau spread depends on synaptic connections rather than spatial proximity [344]. These results have further been supported by *in vitro* studies showing that enhanced synaptic connectivity

⁴ Tetracycline-controlled transcriptional activation – or *tTa* –, is a method of inducible gene expression by turning transcription on or off in the presence of a tetracycline antibiotic, such as doxycycline.

facilitates the spread of pathogenic tau [345]. Importantly, pathological tau accumulation takes place predominantly in principal neurons [346], and therefore most likely spreads along excitatory projection pathways.

Accumulating evidence now strongly suggests that the spread of A β also depends on excitatory projections across principal cells. Previous *in vitro* data have shown that soluble oligomeric A β can spread transsynaptically [347, 348], thus suggesting that the spread of early intraneuronal A β also depends on cellular projection pathways. Interestingly, the process of tau spread through neuronal projection pathways has been found to be accelerated by the presence of A β in AD patients [341, 349]. This is in line with our findings in *Paper V*, showing

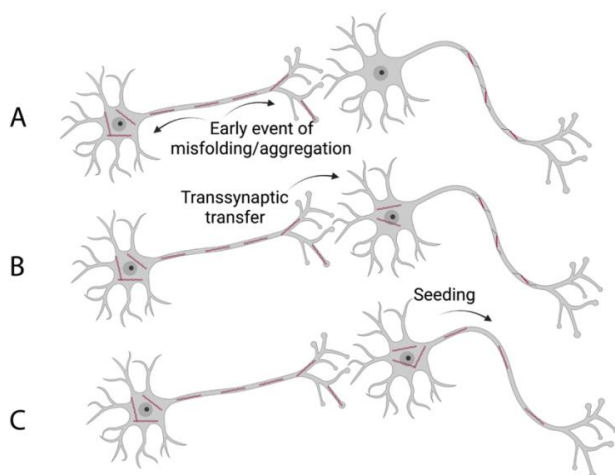


Figure 13. Pathological spreading in a neuron-to-neuron manner. A) Intracellular proteins (such as A β and tau) become misfolded and subsequently aggregate. B) The aggregated proteins are transferred from somata or axons across the synapse to dendrites of a nearby neuron. C) Pathological seeds, or aggregated proteins, travel from the dendrites to soma and axons of the second neuron. © Christiana Bjørkli, figure created in Biorender.com.

that early intraneuronal A β builds-up in LEC layer II and affects downstream connected hippocampal subregions.

Subregions of EC and the hippocampus form a critical functional circuitry that collects cortical information together into cohesive representations [123]. Neither human imaging nor autopsy studies have pointed to a precise regional origin where A β deposition begins, and it has been suggested that this pathology

appears multifocally and then encompasses the majority of association cortex – i.e., *parts of the cortex that receives information from primary sensory cortices* [22, 23, 350, 351]. Moreover, it has been shown that APP can be transported anterogradely via perforant path projections from EC to DG in rats [352], and mice expressing transgene-derived APP in superficial layers of EC and pre- and parasubiculum have high levels of soluble A β and amyloid plaque deposits in perforant path terminal fields in DG [353]. Based on our findings in *Paper V*, the perforant path appears to be highly involved in the origin of intraneuronal A β build-up.

We found that when LEC layer II projection neurons were inhibited over longer periods of time in *Paper V*, the amount of intraneuronal A β -positive neurons in hippocampal subregions was reduced. This is in line with previous research indicating that reelin-positive neurons in LEC layer II of rodents were the first to accumulate intraneuronal A β , a pattern that was reflected in postmortem AD brains as well [354]. Crucially, early seeding activity of A β and tau are present prior to histopathological markers in rodents and AD patients [331, 355]. In *Paper V* we show more reelin- and intraneuronal A β -positive cells in the portion of LEC located closest to the rhinal sulcus/fissure, akin to the first traces of NFT deposition in patients [22].

Despite the contemporary hypothesis of transsynaptic spreading of tau pathology, several recent findings have begun to question whether tau spreads throughout the brain in this manner [356-359]. For instance, a comprehensive histopathological study of postmortem AD brains showed that dendritic tau pathology in the temporal allocortex – *i.e.*, *cerebral cortex that is not part of the neocortex* –, spread in a direction opposite to currently known anterograde hippocampal connectivity [360]. Findings from this study align well with our findings in *Paper IV*, where endogenous human tau load in CA1 of 3xTg AD mice appeared to spread retrogradely to CA3 and the hilar mossy cells of DG and most likely influenced our tau injections in LEC layer II. Like our findings from *Paper IV*, other inoculation studies that have overexpressed tau suggest that transfected tau is taken up by axons and that tau seeding can occur in distant brain regions, rather than tau transsynaptic spread [262].

Tau pathology is usually found in the EC of older adults, including those without simultaneous A β pathology [361, 362]. Therefore, the mechanisms that cause tau to spread from EC and to the hippocampus may be key to understanding, and ultimately preventing the development of AD. Based on our findings in *Paper IV*, tau deposition in the 3xTg AD mouse after overexpression in LEC layer II causes tau to transfer from LEC to DG in an expected anterograde sequence⁵, as well as transferring in an unexpected reverse (or retrograde) sequence, from brain regions with already-present tau pathology in 3xTg AD mice – *such as CA1* –, and thereby causing tau deposition in DG.

⁵ However, tau recipient neurons were unexpectedly observed in hilar mossy cells, and not in granule cells which receive unidirectional projections from LEC layer II.

6.4. Future directions

There has been a considerable amount of research on potential blood-based biomarkers in AD that identify the intricacy of the pathophysiology of the disease [363-365], but none yet fulfil the diagnostic accuracy of CSF/PET core biomarkers. However, it has been found that plasma biomarkers (i.e., blood exosome protein profiles) could predict conversion from MCI to dementia [366]. Other promising results include plasma A β biomarkers using immunoprecipitation coupled with mass spectrometry [367]. Other findings indicate that plasma A β_{42} and p-tau_{181/217} show an association to A β and tau load in the brain and comparable accuracy to their CSF and PET counterparts [368-372]. Moreover, plasma NfL levels have been found to correlate with brain atrophy on structural MRI [373, 374]. Interestingly, plasma NfL, p-tau₁₈₁ and A β ratio measures are significantly altered in AD [375], and the association between plasma p-tau levels and NfL correlated most strongly with AD. The ideal screening method, however, would be a blood-based biomarker that separates AD from other dementias, while it monitors disease progression and effects of therapeutic interventions.

Future targets for AD treatment include simultaneous blood and brain microdialysis to assess BBB permeability of chemicals [376]. Methods for drug delivery that bypasses the BBB include focused ultrasound with combined intravenous injections of microbubbles⁶ in order to widen endothelial clefts and tight-junctions [377]. These microbubbles can also be used as a drug delivery tool by itself, by for instance attaching molecules to the shell [378]. There are other novel ways to administer drugs that bypass the BBB, and nanocarriers appear promising as an alternative route of administration to intranasal and intra-carotid drug delivery [379]. Moreover, nanovesicles derived from exosomes are a potential new lipid nanocarrier of genes, proteins, and drugs [380-382]. However, only exosomes isolated from brain endothelial cells were able to cross the BBB and deliver cargo into the brain [383]. Viral vector delivery systems are currently widely used for gene modification in experimental models [384], and can provide long-term expression of the transgene, especially with AAVs [385]. However, bypassing the BBB for genetic modification is currently limited to intracerebral injections, and in the future, circuit- and cell-type specific tools, – *such as enhancer-driven*

⁶ The most common type of ultrasound contrast agents are encapsulated microbubbles.

gene expression (EDGE) [386] – could be combined with novel methods to deliver therapies across the barrier.

There appears to be a long road to restoring neural circuits for the treatment of AD. For instance, neural stem cell transplants have been shown to improve cognition in mice models of AD, but no neural replacement was observed, and the grafted cells instead differentiated into astrocytes [387]. On the other hand, directly targeting the activity of brain networks might help restore memory in patients. Clinical trials that used deep brain stimulation (DBS) techniques to directly manipulate network activity in AD patients reported positive memory outcomes [388, 389]. In animals, optogenetic techniques that excite cells in the hippocampus led to an increased number of dendritic spines, which restored memory and learning [390]. This latter study is particularly interesting since despite considerable memory impairment following neuronal degeneration, the restoration of synapses could restore recall performance. This follows research that suggests that synapse protection is necessary for halting AD pathophysiology [391, 392], and suggests that memories in AD might be inaccessible rather than lost. Taken together, the experiments described above demonstrate that interventions at both the network and circuit levels have the potential to restore cellular health and circuit integrity and could thus provide new directions for restoring impaired memory in AD patients.

7. Concluding remarks

In summary, the mouse appears to successfully model several important aspects of the complex aetiology of AD in patients. The 3xTg AD mouse models A β and tau neuropathology, the two defining neuropathological hallmarks of the disease, as well as similarity in fluid biomarkers to patients across the disease continuum. Moreover, we have yielded original insights into the function of two repurposed drugs and their effect in attenuating A β and tau pathology. We would strongly argue that to develop an effective treatment for AD, the models need to be kept simple to understand the complexity of biochemical pathways that each intervention may affect. We also show that vulnerable cell-types are involved in the spread of neuropathology in AD, and that this transfer appears to be between highly interconnected regions of the brain. According to our findings, the entorhinal-hippocampal neurocircuitry appears to be strongly involved in the regulation of intraneuronal A β and in the propagation of tau proteins. We have demonstrated original results in terms of origin and spread of intraneuronal A β in the brain, prior to the formation of amyloid plaques and NFTs. Based on our findings, early intervention strategies that can promote synaptic growth and harness cellular clearance mechanisms for removal of protein aggregates could lead to an effective treatment in AD.

8. References

1. Kraepelin, E., *Psychiatrie: ein lehrbuch für studierende und ärzte*. 1910, Leipzig, Germany Johann Ambrosius Barth.
2. Kraepelin, E., *Memoirs* 1987, Berlin, Germany Springer-Verlag
3. Pardridge, W.M., *CSF, blood-brain barrier, and brain drug delivery*. *Expert Opin Drug Deliv*, 2016. **13**(7): p. 963-975.
4. Witter, M.P., *The perforant path: projections from the entorhinal cortex to the dentate gyrus*. *Prog Brain Res*, 2007: p. 43-61.
5. Alzheimer, A., et al., *An English translation of Alzheimer's 1907 paper, "Über eine eigenartige Erkrankung der Hirnrinde"*. *Clin Anat*, 1995. **8**(6): p. 429-31.
6. Crutch, S.J., R. Isaacs, and M.N. Rossor, *Some workmen can blame their tools: artistic change in an individual with Alzheimer's disease*. *Lancet*, 2001. **357**(9274): p. 2129-2133.
7. Wegmann, S., et al., *Experimental evidence for the age dependence of tau protein spread in the brain*. *Sci Adv*, 2019. **5**(6): p. eaaw6404.
8. Nathalie, P. and O. Jean-Noël, *Processing of amyloid precursor protein and amyloid peptide neurotoxicity*. *Curr Alzheimer Res*, 2008. **5**(2): p. 92-9.
9. LaFerla, F.M., K.N. Green, and S. Oddo, *Intracellular amyloid-beta in Alzheimer's disease*. *Nat Rev Neurosci*, 2007. **8**(7): p. 499-509.
10. Suh, J., et al., *Entorhinal cortex layer III input to the hippocampus is crucial for temporal association memory*. *Science*, 2011. **334**(6061): p. 1415-20.
11. Cole, S.L. and R. Vassar, *BACE1 structure and function in health and Alzheimer's disease*. *Curr Alzheimer Res*, 2008. **5**(2): p. 100-20.
12. Stockley, J.H. and C. O'Neill, *The proteins BACE1 and BACE2 and beta-secretase activity in normal and Alzheimer's disease brain*. *Biochem Soc Trans*, 2007. **35**(Pt 3): p. 574-6.
13. Postina, R., *A closer look at alpha-secretase*. *Curr Alzheimer Res*, 2008. **5**(2): p. 179-86.
14. Nilssen, E.S., et al., *Neurons and networks in the entorhinal cortex: A reappraisal of the lateral and medial entorhinal subdivisions mediating parallel cortical pathways*. *Hippocampus*, 2019. **29**(12): p. 1238-1254.
15. Steward, O. and S.A. Scoville, *Cells of origin of entorhinal cortical afferents to the hippocampus and fascia dentata of the rat*. *J Comp Neurol*, 1976. **169**(3): p. 347-70.
16. Kaether, C., C. Haass, and H. Steiner, *Assembly, trafficking and function of gamma-secretase*. *Neurodegener Dis*, 2006. **3**(4-5): p. 275-83.
17. Witter, M.P., et al., *Cortico-hippocampal communication by way of parallel parahippocampal-subicular pathways*. *Hippocampus*, 2000. **10**(4): p. 398-410.
18. Iqbal, K., et al., *Tau in Alzheimer disease and related tauopathies*. *Curr Alzheimer Res*, 2010. **7**(8): p. 656-64.
19. Graeber, M.B., *No man alone: the rediscovery of Alois Alzheimer's original cases*. *Brain Pathol*, 1999. **9**(2): p. 237-40.
20. Maurer, K., S. Volk, and H. Gerbaldo, *Auguste D and Alzheimer's disease*. *Lancet*, 1997. **349**(9064): p. 1546-9.
21. Cipriani, G., et al., *Alzheimer and his disease: a brief history*. *Neurol Sci*, 2011. **32**(2): p. 275-9.
22. Braak, H. and E. Braak, *Neuropathological staging of Alzheimer-related changes*. *Acta Neuropathol*, 1991. **82**(4): p. 239-59.
23. Thal, D.R., et al., *Phases of A beta-deposition in the human brain and its relevance for the development of AD*. *Neurology*, 2002. **58**(12): p. 1791-800.
24. Pearce, J.M.S., *Alzheimer's disease*. *J Neurol Neurosurg Psychiatry*, 2000. **68**(3): p. 348.
25. Katzman, R., *The Prevalence and Malignancy of Alzheimer Disease: A Major Killer*. *Arch Neurol*, 1976. **33**(4): p. 217-218.

26. Minati, L., et al., *Current concepts in Alzheimer's disease: a multidisciplinary review*. Am J Alzheimers Dis Other Demen, 2009. **24**(2): p. 95-121.
27. Galvin, J.E., *Prevention of Alzheimer's Disease: Lessons Learned and Applied*. J Am Geriatr Soc, 2017. **65**(10): p. 2128-2133.
28. Bekris, L.M., et al., *Genetics of Alzheimer disease*. J Geriatr Psychiatry Neurol, 2010. **23**(4): p. 213-227.
29. Serretti, A., P. Olgianti, and D. De Ronchi, *Genetics of Alzheimer's disease. A rapidly evolving field*. J Alzheimers Dis, 2007. **12**(1): p. 73-92.
30. Azevedo, F.A., et al., *Equal numbers of neuronal and nonneuronal cells make the human brain an isometrically scaled-up primate brain*. J Comp Neurol, 2009. **513**(5): p. 532-41.
31. Mott, R.T. and C.M. Hulette, *Neuropathology of Alzheimer's disease*. Neuroimaging Clin N Am, 2005. **15**(4): p. 755-65, ix.
32. Nussbaum, J.M., et al., *Prion-like behaviour and tau-dependent cytotoxicity of pyroglutamylated amyloid- β* . Nature, 2012. **485**(7400): p. 651-5.
33. Frost, B., R.L. Jacks, and M.I. Diamond, *Propagation of tau misfolding from the outside to the inside of a cell*. J Biol Chem, 2009. **284**(19): p. 12845-52.
34. Kaye, R., et al., *Conformation dependent monoclonal antibodies distinguish different replicating strains or conformers of prefibrillar A β oligomers*. Mol Neurodegener, 2010. **5**: p. 57.
35. Kfoury, N., et al., *Trans-cellular propagation of Tau aggregation by fibrillar species*. J Biol Chem, 2012. **287**(23): p. 19440-51.
36. Clavaguera, F., et al., *Transmission and spreading of tauopathy in transgenic mouse brain*. Nat Cell Biol, 2009. **11**(7): p. 909-13.
37. De Calignon, A., et al., *Propagation of tau pathology in a model of early Alzheimer's disease*. Neuron, 2012. **73**(4): p. 685-97.
38. Liu, L., et al., *Trans-synaptic spread of tau pathology in vivo*. PLoS One, 2012. **7**(2): p. e31302.
39. Lu, J.X., et al., *Molecular structure of β -amyloid fibrils in Alzheimer's disease brain tissue*. Cell, 2013. **154**(6): p. 1257-68.
40. Walker, L.C., et al., *Exogenous induction of cerebral beta-amyloidosis in betaAPP-transgenic mice*. Peptides, 2002. **23**(7): p. 1241-7.
41. Irwin, D.J., *Tauopathies as clinicopathological entities*. Parkinsonism Relat Disord, 2016. **22 Suppl 1**(0 1): p. S29-S33.
42. Kövari, E., et al., *The relationship between cerebral amyloid angiopathy and cortical microinfarcts in brain ageing and Alzheimer's disease*. Neuropathol Appl Neurobiol, 2013. **39**(5): p. 498-509.
43. Hardy, J.A. and G.A. Higgins, *Alzheimer's disease: the amyloid cascade hypothesis*. Science, 1992. **256**(5054): p. 184-5.
44. El-Agnaf, O.M., et al., *Oligomerization and toxicity of beta-amyloid-42 implicated in Alzheimer's disease*. Biochem Biophys Res Commun, 2000. **273**(3): p. 1003-7.
45. Meyer-Luehmann, M., et al., *Rapid appearance and local toxicity of amyloid-beta plaques in a mouse model of Alzheimer's disease*. Nature, 2008. **451**(7179): p. 720-4.
46. Haass, C. and D.J. Selkoe, *Soluble protein oligomers in neurodegeneration: lessons from the Alzheimer's amyloid beta-peptide*. Nat Rev Mol Cell Biol, 2007. **8**(2): p. 101-12.
47. Glabe, C., *Intracellular mechanisms of amyloid accumulation and pathogenesis in Alzheimer's disease*. J Mol Neurosci, 2001. **17**(2): p. 137-45.
48. Gouras, G.K., et al., *Intraneuronal beta-amyloid accumulation and synapse pathology in Alzheimer's disease*. Acta Neuropathol, 2010. **119**(5): p. 523-41.
49. D'Andrea, M.R., et al., *Evidence that neurones accumulating amyloid can undergo lysis to form amyloid plaques in Alzheimer's disease*. Histopathology, 2001. **38**(2): p. 120-34.
50. Gouras, G.K., et al., *Intraneuronal Abeta42 accumulation in human brain*. Am J Pathol, 2000. **156**(1): p. 15-20.

51. Gyure, K.A., et al., *Intraneuronal abeta-amyloid precedes development of amyloid plaques in Down syndrome*. Arch Pathol Lab Med, 2001. **125**(4): p. 489-92.
52. LaFerla, F.M., et al., *Neuronal cell death in Alzheimer's disease correlates with apoE uptake and intracellular Abeta stabilization*. J Clin Invest 1997. **100**(2): p. 310-320.
53. Langui, D., et al., *Subcellular topography of neuronal Abeta peptide in APPxPS1 transgenic mice*. Am J Clin Pathol 2004. **165**(5): p. 1465-1477.
54. Skovronsky, D.M., R.W. Doms, and V.M. Lee, *Detection of a novel intraneuronal pool of insoluble amyloid beta protein that accumulates with time in culture*. J Cell Biol, 1998. **141**(4): p. 1031-1039.
55. Wirths, O., et al., *Intraneuronal Abeta accumulation precedes plaque formation in beta-amyloid precursor protein and presenilin-1 double-transgenic mice*. Neurosci Lett, 2001. **306**(1-2): p. 116-20.
56. Almeida, C.G., et al., *Beta-amyloid accumulation in APP mutant neurons reduces PSD-95 and GluR1 in synapses*. Neurobiol Dis, 2005. **20**(2): p. 187-98.
57. Casas, C., et al., *Massive CA1/2 neuronal loss with intraneuronal and N-terminal truncated Abeta42 accumulation in a novel Alzheimer transgenic model*. Am J Pathol, 2004. **165**(4): p. 1289-300.
58. Moolman, D.L., et al., *Dendrite and dendritic spine alterations in Alzheimer models*. J Neurocytol, 2004. **33**(3): p. 377-87.
59. Mori, C., et al., *Intraneuronal Abeta42 accumulation in Down syndrome brain*. Amyloid, 2002. **9**(2): p. 88-102.
60. Mucke, L., et al., *High-level neuronal expression of abeta 1-42 in wild-type human amyloid protein precursor transgenic mice: synaptotoxicity without plaque formation*. J Neurosci, 2000. **20**(11): p. 4050-8.
61. Oddo, S., et al., *Triple-Transgenic Model of Alzheimer's Disease with Plaques and Tangles*. Neuron, 2003. **39**(3): p. 409-421.
62. Spires, T.L., et al., *Dendritic spine abnormalities in amyloid precursor protein transgenic mice demonstrated by gene transfer and intravital multiphoton microscopy*. J Neurosci, 2005. **25**(31): p. 7278-87.
63. Takahashi, R.H., et al., *Intraneuronal Alzheimer abeta42 accumulates in multivesicular bodies and is associated with synaptic pathology*. Am J Pathol, 2002. **161**(5): p. 1869-79.
64. Yang, A.J., et al., *Intracellular accumulation of insoluble, newly synthesized abeta1-42 in amyloid precursor protein-transfected cells that have been treated with Abeta1-42*. J Biol Chem, 1999. **274**(29): p. 20650-6.
65. Bahr, B.A., et al., *Amyloid beta protein is internalized selectively by hippocampal field CA1 and causes neurons to accumulate amyloidogenic carboxyterminal fragments of the amyloid precursor protein*. J Comp Neurol, 1998. **397**(1): p. 139-47.
66. Burdick, D., et al., *Preferential adsorption, internalization and resistance to degradation of the major isoform of the Alzheimer's amyloid peptide, A beta 1-42, in differentiated PC12 cells*. Brain Res, 1997. **746**(1-2): p. 275-84.
67. Yang, A.J., et al., *Intracellular A beta 1-42 aggregates stimulate the accumulation of stable, insoluble amyloidogenic fragments of the amyloid precursor protein in transfected cells*. J Biol Chem, 1995. **270**(24): p. 14786-92.
68. Clifford, P.M., et al., *Abeta peptides can enter the brain through a defective blood-brain barrier and bind selectively to neurons*. Brain Res, 2007. **1142**: p. 223-36.
69. Yu, C., et al., *Endocytic pathways mediating oligomeric Abeta42 neurotoxicity*. Mol Neurodegener, 2010. **5**: p. 19.
70. Chui, D.H., et al., *Transgenic mice with Alzheimer presenilin 1 mutations show accelerated neurodegeneration without amyloid plaque formation*. Nat Med, 1999. **5**(5): p. 560-4.
71. Knobloch, M., et al., *Intracellular Abeta and cognitive deficits precede beta-amyloid deposition in transgenic arcAbeta mice*. Neurobiol Aging, 2007. **28**(9): p. 1297-306.

72. Kuo, Y.M., et al., *The evolution of A beta peptide burden in the APP23 transgenic mice: implications for A beta deposition in Alzheimer disease*. Mol Med, 2001. **7**(9): p. 609-18.
73. Li, Q.X., et al., *Intracellular accumulation of detergent-soluble amyloidogenic A beta fragment of Alzheimer's disease precursor protein in the hippocampus of aged transgenic mice*. J Neurochem, 1999. **72**(6): p. 2479-87.
74. Lord, A., et al., *The Arctic Alzheimer mutation facilitates early intraneuronal Abeta aggregation and senile plaque formation in transgenic mice*. Neurobiol Aging, 2006. **27**(1): p. 67-77.
75. Oakley, H., et al., *Intraneuronal beta-amyloid aggregates, neurodegeneration, and neuron loss in transgenic mice with five familial Alzheimer's disease mutations: potential factors in amyloid plaque formation*. J Neurosci, 2006. **26**(40): p. 10129-40.
76. Oddo, S., et al., *A dynamic relationship between intracellular and extracellular pools of Abeta*. Am J Pathol, 2006. **168**(1): p. 184-94.
77. Glenner, G.G. and C.W. Wong, *Alzheimer's disease: initial report of the purification and characterization of a novel cerebrovascular amyloid protein*. Biochem Biophys Res Commun, 1984. **120**(3): p. 885-90.
78. Masters, C.L. and D.J. Selkoe, *Biochemistry of amyloid β -protein and amyloid deposits in Alzheimer disease*. Cold Spring Harb Perspect Med, 2012. **2**(6): p. a006262.
79. Dickson, D.W., *Neuropathology of non-Alzheimer degenerative disorders*. Int J Clin Exp Pathol, 2009. **3**(1): p. 1-23.
80. Dickson, T.C. and J.C. Vickers, *The morphological phenotype of beta-amyloid plaques and associated neuritic changes in Alzheimer's disease*. Neuroscience, 2001. **105**(1): p. 99-107.
81. Gomez-Isla, T., et al., *Neuropathology of Alzheimer's disease*. Handb Clin Neurol, 2008. **89**: p. 233-43.
82. Serrano-Pozo, A., et al., *Neuropathological alterations in Alzheimer disease*. Cold Spring Harb Perspect Med, 2011. **1**(1): p. a006189.
83. Spire-Jones, T.L. and B.T. Hyman, *The intersection of amyloid beta and tau at synapses in Alzheimer's disease*. Neuron, 2014. **82**(4): p. 756-771.
84. Tagliavini, F., et al., *Preamyloid deposits in the cerebral cortex of patients with Alzheimer's disease and nondemented individuals*. Neurosci Lett, 1988. **93**(2-3): p. 191-6.
85. Hansen, D.V., J.E. Hanson, and M. Sheng, *Microglia in Alzheimer's disease*. J Cell Biol, 2018. **217**(2): p. 459-472.
86. McLean, C.A., et al., *Soluble pool of Abeta amyloid as a determinant of severity of neurodegeneration in Alzheimer's disease*. Ann Neurol, 1999. **46**(6): p. 860-6.
87. McDonald, J.M., et al., *The presence of sodium dodecyl sulphate-stable Abeta dimers is strongly associated with Alzheimer-type dementia*. Brain, 2010. **133**(Pt 5): p. 1328-41.
88. Klein, W.L., *Synaptic targeting by A beta oligomers (ADDLS) as a basis for memory loss in early Alzheimer's disease*. Alzheimers Dement, 2006. **2**(1): p. 43-55.
89. Lambert, M.P., et al., *Diffusible, nonfibrillar ligands derived from Abeta1-42 are potent central nervous system neurotoxins*. Proc Natl Acad Sci U S A, 1998. **95**(11): p. 6448-53.
90. Cleary, J.P., et al., *Natural oligomers of the amyloid-beta protein specifically disrupt cognitive function*. Nat Neurosci, 2005. **8**(1): p. 79-84.
91. Shankar, G.M., et al., *Natural oligomers of the Alzheimer amyloid-beta protein induce reversible synapse loss by modulating an NMDA-type glutamate receptor-dependent signaling pathway*. J Neurosci, 2007. **27**(11): p. 2866-75.
92. Shankar, G.M., et al., *Amyloid-beta protein dimers isolated directly from Alzheimer's brains impair synaptic plasticity and memory*. Nat Med, 2008. **14**(8): p. 837-42.
93. Walsh, D.M., et al., *Naturally secreted oligomers of amyloid beta protein potently inhibit hippocampal long-term potentiation in vivo*. Nature, 2002. **416**(6880): p. 535-9.

94. Walsh, D.M., et al., *The role of cell-derived oligomers of Abeta in Alzheimer's disease and avenues for therapeutic intervention*. Biochem Soc Trans, 2005. **33**(Pt 5): p. 1087-90.
95. Rozkalne, A., B.T. Hyman, and T.L. Spire-Jones, *Calcineurin inhibition with FK506 ameliorates dendritic spine density deficits in plaque-bearing Alzheimer model mice*. Neurobiol Dis, 2011. **41**(3): p. 650-4.
96. Spire-Jones, T.L., et al., *Impaired spine stability underlies plaque-related spine loss in an Alzheimer's disease mouse model*. Am J Pathol, 2007. **171**(4): p. 1304-11.
97. Rozkalne, A., et al., *A single dose of passive immunotherapy has extended benefits on synapses and neurites in an Alzheimer's disease mouse model*. Brain Res, 2009. **1280**: p. 178-85.
98. Spire-Jones, T.L., et al., *Passive immunotherapy rapidly increases structural plasticity in a mouse model of Alzheimer disease*. Neurobiol Dis, 2009. **33**(2): p. 213-20.
99. Renner, M., et al., *Deleterious effects of amyloid beta oligomers acting as an extracellular scaffold for mGluR5*. Neuron, 2010. **66**(5): p. 739-54.
100. Braak, H., et al., *Occurrence of neuropil threads in the senile human brain and in Alzheimer's disease: a third location of paired helical filaments outside of neurofibrillary tangles and neuritic plaques*. Neurosci Lett, 1986. **65**(3): p. 351-5.
101. Braak, H., et al., *Staging of Alzheimer disease-associated neurofibrillary pathology using paraffin sections and immunocytochemistry*. Acta Neuropathol, 2006. **112**(4): p. 389-404.
102. Uchihara, T., et al., *Evolution from pretangle neurons to neurofibrillary tangles monitored by thiazin red combined with Gallyas method and double immunofluorescence*. Acta Neuropathol, 2001. **101**(6): p. 535-9.
103. Goedert, M. and M.G. Spillantini, *A century of Alzheimer's disease*. Science, 2006. **314**(5800): p. 777-81.
104. Kidd, M., *Paired helical filaments in electron microscopy of Alzheimer's disease*. Nature, 1963. **197**: p. 192-3.
105. Spillantini, M.G. and M. Goedert, *Tau pathology and neurodegeneration*. Lancet Neurol, 2013. **12**(6): p. 609-22.
106. Stoothoff, W., et al., *Differential effect of three-repeat and four-repeat tau on mitochondrial axonal transport*. J Neurochem, 2009. **111**(2): p. 417-27.
107. Arnold, S.E., et al., *The topographical and neuroanatomical distribution of neurofibrillary tangles and neuritic plaques in the cerebral cortex of patients with Alzheimer's disease*. Cereb Cortex, 1991. **1**(1): p. 103-16.
108. Wang, J.-Z., et al., *Abnormal Hyperphosphorylation of Tau: Sites, Regulation, and Molecular Mechanism of Neurofibrillary Degeneration*. J Alzheimers Dis, 2013. **33**: p. S123-S139.
109. Köpke, E., et al., *Microtubule-associated protein tau. Abnormal phosphorylation of a non-paired helical filament pool in Alzheimer disease*. J Biol Chem, 1993. **268**(32): p. 24374-84.
110. Alonso, A., et al., *Hyperphosphorylation induces self-assembly of tau into tangles of paired helical filaments/straight filaments*. Proc Natl Acad Sci U S A, 2001. **98**(12): p. 6923-8.
111. Iqbal, K., et al., *Defective brain microtubule assembly in Alzheimer's disease*. Lancet, 1986. **2**(8504): p. 421-6.
112. Ebner, A., et al., *Overexpression of tau protein inhibits kinesin-dependent trafficking of vesicles, mitochondria, and endoplasmic reticulum: implications for Alzheimer's disease*. J Cell Biol, 1998. **143**(3): p. 777-94.
113. Stamer, K., et al., *Tau blocks traffic of organelles, neurofilaments, and APP vesicles in neurons and enhances oxidative stress*. J Cell Biol, 2002. **156**(6): p. 1051-63.
114. Yang, Y., et al., *Inhibition of protein phosphatases induces transport deficits and axonopathy*. J Neurochem, 2007. **102**(3): p. 878-86.

115. Spittaels, K., et al., *Prominent axonopathy in the brain and spinal cord of transgenic mice overexpressing four-repeat human tau protein*. Am J Pathol, 1999. **155**(6): p. 2153-65.
116. Hampel, H., et al., *Alzheimer's disease biomarker-guided diagnostic workflow using the added value of six combined cerebrospinal fluid candidates: Abeta1-42, total-tau, phosphorylated-tau, NFL, neurogranin, and YKL-40*. Alzheimers Dement, 2018. **14**(4): p. 492-501.
117. Palop, J.J. and L. Mucke, *Network abnormalities and interneuron dysfunction in Alzheimer disease*. Nat Rev Neurosci, 2016. **17**(12): p. 777-792.
118. Gomez-Isla, T., et al., *Profound loss of layer II entorhinal cortex neurons occurs in very mild Alzheimer's disease*. J Neurosci, 1996. **16**(14): p. 4491-500.
119. Gallagher, M. and M.T. Koh, *Episodic memory on the path to Alzheimer's disease*. Curr Opin Neurobiol, 2011. **21**(6): p. 929-34.
120. Velayudhan, L., et al., *Entorhinal cortex thickness predicts cognitive decline in Alzheimer's disease*. J Alzheimers Dis, 2013. **33**(3): p. 755-66.
121. Giannakopoulos, P., et al., *Tangle and neuron numbers, but not amyloid load, predict cognitive status in Alzheimer's disease*. Neurology, 2003. **60**(9): p. 1495-500.
122. Price, J.L., et al., *Neuron number in the entorhinal cortex and CA1 in preclinical Alzheimer disease*. Arch Neurol, 2001. **58**(9): p. 1395-402.
123. Eichenbaum, H., A.P. Yonelinas, and C. Ranganath, *The medial temporal lobe and recognition memory*. Annu Rev Neurosci, 2007. **30**: p. 123-52.
124. Hafting, T., et al., *Microstructure of a spatial map in the entorhinal cortex*. Nature, 2005. **436**(7052): p. 801-806.
125. Sargolini, F., et al., *Conjunctive representation of position, direction, and velocity in entorhinal cortex*. Science, 2006. **312**(5774): p. 758-62.
126. Solstad, T., et al., *Representation of geometric borders in the entorhinal cortex*. Science, 2008. **322**(5909): p. 1865-8.
127. Kropff, E., et al., *Speed cells in the medial entorhinal cortex*. Nature, 2015. **523**(7561): p. 419-424.
128. Miao, C., et al., *Parvalbumin and Somatostatin Interneurons Control Different Space-Coding Networks in the Medial Entorhinal Cortex*. Cell, 2017. **171**(3): p. 507-521.e17.
129. Høydal Ø, A., et al., *Object-vector coding in the medial entorhinal cortex*. Nature, 2019. **568**(7752): p. 400-404.
130. Fyhn, M., et al., *Spatial representation in the entorhinal cortex*. Science, 2004. **305**(5688): p. 1258-64.
131. Deshmukh, S.S. and J.J. Knierim, *Representation of non-spatial and spatial information in the lateral entorhinal cortex*. Front Behav Neurosci, 2011. **5**: p. 69.
132. Tsao, A., M.B. Moser, and E.I. Moser, *Traces of experience in the lateral entorhinal cortex*. Curr Biol, 2013. **23**(5): p. 399-405.
133. Tsao, A., et al., *Integrating time from experience in the lateral entorhinal cortex*. Nature, 2018. **561**(7721): p. 57-62.
134. Montchal, M.E., Z.M. Reagh, and M.A. Yassa, *Precise temporal memories are supported by the lateral entorhinal cortex in humans*. Nat Neurosci, 2019. **22**(2): p. 284-288.
135. Witter, M.P., et al., *Architecture of the Entorhinal Cortex A Review of Entorhinal Anatomy in Rodents with Some Comparative Notes*. Front Syst Neurosci, 2017. **11**: p. 46-46.
136. Kobro-Flatmoen, A. and M.P. Witter, *Neuronal chemo-architecture of the entorhinal cortex: A comparative review*. Eur J Neurosci 2019. **50**(10): p. 3627-3662.
137. Canto, C.B., F.G. Wouterlood, and M.P. Witter, *What does the anatomical organization of the entorhinal cortex tell us?* Neural Plast, 2008. **2008**: p. 381243-381243.
138. Strange, B.A., et al., *Functional organization of the hippocampal longitudinal axis*. Nat Rev Neurosci 2014. **15**(10): p. 655-669.
139. Cisse, M., et al., *Reversing EphB2 depletion rescues cognitive functions in Alzheimer model*. Nature, 2011. **469**(7328): p. 47-52.

140. Harris, J.A., et al., *Transsynaptic progression of amyloid-beta-induced neuronal dysfunction within the entorhinal-hippocampal network*. *Neuron*, 2010. **68**(3): p. 428-41.
141. Yassa, M.A., L.T. Muftuler, and C.E. Stark, *Ultra-high-resolution microstructural diffusion tensor imaging reveals perforant path degradation in aged humans in vivo*. *Proc Natl Acad Sci U S A*, 2010. **107**(28): p. 12687-91.
142. Doan, T.P., et al., *Convergent Projections from Perirhinal and Postrhinal Cortices Suggest a Multisensory Nature of Lateral, but Not Medial, Entorhinal Cortex*. *Cell Rep*, 2019. **29**(3): p. 617-627.e7.
143. Scoville, W.B. and M. B., *Loss of recent memory after bilateral hippocampal lesions*. *J Neurol*, 1957. **20**: p. 11-21.
144. Squire, L.R., *Memory and the hippocampus: a synthesis from findings with rats, monkeys, and humans*. *Psychol Rev*, 1992. **99**(2): p. 195-231.
145. Squire, L.R., *Memory and brain*. 1987: Oxford University Press.
146. Tulving, E., *Episodic and semantic memory*, in *Organization of memory*, E. Tulving and W. Donaldson, Editors. 1972, Academic Press: Cambridge, MA. p. 381-403.
147. Bohbot, V.D., et al., *Role of the parahippocampal cortex in memory for the configuration but not the identity of objects: converging evidence from patients with selective thermal lesions and fMRI*. *Front Hum Neurosci*, 2015. **9**: p. 431-431.
148. Bohbot, V.D., et al., *Role of the parahippocampal cortex in memory for the configuration but not the identity of objects: converging evidence from patients with selective thermal lesions and fMRI*. *Front Hum Neurosci*, 2015. **9**(431).
149. Miry, O., J. Li, and L. Chen, *The Quest for the Hippocampal Memory Engram: From Theories to Experimental Evidence*. *Front Behav Neurosci*, 2021. **14**(270).
150. Kragel, J.E., et al., *Distinct cortical systems reinstate the content and context of episodic memories*. *Nat Commun*, 2021. **12**(1): p. 4444.
151. Smith, D.M. and D.A. Bulkin, *The form and function of hippocampal context representations*. *Neurosci Biobehav Rev*, 2014. **40**: p. 52-61.
152. Hainmueller, T. and M. Bartos, *Dentate gyrus circuits for encoding, retrieval and discrimination of episodic memories*. *Nat Rev Neurosci*, 2020. **21**(3): p. 153-168.
153. Pilly, P.K., M.D. Howard, and R. Bhattacharyya, *Modeling Contextual Modulation of Memory Associations in the Hippocampus*. *Front Hum Neurosci*, 2018. **12**: p. 442-442.
154. Hunsaker, M. and R. Kesner, *The operation of pattern separation and pattern completion processes associated with different attributes or domains of memory*. *Neurosci Biobehav Rev*, 2012. **37**.
155. Neunuebel, J. and J. Knierim, *CA3 Retrieves Coherent Representations from Degraded Input: Direct Evidence for CA3 Pattern Completion and Dentate Gyrus Pattern Separation*. *Neuron*, 2014. **81**: p. 416-27.
156. Yassa, M.A., et al., *Pattern separation deficits associated with increased hippocampal CA3 and dentate gyrus activity in nondemented older adults*. *Hippocampus*, 2011. **21**(9): p. 968-979.
157. Yassa, M.A. and C.E.L. Stark, *Pattern separation in the hippocampus*. *Trends Neurosci*, 2011. **34**(10): p. 515-525.
158. Lee, C.-H. and I. Lee, *Impairment of Pattern Separation of Ambiguous Scenes by Single Units in the CA3 in the Absence of the Dentate Gyrus*. *J Neurosci*, 2020. **40**(18): p. 3576.
159. Dillon, S.E., et al., *The impact of ageing reveals distinct roles for human dentate gyrus and CA3 in pattern separation and object recognition memory*. *Sci Rep*, 2017. **7**(1): p. 14069.
160. O'Reilly, K.C., J.M. Alarcon, and J. Ferbinteanu, *Relative contributions of CA3 and medial entorhinal cortex to memory in rats*. *Front Behav Neurosci*, 2014. **8**(292).
161. Siman, R., et al., *A rapid gene delivery-based mouse model for early-stage Alzheimer disease-type tauopathy*. *J Neuropathol Exp Neurol*, 2013. **72**(11): p. 1062-1071.

162. Bjorkli, C., A. Sandvig, and I. Sandvig, *Bridging the Gap Between Fluid Biomarkers for Alzheimer's Disease, Model Systems, and Patients*. Front Aging Neurosci, 2020. **12**(272).
163. Hansson, O., et al., *Association between CSF biomarkers and incipient Alzheimer's disease in patients with mild cognitive impairment: a follow-up study*. Lancet Neurol, 2006. **5**(3): p. 228-34.
164. Mattsson, N., et al., *CSF Biomarkers and Incipient Alzheimer Disease in Patients With Mild Cognitive Impairment*. JAMA, 2009. **302**(4): p. 385-393.
165. Bateman, R.J., et al., *Autosomal-dominant Alzheimer's disease: a review and proposal for the prevention of Alzheimer's disease*. Alzheimers Res Ther, 2011. **3**(1): p. 1.
166. Fleisher, A.S., et al., *Florbetapir PET analysis of amyloid- β deposition in the presenilin 1 E280A autosomal dominant Alzheimer's disease kindred: a cross-sectional study*. Lancet Neurol, 2012. **11**(12): p. 1057-65.
167. Galasko, D., et al., *High cerebrospinal fluid tau and low amyloid beta42 levels in the clinical diagnosis of Alzheimer disease and relation to apolipoprotein E genotype*. Arch Neurol, 1998. **55**(7): p. 937-45.
168. Steinerman, J.R. and L.S. Honig, *Laboratory biomarkers in Alzheimer's disease*. Curr Neurol Neurosci Rep, 2007. **7**(5): p. 381-387.
169. Sjögren, M., et al., *CSF levels of tau, beta-amyloid(1-42) and GAP-43 in frontotemporal dementia, other types of dementia and normal aging*. J Neural Transm, 2000. **107**(5): p. 563-79.
170. Palmqvist, S., N. Mattsson, and O. Hansson, *Cerebrospinal fluid analysis detects cerebral amyloid-beta accumulation earlier than positron emission tomography*. Brain, 2016. **139**(Pt 4): p. 1226-36.
171. Gordon, B.A., et al., *Tau PET in autosomal dominant Alzheimer's disease: relationship with cognition, dementia and other biomarkers*. Brain, 2019. **142**(4): p. 1063-1076.
172. Sjögren, M., et al., *Both total and phosphorylated tau are increased in Alzheimer's disease*. J Neurol Neurosurg Psychiatry, 2001. **70**(5): p. 624-30.
173. Vandermeeren, M., et al., *Detection of tau proteins in normal and Alzheimer's disease cerebrospinal fluid with a sensitive sandwich enzyme-linked immunosorbent assay*. J Neurochem, 1993. **61**(5): p. 1828-34.
174. Blennow, K., et al., *Tau protein in cerebrospinal fluid: a biochemical marker for axonal degeneration in Alzheimer disease?* Mol Chem Neuropathol, 1995. **26**(3): p. 231-45.
175. Itoh, N., et al., *Large-scale, multicenter study of cerebrospinal fluid tau protein phosphorylated at serine 199 for the antemortem diagnosis of Alzheimer's disease*. Ann Neurol, 2001. **50**(2): p. 150-6.
176. Olsson, B., et al., *CSF and blood biomarkers for the diagnosis of Alzheimer's disease: a systematic review and meta-analysis*. Lancet Neurol, 2016. **15**(7): p. 673-684.
177. Zhou, M., et al., *Entorhinal cortex: a good biomarker of mild cognitive impairment and mild Alzheimer's disease*. Rev Neurosci, 2016. **27**(2): p. 185-195.
178. Liu, P.-P., et al., *History and progress of hypotheses and clinical trials for Alzheimer's disease*. Signal Transduct Ther, 2019. **4**(1): p. 29.
179. Salloway, S.P., et al., *Advancing combination therapy for Alzheimer's disease*. Alzheimers Dement, 2020. **6**(1): p. e12073.
180. Ghezzi, L., E. Scarpini, and D. Galimberti, *Disease-modifying drugs in Alzheimer's disease*. Drug Des Devel Ther, 2013. **7**: p. 1471-1478.
181. De Felice, F.G., et al., *Abeta oligomers induce neuronal oxidative stress through an N-methyl-D-aspartate receptor-dependent mechanism that is blocked by the Alzheimer drug memantine*. J Biol Chem, 2007. **282**(15): p. 11590-601.
182. Hardingham, G.E. and H. Bading, *Synaptic versus extrasynaptic NMDA receptor signalling: implications for neurodegenerative disorders*. Nat Rev Neurosci, 2010. **11**(10): p. 682-96.
183. Xia, P., et al., *Memantine Preferentially Blocks Extrasynaptic over Synaptic NMDA Receptor Currents in Hippocampal Autapses*. J Neurosci, 2010. **30**(33): p. 11246.

184. Patel, L. and G.T. Grossberg, *Combination therapy for Alzheimer's disease*. *Drugs Aging*, 2011. **28**(7): p. 539-46.
185. Deardorff, W.J., E. Feen, and G.T. Grossberg, *The Use of Cholinesterase Inhibitors Across All Stages of Alzheimer's Disease*. *Drugs Aging*, 2015. **32**(7): p. 537-547.
186. Ametamey, S.M., et al., *PET studies of 18F-memantine in healthy volunteers*. *Nucl Med Biol*, 2002. **29**(2): p. 227-31.
187. Salabert, A.S., et al., *Radiolabeling of [18F]-fluoroethylnormemantine and initial in vivo evaluation of this innovative PET tracer for imaging the PCP sites of NMDA receptors*. *Nucl Med Biol*, 2015. **42**(8): p. 643-53.
188. Saunders, N.R., et al., *The rights and wrongs of blood-brain barrier permeability studies: a walk through 100 years of history*. *Front Neurosci*, 2014. **8**: p. 404.
189. Niewoehner, J., et al., *Increased brain penetration and potency of a therapeutic antibody using a monovalent molecular shuttle*. *Neuron*, 2014. **81**(1): p. 49-60.
190. Sevigny, J., et al., *The antibody aducanumab reduces A β plaques in Alzheimer's disease*. *Nature*, 2016. **537**(7618): p. 50-6.
191. Growdon, J.H. and S. Corkin, *Neurochemical approaches to the treatment of senile dementia*. *Proc Annu Meet Am Psychopathol Assoc*, 1980. **69**: p. 281-96.
192. Scarpini, E., P. Scheltens, and H. Feldman, *Treatment of Alzheimer's disease: current status and new perspectives*. *Lancet Neurol*, 2003. **2**(9): p. 539-47.
193. Klafki, H.W., et al., *Therapeutic approaches to Alzheimer's disease*. *Brain*, 2006. **129**(Pt 11): p. 2840-55.
194. Rogers, S.L., et al., *A 24-week, double-blind, placebo-controlled trial of donepezil in patients with Alzheimer's disease*. *Donepezil Study Group*. *Neurology*, 1998. **50**(1): p. 136-45.
195. Rösler, M., et al., *Efficacy and safety of rivastigmine in patients with Alzheimer's disease: international randomised controlled trial*. *BMJ*, 1999. **318**(7184): p. 633-8.
196. Raskind, M.A., et al., *Galantamine in AD: A 6-month randomized, placebo-controlled trial with a 6-month extension*. *The Galantamine USA-1 Study Group*. *Neurology*, 2000. **54**(12): p. 2261-8.
197. Samochocki, M., et al., *Galantamine is an allosterically potentiating ligand of neuronal nicotinic but not of muscarinic acetylcholine receptors*. *J Pharmacol Exp Ther*, 2003. **305**(3): p. 1024-36.
198. Folch, J., et al., *Current Research Therapeutic Strategies for Alzheimer's Disease Treatment*. *Neural Plast*, 2016. **2016**: p. 8501693.
199. Schenk, D., et al., *Immunization with amyloid-beta attenuates Alzheimer-disease-like pathology in the PDAPP mouse*. *Nature*, 1999. **400**(6740): p. 173-7.
200. Gilman, S., et al., *Clinical effects of Abeta immunization (AN1792) in patients with AD in an interrupted trial*. *Neurology*, 2005. **64**(9): p. 1553-62.
201. Brody, D.L. and D.M. Holtzman, *Active and passive immunotherapy for neurodegenerative disorders*. *Annu Rev Neurosci*, 2008. **31**: p. 175-93.
202. Dodart, J.C., et al., *Immunization reverses memory deficits without reducing brain Abeta burden in Alzheimer's disease model*. *Nat Neurosci*, 2002. **5**(5): p. 452-7.
203. Takashima, A., *GSK-3 is essential in the pathogenesis of Alzheimer's disease*. *J Alzheimers Dis*, 2006. **9**(3 Suppl): p. 309-17.
204. Bacskai, B.J., et al., *Imaging of amyloid-beta deposits in brains of living mice permits direct observation of clearance of plaques with immunotherapy*. *Nat Med*, 2001. **7**(3): p. 369-72.
205. Tapia-Rojas, C. and N.C. Inestrosa, *Loss of canonical Wnt signaling is involved in the pathogenesis of Alzheimer's disease*. *Neural Regen Res*, 2018. **13**(10): p. 1705-1710.
206. Caricasole, A., et al., *Induction of Dickkopf-1, a negative modulator of the Wnt pathway, is associated with neuronal degeneration in Alzheimer's brain*. *J Neurosci*, 2004. **24**(26): p. 6021-7.
207. Jia, L., J. Piña-Crespo, and Y. Li, *Restoring Wnt/ β -catenin signaling is a promising therapeutic strategy for Alzheimer's disease*. *Mol Brain*, 2019. **12**(1): p. 104.

208. Koch, J.C., et al., *ROCK inhibition in models of neurodegeneration and its potential for clinical translation*. Clin Pharmacol Ther, 2018. **189**: p. 1-21.
209. Purro, S.A., E.M. Dickins, and P.C. Salinas, *The secreted Wnt antagonist Dickkopf-1 is required for amyloid β -mediated synaptic loss*. J Neurosci, 2012. **32**(10): p. 3492-3498.
210. Elliott, C., et al., *A role for APP in Wnt signalling links synapse loss with β -amyloid production*. Transl Psychiatry, 2018. **8**(1): p. 179.
211. Congdon, E.E. and E.M. Sigurdsson, *Tau-targeting therapies for Alzheimer disease*. Nat Rev Neurol, 2018. **14**(7): p. 399-415.
212. Guo, T., et al., *Molecular and cellular mechanisms underlying the pathogenesis of Alzheimer's disease*. Mol Neurodegener, 2020. **15**(1): p. 40.
213. Yim, W.W.-Y. and N. Mizushima, *Lysosome biology in autophagy*. Cell Discovery, 2020. **6**(1): p. 6.
214. Meléndez, A. and B. Levine, *Autophagy in C. elegans*. WormBook, 2009: p. 1-26.
215. Menzies, F.M., et al., *Autophagy and Neurodegeneration: Pathogenic Mechanisms and Therapeutic Opportunities*. Neuron, 2017. **93**(5): p. 1015-1034.
216. VanGuilder, H.D., et al., *Concurrent hippocampal induction of MHC II pathway components and glial activation with advanced aging is not correlated with cognitive impairment*. J Neuroinflammation, 2011. **8**(1): p. 138.
217. Heckmann, B.L., et al., *LC3-Associated Endocytosis Facilitates beta-Amyloid Clearance and Mitigates Neurodegeneration in Murine Alzheimer's Disease*. Cell, 2019. **178**(3): p. 536-551.e14.
218. Liu, J. and L. Li, *Targeting Autophagy for the Treatment of Alzheimer's Disease: Challenges and Opportunities*. Front Mol Neurosci, 2019. **12**(203).
219. Baixauli, F., C. López-Otín, and M. Mittelbrunn, *Exosomes and Autophagy: Coordinated Mechanisms for the Maintenance of Cellular Fitness*. Front Immunol, 2014. **5**(403).
220. Finkbeiner, S., *The Autophagy Lysosomal Pathway and Neurodegeneration*. Cold Spring Harb Perspect Biol, 2020. **12**(3).
221. Kirkin, V., et al., *A role for ubiquitin in selective autophagy*. Mol Cell, 2009. **34**(3): p. 259-69.
222. Rubinsztein, D.C., *The roles of intracellular protein-degradation pathways in neurodegeneration*. Nature, 2006. **443**(7113): p. 780-6.
223. Chesser, A.S., S.M. Pritchard, and G.V. Johnson, *Tau clearance mechanisms and their possible role in the pathogenesis of Alzheimer disease*. Front Neurol, 2013. **4**: p. 122.
224. Keck, S., et al., *Proteasome inhibition by paired helical filament-tau in brains of patients with Alzheimer's disease*. J Neurochem, 2003. **85**(1): p. 115-22.
225. Nixon, R.A. and D.S. Yang, *Autophagy failure in Alzheimer's disease--locating the primary defect*. Neurobiol Dis, 2011. **43**(1): p. 38-45.
226. Rai, S., et al., *The ATG5-binding and coiled coil domains of ATG16L1 maintain autophagy and tissue homeostasis in mice independently of the WD domain required for LC3-associated phagocytosis*. Autophagy, 2019. **15**(4): p. 599-612.
227. Hamano, T., et al., *Autophagy and Tau Protein*. Int J Mol Sci, 2021. **22**(14).
228. Games, D., et al., *Alzheimer-type neuropathology in transgenic mice overexpressing V717F beta-amyloid precursor protein*. Nature, 1995. **373**(6514): p. 523-7.
229. Johnson-Wood, K., et al., *Amyloid precursor protein processing and A beta42 deposition in a transgenic mouse model of Alzheimer disease*. Proc Natl Acad Sci U S A, 1997. **94**(4): p. 1550-1555.
230. Javonillo, D.I., et al., *Systematic Phenotyping and Characterization of the 3xTg-AD Mouse Model of Alzheimer's Disease*. Front Neurosci, 2022. **15**.
231. Caroni, P., *Overexpression of growth-associated proteins in the neurons of adult transgenic mice*. J Neurosci Methods, 1997. **71**(1): p. 3-9.
232. Paxinos, G. and K.B. Franklin, *The Mouse Brain in Stereotaxic Coordinates*. 2007: Elsevier Science.

233. Szymczak, A.L., et al., *Correction of multi-gene deficiency in vivo using a single 'self-cleaving' 2A peptide-based retroviral vector*. Nat Biotechnol, 2004. **22**(5): p. 589-94.
234. Takeda, S., et al., *Novel microdialysis method to assess neuropeptides and large molecules in free-moving mouse*. J Neurosci, 2011. **186**: p. 110-9.
235. Benveniste, H. and N.H. Diemer, *Cellular reactions to implantation of a microdialysis tube in the rat hippocampus*. Acta Neuropathol, 1987. **74**(3): p. 234-8.
236. Benveniste, H., et al., *Regional cerebral glucose phosphorylation and blood flow after insertion of a microdialysis fiber through the dorsal hippocampus in the rat*. J Neurochem, 1987. **49**(3): p. 729-34.
237. A, H., et al., *In vivo brain dialysis of extracellular neurotransmitter and putative transmitter amino acids, in In vivo perfusion and release of neuroactive substances*, B. A and D.-C. R, Editors. 1985, Alan R Liss: New York. p. 473-492.
238. Drijfhout, W.J., et al., *A telemetry study on the chronic effects of microdialysis probe implantation on the activity pattern and temperature rhythm of the rat*. J Neurosci Methods, 1995. **61**(1-2): p. 191-6.
239. Meyding-Lamadé, U., et al., *A new technique: serial puncture of the cisterna magna for obtaining cerebrospinal fluid in the mouse--application in a model of herpes simplex virus encephalitis*. J Exp Anim Sci, 1996. **38**(2): p. 77-81.
240. Tricker, W.J. and D.W. Miller, *Use of osmotic agents in microdialysis studies to improve the recovery of macromolecules*. J Pharm Sci, 2003. **92**(7): p. 1419-27.
241. Liu, L., et al., *Longitudinal observation on CSF Abeta42 levels in young to middle-aged amyloid precursor protein/presenilin-1 doubly transgenic mice*. Neurobiol Dis, 2004. **17**(3): p. 516-23.
242. Liu, L. and K. Duff, *A technique for serial collection of cerebrospinal fluid from the cisterna magna in mouse*. J Vis Exp, 2008(21).
243. Ao, X. and J.A. Stenken, *Microdialysis sampling of cytokines*. Methods, 2006. **38**(4): p. 331-341.
244. Xu, Y., et al., *Quantifying blood-brain-barrier leakage using a combination of evans blue and high molecular weight FITC-Dextran*. J Neurosci Methods, 2019. **325**: p. 108349.
245. Verrees, M. and W.R. Selman, *Management of normal pressure hydrocephalus*. Am Fam Physician, 2004. **70**(6): p. 1071-8.
246. Strazielle, N. and J.F. Ghersi-Egea, *Potential Pathways for CNS Drug Delivery Across the Blood-Cerebrospinal Fluid Barrier*. Curr Pharm Des, 2016. **22**(35): p. 5463-5476.
247. Pardridge, W.M., *Drug delivery to the brain*. J Cereb Blood Flow Metab, 1997. **17**(7): p. 713-31.
248. Brightman, M.W. and T.S. Reese, *Junctions between intimately apposed cell membranes in the vertebrate brain*. J Cell Biol, 1969. **40**(3): p. 648-77.
249. Sellers, K.J., et al., *Amyloid β synaptotoxicity is Wnt-PCP dependent and blocked by fasudil*. Alzheimers Dement, 2018. **14**(3): p. 306-317.
250. Tang, B.L. and Y.C. Liou, *Novel modulators of amyloid-beta precursor protein processing*. J Neurochem, 2007. **100**(2): p. 314-23.
251. Hernandez, I., et al., *A farnesyltransferase inhibitor activates lysosomes and reduces tau pathology in mice with tauopathy*. Sci Transl Med, 2019. **11**(485): p. eaat3005.
252. Nixon, R.A., et al., *Extensive involvement of autophagy in Alzheimer disease: an immuno-electron microscopy study*. J Neuropathol Exp Neurol, 2005. **64**(2): p. 113-22.
253. Wang, Y. and E. Mandelkow, *Degradation of tau protein by autophagy and proteasomal pathways*. Biochem Soc Trans, 2012. **40**(4): p. 644-52.
254. Lim, F., et al., *FTDP-17 mutations in tau transgenic mice provoke lysosomal abnormalities and Tau filaments in forebrain*. Mol Cell Neurosci, 2001. **18**(6): p. 702-14.
255. Schaeffer, V., et al., *Stimulation of autophagy reduces neurodegeneration in a mouse model of human tauopathy*. Brain, 2012. **135**(Pt 7): p. 2169-77.

256. Siman, R., R. Cocca, and Y. Dong, *The mTOR Inhibitor Rapamycin Mitigates Perforant Pathway Neurodegeneration and Synapse Loss in a Mouse Model of Early-Stage Alzheimer-Type Tauopathy*. PLoS One, 2015. **10**(11): p. e0142340.
257. Aldrin-Kirk, P. and T. Bjorklund, *Practical Considerations for the Use of DREADD and Other Chemogenetic Receptors to Regulate Neuronal Activity in the Mammalian Brain*. Methods Mol Biol, 2019. **1937**: p. 59-87.
258. Daniels, R.W., et al., *Expression of multiple transgenes from a single construct using viral 2A peptides in Drosophila*. PLoS one, 2014. **9**(6): p. e100637-e100637.
259. Mandelkow, E.-M. and E. Mandelkow, *Biochemistry and cell biology of tau protein in neurofibrillary degeneration*. Cold Spring Harb Perspect Med, 2012. **2**(7): p. a006247-a006247.
260. Barbier, P., et al., *Role of Tau as a Microtubule-Associated Protein: Structural and Functional Aspects*. Front Aging Neurosci, 2019. **11**(204).
261. Siuda, J., S. Fujioka, and Z.K. Wszolek, *Parkinsonian syndrome in familial frontotemporal dementia*. Parkinsonism Relat Disord 2014. **20**(9): p. 957-964.
262. Hu, W., et al., *Does proteopathic tau propagate trans-synaptically in the brain?* Mol Neurodegener, 2022. **17**(1): p. 21.
263. Gomez, J.L., et al., *Chemogenetics revealed: DREADD occupancy and activation via converted clozapine*. Science, 2017. **357**(6350): p. 503-507.
264. Nagai, Y., et al., *Deschloroclozapine, a potent and selective chemogenetic actuator enables rapid neuronal and behavioral modulations in mice and monkeys*. Nat Neurosci, 2020. **23**: p. 1157–1167.
265. Armbruster, B.N., et al., *Evolving the lock to fit the key to create a family of G protein-coupled receptors potently activated by an inert ligand*. Proc Natl Acad Sci U S A, 2007. **104**(12): p. 5163-8.
266. Vardy, E., et al., *A New DREADD Facilitates the Multiplexed Chemogenetic Interrogation of Behavior*. Neuron, 2015. **86**(4): p. 936-946.
267. Stachniak, T.J., A. Ghosh, and S.M. Sternson, *Chemogenetic synaptic silencing of neural circuits localizes a hypothalamus→midbrain pathway for feeding behavior*. Neuron, 2014. **82**(4): p. 797-808.
268. Wiegert, J.S., et al., *Silencing Neurons: Tools, Applications, and Experimental Constraints*. Neuron, 2017. **95**(3): p. 504-529.
269. Jendryka, M., et al., *Pharmacokinetic and pharmacodynamic actions of clozapine-N-oxide, clozapine, and compound 21 in DREADD-based chemogenetics in mice*. Scientific reports, 2019. **9**(1): p. 4522-4522.
270. Theeuwes, F. and S.I. Yum, *Principles of the design and operation of generic osmotic pumps for the delivery of semisolid or liquid drug formulations*. Ann Biomed Eng, 1976. **4**(4): p. 343-53.
271. Jendryka, M., et al., *Pharmacokinetic and pharmacodynamic actions of clozapine-N-oxide, clozapine, and compound 21 in DREADD-based chemogenetics in mice*. Sci Rep, 2019. **9**(1): p. 4522.
272. El Haj, M. and R.P. Kessels, *Context memory in Alzheimer's disease*. Dement Geriatr Cogn Dis Extra, 2013. **3**(1): p. 342-50.
273. Chun, M.M. and E.A. Phelps, *Memory deficits for implicit contextual information in amnesic subjects with hippocampal damage*. Nat Neurosci, 1999. **2**(9): p. 844-7.
274. Julian, J.B. and C.F. Doeller, *Remapping and realignment in the human hippocampal formation predict context-dependent spatial behavior*. Nat Neurosci, 2021.
275. O'Keefe, J. and J. Dostrovsky, *The hippocampus as a spatial map. Preliminary evidence from unit activity in the freely-moving rat*. Brain Res, 1971. **34**(1): p. 171-5.
276. Alme, C.B., et al., *Place cells in the hippocampus: eleven maps for eleven rooms*. Proc Natl Acad Sci U S A, 2014. **111**(52): p. 18428-35.
277. Leutgeb, S., et al., *Distinct ensemble codes in hippocampal areas CA3 and CA1*. Science, 2004. **305**(5688): p. 1295-8.

278. Diehl, G.W., et al., *Grid and Nongrid Cells in Medial Entorhinal Cortex Represent Spatial Location and Environmental Features with Complementary Coding Schemes*. *Neuron*, 2017. **94**(1): p. 83-92.e6.
279. Fyhn, M., et al., *Hippocampal remapping and grid realignment in entorhinal cortex*. *Nature*, 2007. **446**(7132): p. 190-4.
280. Hafting, T., et al., *Microstructure of a spatial map in the entorhinal cortex*. *Nature*, 2005. **436**(7052): p. 801-6.
281. Nadasdy, Z., et al., *Context-dependent spatially periodic activity in the human entorhinal cortex*. *Proc Natl Acad Sci U S A*, 2017. **114**(17): p. E3516-e3525.
282. Treves, A., et al., *What is the mammalian dentate gyrus good for?* *Neuroscience*, 2008. **154**(4): p. 1155-72.
283. Berron, D., et al., *Strong Evidence for Pattern Separation in Human Dentate Gyrus*. *J Neurosci*, 2016. **36**(29): p. 7569-79.
284. O'Reilly, R.C. and J.L. McClelland, *Hippocampal conjunctive encoding, storage, and recall: avoiding a trade-off*. *Hippocampus*, 1994. **4**(6): p. 661-82.
285. Brock Kirwan, C., et al., *Pattern separation deficits following damage to the hippocampus*. *Neuropsychologia*, 2012. **50**(10): p. 2408-14.
286. Rolls, E.T., *The storage and recall of memories in the hippocampo-cortical system*. *Cell Tissue Res*, 2018. **373**(3): p. 577-604.
287. Jeffery, K.J., *Place cells, grid cells, attractors, and remapping*. *Neural Plast*, 2011. **2011**: p. 182602.
288. Wills, T.J., et al., *Attractor dynamics in the hippocampal representation of the local environment*. *Science (New York, N.Y.)*, 2005. **308**(5723): p. 873-876.
289. Leutgeb, J.K., et al., *Progressive Transformation of Hippocampal Neuronal Representations in "Morphed" Environments*. *Neuron*, 2005. **48**(2): p. 345-358.
290. Ennaceur, A. and K. Meliani, *A new one-trial test for neurobiological studies of memory in rats. III. Spatial vs. non-spatial working memory*. *Behav Brain Res*, 1992. **51**(1): p. 83-92.
291. Wilson, D.I., et al., *Lateral entorhinal cortex is necessary for associative but not nonassociative recognition memory*. *Hippocampus*, 2013. **23**(12): p. 1280-90.
292. Wilson, D.I., et al., *Lateral entorhinal cortex is critical for novel object-context recognition*. *Hippocampus*, 2013. **23**(5): p. 352-366.
293. Franceschini, A., et al., *Dissecting Neuronal Activation on a Brain-Wide Scale With Immediate Early Genes*. *Front Neurosci*, 2020. **14**: p. 569517-569517.
294. Corbett, B.F., et al., *Δ FosB Regulates Gene Expression and Cognitive Dysfunction in a Mouse Model of Alzheimer's Disease*. *Cell Rep*, 2017. **20**(2): p. 344-355.
295. Eckermann, K., et al., *The beta-propensity of Tau determines aggregation and synaptic loss in inducible mouse models of tauopathy*. *J Biol Chem*, 2007. **282**(43): p. 31755-65.
296. Jicha, G.A., et al., *Alz-50 and MC-1, a new monoclonal antibody raised to paired helical filaments, recognize conformational epitopes on recombinant tau*. *J Neurosci Res*, 1997. **48**(2): p. 128-32.
297. Jicha, G.A., et al., *A conformation- and phosphorylation-dependent antibody recognizing the paired helical filaments of Alzheimer's disease*. *J Neurochem*, 1997. **69**(5): p. 2087-95.
298. Tanemura, K., et al., *Formation of tau inclusions in knock-in mice with familial Alzheimer disease (FAD) mutation of presenilin 1 (PS1)*. *J Biol Chem*, 2006. **281**(8): p. 5037-41.
299. Goedert, M., D.S. Eisenberg, and R.A. Crowther, *Propagation of Tau Aggregates and Neurodegeneration*. *Annu Rev Neurosci*, 2017. **40**: p. 189-210.
300. Kerényi, L. and F. Gallyas, *[Errors in quantitative estimations on agar electrophoresis using silver stain]*. *Clin Chim Acta*, 1973. **47**(3): p. 425-36.
301. Braak, H., et al., *Silver impregnation of Alzheimer's neurofibrillary changes counterstained for basophilic material and lipofuscin pigment*. *Stain Technol*, 1988. **63**(4): p. 197-200.

302. D'Andrea, M.R., et al., *The use of formic acid to embellish amyloid plaque detection in Alzheimer's disease tissues misguides key observations*. *Neurosci Lett*, 2003. **342**(1-2): p. 114-8.
303. Ohyagi, Y., et al., *Intraneuronal amyloid beta42 enhanced by heating but counteracted by formic acid*. *J Neurosci Methods*, 2007. **159**(1): p. 134-8.
304. Murakami, K., *Conformation-specific antibodies to target amyloid β oligomers and their application to immunotherapy for Alzheimer's disease*. *Biosci Biotechnol Biochem*, 2014. **78**(8): p. 1293-305.
305. D'Andrea, M.R. and R.G. Nagele, *MAP-2 immunolabeling can distinguish diffuse from dense-core amyloid plaques in brains with Alzheimer's disease*. *Biotech Histochem*, 2002. **77**(2): p. 95-103.
306. Drummond, E. and T. Wisniewski, *Alzheimer's disease: experimental models and reality*. *Acta neuropathologica*, 2017. **133**(2): p. 155-175.
307. Key, D., *Environmental Enrichment Options for Laboratory Rats and Mice*. *Lab Animal*, 2004. **33**(2): p. 39-44.
308. Lydersen, S., *Statistical power: Before, but not after!* *Tidsskr Nor Laegeforen*, 2019. **139**(2).
309. Zahs, K.R. and K.H. Ashe, *'Too much good news' – are Alzheimer mouse models trying to tell us how to prevent, not cure, Alzheimer's disease?* *Trends Neurosci*, 2010. **33**(8): p. 381-389.
310. Onos, K.D., et al., *Enhancing face validity of mouse models of Alzheimer's disease with natural genetic variation*. *PLOS Genetics*, 2019. **15**(5): p. e1008155.
311. Singh, A.K., et al., *Role of TREM2 in Alzheimer's Disease and its Consequences on β - Amyloid, Tau and Neurofibrillary Tangles*. *Curr Alzheimer Res*, 2019. **16**(13): p. 1216-1229.
312. Matarin, M., et al., *A Genome-wide Gene-Expression Analysis and Database in Transgenic Mice during Development of Amyloid or Tau Pathology*. *Cell Rep*, 2015. **10**(4): p. 633-644.
313. Grossman, M., et al., *Cerebrospinal fluid profile in frontotemporal dementia and Alzheimer's disease*. *Ann Neurol*, 2005. **57**(5): p. 721-9.
314. Aguilar, B.J., Y. Zhu, and Q. Lu, *Rho GTPases as therapeutic targets in Alzheimer's disease*. *Alzheimers Res Ther*, 2017. **9**(1): p. 97.
315. Song, Y., et al., *Rho kinase inhibitor fasudil protects against β -amyloid-induced hippocampal neurodegeneration in rats*. *CNS Neurosci Ther*, 2013. **19**(8): p. 603-10.
316. Yu, J.Z., et al., *Multitarget Therapeutic Effect of Fasudil in APP/PS1transgenic Mice*. *CNS Neurol Disord Drug Targets*, 2017. **16**(2): p. 199-209.
317. Guo, M.-F., et al., *Fasudil reduces β -amyloid levels and neuronal apoptosis in APP/PS1 transgenic mice via inhibition of the Nogo-A/NgR/RhoA signaling axis*. *J Integr Neurosci*, 2020. **19**(4): p. 651-662.
318. Boland, B., et al., *Autophagy induction and autophagosome clearance in neurons: relationship to autophagic pathology in Alzheimer's disease*. *J Neurosci*, 2008. **28**(27): p. 6926-37.
319. Herskowitz, J.H., et al., *Pharmacologic inhibition of ROCK2 suppresses amyloid- β production in an Alzheimer's disease mouse model*. *J Neurosci*, 2013. **33**(49): p. 19086-98.
320. Bauer, P.O., et al., *Inhibition of Rho kinases enhances the degradation of mutant huntingtin*. *J Biol Chem*, 2009. **284**(19): p. 13153-64.
321. Koch, J.C., et al., *ROCK2 is a major regulator of axonal degeneration, neuronal death and axonal regeneration in the CNS*. *Cell Death Dis*, 2014. **5**(5): p. e1225.
322. Lingor, P., et al., *ROCK-ALS: Protocol for a Randomized, Placebo-Controlled, Double-Blind Phase IIa Trial of Safety, Tolerability and Efficacy of the Rho Kinase (ROCK) Inhibitor Fasudil in Amyotrophic Lateral Sclerosis*. *Front Neurol*, 2019. **10**: p. 293.
323. Tramutola, A., et al., *Alteration of mTOR signaling occurs early in the progression of Alzheimer disease (AD): analysis of brain from subjects with pre-clinical AD, amnesic mild cognitive impairment and late-stage AD*. *J Neurochem*, 2015. **133**(5): p. 739-49.

324. Weber, A.J. and J.H. Herskowitz, *Perspectives on ROCK2 as a Therapeutic Target for Alzheimer's Disease*. Front Cell Neurosci, 2021. **15**: p. 636017-636017.
325. Niessner, H., et al., *The Farnesyl Transferase Inhibitor Lonafarnib Inhibits mTOR Signaling and Enforces Sorafenib-Induced Apoptosis in Melanoma Cells*. J Invest Dermatol 2011. **131**(2): p. 468-479.
326. Prusiner, S.B., *Some speculations about prions, amyloid, and Alzheimer's disease*. N Engl J Med, 1984. **310**(10): p. 661-3.
327. Peng, C., J.Q. Trojanowski, and V.M. Lee, *Protein transmission in neurodegenerative disease*. Nat Rev Neurol, 2020. **16**(4): p. 199-212.
328. Meisl, G., et al., *In vivo rate-determining steps of tau seed accumulation in Alzheimer's disease*. Sci Adv. **7**(44): p. eabh1448.
329. Walker, L.C., *Prion-like mechanisms in Alzheimer disease*. Handb Clin Neurol, 2018. **153**: p. 303-319.
330. Kane, M.D., et al., *Evidence for seeding of beta -amyloid by intracerebral infusion of Alzheimer brain extracts in beta -amyloid precursor protein-transgenic mice*. J Neurosci, 2000. **20**(10): p. 3606-11.
331. Holmes, B.B., et al., *Proteopathic tau seeding predicts tauopathy in vivo*. Proc Natl Acad Sci U S A, 2014. **111**(41): p. E4376-85.
332. Clavaguera, F., et al., *Invited review: Prion-like transmission and spreading of tau pathology*. Neuropathol Appl Neurobiol, 2015. **41**(1): p. 47-58.
333. Robert, A., M. Schöll, and T. Vogels, *Tau Seeding Mouse Models with Patient Brain-Derived Aggregates*. Int J Mol Sci, 2021. **22**.
334. Takeda, S., et al., *Seed-competent high-molecular-weight tau species accumulates in the cerebrospinal fluid of Alzheimer's disease mouse model and human patients*. Ann Neurol, 2016. **80**(3): p. 355-67.
335. Brettschneider, J., et al., *Spreading of pathology in neurodegenerative diseases: a focus on human studies*. Nat Rev Neurosci, 2015. **16**(2): p. 109-20.
336. Delpech, J.-C., et al., *Wolframin-1-expressing neurons in the entorhinal cortex propagate tau to CA1 neurons and impair hippocampal memory in mice*. Sci Transl Med, 2021. **13**(611): p. eabe8455.
337. Wegmann, S., et al., *Removing endogenous tau does not prevent tau propagation yet reduces its neurotoxicity*. EMBO J, 2015. **34**(24): p. 3028-41.
338. Wang, Y., et al., *The release and trans-synaptic transmission of Tau via exosomes*. Mol Neurodegener, 2017. **12**(1): p. 5.
339. Gibbons, G.S., V.M.Y. Lee, and J.Q. Trojanowski, *Mechanisms of Cell-to-Cell Transmission of Pathological Tau: A Review*. JAMA Neurol, 2019. **76**(1): p. 101-108.
340. Stancu, I.C., et al., *Templated misfolding of Tau by prion-like seeding along neuronal connections impairs neuronal network function and associated behavioral outcomes in Tau transgenic mice*. Acta Neuropathol, 2015. **129**(6): p. 875-94.
341. Vogel, J.W., et al., *Spread of pathological tau proteins through communicating neurons in human Alzheimer's disease*. Nat Commun, 2020. **11**(1): p. 2612.
342. Iba, M., et al., *Synthetic tau fibrils mediate transmission of neurofibrillary tangles in a transgenic mouse model of Alzheimer's-like tauopathy*. J Neurosci, 2013. **33**(3): p. 1024-37.
343. Franzmeier, N., et al., *Functional brain architecture is associated with the rate of tau accumulation in Alzheimer's disease*. Nat Commun, 2020. **11**(1): p. 347.
344. Ahmed, Z., et al., *A novel in vivo model of tau propagation with rapid and progressive neurofibrillary tangle pathology: the pattern of spread is determined by connectivity, not proximity*. Acta Neuropathol, 2014. **127**(5): p. 667-83.
345. Calafate, S., et al., *Synaptic Contacts Enhance Cell-to-Cell Tau Pathology Propagation*. Cell Rep, 2015. **11**(8): p. 1176-83.
346. Fu, H., et al., *A tau homeostasis signature is linked with the cellular and regional vulnerability of excitatory neurons to tau pathology*. Nat Neurosci, 2019. **22**(1): p. 47-56.

347. Nath, S., et al., *Spreading of neurodegenerative pathology via neuron-to-neuron transmission of β -amyloid*. J Neurosci, 2012. **32**(26): p. 8767-77.
348. Domert, J., et al., *Spreading of amyloid- β peptides via neuritic cell-to-cell transfer is dependent on insufficient cellular clearance*. Neurobiol Dis, 2014. **65**: p. 82-92.
349. Adams, J.N., et al., *Cortical tau deposition follows patterns of entorhinal functional connectivity in aging*. Elife, 2019. **8**.
350. Palmqvist, S., et al., *Earliest accumulation of β -amyloid occurs within the default-mode network and concurrently affects brain connectivity*. Nat Commun, 2017. **8**(1): p. 1214.
351. Whittington, A., D.J. Sharp, and R.N. Gunn, *Spatiotemporal Distribution of β -Amyloid in Alzheimer Disease Is the Result of Heterogeneous Regional Carrying Capacities*. J Nucl Med, 2018. **59**(5): p. 822-827.
352. Buxbaum, J.D., et al., *Alzheimer amyloid protein precursor in the rat hippocampus: transport and processing through the perforant path*. J Neurosci, 1998. **18**(23): p. 9629-37.
353. Harris, J.A., et al., *Transsynaptic progression of amyloid- β -induced neuronal dysfunction within the entorhinal-hippocampal network*. Neuron, 2010. **68**(3): p. 428-41.
354. Kobre-Flatmoen, A., A. Nagelhus, and M.P. Witter, *Reelin-immunoreactive neurons in entorhinal cortex layer II selectively express intracellular amyloid in early Alzheimer's disease*. Neurobiol Dis, 2016. **93**: p. 172-183.
355. Furman, J.L., et al., *Widespread tau seeding activity at early Braak stages*. Acta Neuropathol, 2017. **133**(1): p. 91-100.
356. Hu, W., et al., *Hyperphosphorylation determines both the spread and the morphology of tau pathology*. Alzheimers Dement, 2016. **12**(10): p. 1066-1077.
357. Guo, J.L., et al., *Unique pathological tau conformers from Alzheimer's brains transmit tau pathology in nontransgenic mice*. J Exp Med, 2016. **213**(12): p. 2635-2654.
358. Cornblath, E.J., et al., *Computational modeling of tau pathology spread reveals patterns of regional vulnerability and the impact of a genetic risk factor*. Sci Adv, 2021. **7**(24): p. eabg6677.
359. Detrez, J.R., et al., *Regional vulnerability and spreading of hyperphosphorylated tau in seeded mouse brain*. Neurobiol Dis, 2019. **127**: p. 398-409.
360. Braak, H. and K. Del Tredici, *From the Entorhinal Region via the Prosubiculum to the Dentate Fascia: Alzheimer Disease-Related Neurofibrillary Changes in the Temporal Allocortex*. J Neuropathol Exp Neurol, 2020. **79**(2): p. 163-175.
361. Braak, H. and E. Braak, *Frequency of stages of Alzheimer-related lesions in different age categories*. Neurobiol Aging, 1997. **18**(4): p. 351-7.
362. Maass, A., et al., *Comparison of multiple tau-PET measures as biomarkers in aging and Alzheimer's disease*. Neuroimage, 2017. **157**: p. 448-463.
363. Janelidze, S., et al., *Head-to-Head Comparison of 8 Plasma Amyloid- β 42/40 Assays in Alzheimer Disease*. JAMA Neurology, 2021. **78**(11): p. 1375-1382.
364. Fandos, N., et al., *Plasma amyloid β 42/40 ratios as biomarkers for amyloid β cerebral deposition in cognitively normal individuals*. Alzheimers Dement 2017. **8**: p. 179-187.
365. Pérez-Grijalba, V., et al., *Plasma A β 42/40 Ratio Detects Early Stages of Alzheimer's Disease and Correlates with CSF and Neuroimaging Biomarkers in the AB255 Study*. J Prev Alzheimers Dis, 2019. **6**(1): p. 34-41.
366. Fiandaca, M.S., et al., *Identification of preclinical Alzheimer's disease by a profile of pathogenic proteins in neurally derived blood exosomes: A case-control study*. Alzheimers Dement, 2015. **11**(6): p. 600-7.e1.
367. Nakamura, A., et al., *High performance plasma amyloid- β biomarkers for Alzheimer's disease*. Nature, 2018. **554**(7691): p. 249-254.
368. Naveed, M., et al., *Plasma Biomarkers: Potent Screeners of Alzheimer's Disease*. Am J Alzheimers Dis Other Demen, 2019. **34**(5): p. 290-301.
369. Janelidze, S., et al., *Plasma P-tau181 in Alzheimer's disease: relationship to other biomarkers, differential diagnosis, neuropathology and longitudinal progression to Alzheimer's dementia*. Nat Med, 2020. **26**(3): p. 379-386.

370. Karikari, T.K., et al., *Blood phosphorylated tau 181 as a biomarker for Alzheimer's disease: a diagnostic performance and prediction modelling study using data from four prospective cohorts*. *Lancet Neurol*, 2020. **19**(5): p. 422-433.
371. Palmqvist, S., et al., *Discriminative Accuracy of Plasma Phospho-tau217 for Alzheimer Disease vs Other Neurodegenerative Disorders*. *Jama*, 2020. **324**(8): p. 772-781.
372. Thijssen, E.H., et al., *Diagnostic value of plasma phosphorylated tau181 in Alzheimer's disease and frontotemporal lobar degeneration*. *Nat Med*, 2020. **26**(3): p. 387-397.
373. Mattsson, N., et al., *Association of Plasma Neurofilament Light With Neurodegeneration in Patients With Alzheimer Disease*. *JAMA Neurol*, 2017. **74**(5): p. 557-566.
374. Pereira, J.B., E. Westman, and O. Hansson, *Association between cerebrospinal fluid and plasma neurodegeneration biomarkers with brain atrophy in Alzheimer's disease*. *Neurobiol Aging*, 2017. **58**: p. 14-29.
375. Thijssen, E.H., et al., *Diagnostic value of plasma phosphorylated tau181 in Alzheimer's disease and frontotemporal lobar degeneration*. *Nature Medicine*, 2020. **26**(3): p. 387-397.
376. Umezu, T., et al., *Simultaneous blood and brain microdialysis in a free-moving mouse to test blood-brain barrier permeability of chemicals*. *Toxicol Rep*, 2020. **7**: p. 1542-1550.
377. Couture, O., et al., *Review of ultrasound mediated drug delivery for cancer treatment: updates from pre-clinical studies*. *Transl Cancer Res* 2014. **3**(5): p. 494-511.
378. De Temmerman, M.L., et al., *mRNA-Lipoplex loaded microbubble contrast agents for ultrasound-assisted transfection of dendritic cells*. *Biomaterials*, 2011. **32**(34): p. 9128-35.
379. Pandey, P.K., A.K. Sharma, and U. Gupta, *Blood brain barrier: An overview on strategies in drug delivery, realistic in vitro modeling and in vivo live tracking*. *Tissue Barriers*, 2015. **4**(1): p. e1129476-e1129476.
380. El-Andaloussi, S., et al., *Exosome-mediated delivery of siRNA in vitro and in vivo*. *Nat Protoc*, 2012. **7**(12): p. 2112-26.
381. van Dommel, S.M., et al., *Microvesicles and exosomes: opportunities for cell-derived membrane vesicles in drug delivery*. *J Control Release*, 2012. **161**(2): p. 635-44.
382. Sun, D., et al., *Exosomes are endogenous nanoparticles that can deliver biological information between cells*. *Adv Drug Deliv Rev*, 2013. **65**(3): p. 342-7.
383. Yang, T., et al., *Delivery of Small Interfering RNA to Inhibit Vascular Endothelial Growth Factor in Zebrafish Using Natural Brain Endothelia Cell-Secreted Exosome Nanovesicles for the Treatment of Brain Cancer*. *AAPS J*, 2017. **19**(2): p. 475-486.
384. Cummings, J., et al., *Alzheimer's disease drug development pipeline: 2020*. *Alzheimers Dement*, 2020. **6**(1): p. e12050.
385. Fu, H. and D.M. McCarty, *Crossing the blood-brain-barrier with viral vectors*. *Curr Opin Virol*, 2016. **21**: p. 87-92.
386. Blankvoort, S., L.A.L. Descamps, and C. Kentros, *Enhancer-Driven Gene Expression (EDGE) enables the generation of cell type specific tools for the analysis of neural circuits*. *Neurosci Res*, 2020. **152**: p. 78-86.
387. Blurton-Jones, M., et al., *Neural stem cells improve cognition via BDNF in a transgenic model of Alzheimer disease*. *Proc Natl Acad Sci U S A*, 2009. **106**(32): p. 13594-9.
388. Laxton, A.W., et al., *A phase I trial of deep brain stimulation of memory circuits in Alzheimer's disease*. *Ann Neurol*, 2010. **68**(4): p. 521-34.
389. Kuhn, J., et al., *Deep Brain Stimulation of the Nucleus Basalis of Meynert in Early Stage of Alzheimer's Dementia*. *Brain Stimul*, 2015. **8**(4): p. 838-9.
390. Roy, D.S., et al., *Memory retrieval by activating engram cells in mouse models of early Alzheimer's disease*. *Nature*, 2016. **531**(7595): p. 508-12.
391. Chami, M. and F. Checler, *Alterations of the Endoplasmic Reticulum (ER) Calcium Signaling Molecular Components in Alzheimer's Disease*. *Cells*, 2020. **9**(12).

392. Del Prete, D., F. Checler, and M. Chami, *Ryanodine receptors: physiological function and deregulation in Alzheimer disease*. *Mol Neurodegener*, 2014. **9**(1): p. 21.
393. Bjorkli, C., K. Hovde, and B. Monterotti, *Nissl (Cresyl Violet) staining*. protocols.io 2019.
394. Bjorkli, C. and M.J. Lagartos-Donate, *Gallyas-silver stain*. protocols.io, 2022.
395. Bjorkli, C., *Peroxidase/DAB protocol*. protocols.io, 2022.

Supplementary material

Supplementary Table 1: Key resources

| Reagent type (species) or resource | Designation | Information | Identifiers/reference |
|--|--|--|---|
| Strain, strain background (<i>Mus musculus</i>) | 3xTg AD | B6;129- Psen1 ^{tm1MpmTg} (APPSwe,tauP301L)1Lfa/Mmjax | MMRRC Strain #034830-JAX; RRID: MMRRC_034830-MU; PMID: 12895417 |
| Strain, strain background (<i>Mus musculus</i>) | APP/PS1 | B6.Cg-Tg(Thy1-APPSw,Thy1-PSEN1*L166P)21Jckr | MGI, Cat# 5313530; RRID: MGI:5313530; PMID: 16906128 |
| Strain, strain background (<i>Mus musculus</i>) | B6129 | B6129SF2/J | Strain #:101045; RRID: IMSR_JAX:101045 |
| Genetic reagent (virus) | AAV-CBA-GFP-2A-P301L-Tau (serotype 8) | Viral Vector Core at Kavli Institute for Systems Neuroscience; contact Dr Nair, rajeevkumar.r.nair@ntnu.no | Gifted by Bradley Hyman's lab, Harvard Medical School; PMID: 31249873 |
| Genetic reagent (virus) | AAV-CMV-GFP (serotype 8) | Viral Vector Core at Kavli Institute for Systems Neuroscience; contact see above | Agilent Technologies Cat# 240071 |
| Genetic reagent (virus) | AAV-CaMKII-hM4D _{mCherry} (serotypes 1/2 and 8) | Viral Vector Core at Kavli Institute for Systems Neuroscience; contact see above | RRID: Addgene_114469; RRID: Addgene_161576 |
| Genetic reagent (virus) | AAV-CaMKII-mCherry | Viral Vector Core at Kavli Institute for Systems | RRID: Addgene_114469 |

| | | | |
|----------|--|---|--|
| | (serotypes 1/2 and 8) | Neuroscience; contact see above | |
| Antibody | Mouse anti-A β (McSA1)* | Targets the N-terminal amino acids 1-12 of human A β | MediMabs Cat# MM-0015-1P, RRID: AB_1807985 |
| Antibody | Anti-A β_{42} (rabbit polyclonal)* | A β_{42} (pre-oligomers) | Tecan (IBL) Cat# JP28051, RRID: AB_2341462 |
| Antibody | Anti-Iba1 (mouse monoclonal) | Ionized calcium binding adaptor molecule 1 (Iba1) | Abcam Cat# ab15690, RRID: AB_2224403 |
| Antibody | Anti-oligomer A11 (rabbit polyclonal) | Soluble A β_{40} /oligomeric A β_{42} (pre-fibrils) | Thermo Fisher Scientific Cat# AHB0052, RRID: AB_2536236 |
| Antibody | Anti-amyloid fibrils OC (rabbit polyclonal)* | Amyloid fibrils/fibrillar oligomers (protofibrils) | Millipore Cat# AB2286, RRID: AB_1977024 |
| Antibody | Anti-mCherry (mouse monoclonal) | mCherry fluorescent protein | Clontech Cat# 632543 |
| Antibody | Anti-RFP (rat monoclonal) | Red fluorescent protein | Fitzgerald Industries International Cat# 10R-6753, RRID: AB_11200675 |
| Antibody | Anti-cFos (mouse monoclonal) | Immediate-early gene cFos | Abcam Cat# ab208942, RRID: AB_2747772 |
| Antibody | Anti-p44/42 MAP kinase (rabbit polyclonal) | Phospho-p44/42 MAPK (Erk1/2) | Cell Signaling Technology Cat# 9101, RRID: AB_331646 |

| | | | |
|----------|---|--|---|
| Antibody | Anti-reelin (mouse monoclonal) | 164-496 mReelin, clone G10 | Millipore Cat# MAB5364, RRID: AB_2179313 |
| Antibody | Anti-phospho-tau AT8 (mouse monoclonal) | Tau phosphorylated at serine 202 and threonine 205 | Thermo Fisher Scientific Cat# MN1020, RRID: AB_223647 |
| Antibody | Anti-tau HT7 (mouse monoclonal) | Recognized tau ₁₅₉₋₁₆₃ and does not cross-react with murine tau | Thermo Fisher Scientific Cat# MN1000, RRID: AB_2314654; PMID: 1729400 |
| Antibody | Anti-tau MC1 (mouse monoclonal) | Conformation specific, detects misfolded tau relevant to tauopathy | Gifted by Peter Davies, Department of Pathology, Albert Einstein College of Medicine |
| Antibody | Anti-GFP (chicken polyclonal) | Green fluorescent protein | Abcam Cat# ab13970, RRID: AB_300798 |
| Antibody | Anti-TREM2 (rabbit monoclonal) | TREM2 receptor | Thermo Fisher Scientific Cat# MA5-30971, RRID: AB_2786636 |
| Antibody | Anti-MAP2 (rabbit monoclonal) | Microtubule-associated protein 2 | Abcam Cat# ab183830, RRID: AB_2895301; PMID: 12083391 |
| Antibody | Anti-LAMP1 (rabbit polyclonal) | Lysosomal associated membrane protein 1 | Sigma-Aldrich Cat# L1418, RRID: AB_477157 |

| | | | |
|-------------------------|-------------------------------------|----------------------|---|
| Antibody | Anti-NeuN (rabbit monoclonal) | Neuronal labelling | Abcam Cat# ab177487, RRID: AB_2532109 |
| Antibody | Goat anti-mouse IgG (AF 657) | Secondary antibody | Thermo Fisher Scientific Cat# A-21235, RRID: AB_2535804 |
| Antibody | Goat anti-mouse IgG (AF 546) | Secondary antibody | Thermo Fisher Scientific Cat# A-11030, RRID: AB_2534089 |
| Antibody | Goat anti-mouse IgG (AF 488) | Secondary antibody | Thermo Fisher Scientific Cat# A28175, RRID: AB_2536161 |
| Antibody | Goat anti-chicken IgY (AF 488) | Secondary antibody | Thermo Fisher Scientific Cat# A-11039, RRID: AB_2534096 |
| Antibody | Goat anti-rabbit IgG (AF 488) | Secondary antibody | Molecular Probes Cat# A-11008, RRID: AB_143165 |
| Antibody | Goat anti-rabbit IgG (AF 546) | Secondary antibody | Thermo Fisher Scientific Cat# A-11035, RRID: AB_2534093 |
| Antibody | Goat anti-rabbit IgG (H+L) (AF 635) | Secondary antibody | Thermo Fisher Scientific Cat# A-31577, RRID: AB_2536187 |
| Chemical compound, drug | Fasudil | Rho kinase inhibitor | Selleck Chemicals Cat# S1573; PMID: 29055813 |

| | | | |
|-------------------------|---|---|--|
| Chemical compound, drug | Lonafarnib | Farnesyltransferase inhibitor with antitumor activity | Cayman Chemical Cat# CAY11746-1 mg; PMID: 30918111 |
| Chemical compound, drug | Deschloroclozapine | Muscarinic DREADDs agonist | MedChemExpress Cat# HY-42110; PMID: 32632286 |
| Chemical compound, drug | DAPI (4',6-Diamidino-2-Phenylindole, Dihydrochloride) | Nuclear and chromosome counterstain | Thermo Fisher Scientific Cat# D1306, RRID: AB_2629482 |
| Chemical compound, drug | Nissl (cresyl violet) | RNA labelling | See Bjorkli et al. (2019) ⁷ for chemicals and protocol |
| Chemical compound, drug | Gallyas-silver staining | Modified silver impregnation of NFTs | See Bjorkli & Lagartos-Donate (2022) ⁸ for chemicals and protocol |
| Chemical compound, drug | DAB | Chromogen for detecting antibodies | See Bjorkli (2022) ⁹ for chemicals and protocol |
| Software | GraphPad Prism, version 9 | Statistics and data visualization software | |
| Software | Zeiss ZEN lite | Microscope software | |
| Software | Ilastik | Cell counting software | PMID: 31570887 |
| Software | ANY-maze – Stoelting Co. | Video tracking software | |

*Labels amyloid plaques

⁷ 393. Bjorkli, C., K. Hovde, and B. Monterotti, *Nissl (Cresyl Violet) staining*. protocols.io 2019.

⁸ 394. Bjorkli, C. and M.J. Lagartos-Donate, *Gallyas-silver stain*. protocols.io, 2022.

⁹ 395. Bjorkli, C., *Peroxidase/DAB protocol*. Ibid.

PAPERS I – V

Paper I



Bridging the Gap Between Fluid Biomarkers for Alzheimer's Disease, Model Systems, and Patients

Christiana Bjorkli^{1*}, Axel Sandvig^{1,2,3} and Ioanna Sandvig¹

¹ Sandvig Group, Department of Neuromedicine and Movement Science, Faculty of Medicine and Health Sciences, Norwegian University of Science and Technology, Trondheim, Norway, ² Institute of Neuromedicine and Movement Science, Department of Neurology, St. Olavs Hospital, Trondheim, Norway, ³ Department of Pharmacology and Clinical Neurosciences, Division of Neuro, Head, and Neck, University Hospital of Umeå, Umeå, Sweden

Alzheimer's disease (AD) is a debilitating neurodegenerative disease characterized by the accumulation of two proteins in fibrillar form: amyloid- β (A β) and tau. Despite decades of intensive research, we cannot yet pinpoint the exact cause of the disease or unequivocally determine the exact mechanism(s) underlying its progression. This confounds early diagnosis and treatment of the disease. Cerebrospinal fluid (CSF) biomarkers, which can reveal ongoing biochemical changes in the brain, can help monitor developing AD pathology prior to clinical diagnosis. Here we review preclinical and clinical investigations of commonly used biomarkers in animals and patients with AD, which can bridge translation from model systems into the clinic. The core AD biomarkers have been found to translate well across species, whereas biomarkers of neuroinflammation translate to a lesser extent. Nevertheless, there is no absolute equivalence between biomarkers in human AD patients and those examined in preclinical models in terms of revealing key pathological hallmarks of the disease. In this review, we provide an overview of current but also novel AD biomarkers and how they relate to key constituents of the pathological cascade, highlighting confounding factors and pitfalls in interpretation, and also provide recommendations for standardized procedures during sample collection to enhance the translational validity of preclinical AD models.

OPEN ACCESS

Edited by:

Jiehui Jiang,
Shanghai University, China

Reviewed by:

Parnetti Lucilla,
University of Perugia, Italy
Ville Leinonen,
University of Eastern Finland, Finland

*Correspondence:

Christiana Bjorkli
christiana.bjorkli@ntnu.no

Received: 31 May 2020

Accepted: 06 August 2020

Published: 02 September 2020

Citation:

Bjorkli C, Sandvig A and Sandvig I
(2020) Bridging the Gap Between
Fluid Biomarkers for Alzheimer's
Disease, Model Systems,
and Patients.
Front. Aging Neurosci. 12:272.
doi: 10.3389/fnagi.2020.00272

Keywords: Alzheimer's disease, translational research, biomarkers, cerebrospinal fluid, screening tools

INTRODUCTION

Due to an increasingly elderly population, patients with Alzheimer's disease (AD) constitute a growing public health problem, thus developing methods for early diagnosis of the disease will become pertinent as there of yet exists no cure. The disease typically manifests through a progressive decline in cognitive and behavioral functions that severely impact the ability of AD patients to independently perform daily tasks. As a result, the associated socioeconomic cost and burden to the healthcare system are very high, with annual healthcare expenditure exceeding billions of dollars. Based on the early findings by Alzheimer et al. (1995), we now know that the neuropathological hallmarks of AD include intracellular neurofibrillary tangles (NFTs) composed of misfolded tau protein, and extracellular amyloid plaques comprising aggregated amyloid- β (A β). The pathological

protein accumulation in AD follows a predictable spatiotemporal pattern where certain areas become affected before others, including the entorhinal cortex (EC) and the hippocampus (Serrano-Pozo et al., 2011). In late stage AD, up to 90% of cells are lost in EC layer II (Gomez-Isla et al., 1996). The initial A β deposits present as plaques in the temporal neocortex, before progressing to the EC and the hippocampus (**Box 1**; Thal et al., 2002). Meanwhile, initial tangle formation begins in the most lateral portions of EC layer II, followed by the hippocampus, before appearing in areas of the neocortex (**Box 1**; Braak and Braak, 1991). The anatomical and temporal progression of A β and tau pathology, and subsequently neurodegeneration, has led to the postulation that A β acts as an initiator of the disease progression that results in tau-mediated neurodegeneration (Freudenberg-Hua et al., 2018).

Many variants of the amyloid cascade hypothesis have been proposed over the years; and this hypothesis argues that the deposition of A β is the initial and causative step for developing AD (Hardy and Higgins, 1992). According to this hypothesis, A β deposition causes disruption of calcium homeostasis in cells, resulting in molecular lesions, NFTs, oxidative stress, inflammation, excitotoxicity, and eventually cell death. The main counter argument for this hypothesis has been that amyloid plaque burden has a low correlation with the severity of clinical symptoms of AD, unlike that of NFTs and neurodegeneration (Terry et al., 1991; Arriagada et al., 1992). In line with this, amyloid plaque deposition commonly plateaus with time, despite declining cognition in AD (Engler et al., 2006). Therefore, the majority in the AD research field now focus on soluble, intracellular A β oligomers as a possible initiator of the development of the disease (**Figure 1**).

Amyloid- β can exist in multiple assembly forms, ranging from monomeric to oligomeric and fibrillar forms (**Figure 1**). As a monomer, A β does not seem to be toxic, whereas oligomeric or fibrillar forms have been found to be potent blockers of long-term potentiation (LaFerla et al., 2007). Research suggests that levels of soluble A β oligomers are better correlated with disease severity than amyloid plaques mainly consisting of insoluble A β fibrillar species (Arriagada et al., 1992; Lue et al., 1999; McLean et al., 1999; Naslund et al., 2000; Haass and Selkoe, 2007). When produced intracellularly, A β oligomers expose flexible hydrophobic surfaces that might contribute to trapping vital proteins and, in this way, they can subtly damage and predispose vulnerable neurons to the formation of intracellular tau aggregates (Campioni et al., 2010). Thus, tau pathology in AD appears to be a downstream, effect of the presence of A β oligomers (**Figure 1**). In line with this, a link has been made between increased amounts of intracellular A β and neurodegeneration, while clearing of intracellular A β has been shown to revert AD-related memory deficits in animals modeling AD (Billings et al., 2005). An explanation for the weak correlation between cognitive decline and plaque load could be that insoluble fibrillar A β species might serve as reservoirs for smaller oligomeric A β , thus sequestering these away from neurons (Mucke and Selkoe, 2012; **Figure 1**).

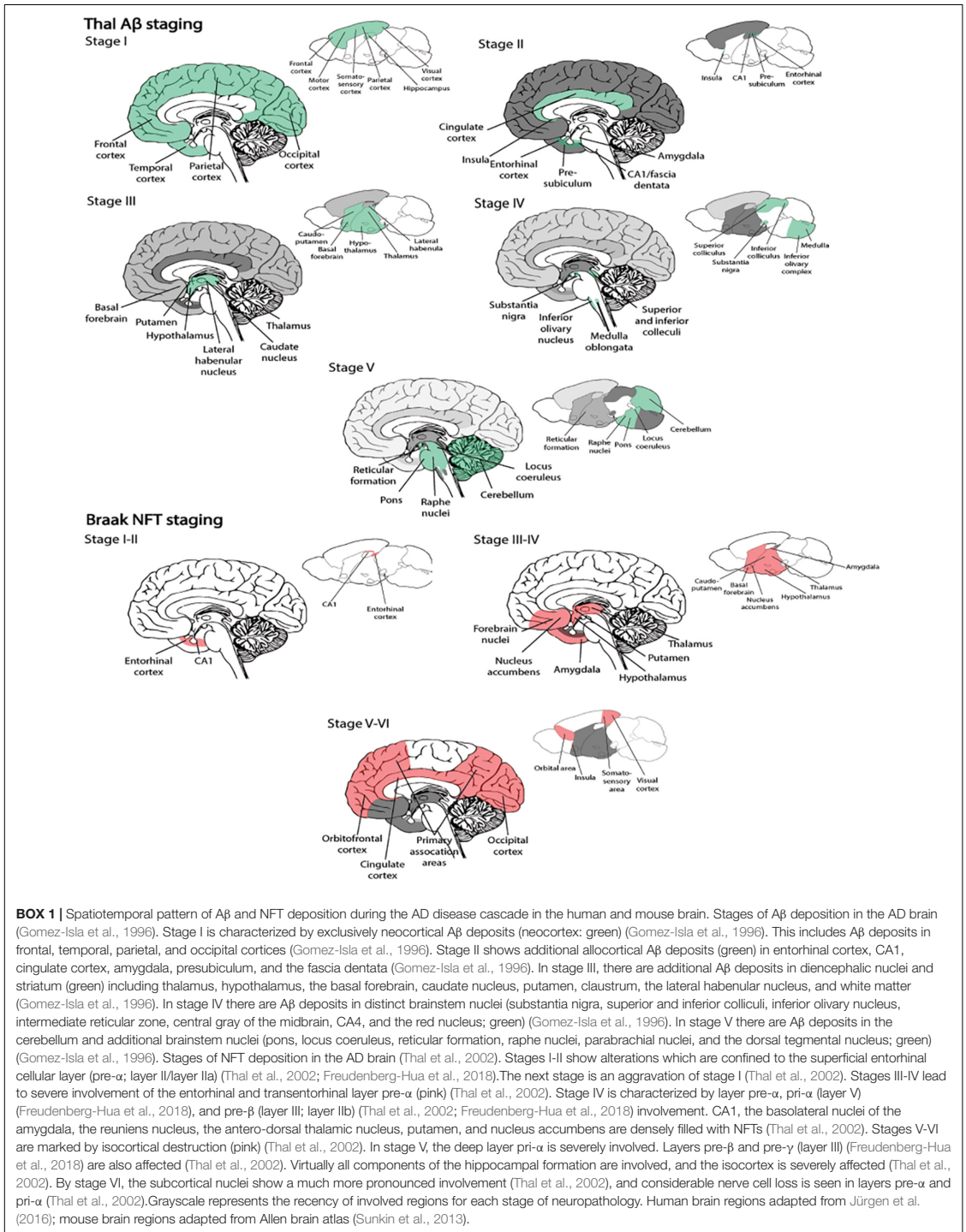
The manner in which pathology progresses in model systems and human patients with AD has mostly been

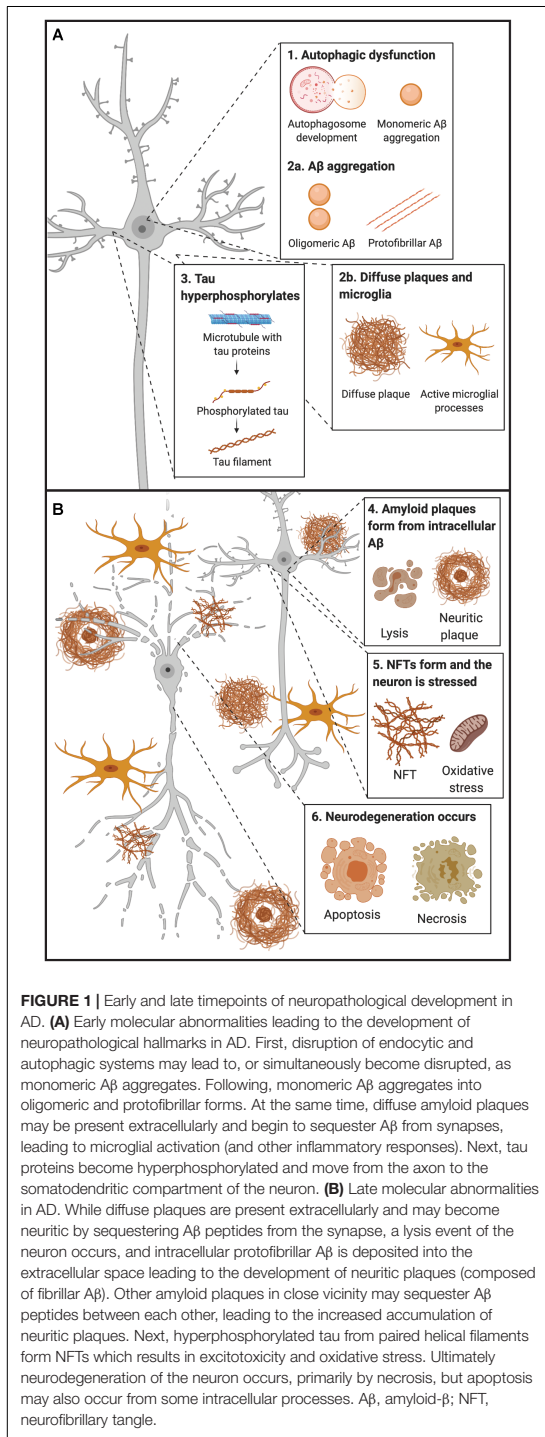
investigated separately resulting in little or poor translational value. As such, the translational aspect of staging the AD molecular disease cascade between preclinical models and human AD patients has remained inadequate. Despite intense investigation into disease cause and mechanisms of neurodegeneration, there is currently no cure or unequivocal evidence as to the exact nature of its underlying cause. Still, there seems to be consensus as to the fact that the success of treatments is primarily contingent on whether they can target disease-related pathology at early onset. This suggests that we are urgently in need of better tools for early onset diagnosis, before evolving pathology severely affects brain function, as well as better tools for monitoring pathological progression.

This effectively means, to translate discoveries made in preclinical models to the clinic, we must bridge the gap between model systems and patients with AD by improving the robustness and predictive validity of screening tools. For instance, the current dominant view is that A β 42 accumulates extracellularly first, and thereby leads to the formation of amyloid plaques. However, several studies of brain tissue from animal models and human patients have begun to challenge this notion. In this paper, we explore potential early screening tools for the diagnosis of AD and also provide links between the extensive research done in preclinical models to human clinical applications. Specifically, we review how screening in AD patients can become more precise by the use of novel cerebrospinal fluid (CSF) biomarkers and by following recommendations for standardized procedures during CSF sample collections. We also focus on how intracellular events of A β and tau aggregation eventually lead to extracellular deposition and the presence of neuropathological hallmarks, and how current tools can predict, diagnose and potentially treat models and patients at various timepoints of the disease.

AD BIOMARKERS – TYPE AND DEFINITION

When defining an AD biomarker, many agree that it is a measurable indicator within a patient that can help to test and monitor the progress of pathology (Hane et al., 2017). The ideal fluid biomarker for AD would be consistent, reproducible, non-invasive, simple to measure, inexpensive, and easy to implement into the clinic and the primary care setting (Davies et al., 1998; Wang et al., 2012; Bjerke and Engelborghs, 2018; Molinuevo et al., 2018). Such biomarkers should be able to identify the clinical disease stage of the patient and also monitor treatment effects. Conventionally, patients with overt dementia are diagnosed with around 85% specificity (but at much lower rates in patients with early stage AD), but the ideal biomarker should exceed this rate (Davies et al., 1998). There is thus an urgent need for a specific marker for early detection in these patients. Various biomarkers that can detect early AD in both preclinical models and patients have been proposed. For instance, it would be preferable to have a biomarker that can detect intracellular events prior to the deposition of amyloid plaques and NFTs. In line





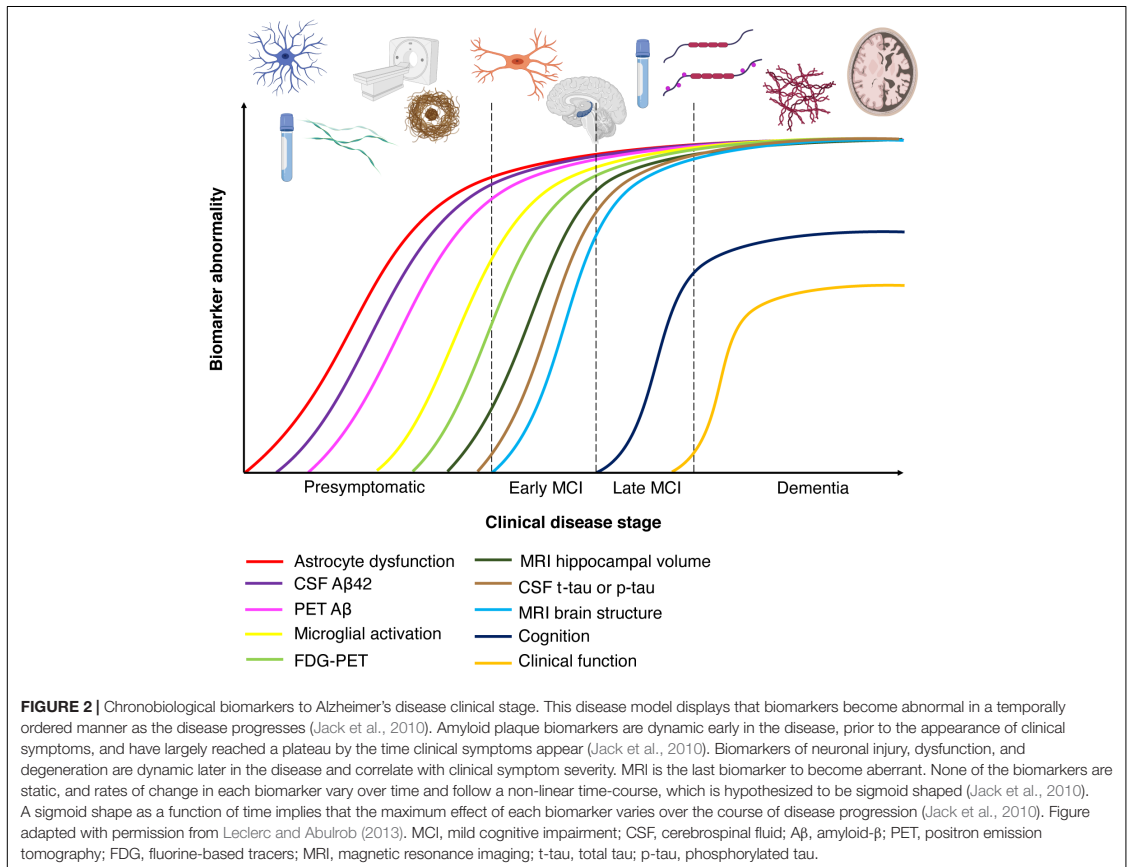
with this, when diagnosing patients based on physical symptoms, reduced memory recall manifests in many diseases other than AD (Hane et al., 2017), highlighting the need for preclinical markers specific to AD.

Furthermore, AD has a long preclinical phase (**Figure 2**) consisting of three stages. In the first stage, monomeric and oligomeric A β aggregates inside neurons and subsequently onto neuronal surfaces and synapses as the concentration in the CSF reservoir diminishes. At this stage, current methods cannot detect the changes caused by A β aggregation in neurons and synapses (Hane et al., 2017). During the second stage, certain CSF biomarkers such as increased CSF tau, hypometabolism in the posterior cingulate, and cortical thinning become detectable (Hane et al., 2017). In the third stage, the patient experiences subtle symptoms while CSF A β decreases and CSF tau increases (Hane et al., 2017). Therefore, biomarker trajectories may differ as a function of the stage to which patients belong along the neuropathological cascade.

Neuroimaging Biomarkers in AD

Imaging Amyloid and Tau Burden

Substantial advances have been made in the detection AD biomarkers using neuroimaging. In terms of imaging amyloid burden, positron emission tomography (PET) scans with radiolabeled tracers specific to A β have become fairly common in AD research. PET amyloid ligands allows for quantification of amyloid deposition in patients, and binding of these ligands predates the development of clinical symptoms of AD by 7–15 years (Jack et al., 2013; Roe et al., 2013). [11 C]Pittsburgh Compound-B (PiB), a derivative of the fluorescent benzothiazole dye thioflavin T, enables for non-invasive imaging of fibrillar A β deposits (Klunk et al., 2004; Johnson et al., 2009). Importantly, this imaging tool is only able to detect extracellular A β deposition, and not intracellular A β accumulation. The Alzheimer's Disease Neuroimaging Initiative (ADNI) suggests that PiB can predict cognitive decline and brain atrophy in patients with mild cognitive impairment (MCI; represents a transition toward diagnosable dementia) (Weiner et al., 2010). Amyloid imaging is now usually performed by the use of fluorine-based tracers (18 F or FDG) and points to the parietal cortices as the earliest sites of amyloid deposition (**Figure 2**; Dickerson et al., 2009). The specific brain regions (posterior cingulate, retrosplenial cortex, and precuneus) are heavily connected with the medial temporal lobes (MTLs) (Ranganath and Ritchey, 2012), which are sites of early AD-related neuropathology. Tau imaging, by the use of selective PET tracers, is able to detect tau depositions that follow Braak staging of NFT pathology (**Figure 2**; Schöll et al., 2015; Cho et al., 2016; Maass et al., 2017). PET ligands have also been developed that are specific for paired-helical filament tau (Leuzy et al., 2019; Scholl et al., 2019). Post-mortem studies of AD patients indicate that, unlike amyloid plaque deposition, NFT density correlates with neurodegeneration and cognitive impairment (Duyckaerts et al., 1987; Braak and Braak, 1997). However, disentangling primary age-related tauopathy (PART) and AD may be a great challenge as there is considerable overlap in the MTL.



FDG-PET – Cerebral Glucose Hypometabolism

Positron emission tomography imaging has been used to examine brain glucose abnormalities in aging, MCI and AD (de Leon et al., 1983). FDG can be used as a metabolic marker and reduced hippocampal metabolism has been observed in patients with MCI and AD (Mosconi et al., 2005; **Figure 2**). FDG-PET is a sensitive biomarker for neuronal and synaptic degeneration (Zimmer et al., 2017), and in line with this, research indicates that cerebral glucose hypometabolism is a downstream marker of neurodegeneration. Thus, this imaging method is able to detect patients at a later timepoint in the course of AD. Studies (Kuhl et al., 1982) have demonstrated that in older ages cerebral glucose metabolism decreases, and that the MTLs, the posterior cingulate cortex and the precuneus show the least age-dependent change. These regions express significant hypometabolism in AD (Márquez and Yassa, 2019), and Mosconi et al. (2008) showed that FDG-PET could be used to differentiate healthy subjects from AD patients with 98 to 99% specificity. Recent work by ADNI 2 PET Core has examined how FDG-PET and amyloid PET can be combined to track progression of AD. For instance, they demonstrated that amyloid PET is negatively associated with

temporoparietal metabolism (Landau et al., 2012). Amyloid PET is associated with cognitive change in healthy subjects, whereas FDG-PET imaging is able to demonstrate cognitive change in MCI patients (Jagust et al., 2015). This is consistent with the spatiotemporal progression model of AD (**Figure 2**), where amyloid progression precedes neurodegeneration.

Imaging Connectivity – Resting-State Functional Magnetic Resonance Imaging

Functional magnetic resonance imaging (fMRI) techniques use blood-oxygenation-level-dependent (BOLD) contrast, which is associated with neuronal population activity. Resting-state fMRI studies examine the correlation of the BOLD signal and anatomical regions of interest at a temporal scale by analyzing spontaneous fluctuations in brain connectivity (Biswal et al., 1995; Fox and Raichle, 2007). In preclinical stages of AD, resting-state fMRI signals have been linked to metabolic changes (indexed by PET) and found to precede neurodegeneration (Sheline and Raichle, 2013). Therefore, this imaging tool is able to detect patients at some point immediately before or after amyloid plaque deposition, prior to the development of NFTs

and associated neurodegeneration. Most of these analyses have focused on the default mode network (Gusnard et al., 2001; Raichle et al., 2001), a network consisting of the MTL, the medial prefrontal cortex, posterior cingulate cortex, anterior cingulate cortex, parietal cortex, and precuneus (Greicius and Menon, 2004; Buckner et al., 2008). These regions overlap with the spatial pattern of amyloid and tau pathology (Buckner et al., 2008). In addition to changes in the default mode network, some studies have suggested that connectivity within the MTL may also be disrupted in AD (Yassa et al., 2011), such as the connectivity between EC and hippocampus [dentate gyrus (DG) and cornu ammonis field 3 (CA3)].

Cortical Thinning and Volume Loss – Structural MRI

Compared with functional imaging modalities, structural MRI provides an overview of anatomical changes in high resolution. Research has shown that in AD patients there is a decrease in brain volume associated with cortical thinning and gyral loss (Figure 2; Uylings and de Brabander, 2002), especially in the prefrontal cortex and hippocampus (Jack et al., 2000; Raz et al., 2005). Thus, this imaging tool can detect patients in which neurodegeneration has begun to occur. Studies in aged rodents and monkeys have demonstrated that hippocampal cells do not undergo frank cell loss with healthy aging (Rapp and Gallagher, 1996; Rasmussen et al., 1996; Rapp et al., 2002); in contrast, this is observed in the prefrontal cortex (Peters et al., 1994; Smith et al., 2004; Stranahan et al., 2012). Recently, cortical thinning of the EC has been shown to be a sensitive marker for structural alterations in both patients with MCI and AD (Holland et al., 2012a). EC thickness has been found to diminish prior to, and thereby predict, hippocampal atrophy (Desikan et al., 2010, 2011, 2012; Eskildsen et al., 2013). Several recent studies using the ADNI data have shown that older adults with CSF A β and phosphorylated-tau (p-tau) present with volume loss in EC (Desikan et al., 2012; Holland et al., 2012b).

White Matter Integrity – Diffusion Tensor Imaging

Studies using diffusion tensor imaging (DTI) in MCI and AD patients show a decrease in brain white matter integrity but with most prominent changes in MTLs (Bozzali et al., 2002; Naggara et al., 2006; Xie et al., 2006; Huang et al., 2007; Chua et al., 2008). DTI studies have focused primarily on the fornix as this region links the limbic system with the rest of the brain. Fornix lesions have been found to reproduce memory and learning deficits linked to hippocampal damage in rats (Sutherland et al., 1982; McDonald and White, 1993) and monkeys (Gaffan et al., 1984; Gaffan, 1992, 1994). The perforant path connects EC layer II neurons to the hippocampal DG and CA3 (Witter, 2007) and is critical for normal hippocampal function (Hyman et al., 1986). The integrity of this pathway is reduced in aged rats with memory loss (Geinisman et al., 1992; Smith et al., 2000). Perforant path lesions also result in EC layer II neuronal loss (Peterson et al., 1994), i.e., at the site where neurodegeneration is first observed in AD patients. Thus, similarly to structural MRI, this imaging tool can detect AD patients at the timepoint at which neurodegeneration has occurred. *In vivo* biomarkers, such as those derived from brain imaging, are crucial for

accurate diagnosis of AD, but does not support diagnosis during preclinical stages. Additionally, molecular imaging is expensive and not easily accessible to the clinical population.

CSF Biomarkers in AD

The current approach to diagnosing AD patients involves assessing patient history, clinical examinations, and detection of underlying pathology using biomarkers during stages of the disease (Ramesh et al., 2018b), with the latter having a diagnostic accuracy between 82 and 84% (Engelborghs et al., 2008). The clinical staging of AD usually lasts about 9–10 years (Heyman et al., 1996), however, researchers have found that the neuropathology of AD starts 20–30 years before the onset of clinical symptoms (Selkoe, 2001; Sperling et al., 2011). Thus, it is likely that, with current means, clinical diagnosis is only feasible at a late stage of the disease. Imaging tools are invaluable methods to diagnose AD patients, but additional methods are needed to detect AD pathology at an earlier stage of the disease cascade, where intervention may be able to delay, even, halt disease progression. By developing better screening and detection tools, early interventions at the preclinical stages of the disease should be possible.

Clearance of abnormal proteins by drainage into the CSF is an endogenous neuroprotective function of the brain. Clinical AD diagnosis is conducted by sampling CSF and analyzing aberrant protein levels within the sample. CSF fills the ventricular system in the brain and spinal cord (Barten et al., 2017) and research evidence suggests that the composition of CSF at any given time reflects true biochemical changes that occur in the brain (Lee et al., 2019). Most of the CSF is generated by the choroid plexus but a significant fraction derives from the interstitial fluid (ISF) in the brain and spinal cord parenchyma. ISF is the circulating CSF that bathes brain tissue (Barten et al., 2017), whereas the choroid plexus connects to nearby permeable capillaries with tight junctions and produces CSF using the aquaporin-1 water channel as well as directional ionic transporters (Speake et al., 2001; Brinker et al., 2014). In terms of CSF production and volume, studies have shown that it can change with age, disease, and time of day. For instance, CSF production increases from 0.4 to 1.4 μ L/min between 8 and 12 weeks of age in the rat (Karimy et al., 2015). Interestingly, CSF volume has been found to increase during neurodegeneration (Barten et al., 2017), which may be related to the increase in atrophy and substance loss of the brain. It is therefore vital to keep these changes in CSF production in mind when comparing healthy subjects to AD patients, and when comparing preclinical with clinical findings.

Temporal Course of AD Biomarkers

Amyloid- β level changes is the first biomarker abnormality seen in AD patients, which can either be in the form of an upregulation in plasma and CSF in cognitively normal individuals (Figure 2). The increased levels seen in CSF A β 40 and A β 42 in AD patients is thought to reflect extracellular A β deposits prior to the accumulation of amyloid plaques (Murphy and LeVine, 2010). However, it is important to note that A β oligomers can form intracellularly before being deposited extracellularly, and currently this cannot be detected with existing biomarkers.

Moreover, A β deposition detected by PET ligands can be seen as early as 15 years prior to onset of AD symptoms (Figure 2; Shen et al., 2018). The next stage of biomarker alteration include neuronal injury, shown by increased levels of CSF total tau protein (t-tau) and tau phosphorylated at threonine 181 (p-tau181/p-tau), and brain atrophy revealed by structural MRI, and synaptic loss and neurodegeneration detected by DTI or FDG-PET (Figures 2, 3; Shen et al., 2018).

Core CSF Biomarkers for Diagnosis

Currently, CSF biomarkers are the only variety of fluid markers used for diagnosis of early AD, however, they have proven difficult to implement in the clinic due to their limited accessibility and the invasive nature of CSF collection (Lee et al., 2019). There are three core CSF biomarkers for AD diagnosis; A β 42, t-tau, and p-tau (Shen et al., 2018). Using a combination of the core AD biomarkers is a better approach compared to using the biomarkers individually, especially for differential diagnosis (Engelborghs et al., 2008). Lower concentrations of CSF A β 42 and higher concentrations of t-tau have been used to distinguish AD patients from healthy age-matched controls and to predict the conversion of MCI to AD (Frölich et al., 2017). To develop a non-invasive and effective measure of preclinical stages in AD, early abnormal AD biomarkers in preclinical models and patients need to be translated and assessed, followed by methodological developments of screening tools that are successful in system models that mirror the disease progression seen in patients.

CLASSIFICATION OF AD BIOMARKERS

Alzheimer's disease biomarkers may be open to different interpretations, however, there is an international classification system proposed by the National Institute of Aging (NIH) and the Alzheimer's Association (NIA-AA) that can aid in grouping them. In 2018, CSF biomarkers could be used in conjunction with neuroimaging for the first time to diagnose AD patients (Lee et al., 2019). The *A/T/N system* (Table 1) is a suggested grouping by Jack et al. (2016) based on the framework from the NIH and NIA-AA, where the *A* refers to the A β pathology measured either by PET or CSF A β 42, the *T* represents tangle pathology and is assessed by either PET or CSF p-tau, and the *N* stands for neurodegeneration or neuronal injury detected by either FDG-PET, structural MRI, or CSF t-tau (Jack et al., 2016). Imaging techniques have found amyloid PET to be most reliable, whereas MRI and FDG-PET scans often are unable to distinguish AD more from other neurodegenerative disorders (Johnson et al., 2012). It is important to note that fluid biomarkers are more available and affordable compared to MRI and PET (Lee et al., 2019).

A β as a Biomarker for AD

Amyloid- β production occurs at the C-terminal fragment of amyloid precursor protein (APP) by cleavage of APP by β -secretase (BACE1) to form C99, followed by cleavage of C99 by presenilin (PSEN) 1 or PSEN2, two enzymatic components of γ -secretase (Haass and De Strooper, 1999). Following

TABLE 1 | AT(N) biomarker grouping of the NIA-AA framework.

| Biomarker class | CSF marker | Imaging marker |
|-----------------------|---|-----------------------|
| Amyloid (A) | CSF A β 42 or A β 42:A β 40 ratio | Amyloid PET |
| Tau (T) | CSF p-tau | Tau PET |
| Neurodegeneration (N) | CSF t-tau | Anatomic MRI; FDG-PET |

Adapted from Jack et al. (2016). NIH, National Institute on Aging; NIA-AA, Alzheimer's Association; CSF, cerebrospinal fluid; A β , amyloid- β ; p-tau, phosphorylated tau; t-tau, total tau; PET, positron emission tomography; MRI, magnetic resonance imaging; FDG, fluorine-based tracers.

production, A β 42 aggregates and accumulates intracellularly and/or extracellularly until a critical threshold is reached, where CSF A β 42 decreases as the peptide sequesters in amyloid plaques in the brain parenchyma (Cirrito et al., 2003; Hong et al., 2011). The long delay in the emergence of plaque deposits even in the presence of increased A β 42, suggests an initial slow process where monomeric A β forms small aggregates, followed by further A β polymerization (Harper and Lansbury, 1997). The AD field cannot yet explain exactly how A β pathology initiates, but further research on the generation of intracellular A β monomers, their recycling, and their aggregation into oligomeric A β may yield some answers.

One of the most widely used biomarkers in AD diagnostic research is the measurement of A β 42 and A β 40 in CSF (Figure 3; Rogeberg et al., 2015). Although A β 40 is present at about 10–20 times higher concentration in CSF, A β 42 is more prone to aggregate and shown to correlate better with AD neuropathology (Mehta et al., 2001; Hellstrand et al., 2010; Murphy and LeVine, 2010; Savage et al., 2014). It has been found that cognitively normal older adults that developed dementia in older ages had low CSF A β 42 but not A β 40 levels (Blennow et al., 2015). These findings can be explained in part by how A β aggregates to form soluble oligomers, which can exist in multiple forms and are neurotoxic (Haass and Selkoe, 2007), and which finally conform to diffuse and dense plaques. Recent studies support the notion that accumulation of the A β peptide arises from an imbalance in the production and clearance of A β and that the ability to clear A β diminishes with age (Wildsmith et al., 2013). An attractive early biomarker for AD is CSF A β 42, given that both CSF t-tau and p-tau changes occur at a later time point in the disease process closer to clinically detectable dementia (Buchhave et al., 2012). Furthermore, measurement of the CSF A β 42:A β 40 ratio is superior to A β 42 alone when distinguishing between MCI patients who progress and those that do not progress to AD dementia (Hansson et al., 2007; Lee et al., 2019). When comparing A β fluid biomarkers and imaging biomarkers, studies have shown that CSF A β 42 can detect amyloid pathology earlier than amyloid PET imaging (Figure 3; Palmqvist et al., 2016).

There appears to be a lack of consensus regarding CSF A β concentrations in AD patients. For instance, researchers have found that CSF A β 42 concentrations increase (Nakamura et al., 1994; Bouwman et al., 2007), decrease (Kanai et al., 1998; Tapiola et al., 2000; Wahlund and Blennow, 2003; Mollenhauer et al., 2005; de Leon et al., 2006; Beckett et al., 2010), or experience

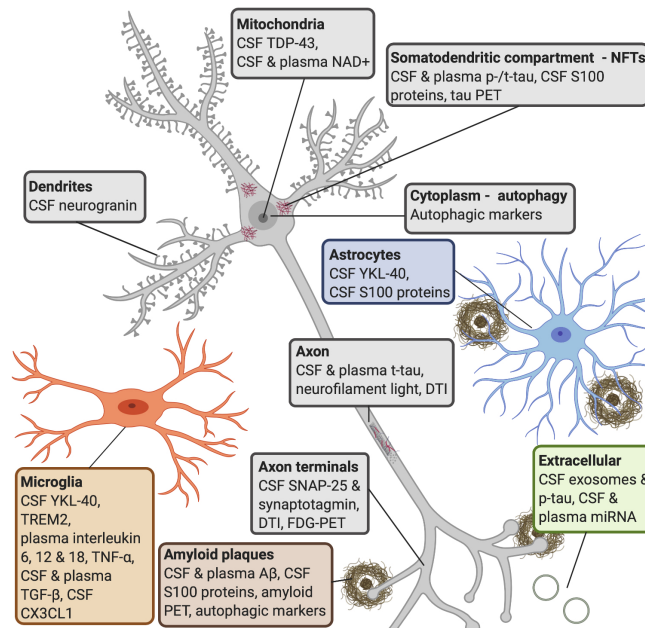


FIGURE 3 | AD molecular processes that can be detected by biomarkers. **Amyloid plaques:** a widely used biomarker for diagnosis in AD is the concentration of CSF A β 42 and A β 40 (Roggeberg et al., 2015). Studies have shown that CSF A β 42 can detect amyloid pathology earlier than amyloid PET imaging (Palmqvist et al., 2016). Some research shows that serum A β 42 levels do not correlate with CSF levels (Liu et al., 2004), whereas others have found that plasma A β can be measured with good sensitivity (Lee et al., 2019). Several S100 proteins (S100B, S100A1, S100A6, S100A8, S100A9, and S100A12) are found within amyloid plaques and in astrocytes and/or microglia near amyloid deposits (Boom et al., 2004; Shepherd et al., 2006; Walker et al., 2006; Ha et al., 2010; Afanador et al., 2014; Lodeiro et al., 2017). **NFTs:** increased CSF tau is a sensitive biomarker for neurodegeneration, but CSF p-tau is more specific to neurodegeneration linked to AD (Lewczuk et al., 2004; Blennow et al., 2015). P-tau is secreted via exosomal release, and reaches the CSF (Saman et al., 2012). Increased levels of CSF t-tau and p-tau can predict the progression of cognitive symptoms better than CSF A β 42 (El Kadmiri et al., 2018), but the diagnostic utility of CSF t-tau and p-tau are improved when measured in combination with A β 42 (Dubois et al., 2014). Increased plasma tau observed in AD patients compared to MCI patients and healthy controls (Mattsson et al., 2016; Pase et al., 2019). S100B and S100A9 are found within NFTs (Sheng et al., 1994, 1997; Shepherd et al., 2006). **Autophagy:** late stages of autophagy is disrupted in AD patients, as an accumulation of autophagic vesicles can be observed in dystrophic neurites (Komatsu et al., 2006), and is observed prior to extracellular A β deposition (Mehrpour et al., 2010; Nixon and Yang, 2011). **Microglia:** YKL-40 is expressed by microglia. CSF TREM2 is associated with higher CSF t-tau and p-tau levels, probably reflecting a corresponding change in microglia activation in response to neurodegeneration (Suarez-Calvet et al., 2016). It has been shown that AD patients have higher levels of interleukin-6, 12, and 18, TNF- α and TGF- β , in blood, and higher levels of TGF- β in CSF, compared to healthy controls (Swardfager et al., 2010). Decreases in CSF neuronal CX3CL1 is found in AD patients (Perea et al., 2018). **Astrocytes:** YKL-40 is expressed in astrocytes near A β plaques (Craig-Schapiro et al., 2010) and correlates positively with tau pathology (Querol-Vilaseca et al., 2017; Janelidze et al., 2018). **Axon terminals:** CSF levels of SNAP-25 (Brinkmalm et al., 2014; Sutphen et al., 2018) and synaptotagmin (Ohrlfelt et al., 2016) have been found at elevated levels in patients with AD or MCI compared with control subjects. Synaptic neurodegeneration can be detected by DTI or FDG-PET (Shen et al., 2018). **Dendrites:** increased CSF neurogranin is found in MCI and AD patients as compared with healthy controls (Thorsell et al., 2010; De Vos et al., 2015). **Axon:** increased neurofilament light is observed in response to axonal damage, which occurs in AD. The core CSF biomarkers (A β 42, t-tau, and p-tau) and CSF neurofilament light levels strongly correlated with AD (Olsson et al., 2016). Blood levels of this protein strongly correlate with its CSF levels (Gisslen et al., 2016; Kuhle et al., 2016; Rojas et al., 2016). **Mitochondria:** studies have shown that TDP-43 contributes to neuroinflammation and may have a role in mitochondrial and neuronal dysfunction (James et al., 2016). NAD⁺ levels can be detected in CSF and plasma in early AD. **Extracellular:** miRNAs released from exosomes appear to be associated with neurodegenerative aspects in AD (Wang et al., 2008, 2012; Chen et al., 2017). Studies have reported that changes in levels of blood miRNA distinguished AD patients from healthy controls with 93% accuracy (Leidinger et al., 2013; Swarbrick et al., 2019). AD, Alzheimer's disease; CSF, cerebrospinal fluid; A β , amyloid- β ; PET, positron emission tomography; NFTs, neurofibrillary tangles; p-tau, phosphorylated tau; t-tau, total tau; MCI, mild cognitive impairment; TREM2, triggering receptor expressed on myeloid cells 2; TNF- α , tumor necrosis factor- α ; TGF- β , transforming growth factor- β ; CX3CL1, CX3 chemokine ligand 1; SNAP-25, synaptosomal-associated protein 25; TDP-43, transactive response element (TAR) deoxyribonucleic acid (DNA)-binding protein 43; NAD⁺, oxidized nicotinamide adenine dinucleotide; miRNA, microRNA.

no significant change (Andreassen et al., 1998, 1999a; Hoglund et al., 2005; Andersson et al., 2008; Brys et al., 2009; Stomrud et al., 2010) during the disease. The prevailing explanation for a reduced amount of A β in later stages of AD is that as the pathology progresses, more A β , especially A β 42, aggregates into

plaques in the brain, which effectively means that less A β can diffuse from the brain to the CSF. Another explanation may be that A β first accumulates intracellularly, and neurodegeneration releases A β in the extracellular compartment, increasing CSF A β levels, and subsequently accumulates onto neuronal surfaces and

in synapses as it clears away from the CSF. As neurodegeneration occurs, less A β is produced and therefore smaller amounts will accumulate in the CSF and subsequently in the brain, where A β will reach plateau levels. Alternatively, reduced CSF A β 42 might follow neuronal dysfunction, which results in decreased metabolism of APP and A β . It is important to note that this is unlikely in transgenic mice, as A β 42 levels in the CSF decline, while its levels in the brain keep rising. Also, when above a certain level, parts of CSF A β 42 may aggregate into a large assembly that antibodies of currently used enzyme-linked immunosorbent assay (ELISA) kits cannot capture (Pitschke et al., 1998; Liu et al., 2004). These seemingly disparate findings regarding CSF A β concentrations may therefore reflect different timepoints of the disease progression.

With regard to studies using A β as a fluid biomarker for AD, studies have shown that concentrations of CSF A β 42 increased between 5 and 7 months of age, but not between 8 and 13 months of age in an APP/PS1 mouse model (Liu et al., 2004). This was despite a rapid increase in brain levels of A β 42 (Liu et al., 2004). However, between 6 and 9 months of age in another APP/PS1 mouse model with a more aggressive AD phenotype a decline in CSF A β 42 levels was reported (Liu et al., 2004). Based on these findings, it appears that CSF A β 42 may initially reflect the rate of A β 42 production (most likely in the synaptic cleft), but after reaching a critical threshold, CSF A β 42 levels stay in equilibrium until plaque formation leads to their decrease (Liu et al., 2004). Consistent with this notion, CSF A β 42 levels have a strong link with the deposition of amyloid plaques, whereby an inverse correlation between A β 42 levels, plaques (Strozyk et al., 2003) and amyloid PET is observed (Toledo et al., 2015; Leuzy et al., 2016; Niemantsverdriet et al., 2017). This implies that as A β aggregates and forms plaques in the brain, lower levels of the protein diffuse into the CSF (Lee et al., 2019).

Compared to tau as a fluid biomarker, the drop in CSF A β 42 should precede the increase in CSF tau proteins. This notion is supported by biomarker studies in sporadic AD patients demonstrating that a decrease in CSF A β 42 was the earliest change reported (Skoog et al., 2003; Gustafson et al., 2007), while in patients with familial AD reductions in CSF A β 42 and elevations in tau occur around 10–15 years prior to symptom development (Bateman et al., 2012; Ringman et al., 2012). Similar to A β , tau can also change its conformation to prion-like oligomers and there is evidence for misfolded A β initiating tau misfolding (Pulawski et al., 2012; Nussbaum et al., 2013). Therefore, A β appears to be an initiator of tau pathology and subsequent neurodegeneration.

Tau as a Biomarker for AD

Tau is a microtubule-associated protein comprising six human isoforms and is located in neuronal axons (Barten et al., 2011; Khan and Bloom, 2016). A characteristic of many neurons in AD is that tau is hyperphosphorylated and translocated from axons to the somatodendritic compartment, where it becomes misfolded and aggregates. Tau aggregates develop intracellularly and may thus trap functional proteins adding to microtubule destabilization, cellular dysfunction and eventually neurodegeneration (Benilova et al., 2012). Intracellular trafficking

is dependent on the phosphorylation of tau in order to separate tau from microtubules, allowing transport, followed by dephosphorylation in order to return tau into microtubules (Avila et al., 2004). It has been proposed that A β pathology drives the abnormal phosphorylation of tau in AD (Bakota and Brandt, 2016; Khan and Bloom, 2016). However, transgenic mice modeling A β pathology alone do not develop NFTs endogenously (Lee and Trojanowski, 2001), while intracerebral injections of human mutated and/or aggregated tau are necessary to observe this neuropathological hallmark (Clavaguera et al., 2013; Ahmed et al., 2014; Kaufman et al., 2017; Lewczuk et al., 2017; Mudher et al., 2017; Narasimhan et al., 2017; He et al., 2018). Tau aggregates and NFTs are produced in the cytoplasm under pathological conditions, when tau changes its conformation from a highly soluble state to one with a high β -sheet content and is hyperphosphorylated (Yamada et al., 2015). Studies have shown that the elevation in CSF tau in AD is due to axonal loss and neuronal death, leading to the release of the intracellular protein (Blennow and Hampel, 2003; Hampel et al., 2010). However, despite significant neurodegeneration and tau pathology, CSF tau is not elevated in other pure tauopathies (Grossman et al., 2005; Bian et al., 2008). This suggests that cell death may not be the only mechanism responsible for CSF tau elevations in AD (Jack et al., 2010).

When using tau as a fluid biomarker for AD, increased CSF concentrations of the protein constitutes a sensitive marker for neurodegeneration, but an entirely unspecific one for AD (Figure 3). However, the increased concentration of p-tau molecules seems much more AD specific (Figure 3; Lewczuk et al., 2004; Blennow et al., 2015). P-tau is secreted via exosomal release, and reaches the CSF (Saman et al., 2012; Figure 3). CSF p-tau levels are usually stable in other dementias, whereas both CSF p-tau and t-tau levels can be used to distinguish AD patients from healthy controls, suggesting that CSF tau is an important biomarker for differential dementia diagnosis (Blennow et al., 2015). In addition, high CSF t-tau and p-tau can predict the progression of cognitive symptoms better than CSF A β 42 (El Kadmiri et al., 2018; Figure 3). Researchers have found correlations between p-tau in CSF and NFTs in the brain (Clark et al., 2003; Buerger et al., 2006; Tapiola et al., 2009; de Souza et al., 2012), and CSF t-tau has been found to correlate with neurodegeneration (Lee et al., 2019). Importantly, the utility of CSF p-tau and t-tau for AD diagnosis is markedly improved when measured together with CSF A β 42 (Figure 3; Dubois et al., 2014).

To examine CSF tau levels in rodents, researchers have used P301S human tau transgenic mice and found that ISF tau was at fivefold higher levels compared to endogenous tau, in line with its elevated levels of expression (Yamada et al., 2011). It is important to keep this in mind when comparing CSF tau between rodents and patients, as the CSF tau from rodents might be contaminated by ISF tau levels, and the CSF levels may not reflect the actual tau levels expressed in the brain. Studies have found that tau in brain tissue is approximately 50,000-fold more abundant than its levels in the CSF (Barten et al., 2011). In humans, patients with sporadic AD display longitudinal increases in tau when low levels of tau were detectable early in the disease course, but no differences (or

increases) have been observed in tau in patients with high levels of tau at baseline (Kanai et al., 1998; Sunderland et al., 1999).

Compared to A β , which aggregates broadly in the brain parenchyma and the perivascular space, tau readily drains into CSF. In contrast to A β , tau levels increase in the CSF with the progression of AD (Olsson et al., 2016). Changes in CSF A β 42 precede changes in CSF tau, consistent with the proposition that A β affects and drives CSF tau levels (Jack et al., 2010). However, further research is needed to explain whether A β and tau pathology represent early initiators of neurodegeneration and cognitive decline, or merely downstream effects of other early pathophysiological events in AD.

Neuroinflammatory Biomarkers

Inflammation is now considered another core feature of AD as it relates to the pathogenesis of the disease and also serves as a link between amyloid plaques and NFTs (Akama and Van Eldik, 2000; Akiyama et al., 2000). Inflammatory response has now been reported in post-mortem tissues of AD patients (Gomez-Nicola and Boche, 2015) and is routinely observed in preclinical models. The presence of inflammation in the brain of AD patients was initially thought to be a consequence of the accumulating neurodegeneration present at late stages of the disease. However, a substantial body of research now demonstrates that a persistent immune response in the brain not only is associated with neurodegeneration, but it also exacerbates A β and tau pathology (Figure 1). Inflammatory markers may be able to give evidence to intracellular abnormalities early in the course of AD, prior to extracellular A β deposition (marked by an increase in CSF A β 40/A β 42 and amyloid PET) as evidence points to a dysfunction in autophagic processes in AD patients (Figure 1; Menzies et al., 2015). Moreover, there have been reports of immune-related proteins and cells opposed to amyloid plaques (Figure 1; Griffin et al., 1989). In line with this, it has been suggested that inflammation may provide a link between the initial A β pathology and subsequent development of NFTs (Kitazawa et al., 2004; Rhein et al., 2009; Garwood et al., 2011; Nisbet et al., 2015).

Autophagic Markers

One way for intracellular accumulation of A β peptides to occur is through a disruption in the autophagic and lysosomal clearance systems. In this way, autophagic markers could ultimately serve as the earliest biomarker to diagnose AD patients, as this process may likely initiate the aggregation of monomeric A β into oligomeric A β intracellularly (Figure 1). Autophagy is a complex process, in which a vesicle known as the phagophore elongates around the cytoplasmic components selected for degradation. The recognition of these components are dependent on the lipidated form of the microtubule-associated protein light chain 3 (LC3) (Milisav et al., 2015). The late stage of autophagy depends on the successful fusion of the autophagosome with the lysosome, which then degrades and recycles the autophagosome cargo. There is evidence supporting that the late stage of autophagy is disrupted in AD, as accumulation of autophagic vesicles can be observed in dystrophic neurites (components of dense plaques) (Komatsu et al., 2006), and these are observed prior

to extracellular A β deposition in model systems and patients (Figure 3; Mehrpour et al., 2010; Nixon and Yang, 2011).

The above findings suggest that autophagy dysfunction leads to the accumulation of intracellular A β by avoiding proper degradation and/or recycling. In line with this, researchers have found that LC3-associated endocytosis is used to clear and recycle A β surface receptors (Heckmann et al., 2019). In model systems with LC3-associated endocytosis disrupted, an increase in extracellular A β deposition, NFTs, neurodegeneration and behavioral deficits was observed. Another line of research found that autophagic markers were significantly increased in AD patients compared with control subjects (Cho et al., 2019). Furthermore, other studies suggest that metabolism of A β and tau is crucially influenced by autophagy (Uddin et al., 2018). Recent evidence suggests that A β monomers and oligomers modulate autophagy differently in neurons. Monomers have been found to stimulate autophagy, increasing autophagosome rates and elevation of LC3 protein levels, while simultaneously impairing the lysosomal pathway affecting the autophagy efflux, leading to autophagosome accumulation (Menzies et al., 2015). By contrast, A β oligomers do not cause a significant increase in LC3 protein levels nor affect efflux of autophagic vacuoles (Menzies et al., 2015), which suggests that an increase in intracellular A β monomers may be the result of a defective autophagic system. This fits the proposition that autophagic disruption and accumulation of A β monomers constitute some of the earliest events in the AD cascade (Figure 1). The exact cascade by which autophagy can degrade amyloid plaques is still not known, however, microglial autophagy appears to play an important role.

Glial Cells and Markers

Neuroinflammation involving astrocytes, microglia, and secreted compounds like reactive oxygen species, cytokines, and chemokines are key pathophysiological processes assessed when diagnosing AD (Ramesh et al., 2018a). Microglia and astrocytes are the two types of glial cells primarily affected (McGeer et al., 1987; Rogers et al., 1988; Bronzuoli et al., 2016), which in turn affect the clearance and production of A β 42 (Hickman et al., 2008; Liu et al., 2017). Glial cells also affect the development and propagation of tau pathology (Asai et al., 2015) and thus influence disease progression and severity (Block et al., 2007; Calsolaro and Edison, 2016). Importantly, if glial cells are activated for too long, they can become pro-inflammatory (Bronzuoli et al., 2016). Chitinase-3-like protein 1 (or YKL-40) is an inflammatory marker expressed by microglia and astrocytes (Figure 3). In AD, YKL-40 is expressed in astrocytes near A β plaques (Craig-Schapiro et al., 2010) and correlates positively with tau pathology (Figure 3; Querol-Vilaseca et al., 2017; Janelidze et al., 2018).

Another glial marker is triggering receptor expressed on myeloid cells 2 (TREM2), which is an inflammatory cell-surface receptor. Loss-of-function mutations of TREM2 are associated with an increased risk of developing AD (Suarez-Calvet et al., 2016). Researchers have found that TREM2 phagocytose A β in early AD stages (Jay et al., 2017). A rare mutation in the TREM2 gene affects the phagocytic activity of microglia and consequently

contributes to accumulation of A β (Kleinberger et al., 2014; Ramesh et al., 2018b). With regard to TREM2 measured in CSF, studies have shown increased levels to be associated with higher CSF t-tau and p-tau levels, probably reflecting a corresponding change in microglia activation in response to neurodegeneration (Figure 3; Suarez-Calvet et al., 2016). Relevant research findings imply that neuroinflammation is a robust biomarker even at pre-symptomatic stages (Janelidze et al., 2018). In line with this, high levels of inflammatory biomarkers are associated with increased CSF levels of t-tau (Janelidze et al., 2018). Interestingly, PET studies have revealed increased microglial activation in the precuneus (Hamelin et al., 2016; Fan et al., 2017), a region in the default mode network that displays early A β deposits in AD (Palmqvist et al., 2017).

Cytokines

With regard to cytokines, it has been shown that AD patients have higher levels of interleukin-6, 12, and 18, tumor necrosis factor- α (TNF- α), and transforming growth factor- β (TGF- β), in blood, and higher levels of TGF- β in CSF, compared to healthy controls (Figure 3; Swardfager et al., 2010). Endothelial growth factor receptor 1 (also known as Flt-1), has been found to be upregulated in entorhinal cortical sections from human AD brains and in human microglia following treatment of A β 42 (Ryu et al., 2009). Following neuroinflammation, oxidative stress in the intracellular environment occurs. Oxidative stress plays an important role in the early stages of AD (Oh et al., 2010) and its associated signaling cascades are being investigated and explored for biomarkers. For instance, higher reactive oxygen species levels lead to post-translational modification of proteins, toxic cell damage, fragmentation and aggregation of A β (Brinkmalm et al., 2014). One type of reactive oxygen species are sulfatides, which have been found to be depleted in both gray and white matter of AD patients, and results in decreased hippocampal volume and cognitive decline (Ramesh et al., 2018b).

Since neuroinflammation occurs in AD brains, the levels of several S100 proteins are increased and some of the proteins play roles related to the processing of APP, regulation of A β levels and tau phosphorylation. S100A1, S100A6, and S100B have been found to be involved in the disassembly of microtubules and tau protein release (Zimmer et al., 2005; Roltsch et al., 2010; Wruck et al., 2016; Sidoryk-Wegrzynowicz et al., 2017), while S100B and S100A9 are found within NFTs (Figure 3; Sheng et al., 1994, 1997; Shepherd et al., 2006). Traumatic brain injury (TBI) has been found to predispose people to developing AD (Johnson et al., 2010). Interestingly, TBI results in an increase in S100A1 and S100B levels in plasma and CSF in patients (de Bussard et al., 2005). Research has shown that levels of S100B originating from necrotic tissue might enhance or amplify neurodegeneration by apoptosis (Sedaghat and Notopoulos, 2008). Thus, various S100 proteins could be a link between neurodegenerative diseases induced by brain damage. Comorbidities often accompany a diagnosis of AD, thus the spectrum of pathological processes that can end in AD at different degrees of severity and symptomatology needs to be kept in mind in order to accurately diagnose and treat patients. Additionally, S100 proteins may serve as an early biomarker for

a later AD diagnosis in patients with TBI or other comorbidities that increase S100 levels.

Moreover, several S100 proteins are implicated in the amyloidogenic pathway of APP cleavage. S100A9 regulates γ -secretase and BACE1 expression and activity (Kummer et al., 2012; Li et al., 2014), and S100B and S100A1 regulate APP levels (Zimmer et al., 2005; Anderson et al., 2009; Mori et al., 2010). S100A7, S100A8, S100A9, and S100B have been found to influence A β levels (Qin et al., 2009; Lee et al., 2013; Lodeiro et al., 2017; Cristovao et al., 2018). Moreover, S100B and S100A6 have been found to reduce zinc levels and senile plaque load in preclinical models (Roltsch et al., 2010; Hagemeyer et al., 2017; Tian et al., 2019). S100A1, S100A9, and S100B proteins can interact and alter the aggregated A β and is found to co-aggregate with A β peptides (Zimmer et al., 2005; Shepherd et al., 2006; Ha et al., 2010; Mori et al., 2010; Chang et al., 2012; Afanador et al., 2014; Cristovao et al., 2018). In line with this, several S100 proteins (S100B, S100A1, S100A6, S100A8, S100A9, and S100A12) are present in amyloid plaques and in astrocytes and/or microglia near amyloid deposits (Figure 3; Boom et al., 2004; Shepherd et al., 2006; Walker et al., 2006; Ha et al., 2010; Afanador et al., 2014; Lodeiro et al., 2017).

Chemokines

In order to maintain brain homeostasis, microglia establish continuous communication with neurons and astrocytes, through the expression and secretion of chemokines (Mennicken et al., 1999). The CX3 chemokine ligand 1 (CX3CL1; or fractalkine), is predominantly expressed in neurons (Bazan et al., 1997) and interacts with the CX3 chemokine receptor 1 (CX3CR1) exclusively present in microglia (Imai et al., 1997; Maciejewski-Lenoir et al., 1999). The CX3CL1/CX3CR1 tandem allows for direct communication between neurons and microglia (Harrison et al., 1998; Sheridan and Murphy, 2013), and it has been suggested that this axis becomes impaired in AD patients (Bolos et al., 2017). Consistent with this, neuronal CX3CL1 is found to be decreased in CSF from AD patients compared to MCI and control subjects (Figure 3; Perea et al., 2018). Furthermore, researchers have aimed to regulate neuroinflammation in tau depositing mouse lines by overexpressing CX3CL1 and found that it significantly reduced tau pathology, ameliorated neuronal loss, reduced microgliosis (Nash et al., 2013) as well as rescuing cognitive function (Finneran et al., 2019). In another line of research, it has been found that when microglia are transferred from tau depositing knock-out *Cx3cr1* mice, hyperphosphorylation of endogenous murine tau is observed (Maphis et al., 2015). Disruption of CX3CL1 signaling in amyloid depositing mouse lines has shown reduced pathology due to increased microglial phagocytosis of amyloid plaques (Lee et al., 2010).

Synaptic Neurodegeneration Markers

There is of yet no established or reliable biomarker test for synaptic degeneration, which is considered a crucial feature for the development of AD-related cognitive decline. The ability to monitor neurodegeneration as a downstream effect of synaptic dysfunction would be an important advantage for

early AD diagnosis and in clinical trials related to drug testing. Synaptotagmin, a pre-synaptic calcium sensor vesicle protein, facilitates neurotransmitter release from the synaptic vesicle by exocytosis and also functions as an essential vesicle cargo molecule in hippocampal neurons (Leinenbach et al., 2014). Various studies have shown a decrease in synaptotagmin-1 in AD patients (Mattsson et al., 2011).

Another marker for synaptic degeneration is synaptosomal-associated protein 25 (SNAP-25), which is an essential component of the soluble N-ethylmaleimide-sensitive fusion protein attachment protein receptors (SNARE) complex that mediates synaptic communication by initiating fusion of synaptic vesicles (Olsson et al., 2016). A negative correlation has been found between SNAP-25 and cognitive decline, suggesting that this is a promising novel CSF biomarker for AD (Andreassen et al., 1999b). Overall, CSF levels of SNAP-25 (Brinkmalm et al., 2014; Sutphen et al., 2018) and synaptotagmin (Öhrfelt et al., 2016) have been assessed and found at elevated levels in patients with AD or MCI compared with control subjects (Figure 3). Another marker for synaptic neurodegeneration is neurogranin, which plays an important role in synaptic plasticity and long-term potentiation processes (Geppert et al., 1994; Sudhof and Rizo, 1996; Thorsell et al., 2010). Neurogranin has also been found at increased levels in CSF of patients with MCI and dementia due to developing AD as compared with healthy controls (Figure 3; Thorsell et al., 2010; De Vos et al., 2015). CSF neurogranin concentrations have been found at increased levels in patients that have reached the threshold for A β PET detection (Palmqvist et al., 2019), and also CSF neurogranin and tau levels have been found to correlate strongly (Thorsell et al., 2010; De Vos et al., 2015).

Novel Biomarkers for AD

Many biomarkers are now being investigated as complimentary to the core AD biomarkers. One such biomarker is neurofilament light, which is a marker of neuronal integrity reflecting axonal damage of the subcortical white matter (Petzold, 2005; Jahn and Fasshauer, 2012; Neselius et al., 2012; Kuhle et al., 2015; Zetterberg et al., 2016). Neurofilament light is released from axons into the extracellular space during healthy aging, which results in increased CSF level concentrations (Figure 3). The release of neurofilament light is accelerated during axonal damage, which occurs in AD (Figure 3). A recent meta-analysis showed that the core CSF biomarkers (A β 42, t-tau, and p-tau) and CSF neurofilament light levels strongly correlated with AD (Figure 3; Olsson et al., 2016). Importantly, CSF neurofilament light levels have been shown to be higher in AD (Sjogren et al., 2001; Pijnenburg et al., 2007; Zetterberg et al., 2016; Alcolea et al., 2017; Lista et al., 2017). Blood neurofilament levels strongly correlate with CSF levels (Figure 3; Gisslen et al., 2016; Kuhle et al., 2016; Rojas et al., 2016), and blood neurofilament light concentrations have been found at increased levels in many forms of neurodegenerative disease (Gisslen et al., 2016; Kuhle et al., 2016; Rohrer et al., 2016; Rojas et al., 2016; Steinacker et al., 2016, 2017; Weydt et al., 2016; Mattsson et al., 2017a) and have proven almost as reliant as CSF analysis in monitoring treatment outcome in patients (Bacioglu et al., 2016; Disanto

et al., 2017). Another novel biomarker is the transactive response element (TAR) deoxyribonucleic acid (DNA)-binding protein 43 (TDP-43) protein, which can become pathologic if triggered by A β peptides. Studies have shown that TDP-43 contributes to neuroinflammation and may have a role in mitochondrial and neuronal dysfunction (Figure 3; James et al., 2016). In accordance with this, TDP-43 pathology has been observed in some AD cases (Amador-Ortiz et al., 2007; Chang et al., 2015; James et al., 2016). Another novel biomarker is oxidized nicotinamide adenine dinucleotide (NAD⁺; involved in mitochondrial homeostasis), which has been found to decrease during healthy aging, but even more rapidly in neurodegenerative diseases (Figure 3; Lautrup et al., 2019). This could be related to the observed decrease in neuronal metabolism that occurs during healthy aging, but this is accelerated in the AD brain. NAD⁺ levels can be detected in CSF and plasma early during the disease progression, and in combination with core biomarkers, it presents as a novel preclinical biomarker for AD (Figure 3).

Neuropathology is associated with a distinct subset of cells in specific regions in the brain and this makes the identification of relevant biomarker molecules a challenge. The transport of macromolecules from the brain to the CSF and blood, mediated by extracellular vesicles, presents a promising source of central nervous system (CNS)-specific biomarkers (Thompson et al., 2016). One such trafficking macromolecule is exosomes, which can be picked up in CSF. An increasing body of evidence suggests that exosomal proteins and microRNAs (miRNAs) may constitute novel biomarkers for clinical AD diagnosis (Van Giau and An, 2016). miRNAs released from exosomes appear to be associated with neurodegenerative aspects in AD (Figure 3; Wang et al., 2008, 2012; Chen et al., 2017). miRNAs are a class of small non-coding RNAs which regulate over 50% of protein-coding genes, and miRNA-107 has been found to be downregulated in AD brains (Van Giau and An, 2016; Fransquet and Ryan, 2018; Ramesh et al., 2018b). Accumulating evidence presents that miRNAs regulate A β production, NFT formation, and neurodegeneration by targeting different genes (Wang et al., 2008; Van Giau and An, 2016). Research has also identified BACE1 as a target of miRNA-107, connecting the level of miRNA-107 to A β formation and neuronal pathogenesis (Wang et al., 2008).

CSF AND BLOOD-BASED BIOMARKERS

Although protein content is lower in CSF compared to blood, CSF holds great value for developing consistent biomarkers for AD as it reflects biochemical changes in the brain by direct interaction with the extracellular space (Hampel et al., 2012). At present, there is no approved blood biomarker for AD (Stadtman and Levine, 2003). It is important to note, however, that blood biomarkers have lower sensitivity and specificity than CSF biomarkers, and this can be attributed to the fact that the blood-brain barrier (BBB) prevents diffusion of analytes into the blood via a filtering mechanism (Lee et al., 2019). Furthermore, one complication of measuring CNS biomarkers in blood is that many of the analytes are produced in the

periphery as well as in the brain, and thus the source of detectable change may be difficult to determine (Barten et al., 2017). However, there is currently an urgent need within the field to develop blood-based biomarkers which are inexpensive and which can detect early neuropathological changes in AD (Hane et al., 2017). For instance, detection of autophagic markers in plasma could serve as an early biomarker for AD (Cho et al., 2019). Blood test sampling is routinely performed in the clinic, it is minimally invasive, cheap and suitable for recurrent measurements (Shen et al., 2018).

When comparing A β levels in blood and CSF, some researchers have found that serum A β 42 levels do not correlate with CSF levels (Figure 3; Liu et al., 2004). However, contrary to this, others have found that plasma A β can be measured with good sensitivity (Figure 3; Lee et al., 2019). A β can easily penetrate the BBB and is therefore an attractive blood biomarker candidate (Lee et al., 2019). Indeed, studies have shown that cerebral amyloid deposits may be sourced in the periphery, while other studies suggest that amyloid deposits in cerebral vessels may originate from circulating A β peptides (Yankner and Mesulam, 1991; Chen et al., 1995; DeMattos et al., 2002; Lee et al., 2019). Plasma A β and A β -approximate peptide concentrations have been reported to be consistent with amyloid PET results (Kaneko et al., 2014). Moreover, levels of A β 42 and the ratio of A β 42:A β 40 in plasma have been shown to correlate with CSF concentrations and with amyloid PET (Janelidze et al., 2016; Verberk et al., 2018). However, it is important to note that some researchers have found that reduction of A β in the periphery does not reduce brain A β levels (Georgievska et al., 2015) [but see Jin et al. (2017)].

To date, neurofilament light is the only biomarker that is translatable from plasma to CSF, and therefore holds great promise as a clinical tool to predict cognitive decline and neurodegeneration in AD (Figure 3; Zetterberg et al., 2016; Mattsson et al., 2017a; Lewczuk et al., 2018). Furthermore, it has been shown that measurements in blood and CSF levels strongly correlate and that neurofilament light increases coincided with the onset and progression of corresponding amyloid pathology in the brain (Figure 3; Bacioglu et al., 2016). Studies have shown that plasma neurofilament light can be used as a non-invasive biomarker that strongly correlates with neurodegeneration in human AD patients (Mattsson et al., 2019). Moreover, plasma t-tau levels can be used for screening and prognosis of cognitive decline in patients where CNS injury has been ruled out (Molinuevo et al., 2018). However, there are decreased amounts of tau in plasma compared to CSF (Barten et al., 2017; Mattsson et al., 2017b), but increases have been found in plasma of AD patients when compared to MCI patients and healthy controls (Figure 3; Mattsson et al., 2016; Pase et al., 2019). Studies looking at circulating RNA biomarkers for AD have reported that changes in levels of blood miRNA distinguished AD patients from healthy controls with 93% accuracy (Figure 3; Leidinger et al., 2013; Swarbrick et al., 2019). Therefore, blood miRNAs could be an addition to the biomarker toolbox for diagnosing AD patients. For a more extensive review on comparisons between CSF and blood biomarkers in AD, and developments in biochemical analyses of blood, see Ashton et al. (2020).

METHODS FOR CSF SAMPLING

CSF Collection in Human Patients

The most commonly used method for sampling CSF in human patients is by lumbar puncture. Clinically, lumbar punctures are routinely performed for diagnosing multiple brain disorders (e.g., meningitis, encephalitis, multiple sclerosis) and for the administration of spinal anesthesia and chemotherapy. However, there are several limitations associated with the use of lumbar punctures, such as associated pain during and after the sampling (including post-puncture headache) in patients (Blennow et al., 2015). Additionally, CSF sampling in patients who cannot cognitively consent to the procedure is ethically problematic. One also needs to keep in mind that A β is higher in lumbar CSF (Brandner et al., 2014), and tau is higher in ventricular CSF (Tarnaris et al., 2011; Pyykkö et al., 2014; Herukka et al., 2015) when using this method for CSF collections. However, the timing of intraventricular CSF sampling will likely affect concentrations of A β and tau, for example whether the sample is taken immediately after the insertion of a ventricular catheter. Research suggests that increased ventricular CSF tau concentrations may be caused by the sampling procedure itself, whereby neurons affected by the insertion of the needle for spinal tap increasingly release tau molecules (Brandner et al., 2014). In line with this, CSF samples taken shortly after surgery often have elevated tau and neurofilament light levels (Barten et al., 2017). CSF flow rate is slower in lumbar regions compared to cephalic regions (Sweetman and Linninger, 2011), and this may additionally cause the differences in concentrations of analytes. However, contradictory evidence suggests that p- and t-tau concentrations are 20–30% lower in intraventricular CSF, compared to lumbar CSF, and that this initial upregulation post-surgery is stable in patients irrespective of brain A β pathology (Leinonen et al., 2019).

CSF Collection in Animal Models

The most commonly used method for sampling CSF in rodents is collections from the cisterna magna, however, this sampling method usually constitutes a terminal procedure. Collections from the cisterna magna in preclinical models for *in vivo* sampling of CSF have proven a valuable technique for studying treatment outcomes after drug delivery to the CNS. This CSF sampling method offers the advantage of serial sampling without the confound of anesthesia, with the added benefit of using animals as their intrinsic controls (Amen et al., 2017). Another technique involves inverting animals during CSF collection in order to drain spinal CSF into the cisterna magna (DeMattos et al., 2002). An alternative technique involves collecting CSF by puncturing the membrane by suction using a pipette (DeMattos et al., 2002; Barten et al., 2011). One major limitation of collections from the cisterna magna in preclinical models is the small volume of CSF that can be obtained. In transgenic mice, the average volume is approximately 5–15 μ l for terminal sampling (Liu and Duff, 2008). For serial sampling, a maximum of 7–8 μ l can be safely taken each time at an interval of 2–3 months (Liu and Duff, 2008).

Microdialysis is an alternative CSF sampling technique, which allows continuous *in vivo* sampling of molecules within the extracellular space (Takeda et al., 2011), which may help circumvent some of the above limitations. Sampling using this method relies on diffusion of analytes across a semi-permeable dialysis membrane (Takeda et al., 2011). This method is advantageous over other CSF sampling techniques as it enables serial sampling that follows the dynamic temporal alterations of a target molecule without necessitating the collection of biopsy samples or sacrifice (Meyding-Lamadé et al., 1996; Trickler and Miller, 2003; Liu et al., 2004; Liu and Duff, 2008). Importantly, each preclinical model can serve as their own intrinsic control in order to reduce inter-animal variability and the number of animals used in experiments. One limitation of this method, however, is detection of large molecules due to adsorption in tubing and the dialysis membrane, as well as low concentration of analytes in the target tissue (Ao and Stenken, 2006). Furthermore, histochemical techniques have revealed that severe gliosis around implanted devices such as microdialysis cannulas takes place at about 4 days after the surgery (Hamberger et al., 1985; Benveniste and Diemer, 1987; Benveniste et al., 1987). Reports suggest that a complete recovery of physiological functions occurs at the earliest at 5–7 days after the implantation surgery (Drijfhout et al., 1995).

CSF AD BIOMARKERS AND TREATMENT

Studies suggest that the neuropathological events that occur in AD may disturb physiological functions of the BBB and thereby distribution of drugs to the brain (Pahnke et al., 2014; Vellonen et al., 2017). Drug molecules in the peripheral circulation are controlled and limited from entry into the brain by the BBB, while dysfunction of the BBB has been associated with neurodegeneration (Vellonen et al., 2017). Furthermore, AD drugs may not be transported to their site of action due to a dysfunctional BBB. This may lead to an increase of the drug in the brain leading to unwanted effects, or decreased drug circulation leading to an insufficient response (Vellonen et al., 2017). Many agents are better dosed directly into the CSF than peripherally because of limited permeability of the drug through the BBB (Barten et al., 2017). The presence of A β plaques, brain atrophy and dilated ventricles in the AD brain may affect the distribution of drugs in brain tissue (Vellonen et al., 2017). CSF levels of autophagic markers, A β and tau may help select an appropriate AD treatment for the timepoint of diagnosis. The CSF pharmacokinetics of a treatment after administration may show how well the drug entered the CNS. Therefore, levels of CSF autophagic markers or A β could be a pharmacodynamic marker of inhibited A β production (Dockens et al., 2012; Albright et al., 2013; Coric et al., 2015), and, in a longer term, CSF tau decreases could be a downstream functional marker of reduced neurodegeneration (Riekse et al., 2006).

Assessing Autophagy in CSF Samples

Inductors of autophagy could be used in order to halt or stop the development and progression of A β pathology in model systems and patients with AD. Trehalose, an inductor of autophagy,

was found to significantly improve memory and learning tasks in APP/PS1 mice (Rami, 2009). Importantly, A β deposits were found to be significantly reduced in the hippocampus of these mice (Rami, 2009). Furthermore, the induction of autophagy by rapamycin in another model system was found to improve cognitive performance through the degradation of extracellular A β depositions (Rami, 2009), and has been found by others to inhibit tau pathology (Caccamo et al., 2010). In AD, changes in early endocytosis and autophagy can be detected in CSF (Armstrong et al., 2014). Moreover, some work within the AD field has focused on lysosomal proteins, as they can be found in and around amyloid plaques and is present in CSF (Cataldo and Nixon, 1990; Schwagerl et al., 1995). It is now widely believed that the deposition of A β is an early initiator of neurodegeneration in AD, thus finding methods that can reduce A β or enhance its clearance could be a strong therapeutic target. In this sense, autophagy appears to be the first line of defense against accumulation of A β .

Assessing A β Pathology in CSF Samples

Cerebrospinal fluid A β 40 and A β 42 may be useful (in addition to other biomarkers) in assessing efficacy of drugs such as BACE1 inhibitors, which selectively decrease toxic forms of A β (Kennedy et al., 2016). For instance, when CSF levels of A β 42 are still rising during early stages of amyloid pathology, decreased levels of CSF A β 42 measured after treatment would show a successful outcome, but at a later stage in amyloid pathology the same finding may indicate accelerated plaque formation (Liu et al., 2004). Anti-amyloid agents are most likely more effective during early AD since deposition of the protein begins many years before diagnosis (Musiek and Holtzman, 2015). Promoting the elimination of A β by enzymatic degradation or by clearance enhancement may halt both the aggregation and the accumulation of the peptide (Menendez-Gonzalez et al., 2018). The choroid plexus is known to produce A β (Krzyszczanowska and Carro, 2012), thus the effect of A β synthesis inhibitors on CSF A β is bound to reflect changes both sourced in the brain and in the choroid plexus. In addition, evidence suggests that the choroid plexus can remove substances, such as A β , from the CSF (Matsumoto et al., 2015).

BACE1 Inhibitors

A potent BACE1 inhibitor known as Verubecestat has been shown to reduce plasma, CSF and brain levels of A β 40, A β 42, and soluble APP β (a direct product of BACE1 enzymatic activity) after short- and long-term administration in rats and monkeys (Kennedy et al., 2016). Recently, a study in healthy elderly AD subjects who received treatment with a BACE1 inhibitor showed no alterations in CSF BACE1 levels following treatment, but revealed a strong link between levels of CSF BACE1 and downstream markers such as CSF A β 42 (Timmers et al., 2017). Genetic deletion of BACE1 eliminated A β production and resolved the amyloid plaques and cognitive deficits observed in transgenic mice over-expressing human APP with familial AD mutations (Dominguez et al., 2005; McConlogue et al., 2007; Ohno et al., 2007). Researchers have demonstrated that long-term BACE1 inhibition diminishes CSF tau levels both in early

depositing APP transgenic mice and APP transgenic mice with moderate A β pathology (Schelle et al., 2017). Overall, BACE1 inhibition appears to not only reduce A β generation, but also downstream AD neuropathology (Schelle et al., 2017).

γ -Secretase Inhibitors

γ -secretase inhibitors have also proven promising as a therapeutic approach; APP/PS1 mice treated with this compound displayed that a modest decrease (~30%) of A β in ISF was enough to halt amyloid plaque development (Yan et al., 2009). Also, NGP 555 (a γ -secretase inhibitor) has been shown to shift amyloid peptide production to the smaller, non-aggregating forms of amyloid (Olsson et al., 2014; Kounnas et al., 2017). Inhibition of γ -secretase has initially been unsuccessful as a therapeutic target (Cummings, 2010), but more recent compounds have been shown to avoid notch-related toxicity and side effects (Basi et al., 2010; Imbimbo et al., 2010). One failure of slowing A β production in patients may be that non-homogenous groups of patients have been included in the trials, and that the treatment has been administered too late in the disease course or has been too short (Bjerke and Engelborghs, 2018). In line with this, some clinical trials have reported changes in CSF A β 42, but no improvement in clinical endpoints (Ritter and Cummings, 2015).

COMPARATIVE BIOMARKING

Studies aiming to translate findings between AD system models and patients found that tau derived from AD brains injected into susceptible mouse models induced prion-like tau aggregation (Skachokova et al., 2019). CSF from AD or MCI patients injected into the hippocampus of young P301S tau transgenic mice increased tau phosphorylation and NFT formation 4 months following injection. Post-seeding, the injections accentuated tau pathology in the contralateral hippocampus of the mice, indicative of spreading (Skachokova et al., 2019). Other researchers found that peritoneal dialysis reduced plasma A β levels in both chronic kidney disease patients and APP/PS1 mice. ISF A β levels in APP/PS1 mice immediately decreased after reducing blood A β by peritoneal dialysis. The treatment also attenuated other AD-type pathologies, including inflammation, tau hyperphosphorylation, neurodegeneration, synaptic dysfunction, and rescued the behavioral deficits of the mice. Importantly, the A β phagocytic function of microglia was enhanced in APP/PS1 mice after peritoneal dialysis (Jin et al., 2017). Current strategies for clearing A β focus on introducing agents into the brain (Jin et al., 2017), but this likely causes adverse effects such as neuroinflammation and tissue scarring (Iijima-Ando et al., 2008; Liu et al., 2012), in addition to increased endogenous tau levels.

The ABC Scoring System

Well-characterized mouse models hold great translational value given that identifying patients at preclinical AD stages has proven difficult (Bacioglu et al., 2016). However, there are important differences between species, which should be kept in mind while interpreting results (Barten et al., 2017). The ideal

TABLE 2 | The ABC scoring system developed by NIA-AA.

| Assessment | NIA-AA scoring |
|--|-------------------|
| A β plaques | A0 (not) |
| | A1 (low) |
| | A2 (intermediate) |
| NFTs, including pretangles and threads | A3 (high) |
| | B0 (not) |
| | B1 (low) |
| Neuritic and diffuse plaque density | B2 (intermediate) |
| | B3 (high) |
| | C0 (not) |
| | C1 (sparse) |
| | C2 (moderate) |
| | C3 (frequent) |

The scoring system can be used to help assess and validate the neuropathological features of AD in mouse lines that are potential preclinical models for AD research. Reproduced with permission from Keene et al. (2016). NIA-AA, Alzheimer's Association; A β , amyloid- β ; NFT, neurofibrillary tangle.

translational model for AD would require A β and tau deposition in a pathological manner and disease-relevant accumulation of amyloid plaques and tangles similar to that seen in AD patients (Keene et al., 2016). The ABC scoring system (Table 2) can be used to determine the level of AD neuropathological change in both system models and patients. The ABC score is generated by a summary of measures of amyloid plaque distribution A0 to A3 (Thal stages), NFT distribution B0 to B3 (Braak stages), and cortical neuritic plaque density C0 to C3 [Consortium to Establish a Registry for Alzheimer's Disease (CERAD) score] (Keene et al., 2016). The ideal translational model system of human AD would display amyloid plaques and NFTs in a spatial and temporal manner correlating with "no" or "low" AD pathology at early ages, progressing to "intermediate" and "high" AD pathology at older ages or in the presence of gene mutations related to neuropathological development (Keene et al., 2016).

In terms of the specifics of the ABC scoring system (Table 2), scoring of diffuse A β plaques is based on assessment in the cerebral cortex, hippocampus, striatum, midbrain, brainstem, and cerebellum (Box 1) according to staging established by Thal et al. (2002) resulting in a Thal phase 0–5, which is translated into the NIA-AA score of A0–A3. Meanwhile, scores for NFTs are determined in the *trans*-entorhinal cortex, corpora ammonis, fronto-parietal cortex, and primary visual cortex (Box 1) to generate a Braak stage (Braak and Braak, 1991), which is translated into the NIA-AA score of B0–B3. Since most existing mouse models do not generate NFTs, the NIH have developed a modified B score for p-tau pathology, including distribution of pre-tangles and threads. In addition, most existing mouse models do not form neuritic plaques (contains fibrillar A β), so a C score for CERAD (Sperling et al., 2011) neuritic plaque density (none, sparse, moderate, or frequent) and a modified C score for diffuse plaque (does not contain fibrillar A β) density are generated from frontal and parietal cortex. Considering that behavioral data from mice have replication issues and are challenging to translate to patients, memory testing *per se* should not constitute a validation criterion or a drug testing endpoint (Keene et al., 2016).

CSF Collection Methods

When translating CSF biomarkers between system models and patients, an advantage with subcutaneous access systems is that drugs can be dosed and also samples can be obtained from unanesthetized animals, as is typical with humans, and without the confound of anesthesia on CSF production or flow. It has been shown that anesthesia can cause disturbances in neurotransmitter density and cell metabolism, and therefore most times, it is desirable to perform experiments on non-anesthetized animals (Kehr, 1999). It is important to note that in most rodent studies, CSF is collected from the cisterna magna above the spinal column, whereas in humans most CSF is collected from the lumbar spinal vertebrae, and therefore drainage from this latter area in preclinical models has a translational advantage (Barten et al., 2017).

Due to the difficulties in collecting CSF samples from preclinical models the quality of the sample may be comprised, and therefore should be tested. The quality of the sample is most often affected by blood and brain-derived protein contamination (Barten et al., 2017). It is critical to minimize blood-contamination when analytes of interest are found in much higher concentration in the blood compared to the CSF, such as the 1:50,000-fold gradient of tau. Another major contamination source of CSF is proteins released in the brain during the collection procedure; this has a higher impact on tau levels compared to A β (Barten et al., 2005).

Furthermore, biomarker development for clinical utility is currently being hampered as comparisons of measurements and techniques between laboratories tend to be unreliable. Factors that may induce variability include storage in different tube types, different aliquot volumes, and the number of freeze-thaw cycles performed, which significantly influences CSF biomarker concentrations (Clough, 2005; Bjerke and Engelborghs, 2018). For instance, CSF A β 42 measures have been found to be greatly influenced by pre-analytical factors such as the type of collection tube used and the number of freeze-thaw cycles of the sample (Perret-Liaudet et al., 2012b; Toombs et al., 2013; Leitão et al., 2015). Various studies have determined the importance of tube types when collecting CSF samples, highlighting that it is crucial to use polypropylene vials (Perret-Liaudet et al., 2012a), and that the tubes are filled to enhance the volume to surface ratio (Perret-Liaudet et al., 2012a). Ultimately there is poor standardization of biobanking protocols and assay consistency, a fact that hampers novel biomarker discoveries and replication of important findings (Teunissen et al., 2018).

One of the reasons why non-human primates are being preferred over canine or rodent species in CSF studies is that they share an upright orientation of the spinal column akin to humans (Spector et al., 2015). Moreover, the difference in brain size (and thereby CSF volume) between mice and humans is over 3000 times, whereas macaque brains are 10- to 20-fold smaller than human brains. Therefore, the distance from the CSF compartments to deeper regions of the brain significantly varies across species and likely influences the exchange analytes (Spector et al., 2015). Nevertheless, most differences across species are otherwise minor, including the volume ratio of CSF to the brain, ranging from 9 to 18% across species

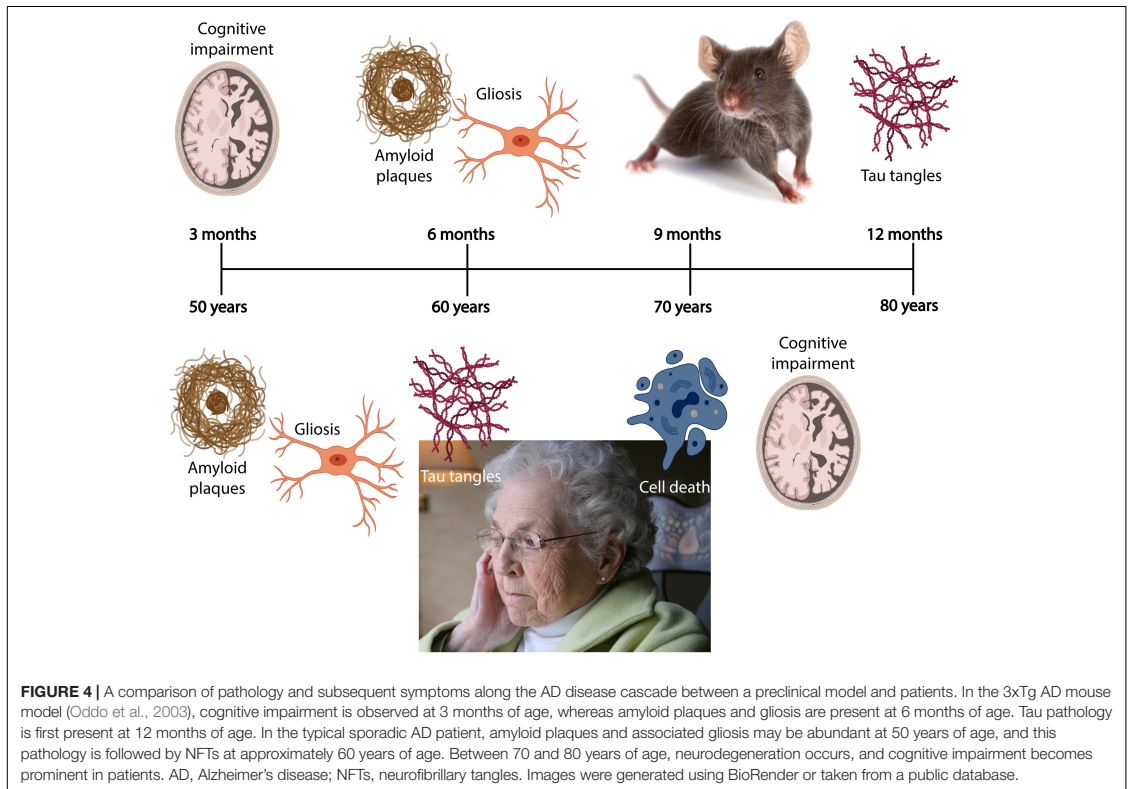
(Barten et al., 2017). CSF turnover per day is also similar between humans and macaques, but is approximately 2-fold higher for rats and 3-fold higher for mice (Barten et al., 2017). The higher turnover rate for rodents can be explained by movement of CSF initiated by the ventricles and arterial pressure as a result of a fast heartbeat, which creates an increase in back- and-forth movement of the CSF (Feinberg and Mark, 1987; Sweetman and Linninger, 2011).

The Physiology of CSF

The exchange of CSF analytes (including therapeutics) may be highly different between patients and rodents as the latter have a much faster heart rate. However, this factor has not been studied. Non-human primates are most likely better preclinical *in vivo* models for biomarker translation because body weight-based allometric scaling is comparable (Karelina et al., 2017). Moreover, ventricular CSF from AD patients has been found to contain a rare high-molecular-weight tau species that was found to exert high seeding activity (Takeda et al., 2016). This needs to be kept in mind when comparing CSF samples gathered from different regions. Moreover, the sleep-wake cycle regulates ISF and CSF levels of A β in AD (Holth et al., 2019), and it has been shown that chronic sleep deprivation increases A β plaques. Mouse ISF tau was found to increase \sim 90% during normal wakefulness versus sleep and \sim 100% during sleep deprivation. The relevant study found that sleep deprivation significantly increased CSF A β by 30% (Lucey et al., 2018). This means that the time of day is bound to influence A β levels in CSF, which suggests that the timing of sampling needs to be chosen with care and kept consistent between clinical sampling and experiments for correct comparisons.

The Efficacy of Drugs

One major drawback of comparative biomarking is the translatability of AD drugs from animal models to human clinical trials. Compared to preclinical models, AD pathology in patients develops over decades rather than over months. Longitudinal studies in AD system models may determine the initiation and progression of biomarkers that allow for evaluation of disease-modifying drugs. For example, research shows that BACE1 inhibitors can decrease both plasma and CSF A β 40 and A β 42 concentrations in mice, guinea pigs (Tagawa et al., 1991), and non-human primates (Sankaranarayanan et al., 2009; Gravenfors et al., 2012; Jeppsson et al., 2012; Wu et al., 2012). A separate study found that a γ -secretase inhibitor reduced CSF A β production in rhesus monkeys without a subsequent rise in A β production (Cook et al., 2010). Candidates for therapeutics could be further addressed by extending these findings to translational transgenic AD models and may ultimately offer insights into mechanisms of the disease. Furthermore, increased plasma levels of interleukin-10 has been shown following A β immunotherapy in Tg2576 mice (Town et al., 2002; Kim et al., 2007). In a separate study, researchers found that peripheral structures play important roles in clearing A β sourced from the brain, suggesting that removing A β from the blood may also be effective as an AD therapy (Jin et al., 2017).



γ -secretase modulators have proven especially useful as therapeutic candidates because they do not alter the total amount of A β peptides produced by γ -secretase activity, instead, they spare the products of other γ -secretase processing, such as notch (Toyn et al., 2016). Importantly, these compounds do not accelerate the production of the potentially toxic product BACE1-C-terminal fragment (C99) (Toyn et al., 2016). In all species, research suggests that γ -secretase modulator treatment decrease A β 42 and A β 40 levels while increasing A β 38 and A β 37 by a corresponding amount. Therefore, the mechanism of action of γ -secretase modulators may translate well across species, validating its therapeutic strategy for utility in AD (Toyn et al., 2016).

Other translational research across species has shown increased levels of plasma interleukin-10 following A β immunotherapy in Tg2576 mice (Town et al., 2002; Kim et al., 2007). Thereby, translation of inflammatory mechanisms and their peripheral markers may benefit from investigation of changes in microglial markers. However, when interpreting and comparing immune markers from mice caution is warranted, as recent evidence suggests that these markers do not translate well to human inflammatory diseases (Seok et al., 2013). Moreover, increased levels of isoprostanes have been shown in Tg2576 mice prior to plaque formation (Pratico et al., 2001), suggesting

isoprostane levels may be useful as a predictive biomarker. Neurofilament light in bodily fluid constitutes a biomarker of neurodegeneration reflecting its translational value in system models and in clinical settings (Bacioglu et al., 2016).

Comparative AD Neuropathology

The earliest (current) detectable A β deposition in humans is the formation of diffuse plaques, whereas in the brain of Tg2576 mice diffuse plaques are not observed until 12 months of age, which is 4 months after biochemically detectable alterations of A β (Kawarabayashi et al., 2001). The most common observation in AD patients is minor amounts of A β 40 deposited in the brain, whereas in 33% of patients great amounts of this A β variant are detected. Intriguingly, this latter group of patients also display substantial amyloid angiopathy (amyloid build up on the walls of the arteries in the brain) (Gravina et al., 1995). Similarly, the Tg2576 mouse model displays marked angiopathy and the deposition of a large amount of A β 40 (Gravina et al., 1995). Generally CSF A β 40 levels are much higher in patients compared to mice, while brain concentrations are similar (Karelina et al., 2017). In terms of plasma concentrations of A β 40, this is highly similar between patients and mice, and therefore the greater A β 40 concentrations observed in human CSF may likely reflect a higher brain production of the peptide (Karelina et al., 2017).

In terms of the similarity between system models and patients, and specifically transgenic mice and human patients, mice and humans share virtually the same set of genes. Almost every gene found in mice or humans has been observed in a closely related form in the other. To look directly at differences along the AD disease cascade, we compare pathological events between the 3xTg AD mouse model and sporadic AD patients (Figure 4). The 3xTg AD mouse model develops amyloid and tau pathology, including amyloid plaques and NFTs (Oddo et al., 2003). At 3 months of age these mice have developed cognitive impairment (Oddo et al., 2003), whereas at approximately 50 years of age an AD patient has developed amyloid plaques and gliosis (Braak and Del Trecidi, 2015). At 6 months of age, the mice develop amyloid plaques and gliosis (Oddo et al., 2003), while patients develop tau tangles at approximately 60 years of age (Braak and Del Trecidi, 2015). At 70 years of age, patients usually suffer from neurodegeneration because of the presence of tau tangles and exhibit cognitive impairment (Braak and Del Trecidi, 2015). First at 12 months of age will the mice develop tau tangles (Oddo et al., 2003).

There are two important differences observed along the AD disease cascade between the species: first, mice exhibit cognitive impairment prior to tau tangles, whereas cognitive impairment is most likely a result from neurodegeneration caused by NFTs in human patients. Second, one does not observe neuronal death in this mouse model, while neuronal death is thought to be the sole causative pathology for symptom development in AD patients. In line with this, by comparing CSF, plasma and *in vivo* amyloid imaging, cross-sectional data obtained at baseline in individuals from AD families enrolled in the Dominantly Inherited Alzheimer Network (DIAN) show lower concentrations of CSF A β 42 when amyloid plaques accumulate, and elevated concentrations of CSF t-tau and p-tau in mutation carriers 10–20 years prior to symptom onset and detection of cognitive deficits (Fagan et al., 2014). This highlights the need for longitudinal CSF sampling in animals modeling AD, in order to compare biochemical, imaging and behavioral tests against each other, and eventually to patients. However, given the difficulty of identifying patients at preclinical AD stages, it is important to remember that well-characterized preclinical disease models hold great translational value (Mattsson et al., 2017a).

CONCLUSION AND FUTURE DIRECTIONS

Clearly, there is a pressing need for better quality data from model systems investigating biomarkers that can be directly translated to human biomarkers. The core biomarkers (A β 42, t-tau, and p-tau) have been found to translate well across species, whereas biomarkers of inflammation translate to a lesser extent between mouse models and patients. Researchers should use autophagic and synaptic degeneration markers when analyzing samples from preclinical models because these markers appear promising in predicting development of AD. Changes in levels of autophagic markers and neurofilament light correlate

strongly with the core biomarkers of AD, and other novel biomarkers should be tested in combination in preclinical models to validate findings observed in patients. Currently, non-invasive structural and functional imaging can detect AD onset and longitudinally monitor disease progression in AD patients. By the combination of early predictive CSF biomarkers, imaging modalities can be strengthened in their ability to characterize patients along the disease cascade. Additional non-invasive methods for detecting AD biomarkers need to be established, such as blood sampling, which could be used in combination with CSF sampling. CSF sampling is invasive but reflects changes in protein levels in the brain to a greater extent compared to blood-based markers. Another advantage of CSF sampling compared to blood testing is that A β is found in the periphery, so it is difficult to differentiate between brain- and periphery-based A β levels. Additionally, there are greater levels of tau in ISF compared to CSF, so this needs to be controlled for when analyzing CSF samples. Neurofilament light is transferable between CSF and plasma in humans, but this needs to be verified in system models.

Furthermore, large inter- and intra-laboratory variations in biomarker sampling may have great consequences in terms of comparisons of results, while within individual laboratories such variations may affect planning and interpretations of longitudinal studies (Blennow et al., 2015). One also needs to consider differences in the CSF sampling methods used, given that protein levels differ between ventricular and lumbar CSF. Studies have shown that changes in the levels of core biomarkers as measured in CSF may be useful for assessing the efficacy of drugs. When translating findings across species, it is important to use the same scoring or grouping system when assessing changes in biomarkers and observed neuropathology. Ultimately, an early diagnosis by utilizing biomarkers detectable at this stage of disease will be the cornerstone for early identification of patients that are regressing away from the prodromal stage of AD (Teunissen et al., 2018). There is a need for continued progress within the AD biomarker field so that markers can be translated across animal models and clinical populations to serve as a translational bridge between model systems and clinical populations (Sabbagh et al., 2013). We still cannot translate all pathological hallmarks seen in AD patients to preclinical models, and we therefore need to be aware of pertinent differences when comparing AD research across species and bringing findings into the clinic.

AUTHOR CONTRIBUTIONS

All authors contributed to the content of the article, and critically reviewed and edited the manuscript.

FUNDING

This work was supported by the Liaison Committee for Education, Research and Innovation in Central Norway (Samarbeidsorganet HMN- NTNU) grant number 2018/42794.

ACKNOWLEDGMENTS

The authors would like to acknowledge support by the Liaison Committee for Education, Research and

Innovation in Central Norway (Samarbeidsorganet HMN-NTNU), and the Joint Research Committee between St. Olavs Hospital and the Faculty of Medicine and Health Sciences, NTNU.

REFERENCES

- Afanador, L., Roltsch, E. A., Holcomb, L., Campbell, K. S., Keeling, D. A., Zhang, Y., et al. (2014). The Ca²⁺ sensor S100A1 modulates neuroinflammation, histopathology and Akt activity in the PSAPP Alzheimer's disease mouse model. *Cell Calcium* 56, 68–80. doi: 10.1016/j.ceca.2014.05.002
- Ahmed, Z., Cooper, J., Murray, T. K., Garn, K., McNaughton, E., Clarke, H., et al. (2014). A novel in vivo model of tau propagation with rapid and progressive neurofibrillary tangle pathology: the pattern of spread is determined by connectivity, not proximity. *Acta Neuropathol.* 127, 667–683. doi: 10.1007/s00401-014-1254-6
- Akama, K., and Van Eldik, L. (2000). β -Amyloid stimulation of Inducible nitric-oxide synthase in astrocytes Is interleukin- β - and tumor necrosis factor- α (TNF α)-dependent, and involves a TNF α receptor-associated factor- and nfkb-inducing kinase-dependent signaling mechanism. *J. Biol. Chem.* 275, 7918–7924. doi: 10.1074/jbc.275.11.7918
- Akiyama, H., Barger, S., Barnum, S., Bradt, B., Bauer, J., Cole, G. M., et al. (2000). Inflammation and Alzheimer's disease. *Neurobiol. Aging* 21, 383–421. doi: 10.1016/s0197-4580(00)00124-x
- Albright, C. F., Dockens, R. C., Meredith, J. E., Olson, R. E., Slemmon, R., Lentz, K. A., et al. (2013). Pharmacodynamics of selective inhibition of γ -secretase by avagacestat. *J. Pharmacol. Exp. Ther.* 344, 686–695. doi: 10.1124/jpet.112.199356
- Alcolea, D., Vilaplana, E., Suarez-Calvet, M., Illan-Gala, I., Blesa, R., Clarimon, J., et al. (2017). CSF sAPP β , YKL-40, and neurofilament light in frontotemporal lobar degeneration. *Neurology* 89, 178–188. doi: 10.1212/wnl.0000000000004088
- Alzheimer, A., Stelzmann, R. A., Schnitzlein, H. N., and Murtagh, F. R. (1995). An English translation of Alzheimer's 1907 paper, "Über eine eigenartige Erkrankung der Hirnrinde. *Clin. Anat.* 8, 429–431. doi: 10.1002/ca.980080612
- Amador-Ortiz, C., Lin, W. L., Ahmed, Z., Personett, D., Davies, P., Duara, R., et al. (2007). TDP-43 immunoreactivity in hippocampal sclerosis and Alzheimer's disease. *Ann. Neurol.* 61, 435–445. doi: 10.1002/ana.21154
- Amen, E. M., Brecheisen, M., Sach-Peltason, L., and Bergadano, A. (2017). Refinement of a model of repeated cerebrospinal fluid collection in conscious rats. *Lab. Anim.* 51, 44–53. doi: 10.1177/0023677216646069
- Anderson, P. J., Watts, H. R., Jen, S., Gentleman, S. M., Moncaster, J. A., Walsh, D. T., et al. (2009). Differential effects of interleukin-1 β and S100B on amyloid precursor protein in rat retinal neurons. *Clin. Ophthalmol.* 3, 235–242. doi: 10.2147/ophth.s2684
- Andersson, C., Blennow, K., Almkvist, O., Andreasen, N., Engfeldt, P., Johansson, S. E., et al. (2008). Increasing CSF phospho-tau levels during cognitive decline and progression to dementia. *Neurobiol. Aging* 29, 1466–1473. doi: 10.1016/j.neurobiolaging.2007.03.027
- Andreasen, N., Hesse, C., Davidsson, P., Minthon, L., Wallin, A., Winblad, B., et al. (1999a). Cerebrospinal fluid beta-amyloid(1–42) in Alzheimer disease: differences between early- and late-onset Alzheimer disease and stability during the course of disease. *Arch. Neurol.* 56, 673–680. doi: 10.1001/archneur.56.6.673
- Andreasen, N., Minthon, L., Clarberg, A., Davidsson, P., Gottfries, J., Vanmechelen, E., et al. (1999b). Sensitivity, specificity, and stability of CSF-tau in AD in a community-based patient sample. *Neurology* 53, 1488–1494. doi: 10.1212/wnl.53.7.1488
- Andreasen, N., Vanmechelen, E., Van de Voorde, A., Davidsson, P., Hesse, C., Tarvonen, S., et al. (1998). Cerebrospinal fluid tau protein as a biochemical marker for Alzheimer's disease: a community based follow up study. *J. Neurol. Neurosurg. Psychiatry* 64, 298–305. doi: 10.1136/jnnp.64.3.298
- Ao, X., and Stenken, J. A. (2006). Microdialysis sampling of cytokines. *Methods* 38, 331–341. doi: 10.1016/j.ymeth.2005.11.012
- Armstrong, A., Mattsson, N., Appelqvist, H., Janefjord, C., Sandin, L., Agholme, L., et al. (2014). Lysosomal network proteins as potential novel CSF biomarkers for Alzheimer's disease. *Neuromol. Med.* 16, 150–160. doi: 10.1007/s12017-013-8269-3
- Arriagada, P. V., Growdon, J. H., Hedley-Whyte, E. T., and Hyman, B. T. (1992). Neurofibrillary tangles but not senile plaques parallel duration and severity of Alzheimer's disease. *Neurology* 42, 631–639. doi: 10.1212/wnl.42.3.631
- Asai, H., Ikezu, S., Tsunoda, S., Medalla, M., Luebke, J., Haydar, T., et al. (2015). Depletion of microglia and inhibition of exosome synthesis halt tau propagation. *Nat. Neurosci.* 18, 1584–1593. doi: 10.1038/nn.4132
- Ashton, N. J., Hye, A., Rajkumar, A. P., Leuzy, A., Snowden, S., Suárez-Calvet, M., et al. (2020). An update on blood-based biomarkers for non-Alzheimer neurodegenerative disorders. *Nat. Rev. Neurol.* 16, 265–284. doi: 10.1038/s41582-020-0348-0
- Avila, J., Lucas, J. J., Perez, M., and Hernandez, F. (2004). Role of tau protein in both physiological and pathological conditions. *Physiol. Rev.* 84, 361–384. doi: 10.1152/physrev.00024.2003
- Bacioglu, M., Maia, L. F., Preische, O., Schelle, J., Apel, A., Kaeser, S. A., et al. (2016). Neurofilament light chain in blood and csf as marker of disease progression in mouse models and in neurodegenerative diseases. *Neuron* 91, 56–66. doi: 10.1016/j.neuron.2016.05.018
- Bakota, L., and Brandt, R. (2016). Tau biology and Tau-Directed therapies for Alzheimer's disease. *Drugs* 76, 301–313. doi: 10.1007/s40265-015-0529-0
- Barten, D. M., Cadelina, G. W., and Weed, M. R. (2017). Dosing, collection, and quality control issues in cerebrospinal fluid research using animal models. *Handb. Clin. Neurol.* 146, 47–64. doi: 10.1016/B978-0-12-804279-3.00004-6
- Barten, D. M., Cadelina, G. W., Hoque, N., DeCarr, L. B., Guss, V. L., Yang, L., et al. (2011). Tau transgenic mice as models for cerebrospinal fluid tau biomarkers. *J. Alzheimers Dis.* 24(Suppl. 2), 127–141. doi: 10.3233/JAD-2011-110161
- Barten, D. M., Guss, V. L., Corsa, J. A., Loo, A., Hansel, S. B., Zheng, M., et al. (2005). Dynamics of {beta}-amyloid reductions in brain, cerebrospinal fluid, and plasma of {beta}-amyloid precursor protein transgenic mice treated with a {gamma}-secretase inhibitor. *J. Pharmacol. Exp. Ther.* 312, 635–643. doi: 10.1124/jpet.104.075408
- Basi, G. S., Hemphill, S., Brigham, E. F., Liao, A., Aubele, D. L., Baker, J., et al. (2010). Amyloid precursor protein selective gamma-secretase inhibitors for treatment of Alzheimer's disease. *Alzheimers Res. Ther.* 2:36. doi: 10.1186/alzrt60
- Bateman, R. J., Xiong, C., Benzinger, T. L. S., Fagan, A. M., Goate, A., Fox, N. C., et al. (2012). Clinical and biomarker changes in dominantly inherited Alzheimer's disease. *N. Engl. J. Med.* 367, 795–804. doi: 10.1056/NEJMoa1202753
- Bazan, J. F., Bacon, K. B., Hardiman, G., Wang, W., Soo, K., Rossi, D., et al. (1997). A new class of membrane-bound chemokine with a CX3C motif. *Nature* 385, 640–644. doi: 10.1038/385640a0
- Beckett, L. A., Harvey, D. J., Gamst, A., Donohue, M., Kornak, J., Zhang, H., et al. (2010). The Alzheimer's Disease Neuroimaging Initiative: annual change in biomarkers and clinical outcomes. *Alzheimers Dement.* 6, 257–264. doi: 10.1016/j.jalz.2010.03.002
- Benilova, I., Karran, E., and De Strooper, B. (2012). The toxic beta oligomer and Alzheimer's disease: an emperor in need of clothes. *Nat. Neurosci.* 15, 349–357. doi: 10.1038/nn.3028
- Benveniste, H., and Diemer, N. H. (1987). Cellular reactions to implantation of a microdialysis tube in the rat hippocampus. *Acta Neuropathol.* 74, 234–238. doi: 10.1007/bf00688186
- Benveniste, H., Drejer, J., Schousboe, A., and Diemer, N. H. (1987). Regional cerebral glucose phosphorylation and blood flow after insertion of a microdialysis fiber through the dorsal hippocampus in the rat. *J. Neurochem.* 49, 729–734. doi: 10.1111/j.1471-4159.1987.tb0954.x
- Bian, H., Van Swieten, J. C., Leight, S., Massimo, L., Wood, E., Forman, M., et al. (2008). CSF biomarkers in frontotemporal lobar degeneration with known pathology. *Neurology* 70, 1827–1835. doi: 10.1212/01.wnl.0000311445.21321.fc

- Billings, L. M., Oddo, S., Green, K. N., McLaugh, J. L., and LaFerla, F. M. (2005). Intraneuronal Abeta causes the onset of early Alzheimer's disease-related cognitive deficits in transgenic mice. *Neuron* 45, 675–688. doi: 10.1016/j.neuron.2005.01.040
- Biswal, B., Zerrin Yetkin, F., Haughton, V. M., and Hyde, J. S. (1995). Functional connectivity in the motor cortex of resting human brain using echo-planar MRI. *Magn. Reson. Med.* 34, 537–541. doi: 10.1002/mrm.1910340409
- Bjerke, M., and Engelborghs, S. (2018). Cerebrospinal fluid biomarkers for early and differential Alzheimer's disease diagnosis. *J. Alzheimers Dis.* 62, 1199–1209. doi: 10.3233/JAD-170680
- Blennow, K., and Hampel, H. (2003). CSF markers for incipient Alzheimer's disease. *Lancet Neurol.* 2, 605–613. doi: 10.1016/s1474-4422(03)00530-1
- Blennow, K., Dubois, B., Fagan, A. M., Lewczuk, P., de Leon, M. J., and Hampel, H. (2015). Clinical utility of cerebrospinal fluid biomarkers in the diagnosis of early Alzheimer's disease. *Alzheimers Dement.* 11, 58–69. doi: 10.1016/j.jalz.2014.02.004
- Block, M. L., Zecca, L., and Hong, J. S. (2007). Microglia-mediated neurotoxicity: uncovering the molecular mechanisms. *Nat. Rev. Neurosci.* 8, 57–69. doi: 10.1038/nrn2038
- Bolos, M., Llorens-Martin, M., Perea, J. R., Jurado-Arjona, J., Rabano, A., Hernandez, F., et al. (2017). Absence of CX3CR1 impairs the internalization of Tau by microglia. *Mol. Neurodegener.* 12:59. doi: 10.1186/s13024-017-0200-1
- Boom, A., Pochet, R., Authalet, M., Pradier, L., Borghgraef, P., Van Leuven, F., et al. (2004). Astrocytic calcium/zinc binding protein S100A6 over expression in Alzheimer's disease and in PS1/APP transgenic mice models. *Biochim. Biophys. Acta* 1742. doi: 10.1016/j.bbamer.2004.09.011
- Bouwman, F. H., van der Flier, W. M., Schoonenboom, N. S., van Elk, E. J., Kok, A., Rijmen, F., et al. (2007). Longitudinal changes of CSF biomarkers in memory clinic patients. *Neurology* 69, 1006–1011. doi: 10.1212/01.wnl.0000271375.37131.04
- Bozzali, M., Falini, A., Franceschi, M., Cercignani, M., Zuffi, M., Scotti, G., et al. (2002). White matter damage in Alzheimer's disease assessed in vivo using diffusion tensor magnetic resonance imaging. *J. Neurol. Neurosurg. Psychiatry* 72, 742–746. doi: 10.1136/jnnp.72.6.742
- Braak, H., and Braak, E. (1991). Neuropathological staging of Alzheimer-related changes. *Acta Neuropathol.* 82, 239–259. doi: 10.1007/bf03088809
- Braak, H., and Braak, E. (1997). Frequency of stages of Alzheimer-related lesions in different age categories. *Neurobiol. Aging* 18, 351–357. doi: 10.1016/s0197-4580(97)00056-0
- Braak, H., and Del Tredici, K. (2015). Neuroanatomy and pathology of sporadic Alzheimer's disease. *Adv. Anat. Embryol. Cell Biol.* 215, 1–162.
- Brandner, S., Thaler, C., Lelethal, N., Buchfelder, M., Kleindienst, A., Maler, J. M., et al. (2014). Ventricular and lumbar cerebrospinal fluid concentrations of Alzheimer's disease biomarkers in patients with normal pressure hydrocephalus and posttraumatic hydrocephalus. *J. Alzheimers Dis.* 41, 1057–1062. doi: 10.3233/JAD-132708
- Brinker, T., Stopa, E., Morrison, J., and Klinge, P. (2014). A new look at cerebrospinal fluid circulation. *Fluids Barriers CNS* 11:10. doi: 10.1186/2045-8118-11-10
- Brinkmalm, A., Brinkmalm, G., Honer, W. G., Frolich, L., Hausner, L., Minthon, L., et al. (2014). SNAP-25 is a promising novel cerebrospinal fluid biomarker for synapse degeneration in Alzheimer's disease. *Mol. Neurodegener.* 9:53. doi: 10.1186/1750-1326-9-53
- Bronzuoli, M. R., Iacomino, A., Steardo, L., and Scuderi, C. (2016). Targeting neuroinflammation in Alzheimer's disease. *J. Inflamm. Res.* 9, 199–208. doi: 10.2147/jir.S86958
- Brys, M., Pirraglia, E., Rich, K., Rolstad, S., Mosconi, L., Switalski, R., et al. (2009). Prediction and longitudinal study of CSF biomarkers in mild cognitive impairment. *Neurobiol. Aging* 30, 682–690. doi: 10.1016/j.neurobiolaging.2007.08.010
- Buchhave, P., Minthon, L., Zetterberg, H., Wallin, A. K., Blennow, K., and Hansson, O. (2012). Cerebrospinal fluid levels of beta-amyloid 1-42, but not of tau, are fully changed already 5 to 10 years before the onset of Alzheimer dementia. *Arch. Gen. Psychiatry* 69, 98–106. doi: 10.1001/archgenpsychiatry.2011.155
- Buckner, R. L., Andrews-Hanna, J. R., and Schacter, D. L. (2008). The brain's default network: anatomy, function, and relevance to disease. *Ann. N.Y. Acad. Sci.* 1124, 1–38. doi: 10.1196/annals.1440.011
- Buerger, K., Ewers, M., Pirttila, T., Zinkowski, R., Alafuzoff, I., Teipel, S. J., et al. (2006). CSF phosphorylated tau protein correlates with neocortical neurofibrillary pathology in Alzheimer's disease. *Brain* 129, 3035–3041. doi: 10.1093/brain/awl269
- Caccamo, A., Majumder, S., Richardson, A., Strong, R., and Oddo, S. (2010). Molecular interplay between mammalian target of rapamycin (mTOR), amyloid-beta, and Tau: effects on cognitive impairments. *J. Biol. Chem.* 285, 13107–13120. doi: 10.1074/jbc.M110.100420
- Calsolaro, V., and Edison, P. (2016). Neuroinflammation in Alzheimer's disease: current evidence and future directions. *Alzheimers Dement.* 12, 719–732. doi: 10.1016/j.jalz.2016.02.010
- Campioni, S., Mannini, B., Zampagni, M., Pensalfini, A., Parrini, C., Evangelisti, E., et al. (2010). A causative link between the structure of aberrant protein oligomers and their toxicity. *Nat. Chem. Biol.* 6, 140–147. doi: 10.1038/nchembio.283
- Cataldo, A. M., and Nixon, R. A. (1990). Enzymatically active lysosomal proteases are associated with amyloid deposits in Alzheimer brain. *Proc. Natl. Acad. Sci. U.S.A.* 87, 3861–3865. doi: 10.1073/pnas.87.10.3861
- Chang, K. A., Kim, H. J., and Suh, Y. H. (2012). The role of S100a9 in the pathogenesis of Alzheimer's disease: the therapeutic effects of S100a9 knockdown or knockout. *Neurodegener. Dis.* 10, 27–29. doi: 10.1159/000333781
- Chang, X.-L., Tan, M.-S., Tan, L., and Yu, J.-T. (2015). The role of TDP-43 in Alzheimer's disease. *Mol. Neurobiol.* 53, 3349–3359.
- Chen, J. J., Zhao, B., Zhao, J., and Li, S. (2017). Potential roles of exosomal MicroRNAs as diagnostic biomarkers and therapeutic application in Alzheimer's disease. *Neural Plast.* 2017:7027380. doi: 10.1155/2017/7027380
- Chen, M., Inestrosa, N. C., Ross, G. S., and Fernandez, H. L. (1995). Platelets are the primary source of amyloid beta-peptide in human blood. *Biochem. Biophys. Res. Commun.* 213, 96–103. doi: 10.1006/bbrc.1995.2103
- Cho, H., Choi, J. Y., Hwang, M. S., Kim, Y. J., Lee, H. M., Lee, H. S., et al. (2016). In vivo cortical spreading pattern of tau and amyloid in the Alzheimer disease spectrum. *Ann. Neurol.* 80, 247–258. doi: 10.1002/ana.24711
- Cho, S.-J., Lim, H. J., Jo, C., Park, M. H., Han, C., and Koh, Y. H. (2019). Plasma ATG5 is increased in Alzheimer's disease. *Sci. Rep.* 9:4741. doi: 10.1038/s41598-019-41347-2
- Chua, T. C., Wen, W., Slavin, M. J., and Sachdev, P. S. (2008). Diffusion tensor imaging in mild cognitive impairment and Alzheimer's disease: a review. *Curr. Opin. Neurol.* 21, 83–92. doi: 10.1097/WCO.0b013e3282f4594b
- Cirrito, J. R., May, P. C., O'Dell, M. A., Taylor, J. W., Parsadanian, M., Cramer, J. W., et al. (2003). In vivo assessment of brain interstitial fluid with microdialysis reveals plaque-associated changes in amyloid-beta metabolism and half-life. *J. Neurosci.* 23, 8844–8853.
- Clark, C. M., Xie, S., Chittams, J., Ewbank, D., Peskind, E., Galasko, D., et al. (2003). Cerebrospinal fluid tau and beta-amyloid: how well do these biomarkers reflect autopsy-confirmed dementia diagnoses? *Arch. Neurol.* 60, 1696–1702. doi: 10.1001/archneur.60.12.1696
- Clavaguera, F., Akatsu, H., Fraser, G., Crowther, R. A., Frank, S., Hench, J., et al. (2013). Brain homogenates from human tauopathies induce tau inclusions in mouse brain. *Proc. Natl. Acad. Sci. U.S.A.* 110, 9535–9540. doi: 10.1073/pnas.1301175110
- Clough, G. F. (2005). Microdialysis of large molecules. *AAPS J.* 7, E686–E692. doi: 10.1208/aapsj070369
- Cook, J. J., Wildsmith, K. R., Gilberto, D. B., Holahan, M. A., Kinney, G. G., Mathers, P. D., et al. (2010). Acute gamma-secretase inhibition of nonhuman primate CNS shifts amyloid precursor protein (APP) metabolism from amyloid-beta production to alternative APP fragments without amyloid-beta rebound. *J. Neurosci.* 30, 6743–6750. doi: 10.1523/jneurosci.1381-10.2010
- Coric, V., Salloway, S., van Dyck, C. H., Dubois, B., Andreasen, N., Brody, M., et al. (2015). Targeting prodromal Alzheimer Disease with avagacetat: a randomized clinical trial. *JAMA Neurol.* 72, 1324–1333. doi: 10.1001/jamaneuro.2015.0607
- Craig-Schapiro, R., Perrin, R. J., Roe, C. M., Xiong, C., Carter, D., Cairns, N. J., et al. (2010). YKL-40: a novel prognostic fluid biomarker for preclinical Alzheimer's disease. *Biol. Psychiatry* 68, 903–912. doi: 10.1016/j.biopsych.2010.08.025
- Cristovao, J. S., Morris, V. K., Cardoso, L., Leal, S. S., Martinez, J., Botelho, H. M., et al. (2018). The neuronal S100B protein is a calcium-tuned suppressor of amyloid-beta aggregation. *Sci. Adv.* 4, eaq1702. doi: 10.1126/sciadv.aq1702

- Cummings, J. (2010). What can be inferred from the interruption of the semagacestat trial for treatment of Alzheimer's disease? *Biol. Psychiatry* 68, 876–878. doi: 10.1016/j.biopsych.2010.09.020
- Davies, P., Resnick, J., Resnick, B., Gilman, S., Growdon, J. H., Khachaturian, Z. S., et al. (1998). Consensus report of the working group on: "molecular and biochemical markers of Alzheimer's disease. *Neurobiol. Aging* 19, 109–116. doi: 10.1016/S0197-4580(98)00022-0
- de Bussard, C. N., Lundin, A., Karlstedt, D., Edman, G., Bartfai, A., and Borg, J. (2005). S100 and cognitive impairment after mild traumatic brain injury. *J. Rehabil. Med.* 37, 53–57. doi: 10.1080/16501970410015587
- de Leon, M. J., DeSanti, S., Zinkowski, R., Mehta, P. D., Pratico, D., Segal, S., et al. (2006). Longitudinal CSF and MRI biomarkers improve the diagnosis of mild cognitive impairment. *Neurobiol. Aging* 27, 394–401. doi: 10.1016/j.neurobiolaging.2005.07.003
- de Leon, M. J., Ferris, S. H., George, A. E., Christman, D. R., Fowler, J. S., Gentes, C., et al. (1983). Positron emission tomographic studies of aging and Alzheimer disease. *AJNR Am. J. Neuroradiol.* 4, 568–571.
- de Souza, L. C., Chupin, M., Lamari, F., Jardel, C., Leclercq, D., Colliot, O., et al. (2012). CSF tau markers are correlated with hippocampal volume in Alzheimer's disease. *Neurobiol. Aging* 33, 1253–1257. doi: 10.1016/j.neurobiolaging.2011.02.022
- De Vos, A., Jacobs, D., Struyfs, H., Franssen, E., Andersson, K., Portelius, E., et al. (2015). C-terminal neurogranin is increased in cerebrospinal fluid but unchanged in plasma in Alzheimer's disease. *Alzheimers Dement.* 11, 1461–1469. doi: 10.1016/j.jalz.2015.05.012
- DeMattos, R. B., Bales, K. R., Parsadanian, M., O'Dell, M. A., Foss, E. M., Paul, S. M., et al. (2002). Plaque-associated disruption of CSF and plasma amyloid-beta (Aβ) equilibrium in a mouse model of Alzheimer's disease. *J. Neurochem.* 81, 229–236. doi: 10.1046/j.1471-4159.2002.00889.x
- Desikan, R. S., McEvoy, L. K., Thompson, W. K., Holland, D., Brewer, J. B., Aisen, P. S., et al. (2012). Amyloid-beta-associated clinical decline occurs only in the presence of elevated P-tau. *Arch. Neurol.* 69, 709–713. doi: 10.1001/archneurol.2011.3354
- Desikan, R. S., McEvoy, L. K., Thompson, W. K., Holland, D., Roddey, J. C., Blennow, K., et al. (2011). Amyloid-beta associated volume loss occurs only in the presence of phospho-tau. *Ann. Neurol.* 70, 657–661. doi: 10.1002/ana.22509
- Desikan, R. S., Sabuncu, M. R., Schmansky, N. J., Reuter, M., Cabral, H. J., Hess, C. P., et al. (2010). Selective disruption of the cerebral neocortex in Alzheimer's disease. *PLoS One* 5:e12853. doi: 10.1371/journal.pone.0012853
- Dickerson, B. C., Bakkour, A., Salat, D. H., Feczko, E., Pacheco, J., Greve, D. N., et al. (2009). The cortical signature of Alzheimer's disease: regionally specific cortical thinning relates to symptom severity in very mild to mild AD dementia and is detectable in asymptomatic amyloid-positive individuals. *Cereb. Cortex* 19, 497–510. doi: 10.1093/cercor/bhn113
- Disanto, G., Barro, C., Benkert, P., Naegelin, Y., Schadelin, S., Giardiello, A., et al. (2017). Serum Neurofilament light: a biomarker of neuronal damage in multiple sclerosis. *Ann. Neurol.* 81, 857–870. doi: 10.1002/ana.24954
- Dockens, R., Wang, J.-S., Castaneda, L., Sverdlow, O., Huang, S.-P., Slemmon, R., et al. (2012). A placebo-controlled, multiple ascending dose study to evaluate the safety, pharmacokinetics and pharmacodynamics of avagacestat (BMS-708163) in healthy young and elderly subjects. *Clin. Pharmacokinet.* 51, 681–693. doi: 10.1007/s40262-012-0005-x
- Dominguez, D., Tournoy, J., Hartmann, D., Huth, T., Cryns, K., Deforce, S., et al. (2005). Phenotypic and biochemical analyses of BACE1- and BACE2-deficient mice. *J. Biol. Chem.* 280, 30797–30806. doi: 10.1074/jbc.M505249200
- Drijfhout, W. J., Kemper, R. H., Meerlo, P., Koolhaas, J. M., Grol, C. J., and Westerink, B. H. (1995). A telemetry study on the chronic effects of microdialysis probe implantation on the activity pattern and temperature rhythm of the rat. *J. Neurosci. Methods* 61, 191–196. doi: 10.1016/0165-0270(94)00041-e
- Dubois, B., Feldman, H. H., Jacova, C., Hampel, H., Molinuevo, J. L., Blennow, K., et al. (2014). Advancing research diagnostic criteria for Alzheimer's disease: the IWG-2 criteria. *Lancet Neurol.* 13, 614–629. doi: 10.1016/s1474-4422(14)70900-0
- Duyckaerts, C., Brion, J. P., Hauw, J. J., and Flament-Durand, J. (1987). Quantitative assessment of the density of neurofibrillary tangles and senile plaques in senile dementia of the Alzheimer type. Comparison of immunocytochemistry with a specific antibody and Bodian's protargol method. *Acta Neuropathol.* 73, 167–170. doi: 10.1007/BF00693783
- El Kadmiri, N., Said, N., Slassi, I., El Moutawakil, B., and Nadifi, S. (2018). Biomarkers for Alzheimer disease: classical and novel candidates' review. *Neuroscience* 370, 181–190. doi: 10.1016/j.neuroscience.2017.07.017
- Engelborghs, S., De Vreese, K., Van de Castele, T., Vanderstichele, H., Van Everbroeck, B., Cras, P., et al. (2008). Diagnostic performance of a CSF-biomarker panel in autopsy-confirmed dementia. *Neurobiol. Aging* 29, 1143–1159. doi: 10.1016/j.neurobiolaging.2007.02.016
- Engler, H., Forsberg, A., Almkvist, O., Blomquist, G., Larsson, E., Savitcheva, I., et al. (2006). Two-year follow-up of amyloid deposition in patients with Alzheimer's disease. *Brain* 129, 2856–2866. doi: 10.1093/brain/awl178
- Eskildsen, S. F., Coupe, P., Garcia-Lorenzo, D., Fonov, V., Pruessner, J. C., and Collins, D. L. (2013). Prediction of Alzheimer's disease in subjects with mild cognitive impairment from the ADNI cohort using patterns of cortical thinning. *Neuroimage* 65, 511–521. doi: 10.1016/j.neuroimage.2012.09.058
- Fagan, A. M., Xiong, C., Jasele, M. S., Bateman, R. J., Goate, A. M., Benzinger, T. L., et al. (2014). Longitudinal change in CSF biomarkers in autosomal-dominant Alzheimer's disease. *Sci. Transl. Med.* 6:226ra230. doi: 10.1126/scitranslmed.3007901
- Fan, Z., Brooks, D. J., Okello, A., and Edison, P. (2017). An early and late peak in microglial activation in Alzheimer's disease trajectory. *Brain* 140, 792–803. doi: 10.1093/brain/aww349
- Feinberg, D. A., and Mark, A. S. (1987). Human brain motion and cerebrospinal fluid circulation demonstrated with MR velocity imaging. *Radiology* 163, 793–799. doi: 10.1148/radiology.163.3.3575734
- Finneran, D. J., Morgan, D., Gordon, M. N., and Nash, K. R. (2019). CNS-wide over expression of fractalkine improves cognitive functioning in a tauopathy model. *J. Neuroimmune. Pharmacol.* 14, 312–325. doi: 10.1007/s11481-018-9822-5
- Fox, M. D., and Raichle, M. E. (2007). Spontaneous fluctuations in brain activity observed with functional magnetic resonance imaging. *Nat. Rev. Neurosci.* 8, 700–711. doi: 10.1038/nrn2201
- Fransquet, P. D., and Ryan, J. (2018). Micro RNA as a potential blood-based epigenetic biomarker for Alzheimer's disease. *Clin. Biochem.* 58, 5–14. doi: 10.1016/j.clinbiochem.2018.05.020
- Freudenberg-Hua, Y., Li, W., and Davies, P. (2018). The role of genetics in advancing precision medicine for Alzheimer's disease—a narrative review. *Front. Med.* 5:108. doi: 10.3389/fmed.2018.00108
- Frölich, L., Peters, O., Lewczuk, P., Gruber, O., Teipel, S. J., Gertz, H. J., et al. (2017). Incremental value of biomarker combinations to predict progression of mild cognitive impairment to Alzheimer's dementia. *Alzheimers Res. Ther.* 9:84. doi: 10.1186/s13195-017-0301-7
- Gaffan, D. (1992). Amnesia for complex naturalistic scenes and for objects following fornix transection in the rhesus monkey. *Eur. J. Neurosci.* 4, 381–388. doi: 10.1111/j.1460-9568.1992.tb00886.x
- Gaffan, D. (1994). Scene-specific memory for objects: a model of episodic memory impairment in monkeys with fornix transection. *J. Cogn. Neurosci.* 6, 305–320. doi: 10.1162/jocn.1994.6.4.305
- Gaffan, D., Saunders, R. C., Gaffan, E. A., Harrison, S., Shields, C., and Owen, M. J. (1984). Effects of fornix transection upon associative memory in monkeys: role of the hippocampus in learned action. *Q. J. Exp. Psychol. Sec. B* 36, 173–221. doi: 10.1080/14640748408402203
- Garwood, C. J., Pooler, A. M., Atherton, J., Hanger, D. P., and Noble, W. (2011). Astrocytes are important mediators of Aβ-induced neurotoxicity and tau phosphorylation in primary culture. *Cell Death Dis.* 2, e167–e167. doi: 10.1038/cddis.2011.50
- Geinisman, Y., deToledo-Morrell, L., Morrell, F., Persina, I. S., and Rossi, M. (1992). Age-related loss of axospinous synapses formed by two afferent systems in the rat dentate gyrus as revealed by the unbiased stereological disector technique. *Hippocampus* 2, 437–444. doi: 10.1002/hipo.450020411
- Georgievska, B., Gustavsson, S., Lundkvist, J., Neelissen, J., Eketjall, S., Ramberg, V., et al. (2015). Revisiting the peripheral sink hypothesis: inhibiting BACE1 activity in the periphery does not alter beta-amyloid levels in the CNS. *J. Neurochem.* 132, 477–486. doi: 10.1111/jnc.12937
- Geppert, M., Goda, Y., Hammer, R. E., Li, C., Rosahl, T. W., Stevens, C. F., et al. (1994). Synaptotagmin I: a major Ca²⁺ sensor for transmitter release at a central synapse. *Cell* 79, 717–727. doi: 10.1016/0092-8674(94)90556-8

- Gisslen, M., Price, R. W., Andreasson, U., Norgren, N., Nilsson, S., Hagberg, L., et al. (2016). Plasma Concentration of the neurofilament light protein (NFL) is a biomarker of CNS Injury in HIV infection: a cross-sectional study. *EBioMedicine* 3, 135–140. doi: 10.1016/j.ebiom.2015.11.036
- Gomez-Isla, T., Price, J. L., McKeel, D. W. Jr., Morris, J. C., Growdon, J. H., and Hyman, B. T. (1996). Profound loss of layer II entorhinal cortex neurons occurs in very mild Alzheimer's disease. *J. Neurosci.* 16, 4491–4500.
- Gomez-Nicola, D., and Boche, D. (2015). Post-mortem analysis of neuroinflammatory changes in human Alzheimer's disease. *Alzheimers Res. Ther.* 7:42. doi: 10.1186/s13195-015-0126-1
- Gravenfors, Y., Viklund, J., Blid, J., Ginman, T., Karlstrom, S., Kihlstrom, J., et al. (2012). New aminoimidazoles as beta-secretase (BACE-1) inhibitors showing amyloid-beta (A β) lowering in brain. *J. Med. Chem.* 55, 9297–9311. doi: 10.1021/jm300991n
- Gravina, S. A., Ho, L., Eckman, C. B., Long, K. E., Otvos, L. Jr., Younkin, L. H., et al. (1995). Amyloid beta protein (A β) in Alzheimer's disease brain. Biochemical and immunocytochemical analysis with antibodies specific for forms ending at A β 40 or A β 42(43). *J. Biol. Chem.* 270, 7013–7016. doi: 10.1074/jbc.270.13.7013
- Greicius, M. D., and Menon, V. (2004). Default-mode activity during a passive sensory task: uncoupled from deactivation but impacting activation. *J. Cogn. Neurosci.* 16, 1484–1492. doi: 10.1162/0898929042568532
- Griffin, W. S., Stanley, L. C., Ling, C., White, L., MacLeod, V., Perrot, L. J., et al. (1989). Brain interleukin 1 and S-100 immunoreactivity are elevated in down syndrome and Alzheimer disease. *Proc. Natl. Acad. Sci. U.S.A.* 86, 7611–7615. doi: 10.1073/pnas.86.19.7611
- Grossman, M., Farmer, J., Leight, S., Work, M., Moore, P., Van Deerlin, V., et al. (2005). Cerebrospinal fluid profile in frontotemporal dementia and Alzheimer's disease. *Ann. Neurol.* 57, 721–729. doi: 10.1002/ana.20477
- Gusnard, D. A., Raichle, M. E., and Raichle, M. E. (2001). Searching for a baseline: functional imaging and the resting human brain. *Nat. Rev. Neurosci.* 2, 685–694. doi: 10.1038/35094500
- Gustafson, D. R., Skoog, I., Rosengren, L., Zetterberg, H., and Blennow, K. (2007). Cerebrospinal fluid β -amyloid 1–42 concentration may predict cognitive decline in older women. *J. Neurol. Neurosurg. Psychiatry* 78, 461–464. doi: 10.1136/jnnp.2006.100529
- Ha, T. Y., Chang, K. A., Kim, J., Kim, H. S., Kim, S., Chong, Y. H., et al. (2010). S100a9 knockdown decreases the memory impairment and the neuropathology in Tg2576 mice, AD animal model. *PLoS One* 5:e8840. doi: 10.1371/journal.pone.0008840
- Haass, C., and De Strooper, B. (1999). The presenilins in Alzheimer's disease—proteolysis holds the key. *Science* 286, 916–919. doi: 10.1126/science.286.5441.916
- Haass, C., and Selkoe, D. J. (2007). Soluble protein oligomers in neurodegeneration: lessons from the Alzheimer's amyloid beta-peptide. *Nat. Rev. Mol. Cell Biol.* 8, 101–112. doi: 10.1038/nrm2101
- Hagmeyer, S., Cristovao, J. S., Mulvihill, J. J. E., Boeckers, T. M., Gomes, C. M., and Grabrucker, A. M. (2017). Zinc binding to S100B affords regulation of trace metal homeostasis and excitotoxicity in the brain. *Front. Mol. Neurosci.* 10:456. doi: 10.3389/fnmol.2017.00456
- Hamberger, A., Berthold, C.-H., Jacobson, I., Karlsson, B., Lehmann, A., Nyström, B. et al. (1985). "In vivo brain dialysis of extracellular nontransmitter and putative transmitter amino acids" in *Vivo Perfusion and Release of Neuroactive Substances*, eds A. Bayon, and R. Drucker-Colin, (New York, NY: Academic Press Inc), 473–492.
- Hamelin, L., Lagarde, J., Dorothee, G., Leroy, C., Labit, M., Comley, R. A., et al. (2016). Early and protective microglial activation in Alzheimer's disease: a prospective study using 18F-DPA-714 PET imaging. *Brain* 139, 1252–1264. doi: 10.1093/brain/aww017
- Hampel, H., Blennow, K., Shaw, L. M., Hoessler, Y. C., Zetterberg, H., and Trojanowski, J. Q. (2010). Total and phosphorylated tau protein as biological markers of Alzheimer's disease. *Exp. Gerontol.* 45, 30–40. doi: 10.1016/j.exger.2009.10.010
- Hampel, H., Lista, S., and Khachaturian, Z. S. (2012). Development of biomarkers to chart all Alzheimer's disease stages: the royal road to cutting the therapeutic Gordian Knot. *Alzheimers Dement.* 8, 312–336. doi: 10.1016/j.jalz.2012.05.2116
- Hane, F. T., Robinson, M., Lee, B. Y., Bai, O., Leonenko, Z., and Albert, M. S. (2017). Recent progress in Alzheimer's disease research, part 3: diagnosis and treatment. *J. Alzheimers Dis.* 57, 645–665. doi: 10.3233/JAD-160907
- Hansson, O., Zetterberg, H., Buchhave, P., Andreasson, U., Londos, E. F., Minthon, L., et al. (2007). Prediction of Alzheimer's disease using the CSF A β 42/A β 40 ratio in patients with mild cognitive impairment. *Dement. Geriatr. Cogn. Disord.* 23, 316–320. doi: 10.1159/000100926
- Hardy, J. A., and Higgins, G. A. (1992). Alzheimer's disease: the amyloid cascade hypothesis. *Science* 256, 184–185. doi: 10.1126/science.1566067
- Harper, J. D., and Lansbury, P. T. Jr. (1997). Models of amyloid seeding in Alzheimer's disease and scrapie: mechanistic truths and physiological consequences of the time-dependent solubility of amyloid proteins. *Annu. Rev. Biochem.* 66, 385–407. doi: 10.1146/annurev.biochem.66.1.385
- Harrison, J. K., Jiang, Y., Chen, S., Xia, Y., Maciejewski, D., McNamara, R. K., et al. (1998). Role for neuronally derived fractalkine in mediating interactions between neurons and CX3CR1-expressing microglia. *Proc. Natl. Acad. Sci. U.S.A.* 95, 10896–10901. doi: 10.1073/pnas.95.18.10896
- He, Z., Guo, J. L., McBride, J. D., Narasimhan, S., Kim, H., Changolkar, L., et al. (2018). Amyloid-beta plaques enhance Alzheimer's brain tau-seeded pathologies by facilitating neuritic plaque tau aggregation. *Nat. Med.* 24, 29–38. doi: 10.1038/nm.4443
- Heckmann, B. L., Teubner, B. J. W., Tummers, B., Boada-Romero, E., Harris, L., Yang, M., et al. (2019). LC3-Associated endocytosis facilitates beta-amyloid clearance and mitigates neurodegeneration in murine Alzheimer's disease. *Cell* 178, 536.e14–551.e14. doi: 10.1016/j.cell.2019.05.056
- Hellstrand, E., Boland, B., Walsh, D. M., and Linse, S. (2010). Amyloid beta-protein aggregation produces highly reproducible kinetic data and occurs by a two-phase process. *ACS Chem. Neurosci.* 1, 13–18. doi: 10.1021/cn900015v
- Herukka, S. K., Rummukainen, J., Ihalaenen, J., Von Und Zu Fraunberg, M., Koivisto, A. M., Nerg, O., et al. (2015). Amyloid- β and tau dynamics in human brain interstitial fluid in patients with suspected normal pressure hydrocephalus. *J. Alzheimers Dis.* 46, 261–269. doi: 10.3233/JAD-142862
- Heyman, A., Peterson, B., Fillenbaum, G., and Pieper, C. (1996). The consortium to establish a registry for Alzheimer's disease (CERAD). Part XIV: demographic and clinical predictors of survival in patients with Alzheimer's disease. *Neurology* 46, 656–660. doi: 10.1212/wnl.46.3.656
- Hickman, S. E., Allison, E. K., and El Khoury, J. (2008). Microglial dysfunction and defective beta-amyloid clearance pathways in aging Alzheimer's disease mice. *J. Neurosci.* 28, 8354–8360. doi: 10.1523/jneurosci.0616-08.2008
- Hoglund, K., Thelen, K. M., Syversen, S., Sjogren, M., von Bergmann, K., Wallin, A., et al. (2005). The effect of simvastatin treatment on the amyloid precursor protein and brain cholesterol metabolism in patients with Alzheimer's disease. *Dement. Geriatr. Cogn. Disord.* 19, 256–265. doi: 10.1159/000084550
- Holland, D., McEvoy, L. K., and Dale, A. M. (2012a). Unbiased comparison of sample size estimates from longitudinal structural measures in ADNI. *Hum. Brain Mapp.* 33, 2586–2602. doi: 10.1002/hbm.21386
- Holland, D., McEvoy, L. K., Desikan, R. S., and Dale, A. M. (2012b). Enrichment and stratification for predementia Alzheimer disease clinical trials. *PLoS One* 7:e47739. doi: 10.1371/journal.pone.0047739
- Holth, J., Fritsch, S., Wang, C., Pedersen, N., Cirrito, J., Mahan, T., et al. (2019). The sleep-wake cycle regulates brain interstitial fluid tau in mice and CSF tau in humans. *Science* 363, eaav2546. doi: 10.1126/science.aav2546
- Hong, S., Quintero-Monzon, O., Ostaszewski, B. L., Podlisny, D. R., Cavanaugh, W. T., Yang, T., et al. (2011). Dynamic analysis of amyloid beta-protein in behaving mice reveals opposing changes in ISF versus parenchymal A β during age-related plaque formation. *J. Neurosci.* 31, 15861–15869. doi: 10.1523/jneurosci.3272-11.2011
- Huang, J., Friedland, R. P., and Auchs, A. P. (2007). Diffusion tensor imaging of normal-appearing white matter in mild cognitive impairment and early Alzheimer disease: preliminary evidence of axonal degeneration in the temporal lobe. *AJNR Am. J. Neuroradiol.* 28, 1943–1948. doi: 10.3174/ajnr.A0700
- Hyman, B. T., Van Hoesen, G. W., Kromer, L. J., and Damasio, A. R. (1986). Perforant pathway changes and the memory impairment of Alzheimer's disease. *Ann. Neurol.* 20, 472–481. doi: 10.1002/ana.410200406

- Iijima-Ando, K., Hearn, S. A., Granger, L., Shenton, C., Gatt, A., Chiang, H. C., et al. (2008). Overexpression of neprilysin reduces alzheimer amyloid-beta42 (Abeta42)-induced neuron loss and intraneuronal Abeta42 deposits but causes a reduction in cAMP-responsive element-binding protein-mediated transcription, age-dependent axon pathology, and premature death in *Drosophila*. *J. Biol. Chem.* 283. doi: 10.1074/jbc.M710509200
- Imai, T., Hieshima, K., Haskell, C., Baba, M., Nagira, M., Nishimura, M., et al. (1997). Identification and molecular characterization of fractalkine receptor CX3CR1, which mediates both leukocyte migration and adhesion. *Cell* 91, 521–530. doi: 10.1016/s0092-8674(00)80438-9
- Imbimbo, B. P., Giardino, L., Sivilia, S., Giuliani, A., Gusciglio, M., Pietrini, V., et al. (2010). CHF5074, a novel gamma-secretase modulator, restores hippocampal neurogenesis potential and reverses contextual memory deficit in a transgenic mouse model of Alzheimer's disease. *J. Alzheimers Dis.* 20, 159–173. doi: 10.3233/jad-2010-1366
- Jack, C. R. Jr., Bennett, D. A., Blennow, K., Carrillo, M. C., Feldman, H. H., Frisoni, G. B., et al. (2016). A/T/N: an unbiased descriptive classification scheme for Alzheimer disease biomarkers. *Neurology* 87, 539–547. doi: 10.1212/wnl.0000000000002923
- Jack, C. R. Jr., Knopman, D. S., Jagust, W. J., Shaw, L. M., Aisen, P. S., Weiner, M. W., et al. (2010). Hypothetical model of dynamic biomarkers of the Alzheimer's pathological cascade. *Lancet Neurol.* 9, 119–128. doi: 10.1016/s1474-4422(09)70299-6
- Jack, C. R. Jr., Petersen, R. C., Xu, Y., O'Brien, P. C., Smith, G. E., Ivnik, R. J., et al. (2000). Rates of hippocampal atrophy correlate with change in clinical status in aging and AD. *Neurology* 55, 484–489. doi: 10.1212/wnl.55.4.484
- Jack, C. R. Jr., Wiste, H. J., Lesnick, T. G., Weigand, S. D., Knopman, D. S., Vemuri, P., et al. (2013). Brain beta-amyloid load approaches a plateau. *Neurology* 80, 890–896. doi: 10.1212/WNL.0b013e3182840bbe
- Jagust, W. J., Landau, S. M., Koeppe, R. A., Reiman, E. M., Chen, K., Mathis, C. A., et al. (2015). The Alzheimer's disease neuroimaging initiative 2 PET core: 2015. *Alzheimers Dement.* 11, 757–771. doi: 10.1016/j.jalz.2015.05.001
- Jahn, R., and Fasshauer, D. (2012). Molecular machines governing exocytosis of synaptic vesicles. *Nature* 490, 201–207. doi: 10.1038/nature11320
- James, B. D., Wilson, R. S., Boyle, P. A., Trojanowski, J. Q., Bennett, D. A., and Schneider, J. A. (2016). TDP-43 stage, mixed pathologies, and clinical Alzheimer's-type dementia. *Brain* 139, 2983–2993. doi: 10.1093/brain/aww224
- Janelidze, S., Mattsson, N., Stomrud, E., Lindberg, O., Palmqvist, S., Zetterberg, H., et al. (2018). CSF biomarkers of neuroinflammation and cerebrovascular dysfunction in early Alzheimer disease. *Neurology* 91, e867–e877. doi: 10.1212/WNL.0000000000006082
- Janelidze, S., Stomrud, E., Palmqvist, S., Zetterberg, H., van Westen, D., Jeromin, A., et al. (2016). Plasma beta-amyloid in Alzheimer's disease and vascular disease. *Sci. Rep.* 6:26801. doi: 10.1038/srep26801
- Jay, T. R., von Saucken, V. E., and Landreth, G. E. (2017). TREM2 in neurodegenerative diseases. *Mol. Neurodegener.* 12:56. doi: 10.1186/s13024-017-0197-5
- Jeppsson, F., Eketjäll, S., Janson, J., Karlstrom, S., Gustavsson, S., Olsson, L. L., et al. (2012). Discovery of AZD3839, a potent and selective BACE1 inhibitor clinical candidate for the treatment of Alzheimer disease. *J. Biol. Chem.* 287, 41245–41257. doi: 10.1074/jbc.M112.409110
- Jin, W. S., Shen, L. L., Bu, X. L., Zhang, W. W., Chen, S. H., Huang, Z. L., et al. (2017). Peritoneal dialysis reduces amyloid-beta plasma levels in humans and attenuates Alzheimer-associated phenotypes in an APP/PS1 mouse model. *Acta Neuropathol.* 134, 207–220. doi: 10.1007/s00401-017-1721-y
- Johnson, A. E., Jeppsson, F., Sandell, J., Wensbo, D., Neelissen, J. A., Jureus, A., et al. (2009). AZD2184: a radioligand for sensitive detection of beta-amyloid deposits. *J. Neurochem.* 108, 1177–1186. doi: 10.1111/j.1471-4159.2008.05861.x
- Johnson, K. A., Fox, N. C., Sperling, R. A., and Klunk, W. E. (2012). Brain imaging in Alzheimer disease. *Cold Spring Harb. Perspect. Med.* 2, a006213. doi: 10.1101/cshperspect.a006213
- Johnson, V. E., Stewart, W., and Smith, D. H. (2010). Traumatic brain injury and amyloid- β pathology: a link to Alzheimer's disease? *Nat. Rev. Neurosci.* 11, 361–370. doi: 10.1038/nrn2808
- Jürgen, M. K., Milan, M., and George, P. (2016). *Atlas of the Human Brain*, 4th Edn. Cambridge, MA: Academic Press.
- Kanai, M., Matsubara, E., Iseo, K., Urakami, K., Nakashima, K., Arai, H., et al. (1998). Longitudinal study of cerebrospinal fluid levels of tau, A beta1-40, and A beta1-42(43) in Alzheimer's disease: a study in Japan. *Ann. Neurol.* 44, 17–26. doi: 10.1002/ana.410440108
- Kaneko, N., Nakamura, A., Washimi, Y., Kato, T., Sakurai, T., Arahata, Y., et al. (2014). Novel plasma biomarker surrogating cerebral amyloid deposition. *Proc. JPN Acad. Ser. B Phys. Biol. Sci.* 90, 353–364. doi: 10.2183/pjab.90.353
- Karelina, T., Demin, O., Nicholas, T., Lu, Y., Duvvuri, S., and Barton, H. A. (2017). A translational systems pharmacology model for beta kinetics in mouse, monkey, and human. *CPT Pharmacometrics Syst. Pharmacol.* 6, 666–675. doi: 10.1002/psp4.12211
- Karim, J. K., Kahle, K. T., Kurland, D. B., Yu, E., Gerzanich, V., and Simard, J. M. (2015). A novel method to study cerebrospinal fluid dynamics in rats. *J. Neurosci. Methods* 241, 78–84. doi: 10.1016/j.jneumeth.2014.12.015
- Kaufman, S. K., Thomas, T. L., Del Tredici, K., Braak, H., and Diamond, M. I. (2017). Characterization of tau prion seeding activity and strains from formaldehyde-fixed tissue. *Acta Neuropathol. Commun.* 5:41. doi: 10.1186/s40478-017-0442-8
- Kawarabayashi, T., Younkin, L. H., Saido, T. C., Shoji, M., Ashe, K. H., and Younkin, S. G. (2001). Age-dependent changes in brain, CSF, and plasma amyloid (beta) protein in the Tg2576 transgenic mouse model of Alzheimer's disease. *J. Neurosci.* 21, 372–381.
- Keene, C. D., Darvas, M., Kraemer, B., Liggitt, D., Sigurdson, C., and Ladiges, W. (2016). Neuropathological assessment and validation of mouse models for Alzheimer's disease: applying NIA-AA guidelines. *Pathobiol. Aging Age Relat. Dis.* 6:32397. doi: 10.3402/pba.v6.32397
- Kehr, J. (1999). "Monitoring chemistry of brain microenvironment: biosensors, microdialysis and related techniques," in *Modern Techniques in Neuroscience Research*, U. Windhorst, and H. Johansson, (Heidelberg: Springer-Verlag) 41, 1149–1198.
- Kennedy, M. E., Stamford, A. W., Chen, X., Cox, K., Cumming, J. N., Dockendorff, M. F., et al. (2016). The BACE1 inhibitor verubecestat (MK-8931) reduces CNS beta-amyloid in animal models and in Alzheimer's disease patients. *Sci. Transl. Med.* 8:363ra150. doi: 10.1126/scitranslmed.aad9704
- Khan, S. S., and Bloom, G. S. (2016). Tau: the center of a signaling nexus in Alzheimer's disease. *Front. Neurosci.* 10:31. doi: 10.3389/fnins.2016.00031
- Kim, H. D., Tahara, K., Maxwell, J. A., Lalonde, R., Fukuiwa, T., Fujihashi, K., et al. (2007). Nasal inoculation of an adenovirus vector encoding 11 tandem repeats of Abeta1-6 upregulates IL-10 expression and reduces amyloid load in a Mo/Hu APPswe PS1dE9 mouse model of Alzheimer's disease. *J. Gene Med.* 9, 88–98. doi: 10.1002/jgm.993
- Kitazawa, M., Yamasaki, T. R., and LaFerla, F. M. (2004). Microglia as a potential bridge between the amyloid beta-peptide and tau. *Ann. N. Y. Acad. Sci.* 1035, 85–103. doi: 10.1196/annals.1332.006
- Kleinberger, G., Yamanishi, Y., Suarez-Calvet, M., Czirz, E., Lohmann, E., Cuyvers, E., et al. (2014). TREM2 mutations implicated in neurodegeneration impair cell surface transport and phagocytosis. *Sci. Transl. Med.* 6:243ra286. doi: 10.1126/scitranslmed.3009093
- Klunk, W. E., Engler, H., Nordberg, A., Wang, Y., Blomqvist, G., Holt, D. P., et al. (2004). Imaging brain amyloid in Alzheimer's disease with pittsburgh compound-B. *Ann. Neurol.* 55, 306–319. doi: 10.1002/ana.20009
- Komatsu, M., Waguri, S., Chiba, T., Murata, S., Iwata, J., Tanida, I., et al. (2006). Loss of autophagy in the central nervous system causes neurodegeneration in mice. *Nature* 441, 880–884. doi: 10.1038/nature04723
- Kounnas, M. Z., Lane-Donovan, C., Nowakowski, D. W., Herz, J., and Comer, W. T. (2017). NGP 555, a gamma-secretase modulator, lowers the amyloid biomarker, Abeta42, in cerebrospinal fluid while preventing alzheimer's disease cognitive decline in rodents. *Alzheimers Dement.* 3, 65–73. doi: 10.1016/j.trci.2016.09.003
- Krzyzanowska, A., and Carro, E. (2012). Pathological alteration in the choroid plexus of alzheimer's disease: implication for new therapy approaches. *Front. Pharmacol.* 3:75. doi: 10.3389/fphar.2012.00075
- Kuhl, D. E., Metter, E. J., Riege, W. H., and Phelps, M. E. (1982). Effects of human aging on patterns of local cerebral glucose utilization determined by the [18F]fluoro-deoxyglucose method. *J. Cereb. Blood Flow Metab.* 2, 163–171. doi: 10.1038/jcbfm.1982.15
- Kuhle, J., Barro, C., Andreasson, U., Derfuss, T., Lindberg, R., Sandelius, A., et al. (2016). Comparison of three analytical platforms for quantification of the neurofilament light chain in blood samples: eLISA, electrochemiluminescence

- immunoassay and Simoa. *Clin. Chem. Lab. Med.* 54, 1655–1661. doi: 10.1515/cclm-2015-1195
- Kuhle, J., Gaiottino, J., Leppert, D., Petzold, A., Bestwick, J. P., Malaspina, A., et al. (2015). Serum neurofilament light chain is a biomarker of human spinal cord injury severity and outcome. *J. Neurol. Neurosurg.* 86:273. doi: 10.1136/jnnp-2013-307454
- Kummer, M. P., Vogl, T., Axt, D., Griep, A., Vieira-Saecker, A., Jessen, F., et al. (2012). MRP14 deficiency ameliorates amyloid beta burden by increasing microglial phagocytosis and modulation of amyloid precursor protein processing. *J. Neurosci.* 32, 17824–17829. doi: 10.1523/jneurosci.1504-12.2012
- LaFerla, F. M., Green, K. N., and Oddo, S. (2007). Intracellular amyloid-beta in Alzheimer's disease. *Nat. Rev. Neurosci.* 8, 499–509. doi: 10.1038/nrn2168
- Landau, S. M., Mintun, M. A., Joshi, A. D., Koeppe, R. A., Petersen, R. C., Aisen, P. S., et al. (2012). Amyloid deposition, hypometabolism, and longitudinal cognitive decline. *Ann. Neurol.* 72, 578–586. doi: 10.1002/ana.23650
- Lautrup, S., Sinclair, D. A., Mattson, M. P., and Fang, E. F. (2019). NAD(+) in brain aging and neurodegenerative disorders. *Cell Metab.* 30, 630–655. doi: 10.1016/j.cmet.2019.09.001
- Leclerc, B., and Abulrob, A. (2013). Perspectives in molecular imaging using staging biomarkers and immunotherapies in Alzheimer's disease. *Sci. World J.* 2013:589308.
- Lee, E. O., Yang, J. H., Chang, K. A., Suh, Y. H., and Chong, Y. H. (2013). Amyloid-beta peptide-induced extracellular S100A9 depletion is associated with decrease of antimicrobial peptide activity in human THP-1 monocytes. *J. Neuroinflammation* 10:68. doi: 10.1186/1742-2094-10-68
- Lee, J. C., Kim, S. J., Hong, S., and Kim, Y. (2019). Diagnosis of Alzheimer's disease utilizing amyloid and tau as fluid biomarkers. *Exp. Mol. Med.* 51, 1–10. doi: 10.1038/s12276-019-0250-2
- Lee, S., Varvel, N. H., Konerth, M. E., Xu, G., Cardona, A. E., Ransohoff, R. M., et al. (2010). CX3CR1 deficiency alters microglial activation and reduces beta-amyloid deposition in two Alzheimer's disease mouse models. *Am. J. Pathol.* 177, 2549–2562. doi: 10.2353/ajpath.2010.100265
- Lee, V. M., and Trojanowski, J. Q. (2001). Transgenic mouse models of tauopathies: prospects for animal models of Pick's disease. *Neurology* 56, S26–S30. doi: 10.1212/wnl.56.suppl_4.s26
- Leidinger, P., Backes, C., Deutscher, S., Schmitt, K., Mueller, S. C., Frese, K., et al. (2013). A blood based 12-miRNA signature of Alzheimer disease patients. *Genome Biol.* 14, R78. doi: 10.1186/gb-2013-14-7-r78
- Leinenbach, A., Pannese, J., Dullfer, T., Huber, A., Bittner, T., Andreasson, U., et al. (2014). Mass spectrometry-based candidate reference measurement procedure for quantification of amyloid-beta in cerebrospinal fluid. *Clin. Chem.* 60, 987–994. doi: 10.1373/clinchem.2013.220392
- Leinonen, V., Pemberton, D., Van Der Ark, P., Timmers, M., Slemmon, J. R., Janssens, L., et al. (2019). P1-257: longitudinal comparison of Csf biomarkers of neurodegeneration in patients with probable idiopathic normal pressure hydrocephalus (INPH). *Alzheimers Dement.* 15, 337–338. doi: 10.1016/j.jalz.2019.06.812
- Leitão, M. J., Baldeiras, I., Herukka, S.-K., Pikkariainen, M., Leinonen, V., Simonsen, A. H., et al. (2015). Chasing the effects of pre-analytical confounders – a multicenter study on CSF-AD biomarkers. *Front. Neurol.* 6:153. doi: 10.3389/fneur.2015.00153
- Leuzy, A., Chiotis, K., Hasselbalch, S. G., Rinne, J. O., de Mendonca, A., Otto, M., et al. (2016). Pittsburgh compound B imaging and cerebrospinal fluid amyloid-beta in a multicentre European memory clinic study. *Brain* 139, 2540–2553. doi: 10.1093/brain/aww160
- Leuzy, A., Chiotis, K., Lemoine, L., Gillberg, P. G., Almkvist, O., Rodriguez-Vieitez, E., et al. (2019). Tau PET imaging in neurodegenerative tauopathies – still a challenge. *Mol. Psychiatry* 24, 1112–1134. doi: 10.1038/s41380-018-0342-8
- Lewczuk, P., Ermann, N., Andreasson, U., Schultheis, C., Podhorna, J., Spitzer, P., et al. (2018). Plasma neurofilament light as a potential biomarker of neurodegeneration in Alzheimer's disease. *Alzheimers Res. Ther.* 10:71. doi: 10.1186/s13195-018-0404-9
- Lewczuk, P., Esselmann, H., Bibl, M., Beck, G., Maler, J. M., Otto, M., et al. (2004). Tau protein phosphorylated at threonine 181 in CSF as a neurochemical biomarker in Alzheimer's disease: original data and review of the literature. *J. Mol. Neurosci.* 23, 115–122. doi: 10.1385/jmn:23:1-2:115
- Lewczuk, P., Leleental, N., Lachmann, I., Holzer, M., Flach, K., Brandner, S., et al. (2017). Non-phosphorylated tau as a potential biomarker of Alzheimer's disease: analytical and diagnostic characterization. *J. Alzheimers Dis.* 55, 159–170. doi: 10.3233/JAD-160448
- Li, G., Chen, H., Cheng, L., Zhao, R., Zhao, J., and Xu, Y. (2014). Amyloid precursor-like protein 2 C-terminal fragments upregulate S100A9 gene and protein expression in BV2 cells. *Neural Regen. Res.* 9, 1923–1928. doi: 10.4103/1673-5374.145362
- Lista, S., Toschi, N., Baldacci, F., Zetterberg, H., Blennow, K., Kilimann, I., et al. (2017). Diagnostic accuracy of CSF neurofilament light chain protein in the biomarker-guided classification system for Alzheimer's disease. *Neurochem. Int.* 108, 355–360. doi: 10.1016/j.neuint.2017.05.010
- Liu, C. C., Hu, J., Zhao, N., Wang, J., Wang, N., Cirrito, J. R., et al. (2017). Astrocytic LRP1 mediates brain abeta clearance and impacts amyloid deposition. *J. Neurosci.* 37, 4023–4031. doi: 10.1523/jneurosci.3442-16.2017
- Liu, L., and Duff, K. (2008). A technique for serial collection of cerebrospinal fluid from the cisterna magna in mouse. *J. Vis. Exp.* 960. doi: 10.3791/960
- Liu, L., Herukka, S. K., Minkevičienė, R., van Groen, T., and Tanila, H. (2004). Longitudinal observation on CSF Abeta42 levels in young to middle-aged amyloid precursor protein/presenilin-1 doubly transgenic mice. *Neurobiol. Dis.* 17, 516–523. doi: 10.1016/j.nbd.2004.08.005
- Liu, Y. H., Giunta, B., Zhou, H. D., Tan, J., and Wang, Y. J. (2012). Immunotherapy for Alzheimer disease: the challenge of adverse effects. *Nat. Rev. Neurol.* 8, 465–469. doi: 10.1038/nrn2012.118
- Lodeiro, M., Puerta, E., Ismail, M. A., Rodriguez-Rodriguez, P., Ronnback, A., Codita, A., et al. (2017). Aggregation of the inflammatory S100A8 precedes abeta plaque formation in transgenic APP mice: positive feedback for S100A8 and abeta productions. *J. Gerontol. A Biol. Sci. Med. Sci.* 72, 319–328. doi: 10.1093/geron/ghw073
- Lucey, B. P., Hicks, T. J., McLeland, J. S., Toedebusch, C. D., Boyd, J., Elbert, D. L., et al. (2018). Effect of sleep on overnight cerebrospinal fluid amyloid beta kinetics. *Ann. Neurol.* 83, 197–204. doi: 10.1002/ana.25117
- Lue, L. F., Kuo, Y. M., Roher, A. E., Brachova, L., Shen, Y., Sue, L., et al. (1999). Soluble amyloid beta peptide concentration as a predictor of synaptic change in Alzheimer's disease. *Am. J. Pathol.* 155, 853–862. doi: 10.1016/s0002-9440(10)65184-x
- Maass, A., Landau, S., Baker, S. L., Horng, A., Lockhart, S. N., La Joie, R., et al. (2017). Comparison of multiple tau-PET measures as biomarkers in aging and Alzheimer's disease. *Neuroimage* 157, 448–463. doi: 10.1016/j.neuroimage.2017.05.058
- Maciejewski-Lenoir, D., Chen, S., Feng, L., Maki, R., and Bacon, K. B. (1999). Characterization of fractalkine in rat brain cells: migratory and activation signals for CX3CR1-expressing microglia. *J. Immunol.* 163, 1628–1635.
- Maphis, N., Xu, G., Kokiko-Cochran, O. N., Jiang, S., Cardona, A., Ransohoff, R. M., et al. (2015). Reactive microglia drive tau pathology and contribute to the spreading of pathological tau in the brain. *Brain* 138, 1738–1755. doi: 10.1093/brain/aww081
- Márquez, F., and Yassa, M. A. (2019). Neuroimaging biomarkers for Alzheimer's disease. *Mol. Neurodegener.* 14:21. doi: 10.1186/s13024-019-0325-5
- Matsumoto, K., Chiba, Y., Fujihara, R., Kubo, H., Sakamoto, H., and Ueno, M. (2015). Immunohistochemical analysis of transporters related to clearance of amyloid- β peptides through blood-cerebrospinal fluid barrier in human brain. *Histochem. Cell Biol.* 144, 597–611. doi: 10.1007/s00418-015-1366-7
- Mattsson, N., Andreasson, U., Persson, S., Arai, H., Batish, S. D., Bernardini, S., et al. (2011). The Alzheimer's Association external quality control program for cerebrospinal fluid biomarkers. *Alzheimers Dement.* 7, 386.e6–395.e6. doi: 10.1016/j.jalz.2011.05.2243
- Mattsson, N., Andreasson, U., Zetterberg, H., and Blennow, K. (2017a). Association of plasma neurofilament light with neurodegeneration in patients with Alzheimer disease. *JAMA Neurol.* 74, 557–566. doi: 10.1001/jamaneuro.2016.6117
- Mattsson, N., Cullen, N. C., Andreasson, U., Zetterberg, H., and Blennow, K. (2019). Association between longitudinal plasma neurofilament light and neurodegeneration in patients with Alzheimer disease. *JAMA Neurol.* 76, 791–799. doi: 10.1001/jamaneuro.2019.0765
- Mattsson, N., Scholl, M., Strandberg, O., Smith, R., Palmqvist, S., Insel, P. S., et al. (2017b). (18)F-AV-1451 and CSF T-tau and P-tau as biomarkers in Alzheimer's disease. *EMBO Mol. Med.* 9, 1212–1223. doi: 10.15252/emmm.201707809

- Mattsson, N., Zetterberg, H., Janelidze, S., Insel, P. S., Andreasson, U., Stomrud, E., et al. (2016). Plasma tau in Alzheimer disease. *Neurology* 87, 1827–1835. doi: 10.1212/wnl.0000000000003246
- McConlogue, L., Buttini, M., Anderson, J. P., Brigham, E. F., Chen, K. S., Freedman, S. B., et al. (2007). Partial reduction of BACE1 has dramatic effects on Alzheimer plaque and synaptic pathology in APP Transgenic Mice. *J. Biol. Chem.* 282, 26326–26334. doi: 10.1074/jbc.M611687200
- McDonald, R. J., and White, N. M. (1993). A triple dissociation of memory systems: hippocampus, amygdala, and dorsal striatum. *Behav. Neurosci.* 107, 3–22. doi: 10.1037//0735-7044.107.1.3
- McGeer, P. L., Itagaki, S., Tago, H., and McGeer, E. G. (1987). Reactive microglia in patients with senile dementia of the Alzheimer type are positive for the histocompatibility glycoprotein HLA-DR. *Neurosci. Lett.* 79, 195–200. doi: 10.1016/0304-3940(87)90696-3
- McLean, C. A., Cherny, R. A., Fraser, F. W., Fuller, S. J., Smith, M. J., Beyreuther, K., et al. (1999). Soluble pool of Abeta amyloid as a determinant of severity of neurodegeneration in Alzheimer's disease. *Ann. Neurol.* 46, 860–866. doi: 10.1002/1531-8249(199912)46:6<860::aid-ana8<3.0.co;2-m
- Mehrpour, M., Esclatine, A., Beau, I., and Codogno, P. (2010). Overview of macroautophagy regulation in mammalian cells. *Cell Res.* 20, 748–762. doi: 10.1038/cr.2010.82
- Mehta, P. D., Pirttila, T., Patrick, B. A., Barshatzky, M., and Mehta, S. P. (2001). Amyloid beta protein 1-40 and 1-42 levels in matched cerebrospinal fluid and plasma from patients with Alzheimer disease. *Neurosci. Lett.* 304, 102–106. doi: 10.1016/s0304-3940(01)01754-2
- Menendez-Gonzalez, M., Padilla-Zambrano, H. S., Alvarez, G., Capetillo-Zarate, E., Tomas-Zapico, C., and Costa, A. (2018). Targeting beta-amyloid at the CSF: a new therapeutic strategy in Alzheimer's disease. *Front. Aging Neurosci.* 10:100. doi: 10.3389/fnagi.2018.00100
- Mennicken, F., Maki, R., de Souza, E. B., and Quirion, R. (1999). Chemokines and chemokine receptors in the CNS: a possible role in neuroinflammation and patterning. *Trends Pharmacol. Sci.* 20, 73–78. doi: 10.1016/s0165-6147(99)01308-5
- Menzies, F. M., Fleming, A., and Rubinsztein, D. C. (2015). Compromised autophagy and neurodegenerative diseases. *Nat. Rev. Neurosci.* 16, 345–357. doi: 10.1038/nrn3961
- Meyding-Lamadé, U., Ehrhart, K., de Ruiz, H. L., Kehm, R., and Lamadé, W. A. (1996). new technique: serial puncture of the cisterna magna for obtaining cerebrospinal fluid in the mouse—application in a model of herpes simplex virus encephalitis. *J. Exp. Anim. Sci.* 38, 77–81.
- Milisauskas, I., Šuput, D., and Ribariš, S. (2015). Unfolded protein response and macroautophagy in Alzheimer's, Parkinson's and Prion diseases. *Molecules* 20, 22718–22756.
- Molinuevo, J. L., Ayton, S., Batrla, R., Bednar, M. M., Bittner, T., Cummings, J., et al. (2018). Current state of Alzheimer's fluid biomarkers. *Acta Neuropathol.* 136, 821–853. doi: 10.1007/s00401-018-1932-x
- Mollenhauer, B., Bibl, M., Trenkwalder, C., Stiens, G., Cepek, L., Steinacker, P., et al. (2005). Follow-up investigations in cerebrospinal fluid of patients with dementia with Lewy bodies and Alzheimer's disease. *J. Neural. Transm.* 112, 933–948. doi: 10.1007/s00702-004-0235-7
- Mori, T., Koyama, N., Arendash, G. W., Horikoshi-Sakuraba, Y., Tan, J., and Town, T. (2010). Overexpression of human S100B exacerbates cerebral amyloidosis and gliosis in the Tg2576 mouse model of Alzheimer's disease. *Glia* 58, 300–314. doi: 10.1002/glia.20924
- Mosconi, L., Tsui, W. H., De Santi, S., Li, J., Rusinek, H., Convit, A., et al. (2005). Reduced hippocampal metabolism in MCI and AD: automated FDG-PET image analysis. *Neurology* 64, 1860–1867. doi: 10.1212/01.Wnl.0000163856.13524.08
- Mosconi, L., Tsui, W. H., Herholz, K., Pupi, A., Drzezga, A., Lucignani, G., et al. (2008). Multicenter standardized 18F-FDG PET diagnosis of mild cognitive impairment, Alzheimer's disease, and other dementias. *J. Nucl. Med.* 49, 390–398. doi: 10.2967/jnumed.107.045385
- Mucke, L., and Selkoe, D. J. (2012). Neurotoxicity of amyloid beta-protein: synaptic and network dysfunction. *Cold Spring Harb. Perspect. Med.* 2:a006338. doi: 10.1101/cshperspect.a006338
- Mudher, A., Colin, M., Dujardin, S., Medina, M., Dewachter, I., Alavi Naini, S. M., et al. (2017). What is the evidence that tau pathology spreads through prion-like propagation? *Acta Neuropathol. Commun.* 5:99. doi: 10.1186/s40478-017-0488-7
- Murphy, M. P., and LeVine, H. III (2010). Alzheimer's disease and the amyloid-beta peptide. *J. Alzheimers Dis.* 19, 311–323. doi: 10.3233/JAD-2010-1221
- Musiek, E. S., and Holtzman, D. M. (2015). Three dimensions of the amyloid hypothesis: time, space and 'wingmen'. *Nat. Neurosci.* 18, 800–806. doi: 10.1038/nn.4018
- Naggara, O., Oppenheim, C., Rieu, D., Raoux, N., Rodrigo, S., Dalla Barba, G., et al. (2006). Diffusion tensor imaging in early Alzheimer's disease. *Psychiatry Res.* 146, 243–249. doi: 10.1016/j.psychres.2006.01.005
- Nakamura, T., Shoji, M., Harigaya, Y., Watanabe, M., Hosoda, K., Cheung, T. T., et al. (1994). Amyloid beta protein levels in cerebrospinal fluid are elevated in early-onset Alzheimer's disease. *Ann. Neurol.* 36, 903–911. doi: 10.1002/ana.410360616
- Narasimhan, S., Guo, J. L., Changolkar, L., Stieber, A., McBride, J. D., Silva, L. V., et al. (2017). Pathological Tau strains from human brains recapitulate the diversity of tauopathies in nontransgenic mouse brain. *J. Neurosci.* 37, 11406–11423. doi: 10.1523/jneurosci.1230-17.2017
- Nash, K. R., Lee, D. C., Hunt, J. B. Jr., Morganti, J. M., Selenica, M. L., Moran, P., et al. (2013). Fractalkine overexpression suppresses tau pathology in a mouse model of tauopathy. *Neurobiol. Aging* 34, 1540–1548. doi: 10.1016/j.neurobiolaging.2012.12.011
- Naslund, J., Haroutunian, V., Mohs, R., Davis, K. L., Davies, P., Greengard, P., et al. (2000). Correlation between elevated levels of amyloid beta-peptide in the brain and cognitive decline. *Jama* 283, 1571–1577. doi: 10.1001/jama.283.12.1571
- Neselius, S., Brisby, H., Theodorsson, A., Blennow, K., Zetterberg, H., and Marcusson, J. (2012). CSF-Biomarkers in olivary boxing: diagnosis and effects of repetitive head trauma. *PLoS One* 7:e33606. doi: 10.1371/journal.pone.0033606
- Niemantsverdriet, E., Ottoy, J., Somers, C., De Roeck, E., Struyfs, H., Soetewey, F., et al. (2017). The Cerebrospinal fluid abeta1-42/Abeta1-40 ratio improves concordance with amyloid-PET for diagnosing Alzheimer's disease in a clinical setting. *J. Alzheimers Dis.* 60, 561–576. doi: 10.3233/jad-170327
- Nisbet, R. M., Polanco, J. C., Ittner, L. M., and Gotz, J. (2015). Tau aggregation and its interplay with amyloid-beta. *Acta Neuropathol.* 129, 207–220. doi: 10.1007/s00401-014-1371-2
- Nixon, R. A., and Yang, D. S. (2011). Autophagy failure in Alzheimer's disease—locating the primary defect. *Neurobiol. Dis.* 43, 38–45. doi: 10.1016/j.nbd.2011.01.021
- Nussbaum, J. M., Seward, M. E., and Bloom, G. S. (2013). Alzheimer disease: a tale of two prions. *Prion* 7, 14–19. doi: 10.4161/pri.22118
- Oddo, S., Caccamo, A., Shepherd, J. D., Murphy, M. P., Golde, T. E., Kaye, R., et al. (2003). Triple-transgenic model of Alzheimer's disease with plaques and tangles. *Neuron* 39, 409–421. doi: 10.1016/s0896-6273(03)00434-3
- Oh, E. S., Mielke, M. M., Rosenberg, P. B., Jain, A., Fedarko, N. S., Lyketos, C. G., et al. (2010). Comparison of conventional ELISA with electrochemiluminescence technology for detection of amyloid-beta in plasma. *J. Alzheimers Dis.* 21, 769–773. doi: 10.3233/jad-2010-100456
- Ohno, M., Cole, S. L., Yasvoina, M., Zhao, J., Citron, M., Berry, R., et al. (2007). BACE1 gene deletion prevents neuron loss and memory deficits in 5XFAD APP/PS1 transgenic mice. *Neurobiol. Dis.* 26, 134–145. doi: 10.1016/j.nbd.2006.12.008
- Öhrfelt, A., Brinkmalm, A., Dumurgier, J., Brinkmalm, G., Hansson, O., Zetterberg, H., et al. (2016). The pre-synaptic vesicle protein synaptotagmin is a novel biomarker for Alzheimer's disease. *Alzheimers Res. Ther.* 8:41. doi: 10.1186/s13195-016-0208-8
- Olsson, B., Lautner, R., Andreasson, U., Öhrfelt, A., Portelius, E., Bjerke, M., et al. (2016). CSF and blood biomarkers for the diagnosis of Alzheimer's disease: a systematic review and meta-analysis. *Lancet Neurol.* 15, 673–684. doi: 10.1016/s1474-4422(16)00070-3
- Olsson, F., Schmidt, S., Althoff, V., Munter, L. M., Jin, S., Rosqvist, S., et al. (2014). Characterization of intermediate steps in amyloid beta (Abeta) production under near-native conditions. *J. Biol. Chem.* 289, 1540–1550. doi: 10.1074/jbc.M113.498246

- Pahnke, J., Langer, O., and Krohn, M. (2014). Alzheimer's and ABC transporters — new opportunities for diagnostics and treatment. *Neurobiol. Dis.* 72, 54–60. doi: 10.1016/j.nbd.2014.04.001
- Palmqvist, S., Insel, P. S., Stomrud, E., Janelidze, S., Zetterberg, H., Brix, B., et al. (2019). Cerebrospinal fluid and plasma biomarker trajectories with increasing amyloid deposition in Alzheimer's disease. *EMBO Mol. Med.* 11:e11170. doi: 10.15252/emmm.201911170
- Palmqvist, S., Mattsson, N., and Hansson, O. (2016). Cerebrospinal fluid analysis detects cerebral amyloid-beta accumulation earlier than positron emission tomography. *Brain* 139, 1226–1236. doi: 10.1093/brain/aww015
- Palmqvist, S., Schöll, M., Strandberg, O., Mattsson, N., Stomrud, E., Zetterberg, H., et al. (2017). Earliest accumulation of β -amyloid occurs within the default-mode network and concurrently affects brain connectivity. *Nat. Commun.* 8:1214. doi: 10.1038/s41467-017-01150-x
- Pase, M. P., Beiser, A. S., Himali, J. J., Satizabal, C. L., Aparicio, H. J., DeCarli, C., et al. (2019). Assessment of plasma total tau level as a predictive biomarker for dementia and related endophenotypes. *JAMA Neurol.* 76, 598–606. doi: 10.1001/jamaneurol.2018.4666
- Perea, J. R., Lleó, A., Alcolea, D., Fortea, J., Ávila, J., and Bolós, M. (2018). Decreased CX3CL1 levels in the cerebrospinal fluid of patients with Alzheimer's disease. *Front. Neurosci.* 12:609. doi: 10.3389/fnins.2018.00609
- Perret-Liaudet, A., Pelpel, M., Tholance, Y., Dumont, B., Vanderstichele, H., Zorzi, W., et al. (2012a). Cerebrospinal fluid collection tubes: a critical issue for Alzheimer disease diagnosis. *Clin. Chem.* 58, 778–789. doi: 10.1373/clinchem.2011.178368
- Perret-Liaudet, A., Pelpel, M., Tholance, Y., Dumont, B., Vanderstichele, H., Zorzi, W., et al. (2012b). Risk of Alzheimer's disease biological misdiagnosis linked to cerebrospinal collection tubes. *J. Alzheimers Dis.* 31, 13–20. doi: 10.3233/jad-2012-120361
- Peters, A., Leahu, D., Moss, M. B., and McNally, K. J. (1994). The effects of aging on area 46 of the frontal cortex of the rhesus monkey. *Cereb. Cortex* 4, 621–635. doi: 10.1093/cercor/4.6.621
- Peterson, D. A., Lucidi-Phillipi, C. A., Eagle, K. L., and Gage, F. H. (1994). Perforant path damage results in progressive neuronal death and somal atrophy in layer II of entorhinal cortex and functional impairment with increasing postdamage age. *J. Neurosci.* 14, 6872–6885. doi: 10.1523/JNEUROSCI.14-11-06872.1994
- Petzold, A. (2005). Neurofilament phosphoforms: surrogate markers for axonal injury, degeneration and loss. *J. Neurol. Sci.* 233, 183–198. doi: 10.1016/j.jns.2005.03.015
- Pijnenburg, Y. A., Janssen, J. C., Schoonenboom, N. S., Petzold, A., Mulder, C., Stigbrand, T., et al. (2007). CSF neurofilaments in frontotemporal dementia compared with early onset Alzheimer's disease and controls. *Dement. Geriatr. Cogn. Disord.* 23, 225–230. doi: 10.1159/000099473
- Pitschke, M., Prior, R., Haupt, M., and Riesner, D. (1998). Detection of single amyloid β -protein aggregates in the cerebrospinal fluid of Alzheimer's patients by fluorescence correlation spectroscopy. *Nat. Med.* 4, 832–834. doi: 10.1038/nm0798-832
- Pratico, D., Uryu, K., Leight, S., Trojanowski, J. Q., and Lee, V. M. (2001). Increased lipid peroxidation precedes amyloid plaque formation in an animal model of Alzheimer amyloidosis. *J. Neurosci.* 21, 4183–4187.
- Pulawski, W., Ghoshdastider, U., Andrisano, V., and Filipek, S. (2012). Ubiquitous amyloids. *Appl. Biochem. Biotechnol.* 166, 1626–1643. doi: 10.1007/s12010-012-9549-3
- Pyykkö, O. T., Lumela, M., Rummukainen, J., Nerg, O., Seppälä, T. T., Herukka, S.-K., et al. (2014). Cerebrospinal fluid biomarker and brain biopsy findings in idiopathic normal pressure hydrocephalus. *PLoS One* 9:e91974. doi: 10.1371/journal.pone.0091974
- Qin, W., Ho, L., Wang, J., Peskind, E., and Pasinetti, G. M. (2009). S100A7, a novel Alzheimer's disease biomarker with non-amyloidogenic alpha-secretase activity acts via selective promotion of ADAM-10. *PLoS One* 4:e4183. doi: 10.1371/journal.pone.0004183
- Querol-Vilaseca, M., Colom-Cadena, M., Pegueroles, J., San Martín-Paniello, C., Clarimon, J., Belbin, O., et al. (2017). YKL-40 (Chitinase 3-like I) is expressed in a subset of astrocytes in Alzheimer's disease and other tauopathies. *J. Neuroinflammation* 14:118. doi: 10.1186/s12974-017-0893-7
- Raichle, M. E., MacLeod, A. M., Snyder, A. Z., Powers, W. J., Gusnard, D. A., and Shulman, G. L. (2001). A default mode of brain function. *Proc. Natl. Acad. Sci. U.S.A.* 98, 676–682. doi: 10.1073/pnas.98.2.676
- Ramesh, S., Govindarajulu, M., Jones, E., Knowlton, S., Weeks, L., Suppiramaniam, V., et al. (2018a). *Alzheimer's Disease and Treatment*, Reno, NV: MedDocs Publishers.
- Ramesh, S., Govindarajulu, M., Jones, E., Knowlton, S., Weeks, L., Suppiramaniam, V., et al. (2018b). *Current and Novel Biomarkers for Alzheimer's Disease*. Reno, NV: MedDocs Publishers LLC.
- Rami, A. (2009). Review: autophagy in neurodegeneration: firefighter and/or incendiary? *Neuropathol. Appl. Neurobiol.* 35, 449–461. doi: 10.1111/j.1365-2990.2009.01034.x
- Ranganath, C., and Ritchey, M. (2012). Two cortical systems for memory-guided behaviour. *Nat. Rev. Neurosci.* 13, 713–726. doi: 10.1038/nrn3338
- Rapp, P. R., and Gallagher, M. (1996). Preserved neuron number in the hippocampus of aged rats with spatial learning deficits. *Proc. Natl. Acad. Sci. U.S.A.* 93, 9926–9930. doi: 10.1073/pnas.93.18.9926
- Rapp, P. R., Deroche, P. S., Mao, Y., and Burwell, R. D. (2002). Neuron number in the parahippocampal region is preserved in aged rats with spatial learning deficits. *Cereb. Cortex* 12, 1171–1179. doi: 10.1093/cercor/12.11.1171
- Rasmussen, T., Schliemann, T., Sorensen, J. C., Zimmer, J., and West, M. J. (1996). Memory impaired aged rats: no loss of principal hippocampal and subicular neurons. *Neurobiol. Aging* 17, 143–147. doi: 10.1016/0197-4580(95)02032-2
- Raz, N., Lindenberger, U., Rodrigue, K. M., Kennedy, K. M., Head, D., Williamson, A., et al. (2005). Regional brain changes in aging healthy adults: general trends, individual differences and modifiers. *Cereb. Cortex* 15, 1676–1689. doi: 10.1093/cercor/bhi044
- Rhein, V., Song, X., Wiesner, A., Ittner, L. M., Baysang, G., Meier, F., et al. (2009). Amyloid-beta and tau synergistically impair the oxidative phosphorylation system in triple transgenic Alzheimer's disease mice. *Proc. Natl. Acad. Sci. U.S.A.* 106, 20057–20062. doi: 10.1073/pnas.0905529106
- Riekse, R. G., Li, G., Petrie, E. C., Leverenz, J. B., Vavrek, D., Vuletic, S., et al. (2006). Effect of statins on Alzheimer's disease biomarkers in cerebrospinal fluid. *J. Alzheimers Dis.* 10, 399–406. doi: 10.3233/JAD-2006-10408
- Ringman, J. M., Coppola, G., Elashoff, D., Rodriguez-Agudelo, Y., Medina, L. D., Glyys, K., et al. (2012). Cerebrospinal fluid biomarkers and proximity to diagnosis in preclinical familial Alzheimer's disease. *Dement. Geriatr. Cogn. Disord.* 33, 1–5. doi: 10.1159/000335729
- Ritter, A., and Cummings, J. (2015). Fluid biomarkers in clinical trials of Alzheimer's disease therapeutics. *Front. Neurol.* 6:186. doi: 10.3389/fneur.2015.00186
- Roe, C. M., Fagan, A. M., Grant, E. A., Hassenstab, J., Moulder, K. L., Maue Dreyfus, D., et al. (2013). Amyloid imaging and CSF biomarkers in predicting cognitive impairment up to 7.5 years later. *Neurology* 80, 1784–1791. doi: 10.1212/WNL.0b013e3182918ca6
- Rogeberg, M., Wettergreen, M., Nilsson, L. N., and Fladby, T. (2015). Identification of amyloid beta mid-domain fragments in human cerebrospinal fluid. *Biochimie* 113, 86–92. doi: 10.1016/j.biochi.2015.03.022
- Rogers, J., Lubner-Narod, J., Styren, S. D., and Civin, W. H. (1988). Expression of immune system-associated antigens by cells of the human central nervous system: relationship to the pathology of Alzheimer's disease. *Neurobiol. Aging* 9, 339–349. doi: 10.1016/s0197-4580(88)80079-4
- Rohrer, J. D., Woollacott, I. O., Dick, K. M., Brotherhood, E., Gordon, E., Fellows, A., et al. (2016). Serum neurofilament light chain protein is a measure of disease intensity in frontotemporal dementia. *Neurology* 87, 1329–1336. doi: 10.1212/wnl.00000000000003154
- Rojas, J. C., Karydas, A., Bang, J., Tsai, R. M., Blennow, K., Liman, V., et al. (2016). Plasma neurofilament light chain predicts progression in progressive supranuclear palsy. *Ann. Clin. Transl. Neurol.* 3, 216–225. doi: 10.1002/acn.3290
- Roitshch, E., Holcomb, L., Young, K. A., Marks, A., and Zimmer, D. B. (2010). PSAPP mice exhibit regionally selective reductions in gliosis and plaque deposition in response to S100B ablation. *J. Neuroinflammation* 7:78. doi: 10.1186/1742-2094-7-78
- Ryu, J. K., Cho, T., Choi, H. B., Wang, Y. T., and McLarnon, J. G. (2009). Microglial VEGF receptor response is an integral chemotactic component in Alzheimer's disease pathology. *J. Neurosci.* 29, 3–13. doi: 10.1523/jneurosci.2888-08.2009
- Sabbagh, J. J., Kinney, J. W., and Cummings, J. L. (2013). Alzheimer's disease biomarkers in animal models: closing the translational gap. *Am. J. Neurodegener. Dis.* 2, 108–120.
- Saman, S., Kim, W., Raya, M., Visnick, Y., Miro, S., Saman, S., et al. (2012). Exosome-associated tau is secreted in tauopathy models and is selectively

- phosphorylated in cerebrospinal fluid in early Alzheimer disease. *J. Biol. Chem.* 287, 3842–3849. doi: 10.1074/jbc.M111.277061
- Sankaranarayanan, S., Holahan, M. A., Colussi, D., Crouthamel, M. C., Devanarayan, V., Ellis, J., et al. (2009). First demonstration of cerebrospinal fluid and plasma A beta lowering with oral administration of a beta-site amyloid precursor protein-cleaving enzyme 1 inhibitor in nonhuman primates. *J. Pharmacol. Exp. Ther.* 328, 131–140. doi: 10.1124/jpet.108.143628
- Savage, M. J., Kalinina, J., Wolfe, A., Tugusheva, K., Korn, R., Cash-Mason, T., et al. (2014). A sensitive abeta oligomer assay discriminates Alzheimer's and aged control cerebrospinal fluid. *J. Neurosci.* 34, 2884–2897. doi: 10.1523/jneurosci.1675-13.2014
- Schelle, J., Hasler, L. M., Gopfert, J. C., Joos, T. O., Vanderstichele, H., Stoops, E., et al. (2017). Prevention of tau increase in cerebrospinal fluid of APP transgenic mice suggests downstream effect of BACE1 inhibition. *Alzheimers Dement.* 13, 701–709. doi: 10.1016/j.jalz.2016.09.005
- Scholl, M., Maass, A., Mattsson, N., Ashton, N. J., Blennow, K., Zetterberg, H., et al. (2019). Biomarkers for tau pathology. *Mol. Cell Neurosci.* 97, 18–33. doi: 10.1016/j.mcn.2018.12.001
- Schöll, M., Schonhaut, D., Lockhart, S., Vogel, J. W., Baker, S., Schwimmer, H., et al. (2015). IC-01-05: in vivo braak staging using 18F-AV1451 Tau PET imaging. *Alzheimers Dement.* 11:P4. doi: 10.1016/j.jalz.2015.06.006
- Schwagerl, A. L., Mohan, P. S., Cataldo, A. M., Vonsattel, J. P., Kowall, N. W., and Nixon, R. A. (1995). Elevated levels of the endosomal-lysosomal proteinase cathepsin D in cerebrospinal fluid in Alzheimer disease. *J. Neurochem.* 64, 443–446. doi: 10.1046/j.1471-4159.1995.64010443.x
- Sedaghat, F., and Notopoulos, A. (2008). S100 protein family and its application in clinical practice. *Hippokratia* 12, 198–204.
- Selkoe, D. J. (2001). Alzheimer's disease: genes, pathology, and therapy. *Physiol. Rev.* 81, 741–766. doi: 10.1152/physrev.2001.81.2.741
- Seok, J., Warren, H. S., Cuenca, A. G., Mindrinos, M. N., Baker, H. V., Xu, W., et al. (2013). Genomic responses in mouse models poorly mimic human inflammatory diseases. *Proc. Natl. Acad. Sci. U.S.A.* 110, 3507–3512. doi: 10.1073/pnas.1222878110
- Serrano-Pozo, A., Froesch, M. P., Masliah, E., and Hyman, B. T. (2011). Neuropathological alterations in Alzheimer disease. *Cold Spring Harb. Perspect. Med.* 1:a006189. doi: 10.1101/cshperspect.a006189
- Sheline, Y. L., and Raichle, M. E. (2013). Resting state functional connectivity in preclinical Alzheimer's disease. *Biol. Psychiatry* 74, 340–347. doi: 10.1016/j.biopsych.2012.11.028
- Shen, L., Xia, S., Zhang, H., Yao, F., Liu, X., Zhao, Y., et al. (2018). *Precision Medicine: Role of Biomarkers in Early Prediction and Diagnosis of Alzheimer's Disease*. London: IntechOpen.
- Sheng, J. G., Mrak, R. E., and Griffin, W. S. (1994). S100 beta protein expression in Alzheimer disease: potential role in the pathogenesis of neuritic plaques. *J. Neurosci. Res.* 39, 398–404. doi: 10.1002/jnr.490390406
- Sheng, J. G., Mrak, R. E., and Griffin, W. S. (1997). Glial-neuronal interactions in Alzheimer disease: progressive association of IL-1alpha+ microglia and S100beta+ astrocytes with neurofibrillary tangle stages. *J. Neuropathol. Exp. Neurol.* 56, 285–290.
- Shepherd, C. E., Goyette, J., Utter, V., Rahimi, F., Yang, Z., Geczy, C. L., et al. (2006). Inflammatory S100A9 and S100A12 proteins in Alzheimer's disease. *Neurobiol. Aging* 27, 1554–1563. doi: 10.1016/j.neurobiolaging.2005.09.033
- Sheridan, G. K., and Murphy, K. J. (2013). Neuron-glia crosstalk in health and disease: fractalkine and CX3CR1 take centre stage. *Open Biol.* 3:130181. doi: 10.1098/rsob.130181
- Sidoryk-Wegrzynowicz, M., Gerber, Y. N., Ries, M., Sastre, M., Tolkovsky, A. M., and Spillantini, M. G. (2017). Astrocytes in mouse models of tauopathies acquire early deficits and lose neurosupportive functions. *Acta Neuropathol. Commun.* 5:89. doi: 10.1186/s40478-017-0478-9
- Sjogren, M., Blomberg, M., Jonsson, M., Wahlund, L. O., Edman, A., Lind, K., et al. (2001). Neurofilament protein in cerebrospinal fluid: a marker of white matter changes. *J. Neurosci. Res.* 66, 510–516. doi: 10.1002/jnr.1242
- Skachokova, Z., Martinisi, A., Flach, M., Sprenger, F., Naegelin, Y., Steiner-Monard, V., et al. (2019). Cerebrospinal fluid from Alzheimer's disease patients promotes tau aggregation in transgenic mice. *Acta Neuropathol. Commun.* 7:72. doi: 10.1186/s40478-019-0725-3
- Skoog, I., Davidsson, P., Aevarsson, Ö, Vanderstichele, H., Vanmechelen, E., and Blennow, K. (2003). Cerebrospinal fluid beta-amyloid 42 is reduced before the onset of sporadic dementia: a population-based study in 85-year-olds. *Dement. Geriatr. Cogn. Disord.* 15, 169–176. doi: 10.1159/000068478
- Smith, D. E., Rapp, P. R., McKay, H. M., Roberts, J. A., and Tuszynski, M. H. (2004). Memory impairment in aged primates is associated with focal death of cortical neurons and atrophy of subcortical neurons. *J. Neurosci.* 24, 4373–4381. doi: 10.1523/jneurosci.4289-03.2004
- Smith, T. D., Adams, M. M., Gallagher, M., Morrison, J. H., and Rapp, P. R. (2000). Circuit-specific alterations in hippocampal synaptophysin immunoreactivity predict spatial learning impairment in aged rats. *J. Neurosci.* 20, 6587–6593. doi: 10.1523/JNEUROSCI.20-17-06587.2000
- Speake, T., Whitwell, C., Kajita, H., Majid, A., and Brown, P. D. (2001). Mechanisms of CSF secretion by the choroid plexus. *Microsc. Res. Tech.* 52, 49–59. doi: 10.1002/1097-0029(20010101)52:1<49::AID-JEMT7<3.0.CO;2-C
- Spector, R., Robert Snodgrass, S., and Johanson, C. E. (2015). A balanced view of the cerebrospinal fluid composition and functions: focus on adult humans. *Exp. Neurol.* 273, 57–68. doi: 10.1016/j.expneurol.2015.07.027
- Sperling, R. A., Aisen, P. S., Beckett, L. A., Bennett, D. A., Craft, S., Fagan, A. M., et al. (2011). Toward defining the preclinical stages of Alzheimer's disease: recommendations from the National Institute on Aging-Alzheimer's Association workgroups on diagnostic guidelines for Alzheimer's disease. *Alzheimers Dement.* 7, 280–292. doi: 10.1016/j.jalz.2011.03.003
- Stadtman, E. R., and Levine, R. L. (2003). Free radical-mediated oxidation of free amino acids and amino acid residues in proteins. *Amino. Acids* 25, 207–218. doi: 10.1007/s00726-003-0011-2
- Steinacker, P., Blennow, K., Halbgauer, S., Shi, S., Ruf, V., Oeckl, P., et al. (2016). Neurofilaments in blood and CSF for diagnosis and prediction of onset in Creutzfeldt-Jakob disease. *Sci. Rep.* 6:38737. doi: 10.1038/srep38737
- Steinacker, P., Semler, E., Anderl-Straub, S., Diehl-Schmid, J., Schroeter, M. L., Uttner, I., et al. (2017). Neurofilament as a blood marker for diagnosis and monitoring of primary progressive aphasia. *Neurology* 88, 961–969. doi: 10.1212/wnl.0000000000003688
- Stomrud, E., Hansson, O., Zetterberg, H., Blennow, K., Minthon, L., and Londos, E. (2010). Correlation of longitudinal cerebrospinal fluid biomarkers with cognitive decline in healthy older adults. *Arch. Neurol.* 67, 217–223. doi: 10.1001/archneurol.2009.316
- Stranahan, A. M., Jiam, N. T., Spiegel, A. M., and Gallagher, M. (2012). Aging reduces total neuron number in the dorsal component of the rodent prefrontal cortex. *J. Comp. Neurol.* 520, 1318–1326. doi: 10.1002/cne.22790
- Strozyk, D., Blennow, K., White, L. R., and Launer, L. J. (2003). CSF Abeta 42 levels correlate with amyloid-neuropathology in a population-based autopsy study. *Neurology* 60, 652–656. doi: 10.1212/01.wnl.0000046581.81650.d0
- Suarez-Calvet, M., Kleinberger, G., Araque Caballero, M. A., Brendel, M., Rominger, A., Alcolea, D., et al. (2016). sTREM2 cerebrospinal fluid levels are a potential biomarker for microglia activity in early-stage Alzheimer's disease and associate with neuronal injury markers. *EMBO Mol. Med.* 8, 466–476. doi: 10.15252/emmm.201506123
- Sudhof, T. C., and Rizo, J. (1996). Synaptotagmins: c2-domain proteins that regulate membrane traffic. *Neuron* 17, 379–388. doi: 10.1016/s0896-6273(00)80171-3
- Sunderland, T., Wolozin, B., Galasko, D., Levy, J., Dukoff, R., Bahro, M., et al. (1999). Longitudinal stability of CSF tau levels in Alzheimer patients. *Biol. Psychiatry* 46, 750–755. doi: 10.1016/s0006-3223(99)00143-2
- Sunkin, S. M., Ng, L., Lau, C., Dolbeare, T., Gilbert, T. L., Thompson, C. L., et al. (2013). Allen Brain Atlas: an integrated spatio-temporal portal for exploring the central nervous system. *Nucleic Acids Res.* 41, D996–D1008. doi: 10.1093/nar/gks1042
- Sutherland, R. J., Kolb, B., and Whishaw, I. Q. (1982). Spatial mapping: definitive disruption by hippocampal or medial frontal cortical damage in the rat. *Neurosci. Lett.* 31, 271–276. doi: 10.1016/0304-3940(82)90032-5
- Sutphen, C. L., McCue, L., Herries, E. M., Xiong, C., Ladenson, J. H., Holtzman, D. M., et al. (2018). Longitudinal decreases in multiple cerebrospinal fluid biomarkers of neuronal injury in symptomatic late onset Alzheimer's disease. *Alzheimers Dement.* 14, 869–879. doi: 10.1016/j.jalz.2018.01.012
- Swarbrick, S., Wragg, N., Ghosh, S., and Stolzing, A. (2019). Systematic review of miRNA as biomarkers in Alzheimer's disease. *Mol. Neurobiol.* 56, 6156–6167. doi: 10.1007/s12035-019-1500-y

- Swardfager, W., Lanctot, K., Rothenburg, L., Wong, A., Cappell, J., and Herrmann, N. (2010). A meta-analysis of cytokines in Alzheimer's disease. *Biol. Psychiatry* 68, 930–941. doi: 10.1016/j.biopsych.2010.06.012
- Sweetman, B., and Linninger, A. A. (2011). Cerebrospinal fluid flow dynamics in the central nervous system. *Ann. Biomed. Eng.* 39, 484–496. doi: 10.1007/s10439-010-0141-0
- Tagawa, K., Kunishita, T., Maruyama, K., Yoshikawa, K., Kominami, E., Tsuchiya, T., et al. (1991). Alzheimer's disease amyloid beta-clipping enzyme (APP secretase): identification, purification, and characterization of the enzyme. *Biochem. Biophys. Res. Commun.* 177, 377–387. doi: 10.1016/0006-291x(91)91994-n
- Takeda, S., Commins, C., DeVos, S. L., Nobuhara, C. K., Wegmann, S., Roe, A. D., et al. (2016). Seed-competent high-molecular-weight tau species accumulates in the cerebrospinal fluid of Alzheimer's disease mouse model and human patients. *Ann. Neurol.* 80, 355–367. doi: 10.1002/ana.24716
- Takeda, S., Sato, N., Ikimura, K., Nishino, H., Rakugi, H., and Morishita, R. (2011). Novel microdialysis method to assess neuropeptides and large molecules in free-moving mouse. *Neuroscience* 186, 110–119. doi: 10.1016/j.neuroscience.2011.04.035
- Tapiola, T., Alafuzoff, I., Herukka, S. K., Parkkinen, L., Hartikainen, P., Soininen, H., et al. (2009). Cerebrospinal fluid {beta}-amyloid 42 and tau proteins as biomarkers of Alzheimer-type pathologic changes in the brain. *Arch. Neurol.* 66, 382–389. doi: 10.1001/archneurol.2008.596
- Tapiola, T., Pirttilä, T., Mikkonen, M., Mehta, P. D., Alafuzoff, I., Koivisto, K., et al. (2000). Three-year follow-up of cerebrospinal fluid tau, beta-amyloid 42 and 40 concentrations in Alzheimer's disease. *Neurosci. Lett.* 280, 119–122. doi: 10.1016/s0304-3940(00)00767-9
- Tarnaris, A., Toma, A. K., Chapman, M. D., Petzold, A., Keir, G., Kitchen, N. D., et al. (2011). Rostrocaudal dynamics of CSF biomarkers. *Neurochem. Res.* 36, 528–532. doi: 10.1007/s11064-010-0374-1
- Terry, R. D., Masliah, E., Salmon, D. P., Butters, N., DeTeresa, R., Hill, R., et al. (1991). Physical basis of cognitive alterations in Alzheimer's disease: synapse loss is the major correlate of cognitive impairment. *Ann. Neurol.* 30, 572–580. doi: 10.1002/ana.410300410
- Teunissen, C. E., Otto, M., Engelborghs, S., Herukka, S. K., Lehmann, S., Lewczuk, P., et al. (2018). White paper by the society for CSF analysis and clinical neurochemistry: overcoming barriers in biomarker development and clinical translation. *Alzheimers Res. Ther.* 10:30. doi: 10.1186/s13195-018-0359-x
- Thal, D. R., Rub, U., Orantes, M., and Braak, H. (2002). Phases of a beta-deposition in the human brain and its relevance for the development of AD. *Neurology* 58, 1791–1800. doi: 10.1212/wnl.58.12.1791
- Thompson, A. G., Gray, E., Heman-Ackah, S. M., Mager, I., Talbot, K., Andaloussi, S. E., et al. (2016). Extracellular vesicles in neurodegenerative disease - pathogenesis to biomarkers. *Nat. Rev. Neurol.* 12, 346–357. doi: 10.1038/nrneuro.2016.68
- Thorsell, A., Bjerke, M., Gobom, J., Brunhage, E., Vanmechelen, E., Andreasen, N., et al. (2010). Neurogranin in cerebrospinal fluid as a marker of synaptic degeneration in Alzheimer's disease. *Brain Res.* 1362, 13–22. doi: 10.1016/j.brainres.2010.09.073
- Tian, Z.-Y., Wang, C.-Y., Wang, T., Li, Y.-C., and Wang, Z.-Y. (2019). Glial S100A6 degrades beta-amyloid aggregation through targeting competition with Zinc ions. *Aging Dis.* 10, 756–769. doi: 10.14336/AD.2018.0912
- Timmers, M., Barao, S., Van Broeck, B., Tesseur, I., Slemmon, J., De Waepenaert, K., et al. (2017). BACE1 dynamics upon inhibition with a BACE inhibitor and correlation to downstream Alzheimer's disease markers in elderly healthy participants. *J. Alzheimers Dis.* 56, 1437–1449. doi: 10.3233/jad-160829
- Toledo, J. B., Bjerke, M., Da, X., Landau, S. M., Foster, N. L., Jagust, W., et al. (2015). Nonlinear association between cerebrospinal fluid and florbetapir F-18 beta-amyloid measures across the spectrum of Alzheimer disease. *JAMA Neurol.* 72, 571–581. doi: 10.1001/jamaneurol.2014.4829
- Toombs, J., Paterson, R. W., Lunn, M. P., Nicholas, J. M., Fox, N. C., Chapman, M. D., et al. (2013). Identification of an important potential confound in CSF AD studies: aliquot volume. *Clin. Chem. Lab. Med.* 51, 2311–2317. doi: 10.1515/cclm-2013-0293
- Town, T., Vendrame, M., Patel, A., Poetter, D., DelleDonne, A., Mori, T., et al. (2002). Reduced Th1 and enhanced Th2 immunity after immunization with Alzheimer's beta-amyloid(1-42). *J. Neuroimmunol.* 132, 49–59. doi: 10.1016/s0165-5728(02)00307-7
- Toyn, J. H., Boy, K. M., Raybon, J., Meredith, J. E. Jr., Robertson, A. S., Guss, V., et al. (2016). Robust translation of gamma-secretase modulator pharmacology across preclinical species and human subjects. *J. Pharmacol. Exp. Ther.* 358, 125–137. doi: 10.1124/jpet.116.232249
- Trickler, W. J., and Miller, D. W. (2003). Use of osmotic agents in microdialysis studies to improve the recovery of macromolecules. *J. Pharm. Sci.* 92, 1419–1427. doi: 10.1002/jps.10410
- Uddin, M. S., Stachowiak, A., Mamun, A. A., Tzvetkov, N. T., Takeda, S., Atanasov, A. G., et al. (2018). Autophagy and Alzheimer's disease: from molecular mechanisms to therapeutic implications. *Front. Aging Neurosci.* 10:4. doi: 10.3389/fnagi.2018.00004
- Uylings, H. B., and de Brabander, J. M. (2002). Neuronal changes in normal human aging and Alzheimer's disease. *Brain Cogn.* 49, 268–276. doi: 10.1006/brcg.2001.1500
- Van Giau, V., and An, S. S. (2016). Emergence of exosomal miRNAs as a diagnostic biomarker for Alzheimer's disease. *J. Neurol. Sci.* 360, 141–152. doi: 10.1016/j.jns.2015.12.005
- Vellonen, K.-S., Ihalainen, J., Boucay, M.-C., Gosselet, F., Picardat, T., Gynther, M., et al. (2017). Disease-induced alterations in brain drug transporters in animal models of Alzheimer's disease. *Pharm. Res.* 34, 2652–2662. doi: 10.1007/s11095-017-2263-7
- Verberk, I. M. W., Slot, R. E., Verfaillie, S. C. J., Heijst, H., Prins, N. D., van Berckel, B. N. M., et al. (2018). Plasma amyloid as prescreener for the earliest Alzheimer pathological changes. *Ann. Neurol.* 84, 648–658. doi: 10.1002/ana.25334
- Wahlund, L. O., and Blennow, K. (2003). Cerebrospinal fluid biomarkers for disease stage and intensity in cognitively impaired patients. *Neurosci. Lett.* 339, 99–102. doi: 10.1016/s0304-3940(02)01483-0
- Walker, D. G., Link, J., Lue, L. F., Dalsing-Hernandez, J. E., and Boyes, B. E. (2006). Gene expression changes by amyloid beta peptide-stimulated human postmortem brain microglia identify activation of multiple inflammatory processes. *J. Leukoc. Biol.* 79, 596–610. doi: 10.1189/jlb.0705377
- Wang, L. L., Huang, Y., Wang, G., and Chen, S. D. (2012). The potential role of microRNA-146 in Alzheimer's disease: biomarker or therapeutic target? *Med. Hypotheses* 78, 398–401. doi: 10.1016/j.mehy.2011.11.019
- Wang, W. X., Rajeev, B. W., Stromberg, A. J., Ren, N., Tang, G., Huang, Q., et al. (2008). The expression of microRNA miR-107 decreases early in Alzheimer's disease and may accelerate disease progression through regulation of beta-site amyloid precursor protein-cleaving enzyme 1. *J. Neurosci.* 28, 1213–1223. doi: 10.1523/jneurosci.5065-07.2008
- Weiner, M. W., Aisen, P. S., Jack, C. R. Jr., Jagust, W. J., Trojanowski, J. Q., Shaw, L., et al. (2010). The Alzheimer's disease neuroimaging initiative: progress report and future plans. *Alzheimers Dement.* 6, 202.e7–211.e7. doi: 10.1016/j.jalz.2010.03.007
- Weydt, P., Oeckl, P., Huss, A., Muller, K., Volk, A. E., Kuhle, J., et al. (2016). Neurofilament levels as biomarkers in asymptomatic and symptomatic familial amyotrophic lateral sclerosis. *Ann. Neurol.* 79, 152–158. doi: 10.1002/ana.24552
- Wildsmith, K. R., Holley, M., Savage, J. C., Skerrett, R., and Landreth, G. E. (2013). Evidence for impaired amyloid beta clearance in Alzheimer's disease. *Alzheimers Res. Ther.* 5:33. doi: 10.1186/alzrt187
- Witter, M. P. (2007). The perforant path: projections from the entorhinal cortex to the dentate gyrus. *Progress Brain Res.* 163 43–61.
- Wruck, W., Schroter, F., and Adjaye, J. (2016). Meta-analysis of transcriptome data related to hippocampus biopsies and iPSC-Derived neuronal cells from Alzheimer's disease patients reveals an association with FOXA1 and FOXA2 gene regulatory networks. *J. Alzheimers Dis.* 50, 1065–1082. doi: 10.3233/jad-150733
- Wu, G., Sankaranarayanan, S., Wong, J., Tugusheva, K., Michener, M. S., Shi, X., et al. (2012). Characterization of plasma beta-secretase (BACE1) activity and soluble amyloid precursor proteins as potential biomarkers for Alzheimer's disease. *J. Neurosci. Res.* 90, 2247–2258. doi: 10.1002/jnr.23122
- Xie, S., Xiao, J. X., Gong, G. L., Zhang, Y. F., Wang, Y. H., Wu, H. K., et al. (2006). Voxel-based detection of white matter abnormalities in mild Alzheimer disease. *Neurology* 66, 1845–1849. doi: 10.1212/01.wnl.0000219625.776.25.a
- Yamada, K., Cirrito, J. R., Stewart, F. R., Jiang, H., Finn, M. B., Holmes, B. B., et al. (2011). In vivo microdialysis reveals age-dependent decrease of brain interstitial fluid tau levels in P301S human tau transgenic mice. *J. Neurosci.* 31, 13110–13117. doi: 10.1523/JNEUROSCI.2569-11.2011

- Yamada, K., Patel, T. K., Hochgrafe, K., Mahan, T. E., Jiang, H., Stewart, F. R., et al. (2015). Analysis of in vivo turnover of tau in a mouse model of tauopathy. *Mol. Neurodegener.* 10:55. doi: 10.1186/s13024-015-0052-5
- Yan, P., Bero, A. W., Cirrito, J. R., Xiao, Q., Hu, X., Wang, Y., et al. (2009). Characterizing the appearance and growth of amyloid plaques in APP/PS1 mice. *J. Neurosci.* 29, 10706–10714. doi: 10.1523/jneurosci.2637-09.2009
- Yankner, B. A., and Mesulam, M. M. (1991). Seminars in medicine of the Beth Israel Hospital, Boston. beta-Amyloid and the pathogenesis of Alzheimer's disease. *N. Engl. J. Med.* 325, 1849–1857. doi: 10.1056/nejm199112263252605
- Yassa, M. A., Mattfeld, A. T., Stark, S. M., and Stark, C. E. (2011). Age-related memory deficits linked to circuit-specific disruptions in the hippocampus. *Proc. Natl. Acad. Sci. U.S.A.* 108, 8873–8878. doi: 10.1073/pnas.1101567108
- Zetterberg, H., Skillback, T., Mattsson, N., Trojanowski, J. Q., Portelius, E., Shaw, L. M., et al. (2016). Association of cerebrospinal fluid neurofilament light concentration with Alzheimer Disease progression. *JAMA Neurol.* 73, 60–67. doi: 10.1001/jamaneurol.2015.3037
- Zimmer, D. B., Chaplin, J., Baldwin, A., and Rast, M. (2005). S100-mediated signal transduction in the nervous system and neurological diseases. *Cell Mol. Biol.* 51, 201–214.
- Zimmer, E. R., Parent, M. J., Souza, D. G., Leuzy, A., Lecrux, C., Kim, H. I., et al. (2017). [(18)F]FDG PET signal is driven by astroglial glutamate transport. *Nat. Neurosci.* 20, 393–395. doi: 10.1038/nn.4492

Conflict of Interest: The authors declare that the research was conducted in the absence of any commercial or financial relationships that could be construed as a potential conflict of interest.

Copyright © 2020 Bjorkli, Sandvig and Sandvig. This is an open-access article distributed under the terms of the Creative Commons Attribution License (CC BY). The use, distribution or reproduction in other forums is permitted, provided the original author(s) and the copyright owner(s) are credited and that the original publication in this journal is cited, in accordance with accepted academic practice. No use, distribution or reproduction is permitted which does not comply with these terms.

Paper II

Bjorkli, Christiana; Louet, Claire; Flo, Trude Helen; Hemler, Mary Elizabeth; Sandvig, Axel; Sandvig, Ioanna. In Vivo Microdialysis in Mice Captures Changes in Alzheimer's Disease Cerebrospinal Fluid Biomarkers Consistent with Developing Pathology. *Journal of Alzheimer's Disease* 2021 ;Volum 84.(4) s. 1781-1794

This paper is not included due to copyright restrictions

Paper III



OPEN ACCESS

EDITED BY
Senthil S. Gounder,
Johns Hopkins Medicine, United States

REVIEWED BY
Aravinthkumar Jayabalan,
Johns Hopkins University, United States
Aanishaa Jhaldiyal,
Johns Hopkins Medicine, United States
Biao Cai,
Anhui University of Chinese Medicine,
China
Mahmoud Kandeel,
Kafrelsheikh University, Egypt

*CORRESPONDENCE
Christiana Bjorkli,
christiana.bjorkli@ntnu.no

SPECIALTY SECTION
This article was submitted to
Neuropharmacology,
a section of the journal
Frontiers in Pharmacology

RECEIVED 06 April 2022
ACCEPTED 28 June 2022
PUBLISHED 16 August 2022

CITATION
Bjorkli C, Hemler M, Julian JB, Sandvig A
and Sandvig I (2022), Combined
targeting of pathways regulating
synaptic formation and autophagy
attenuates Alzheimer's disease
pathology in mice.
Front. Pharmacol. 13:913971.
doi: 10.3389/fphar.2022.913971

COPYRIGHT
© 2022 Bjorkli, Hemler, Julian, Sandvig
and Sandvig. This is an open-access
article distributed under the terms of the
[Creative Commons Attribution License
\(CC BY\)](https://creativecommons.org/licenses/by/4.0/). The use, distribution or
reproduction in other forums is
permitted, provided the original
author(s) and the copyright owner(s) are
credited and that the original
publication in this journal is cited, in
accordance with accepted academic
practice. No use, distribution or
reproduction is permitted which does
not comply with these terms.

Combined targeting of pathways regulating synaptic formation and autophagy attenuates Alzheimer's disease pathology in mice

Christiana Bjorkli^{1,2*}, Mary Hemler^{1,2}, Joshua B. Julian³,
Axel Sandvig^{1,2,4,5} and Ioanna Sandvig^{1,2}

¹Department of Neuromedicine and Movement Science, Faculty of Medicine and Health Sciences, Norwegian University of Science and Technology, Trondheim, Norway, ²Department of Neurology, St. Olav's Hospital, Trondheim, Norway, ³Princeton Neuroscience Institute, Princeton University, Princeton, NJ, United States, ⁴Department of Clinical Neurosciences, Division of Neuro Head and Neck, Umeå University Hospital, Umeå, Sweden, ⁵Department of Community Medicine and Rehabilitation, Umeå University, Umeå, Sweden

All drug trials completed to date have fallen short of meeting the clinical endpoint of significantly slowing cognitive decline in Alzheimer's disease (AD) patients. In this study, we repurposed two FDA-approved drugs, Fasudil and Lonafarnib, targeting synaptic formation (i.e., Wnt signaling) and cellular clearance (i.e., autophagic) pathways respectively, to test their therapeutic potential for attenuating AD-related pathology. We characterized our 3xTg AD mouse colony to select timepoints for separate and combinatorial treatment of both drugs while collecting cerebrospinal fluid (CSF) using an optimized microdialysis method. We found that treatment with Fasudil reduced A β at early and later stages of AD, whereas administration of Lonafarnib had no effect on A β , but did reduce tau, at early stages of the disease. Induction of autophagy led to increased size of amyloid plaques when administered at late phases of the disease. We show that combinatorial treatment with both drugs was effective at reducing intraneuronal A β and led to improved cognitive performance in mice. These findings lend support to regulating Wnt and autophagic pathways in order to attenuate AD-related pathology.

KEYWORDS

microdialysis, repurposed drugs, Wnt signalling, mTor pathway, amyloid plaques, neurofibrillary tangles

Introduction

Alzheimer's disease (AD) is the leading cause of dementia, and symptoms include progressive neurodegeneration, followed by impairments in memory, cognitive and visuospatial function (De Strooper and Karran, 2016). Neuropathology in AD patients is characterized by extracellular deposits of aggregated amyloid- β (A β ; i.e., amyloid plaques), and neurofibrillary tangles (NFTs) consisting of hyperphosphorylated tau, and eventually abiotrophic neuronal cell death starting in superficial layers of lateral entorhinal cortex (LEC) (Braak and Braak, 1991; Thal et al., 2002; De Strooper and Karran, 2016). Both amyloid plaques and NFTs are believed to disrupt the healthy function of synapses and neurons (Mufson et al., 2016), as well as to impair cellular clearance along autophagic pathways (Baixauli et al., 2014; Liu and Li, 2019). Researchers and clinicians are currently utilizing cerebrospinal fluid (CSF) levels of A β and tau to predict the development and rate of the disease (Snider et al., 2009; Buchhave et al., 2012; Mufson et al., 2016; Bjorkli et al., 2020).

Over the years there have been multiple therapeutic approaches aimed at lowering A β and tau levels. Promising avenues for AD therapeutics include drugs that attenuate synaptic loss and therapies that take advantage of the autophagic system to remove intraneuronal protein aggregates. Both drug targets represent structural and biochemical correlates of cognitive decline in AD. For instance, A β -driven synaptic loss has been found to be dependent on the activation of a branch of Wnt¹ signaling known as the Wnt-planar cell polarity (Wnt-PCP) pathway (Killick et al., 2014) (Supplementary Figure S1A). Drugs that inhibit Rho-associated protein kinase (ROCK) along the Wnt-PCP pathway have been shown to attenuate AD-related pathology, and these include pitavastatin (Hamano et al., 2020), FSD-C10 (Gu et al., 2018), Y-27632 (Herskowitz et al., 2013), and Fasudil (Tang and Liou, 2007; Herskowitz et al., 2013; Elliott et al., 2018; Sellers et al., 2018), among others. A β has been shown to activate Wnt-PCP signaling through its ability to induce Dickkopf-1 (Dkk1), which then blocks the binding interaction between lipoprotein receptor-related protein 6 (LRP6) and frizzled, leading to activation of Wnt-PCP signaling in favor of the canonical Wnt pathway (Bafico et al., 2001; Sellers et al., 2018) (Supplementary Figure S1A). Along the same arm of Wnt-PCP signaling, binding of a Wnt receptor to frizzled causes disheveled to inhibit the activity of glycogen synthase kinase-3 β (GSK-3 β) (Moon et al., 2004), and this serine/threonine kinase contributes to the hyperphosphorylation of tau proteins (Hanger et al., 1992). Fasudil is clinically approved to treat cerebral consequences of subarachnoid haemorrhage, and as a ROCK inhibitor (Supplementary Figure S1A) it shows promise in halting the deleterious downstream effects of A β and tau pathology. Fasudil inhibits the arm of the Wnt-PCP pathway

that promotes the retraction of dendritic spines and synapses through the disheveled associated activator of morphogenesis 1 (Daam1)/Ras homolog family member A (RhoA)/ROCK pathway (Ethell and Pasquale, 2005; Schratz, 2009).

Similarly, it has been shown that autophagic activators can lower the levels of misfolded and aggregated proteins, prevent the spread of tau, and reduce neuronal loss in experimental models (Schaeffer et al., 2012; Siman et al., 2015; Hernandez et al., 2019). Drugs that induce autophagy have been shown to attenuate AD-related pathology, and includes rapamycin (Majumder et al., 2011; Zhang et al., 2017), carbamazepine (Zhang et al., 2017), lithium (Forlenza et al., 2012), memantine (Song et al., 2015), nicotinamide (Liu et al., 2013), resveratrol (Porquet et al., 2014), and Lonafarnib (Hernandez et al., 2019), as well as others. For instance, activation of mammalian target of rapamycin (mTOR) results in activation of downstream components (i.e., 4EBP1 and p70S6K1) (Supplementary Figure S1B) which both initiate cascades resulting in tau hyperphosphorylation and eventual NFTs. mTOR activation also leads to the accumulation of amyloid plaques by inhibiting autophagy, while accumulated A β further induces tau phosphorylation and mTOR activation (Mueed et al., 2019). Lonafarnib is a clinically approved cancer drug, and works as a farnesyltransferase² inhibitor, which acts as an autophagic inducer by inhibiting mTOR and prevents the accumulation of aggregated proteins and reduces cognitive decline (Pan and Yeung, 2005) (Supplementary Figure S1B). The mechanisms of action involves Ras homologue enriched in brain (Rheb) and the phosphatidylinositol 3-kinase (PI3K)/protein kinase B (Akt)/mTOR pathway. Rheb acts downstream of tuberous sclerosis complex 1 (TSC1)/TSC2 and upstream of mTOR to regulate cell growth (Inoki et al., 2003) and activates S6 kinase 1 during amino acid deprivation via mTOR (Avruch et al., 2006).

To date, drugs have fallen short of meeting the clinical endpoint of significantly slowing cognitive decline in AD patients (Gauthier et al., 2016), possibly due to off-target effects since most drugs are unable to cross the blood-brain barrier (BBB). One way of systemically delivering drugs into the brain is by *in vivo* microdialysis (Deguchi, 2002). Here we have used the most complete transgenic mouse model for AD to date, the 3xTg AD mouse, which has been shown by us and others to develop age-dependent amyloid plaque and NFT deposition (Oddo et al., 2003; Javonillo et al., 2022). We used an optimized protocol for intraventricular microdialysis (Bjorkli et al., 2021) to systemically target two promising therapeutic avenues, the Wnt and autophagic pathways, to attenuate A β and tau levels respectively, at the molecular and functional level. Many drugs that target these two pathways have displayed adverse side-effects in experimental models and patients, and we therefore opted to repurpose drugs

1 Wnt is a portmanteau created from the names of two genes, the *Drosophila wingless* gene and the murine homologue integration site 1 gene.

2 Farnesylation is a posttranslational modification of proteins.

that were already approved for clinical use. Fasudil and Lonafarnib were also chosen because they target independent pathways that regulate and/or is affected by both A β and tau pathology. Here we demonstrate that novel combinatorial treatment with both drugs was effective at reducing intraneuronal A β and led to improved context-dependent spatial memory in mice.

Materials and methods

Animals

Thirty 3xTg AD mice (MMRRC Strain #034830-JAX; RRID: MMRRC_034830-MU) (Oddo et al., 2003; Billings et al., 2005) and two control B6129 mice (Strain #:101045; RRID: IMSR_JAX: 101045) were included in these experiments. 3xTg AD mice contain three mutations associated with familial Alzheimer's disease (*APP_{Swe}*, *MAPT_{P301L}*, and *PSEN1_{M146V}*). The donating investigators of the 3xTg AD mouse model have previously communicated to Jackson Laboratories that male transgenic mice may not exhibit all phenotypic traits of AD (Billings et al., 2005). Therefore, only female mice were included in these experiments. See [Supplementary Table S1](#) for key resources used, and [Supplementary Table S2](#) for an overview of the sample size for each experimental condition.

To validate whether our mouse model replicated AD neuropathology as observed in patients, and to assess the possibility of genetic drift in our own colony (Zeldovich, 2017), we characterized the 3xTg AD mouse model. Our findings suggest that genetic drift with phenotypic effects (Masel, 2011) occurred in our mouse colony, but we also confirm that this mouse presents as a valid model for studying AD-related neuropathology.

All housing and breeding of animals was approved by the Norwegian Animal Research Authority and is in accordance with the Norwegian Animal Welfare Act §§ 1-28, the Norwegian Regulations of Animal Research §§ 1-26, and the European Convention for the Protection of Vertebrate Animals used for Experimental and Other Scientific Purposes (FOTS ID 21061). The animals were kept on a 12 h light/dark cycle under standard laboratory conditions (19–22°C, 50%–60% humidity), and had free access to food and water.

Microdialysis guide implantation surgeries

Surgeries were based on previously established protocols (Bjorkli, 2021; Bjorkli et al., 2021), but in brief, implantation surgery was performed to insert microdialysis guide cannulas (CMA 7; CMA Microdialysis AB, Kista, Sweden) into the lateral ventricle of mice. Mice were anesthetized with isoflurane gas (4% induction and 1.5–3% maintenance; IsoFlo vet., Abbott Laboratories, Chicago, IL, United States) prior to being fixed

in a stereotaxic frame (Kopf Instruments; Chicago, IL, United States). Prior to making any incisions, Marcain (0.03–0.18 mg/kg; Aspen Pharma, Ballerup, Denmark) was injected subcutaneously into the scalp and Metacam (5 mg/kg; Boehringer Ingelheim Vetmedica, Copenhagen, Denmark) and Temgesic (0.05–0.1 mg/kg; Invidor United Kingdom, Slough, Great Britain) were administered subcutaneously for intraoperative pain relief. Equal heights of bregma and lambda were measured to ensure that the skull was level for each animal (with \pm 0.1 mm tolerance), as well as two points equally distant from the midline. After leveling the skull, the stereotaxic coordinates were derived to target the lateral ventricle (A/P: –0.1 mm, M/L: +1.2 mm, D/V: –2.75 mm; see [Supplementary Figure S2](#) for histological verification of probe placement). The microdialysis guide cannula was attached to the stereotaxic frame using a guide clip and connection rod for the clip (CMA Microdialysis AB, Kista, Sweden). The skull was drilled through at these coordinates and the guide cannula was slowly lowered into the drilled hole. The guide cannula was attached to the skull with super glue and dental cement (Dentalon Plus; Cliniclans AB, Trelleborg, Sweden). Post-surgery, Metacam and Temgesic were administered within 24 h. The guide cannula was implanted into the right hemisphere of all animals, as we did not observe any lateralization of pathology in the brains of 3xTg AD mice ([Supplementary Figure S3](#)).

Stereotactic viral injections of P301L tau

Mice were treated identically to microdialysis guide implantation surgeries, up until deriving stereotaxic coordinates. To target LEC layer II, a craniotomy was made at 0.5 mm anterior to lambda and ~4 mm lateral (dependent on animal weight) to the midline. A Hamilton microsyringe (Neuro 32-gauge syringe, 5 μ l, Hamilton company, Nevada, United States) was lowered vertically into the brain to a depth ~3.6 mm (dependent on animal weight) from the surface, and 300–1,500 nl of viruses was injected using a microinjector (Nanoliter 2010, World Precision Instruments Inc., United States). We injected the adeno-associated virus (AAV)8 GFP-2a-P301Ltau (with the chicken beta actin [CBA] promoter; hereafter referred to as AAV-tau), generated by Dr. Nair at the Viral Vector Core Facility, at the Kavli Institute for Systems Neuroscience, in Trondheim, Norway. More information regarding AAV-tau can be found in this paper (Wegmann et al., 2019), but in brief, the short 2A peptide cleaves GFP and human tau during translation at the ribosome (Szymczak et al., 2004). This results in neurons transduced with the virus being able to produce GFP and human tau as individual proteins (GFP+/MCI+; donor neurons). Conversely, neurons that receive human tau from cross-neuronal spread have human tau,

but no GFP (GFP-/MC1+; recipient neurons). The microsyringe was kept in place for 5 min prior and after the injection, to minimize potential upward leakage of the viral solution. Metacam was given within 24 h post-surgery. Animals were implanted with microdialysis guide cannulas 2 months following injections.

Push-pull microdialysis apparatus and sampling

Push-pull microdialysis was conducted as previously described (Bjorkli et al., 2021), but in brief a refrigerated fraction collector (CMA 470) was set to 6°C for the storage of collected CSF in 300 µl low-retention polypropylene plastic vials (Harvard Apparatus, Cambridge, MA, United States). Fluorinated ethylene propylene (FEP) peristaltic tubing (CMA Microdialysis AB, Kista, Sweden) was placed inside each plastic vial for collection and connected to the cassette of the peristaltic roller pump (Reglo ICC Digital). This peristaltic FEP tubing was connected to the outlet side of microdialysis probes (β-irrigated 2 mDa microdialysis probe; CMA 7; CMA Microdialysis AB, Kista, Sweden) with a polyethersulfone 2 mm membrane with tubing adapters bathed in 75% ethanol. FEP tubing (CMA Microdialysis AB, Kista, Sweden) was connected to each microsyringe. The FEP tubing was then connected to the inlet part of the microdialysis probes. Transparent cages were prepared with 1.5 cm of bedding, filled water bottles, and treats. Saline or drugs were loaded inside a gastight microsyringe (CMA Microdialysis AB, Kista, Sweden), which was placed into a syringe pump (CMA 4004). The “dead volume” of the FEP outlet tubing (1.2 ml/100 mm) was calculated. 100 cm of FEP outlet tubing was used, and therefore the first 12 ml sampled from each animal were discarded. Prior to inserting the microdialysis probes into the guide cannula, the probe was conditioned in 75% ethanol for better recovery of analytes. At the conclusion of microdialyte sampling, the vials of 60 µl CSF were centrifuged and kept at -80°C until the samples were analyzed with multiplex ELISA.

Intraventricular drug infusions

Previously, researchers have administered a dosage of 10 mg/kg of Fasudil into the lateral ventricle (Sellers et al., 2018) to attenuate Aβ levels, and 80 mg/kg of Lonafarnib orally to attenuate tau levels in mice (Hernandez et al., 2019). Both drugs have previously been delivered using DMSO, which can damage the BBB and mitochondria as well as cause apoptosis (Yuan et al., 2014). Since we had a less effective delivery vehicle than DMSO (Blevins et al., 2002), we conducted pilot experiments to determine effective titers of Fasudil and Lonafarnib, as well as to determine the most effective

duration of infusions. Previous research has shown that ~98% of all small molecules are not transported across the BBB (Pardridge, 2005), whilst other research has shown poor drug transport from CSF to the brain (Yan et al., 1994). Taking drug transport across the BBB, and from CSF into the brain parenchyma into consideration, dosages of both 25, 50 and 80 mg/kg were administered in initial pilot experiments.

In these experiments, a final concentration of 50 mg/kg of Fasudil (10 mM; Selleck Chemicals, Houston, TX, United States) was infused for 14 days in mice and stored at -80°C, whilst a final concentration of 80 mg/kg of Lonafarnib (5 mM; Cayman Chemical, Ann Arbor, MI, United States) was infused for 10 days and stored -20°C between infusions (see [Supplementary Table S1](#) for key resources used). These drug concentrations resulted in no observable side-effects in mice. The same dosages were used during combinatorial infusions of Fasudil and Lonafarnib (administered for a duration of 7 days) in mice ($n = 4$) as the drugs target independent intracellular pathways. All dosages in ml were calculated using; dosage (mg)/concentration (mg/ml) = dose x ml and were infused at a volume of 60 µl at a rate of 1 µl/min using saline as a control vehicle.

To assess the efficacy of oral versus intraventricular drug administration, we mixed 0.6 ml of 50 mg/kg Fasudil and 80 mg/kg Lonafarnib in baby porridge (Nestlé S.A., Vevey, Switzerland) in 3xTg AD mice ($n = 3$). Intraventricular drug infusions were more effective in reducing intraneuronal Aβ accumulation in the dorsal subiculum (dSub) compared to oral administration of the drugs ($t_{65} = 2.54$, $p = 0.0136$, unpaired two-tailed t-test; [Supplementary Figure S4](#)).

As Lonafarnib has previously been shown to increase the activation of lysosomes (Hernandez et al., 2019), we immunolabelled for lysosomal associated membrane protein 1 (LAMP1) in 3xTg AD mice. LAMP1+ neurons in dSub were more prominent in Lonafarnib infused ($n = 4$), compared to vehicle infused mice ($n = 8$), and overlapped with fibrillar OC + amyloid plaques ([Supplementary Figure S5](#)).

Context-dependent spatial memory testing

The basic training and testing protocol of the context-dependent spatial memory task ([Supplementary Figure S6](#)) is described in (Julian et al., 2015). In brief, starting 5 days before the experiment, animals were taught to dig in a brain cup for a food reward (Weetos choco, Nestlé S.A.) in their home cage by providing them once daily with the reward gradually buried deeper under ginger-scented bedding (1 g of ginger for every 100 g of bedding) while being gradually food deprived to maintain 90–95% of their free-feed weight.

Disoriented mice were trained to dig for buried food rewards in two different chambers, one with square boundaries (4 ×

29.25 cm) and one with circle boundaries (157 cm circumference). All chambers were built out of rectangular Legos (2 × 1 cm; Lego A/S, Billund, Denmark), and were 15 cm tall. Rewards were buried under ginger-scented bedding in cups embedded in the chamber floors. Each chamber was surrounded by the same distal cues for orientation. There were four possible reward locations in each chamber, and the rewarded location differed between the square- and circle-chamber relative to the common reference frame provided by the distal cues. Pilot experiments revealed that mice could successfully discriminate the square and circle reward locations above chance after 8 trials. Therefore, the training phase consisted of four training trials per chamber per day for 2 days, with successive trials alternated across chambers (8 trials total in the square-chamber and 8 trials total in the circle-chamber). If a given mouse achieved 66.6% correct performance during training, contextual memory was then tested in 4 testing sessions across 4 days, with 8 trials per session.

During each testing session, the first two trials consisted of spatial memory being tested in the square- and circle-chamber with rewards. In trials 3–6, spatial memory was tested in four chambers with morphed boundary geometry, which continuously ranged from most-square-like to most-circle-like: a pentagon (5 × 31.4 cm), a hexagon (6 × 26.16 cm), an octagon (8 × 19.6 cm), and a decagon (10 × 15.7 cm). During the final two trials of each testing session (trials 7–8), the animals were again tested in the square- and circle-chambers with rewards. The order of the square-, circle-, and morphed-chambers across trials in each session was randomized but was the same for each animal on a given day's session. If a given mouse achieved 66.6% correct performance during testing, contextual memory was tested in an ambiguous half-square half-circle context (the "Squircle") (Julian and Doeller, 2021).

During reward trials, mice were removed from the apparatus and the trial ended after they had found the reward. During unrewarded trials, they were removed, and the trial ended after their first dig, or after 5 min (whichever came later). Chambers were cleaned with ethanol after each trial to remove odor trails. Dig locations and time spent in these locations were calculated using ANY-maze video tracking system (Stoelting Europe) via an overhead, centrally located camera (DMK 22AUC03 USB 2.0 monochrome industrial camera, The imaging Source Europe, Germany).

Proteomic analysis of amyloid- β and tau concentrations in cerebrospinal fluid

The MILLIPLEX[®] MAP human A β and tau magnetic bead panel 4-plex ELISA kit (Millipore, Burlington, MA, United States) and the Bio-Plex 200 System instrument (Biorad, Hercules, CA, United States) were used to assess

simultaneously the concentrations of A β ₄₀, A β ₄₂, total tau (t-tau), and phosphorylated tau at Thr181 (p-tau) in CSF samples. The samples were undiluted and analyzed in duplicates. The lower limit of quantification (LLOQ) for each protein is shown in [Supplementary Figure S7](#).

Tissue processing and immunohistochemistry

Mice were administered a lethal dose of sodium pentobarbital (100 mg/ml; Apotekforeningen, Oslo, Norway) and transcardially perfused with Ringer's solution followed by paraformaldehyde (PFA, 4%; Sigma-Aldrich) in 125 mM phosphate buffer (PB). Brains were extracted and fixed for a minimum of 24 h in PFA at 4°C and transferred to a 2% DMSO solution prepared in PB for 24 h at 4°C. Brains were sectioned coronally at 40 μ m on a freezing-sliding microtome (Microm HM430, ThermoFisher Scientific, Waltham, MA, United States). An incision was made in the non-implanted hemisphere for visualization of the control hemisphere. Immunohistochemical processing was conducted on tissue, see (Bjorkli, 2019; Bjorkli and Lagartos-Donate, 2022) for detailed protocols, and [Supplementary Table S1](#) for key resources.

Previous research has indicated that a differential microtubule-associated protein 2 (MAP2) immunolabeling pattern can distinguish dense-core from diffuse amyloid plaques using DAB (Sigma-Aldrich, St. Louis, MO, United States) as a chromogen (D'Andrea and Nagele, 2002). See (Bjorkli, 2022) for detailed protocol.

One series of each brain was dehydrated in ethanol, cleared in xylene (Merck Chemicals, Darmstadt, Germany) and rehydrated before staining with Cresyl violet (Nissl; 1 g/L) for 3 min to verify probe placement. The sections were then alternatively dipped in ethanol-acetic acid (5 ml acetic acid in 1 L 70% ethanol) and rinsed with cold water until the desired differentiation was obtained, then dehydrated, cleared in xylene and coverslipped with entellan containing xylene (Merck Chemicals).

Sections were scanned using a Mirax-midi slide scanner (objective 20X, NA 0.8; Carl Zeiss Microscopy, Oberkochen, Germany), using either reflected fluorescence (for sections stained with a fluorophore) or transmitted white light (for sections immunolabelled with Nissl DAB, or Gallyas-silver) as the light source.

Quantification of intraneuronal amyloid- β and tau, and amyloid plaques.

Series of sections were chosen randomly and coded to ensure blinding to the investigators. The number of cells containing intraneuronal A β , tau, and amyloid plaques, in dSub and LEC of 3xTg AD mice infused with a vehicle or drugs was estimated with

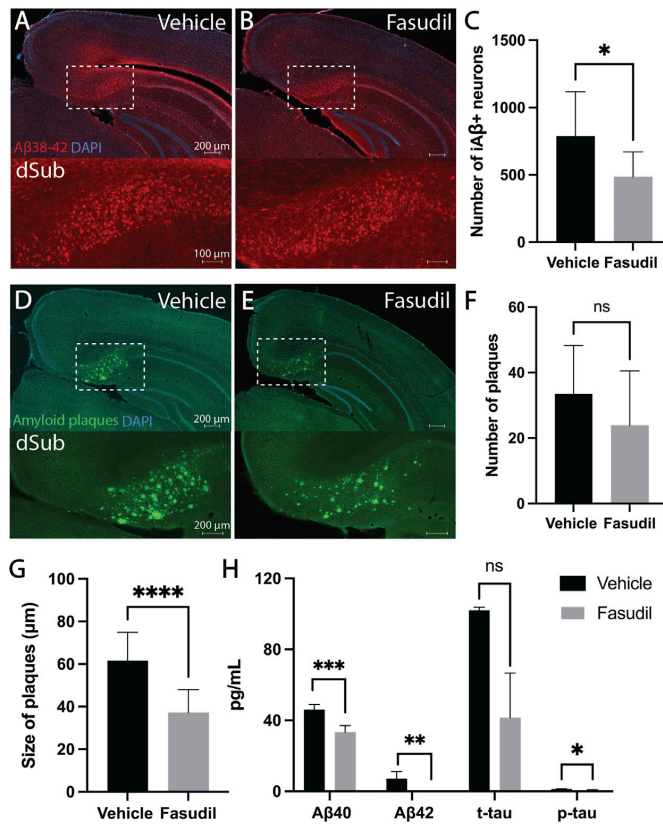


FIGURE 1

Inhibiting the Wnt-PCP pathway attenuated amyloid- β and tau pathology in early and late phase AD. (A) Intraneuronal A β_{38-42} (McSA1; red) in dSub in 3xTg AD mice ($n = 4$) receiving infusions of a vehicle (i.e., saline). DAPI counterstain (blue). (B) A β_{38-42} (McSA1; red) immunoreactivity in dSub in 3xTg AD mice ($n = 6$) receiving infusions of Fasudil. DAPI counterstain (blue). (C) Mean number of A β^+ neurons in dSub of 3xTg AD mice after infusions of a vehicle and Fasudil. Intraneuronal A β in dSub was quantified from at least 7 brain sections for each animal using Ilastik. Error bars denote ± 1 SD, unpaired two-tailed t -test, * $p < 0.05$. (D) Amyloid plaques (amyloid fibrils OC; green) in dSub of 3xTg AD mice ($n = 2$) receiving infusions of a vehicle. DAPI counterstain (blue). (E) Amyloid plaques (amyloid fibrils OC; green) in dSub of 3xTg AD mice ($n = 4$) receiving infusions of Fasudil. DAPI counterstain (blue). (F) Mean number of amyloid plaques in dSub of 3xTg AD mice after infusions of a vehicle and Fasudil. Amyloid plaques in dSub were quantified from at least 4 brain sections for each animal using Ilastik. Error bars denote ± 1 SD, unpaired two-tailed t -test, n. s. non-significant. (G) Mean size of amyloid plaques in dSub of 3xTg AD mice after infusions of a vehicle and Fasudil. Amyloid plaques in dSub were quantified from at least 4 brain sections for each animal using Ilastik. Error bars denote ± 1 SD, unpaired two-tailed t -test, ****; $p < 0.0001$. (H) Mean concentrations of duplicates of A β_{40} , A β_{42} , p-tau and t-tau CSF levels (pg/ml) as measured by multiplex ELISA on the last day of infusion (day 14) of a vehicle ($n = 6$) or Fasudil ($n = 10$) in young and older 3xTg AD mice. Error bars denote ± 1 SD, unpaired two-tailed t -test, ****; $p < 0.001$, **; $p < 0.01$, *; $p < 0.05$. Abbreviations: A β , amyloid- β ; dSub, dorsal subiculum; iA β , intraneuronal A β ; t-tau, total tau; p-tau, phosphorylated tau.

Ilastik using the Density Cell Counting workflow (Berg et al., 2019). dSub and LEC was delineated using cytoarchitectonic features in sections stained with Nissl, based on The Paxinos & Franklin Mouse Brain Atlas (Paxinos and Franklin, 2004). The same surface area and rostrocaudal levels of each brain region was selected, and at least 4 brain sections were used for each infused hemisphere. Damaged regions of brain sections were excluded from analyses to avoid false-positive antibody expression.

Statistics

Effect size (Cohen's D) was calculated based on initial experiments between animals infused with Fasudil and animals infused with a vehicle, and the resulting effects on intraneuronal A β in dSub. Based on each group consisting of $n = 2$ animals, an effect size of 0.75 was calculated (0.8 is considered a large effect size) (Cohen, 1992). Most of the

dataset was normally distributed (Shapiro-Wilk test) and therefore two-tailed, unpaired *t*-tests were used to compare mean differences. For the minor parts of the dataset that was not normally distributed, nonparametric statistical tests were used (Mann-Whitney *U*). Statistical comparisons of behavioral data across vehicle and drug infused mice were conducted based on trial-wise pooling of data across mice separately for each group. Behavioral performance in the morphed environments of the context-dependent spatial memory task (Supplementary Figure S6) was calculated as follows: dig in square-consistent location = 1, dig in circle-consistent location = 0, dig in any other location = 0.5. Context-consistency of reward locations was determined relative to the common reference frame defined by the distal cues shared across all contexts. We then assessed whether performance in the morphed environments was associated with more context-appropriate choices for animals treated with a vehicle compared to drugs. All statistical tests and graphs were made in Prism 9 (GraphPad Software Inc., CA, United States).

Results

Fasudil treatment attenuated amyloid- β and tau pathology in early and late phases of the disease

First, we wanted to assess whether Fasudil (administered for a duration of 14 days) would affect intraneuronal A β which is present already at 1-month-of-age in 3xTg AD mice (Supplementary Figure S8A; Supplementary Table S3). Intraventricular administration of Fasudil in 6 months-old 3xTg AD mice reduced the number of A β + neurons in dSub as compared to vehicle infused mice ($t_{18} = 2.63$, $p = 0.0169$, unpaired two-tailed *t*-test; Figures 1A–C). We then went on to assess the effect of Fasudil on amyloid plaques in 3xTg AD mice, which accumulate at 13-months-of-age (Supplementary Figures S8B,C; Supplementary Table S3). In older 3xTg AD mice (14 months-old), Fasudil infusions moderately reduced the number of dense-core amyloid plaques (Supplementary Figure S9) in dSub as compared to vehicle infused mice (n.s.; Figures 1D–F). The size of amyloid plaques, on the other hand, was effectively reduced in Fasudil, compared to vehicle, treated mice ($t_{26} = 4.69$, $p < 0.0001$, unpaired two-tailed *t*-test; Figures 1D,E,G). We went on to conduct proteomic analyses to assess CSF A β and tau levels following Fasudil treatment (Figure 1H). On average across younger and older mice, Fasudil effectively reduced CSF A β_{40} ($t_6 = 5.96$, $p < 0.001$, unpaired two-tailed *t*-test) and A β_{42} levels ($t_5 = 5.59$, $p < 0.01$, unpaired two-tailed *t*-test). Fasudil treatment also effectively reduced CSF p-tau levels ($t_5 = 2.86$, $p < 0.05$, unpaired two-tailed *t*-test), and moderately reduced CSF t-tau levels (n.s.).

Lonafarnib treatment attenuated amyloid- β and tau pathology in early and late phases of the disease

Similarly, we also wanted to assess whether Lonafarnib (administered for a duration of 10 days) would affect AD-related neuropathology present in early phases of AD. Since previous research suggests that Lonafarnib can reduce tau levels, we assessed not only early intraneuronal A β but also early tau abnormalities following infusions. Lonafarnib did not affect the number of A β + neurons in dSub in young 3xTg AD mice (Supplementary Figure S10). Since the earliest accumulation of non-fibrillar tau (recognized by the MC1 antibody) is not present in 3xTg AD mice until around 9-months-of-age in CA1 (Supplementary Figure S11; Supplementary Table S3), we overexpressed human tau in LEC layer II (an area that is early involved in NFT deposition in AD patients), of 6 months-old 3xTg AD mice (Figure 2A). Lonafarnib infusions moderately reduced the number of tau+ neurons in LEC following injection of AAV-tau (n.s.; Figures 2B–D).

In older 3xTg AD mice (14 months-old), Lonafarnib infusions effectively reduced the number of dense-core amyloid plaques that overlapped with MC1 immunolabelling (Supplementary Figures S9, S12) in dSub as compared to vehicle infused mice ($t_{14} = 3.86$, $p = 0.0017$, unpaired two-tailed *t*-test; Figures 2E–G). The size of amyloid plaques, on the other hand, was moderately increased in Lonafarnib, compared to vehicle, treated mice (n.s.; Figures 2E,F,H). We then conducted proteomic analyses to assess CSF A β and tau levels following Lonafarnib treatment (Figure 2I). On average, across younger (injected with AAV-tau) and older mice, Lonafarnib effectively reduced CSF A β_{40} ($t_6 = 4.53$, $p < 0.01$, unpaired two-tailed *t*-test) and t-tau levels ($t_6 = 4.05$, $p < 0.01$, unpaired two-tailed *t*-test). Lonafarnib treatment moderately reduced CSF A β_{42} (n.s.) and p-tau levels (n.s.).

Combinatorial drug treatment effectively attenuated Alzheimer's disease-related pathology at the molecular and functional level

Since both drugs appeared to reduce AD-related neuropathology, we wanted to assess their combinatorial effects when administered for 7 days during earlier phases of the disease (4-months-of-age). Since these mice were young, the treatment effects on intraneuronal A β in dSub were assessed, without the possibility of assessing amyloid plaques or tau pathology (Supplementary Table S3). Combinatorial treatment

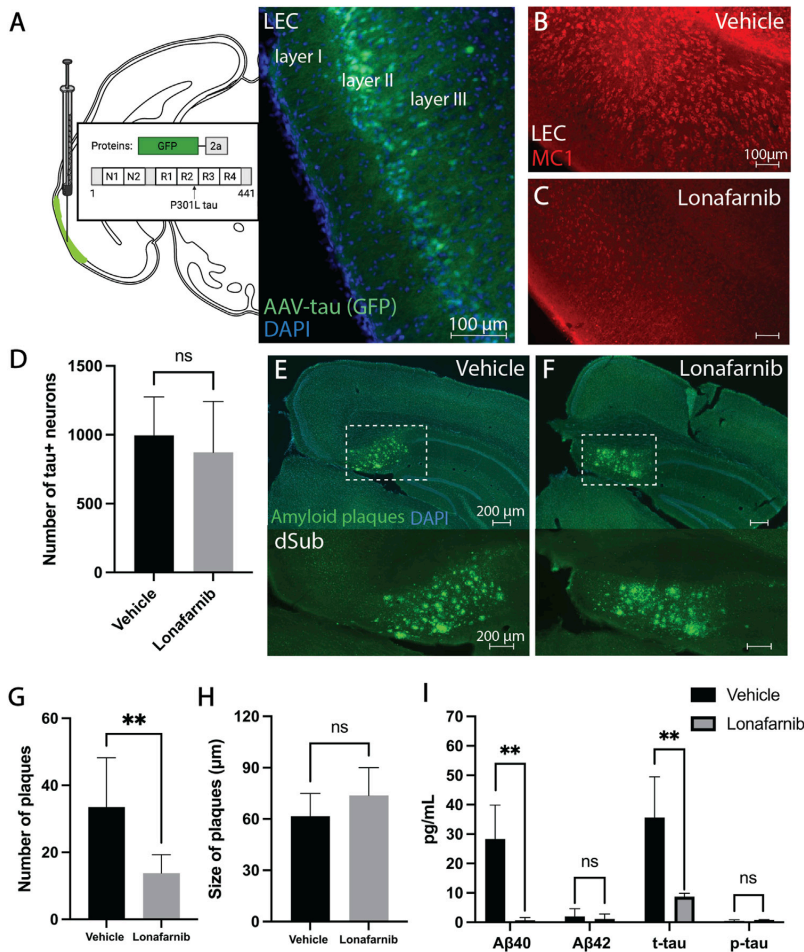


FIGURE 2

Induction of autophagy attenuated amyloid- β and tau pathology in early and late phase AD. (A) Schematic for the injection of AAV8 GFP-2a-P301Ltau (AAV-tau) into LEC layer II (GFP; green) of 3xTg AD mice ($n = 4$), and the proteins encoded in the viral construct. DAPI counterstain (blue). (B) Conformation-specific tau (MC1; red) in LEC of 3xTg AD mice ($n = 2$) receiving infusions of a vehicle (i.e., saline). (C) Conformation-specific tau (MC1; red) in LEC of 3xTg AD mice ($n = 2$) receiving infusions of Lonafarnib. (D) Mean number of tau + neurons in LEC of 3xTg AD mice after infusions of a vehicle and Lonafarnib. Intraneuronal tau in LEC layer II was quantified from at least 4 brain sections for each animal using Ilastik. Error bars denote ± 1 SD, unpaired two-tailed t -test, n.s.: non-significant. (E) Amyloid plaques (amyloid fibrils OC; green) in dSub of 3xTg AD mice ($n = 2$) receiving infusions of a vehicle. DAPI counterstain (blue). (F) Amyloid plaques (amyloid fibrils OC; green) in dSub of 3xTg AD mice ($n = 2$) receiving infusions of Lonafarnib. DAPI counterstain (blue). (G) Mean number of amyloid plaques in dSub of 3xTg AD mice after infusions of a vehicle and Lonafarnib. Amyloid plaques in dSub were quantified from at least 4 brain sections for each animal using Ilastik. Error bars denote ± 1 SD, unpaired two-tailed t -test, **: $p < 0.01$. (H) Mean size of amyloid plaques in dSub of 3xTg AD mice after infusions of a vehicle and Lonafarnib. Amyloid plaques in dSub were quantified from at least 4 brain sections for each animal using Ilastik. Error bars denote ± 1 SD, unpaired two-tailed t -test, n.s.: non-significant. (I) Mean concentrations of duplicates of A β_{40} , A β_{42} , p-tau and t-tau CSF levels (pg/ml) as measured by multiplex ELISA on the last day of infusion (day 10) of a vehicle ($n = 8$) or Lonafarnib ($n = 4$) in young (injected with AAV-tau) and older 3xTg AD mice. Error bars denote ± 1 SD, unpaired two-tailed t -test, **: $p < 0.01$. Abbreviations: GFP, green fluorescent protein; LEC, lateral entorhinal cortex; AAV, adeno-associated virus; dSub, dorsal subiculum; t-tau, total tau; p-tau, phosphorylated tau.

of drugs effectively reduced the number of A β + neurons in dSub of mice ($t_{80} = 4.66$, $p < 0.0001$, unpaired two-tailed t -test; Figures 3A–C).

Proteomic analyses of CSF A β and tau levels (Figure 3D) revealed that on average, combinatorial treatment effectively reduced CSF t-tau ($t_{10} = 2.39$, $p < 0.05$, unpaired two-tailed

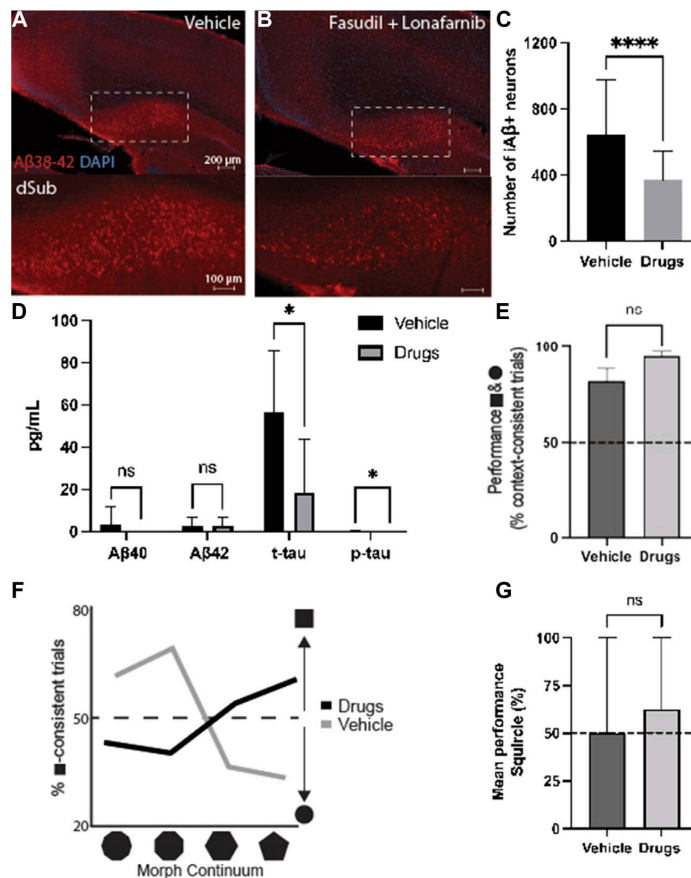


FIGURE 3

Combinatorial targeting of Wnt and mTOR pathways effectively attenuates neuropathology and context-dependent spatial memory deficits. (A) Intraneuronal Aβ₃₈₋₄₂ (McSA1; red) in dSub in 3xTg AD mice ($n = 4$) receiving infusions of a vehicle (i.e., saline). DAPI counterstain (blue). (B) Aβ₃₈₋₄₂ (McSA1; red) immunoreactivity in dSub in 3xTg AD mice ($n = 4$) receiving infusions of Fasudil and Lonafarnib. DAPI counterstain (blue). (C) Mean number of Aβ+ neurons in dSub of 3xTg AD mice after infusions of a vehicle, or Fasudil and Lonafarnib. Intraneuronal Aβ in dSub was quantified from at least 7 brain sections for each animal using Ilastik. Error bars denote ± 1 SD, unpaired two-tailed t -test, **** $p < 0.0001$. (D) Mean concentrations of duplicates of Aβ₄₀, Aβ₄₂, p-tau and t-tau CSF levels (pg/ml) as measured by multiplex ELISA on the last day of infusion (day 7) of a vehicle ($n = 6$) or Fasudil and Lonafarnib ($n = 4$) in young 3xTg AD mice. Error bars denote ± 1 SD, unpaired two-tailed t -test, * $p < 0.05$. (E) Mean behavioral performance (% of trials with context-appropriate choices) in 3xTg AD mice infused with a vehicle ($n = 3$) or Fasudil and Lonafarnib ($n = 4$) in the square- and circle-chambers. Error bars denote ± 1 SD, unpaired two-tailed t -test, n.s.: non-significant. (F) Percentage of trials with square context-consistent digs in 3xTg AD mice infused with a vehicle ($n = 3$) or Fasudil and Lonafarnib ($n = 4$) in each of the four morphed environments, ranging from most circle-like to most square-like in boundary geometry shape. (G) Mean behavioral performance (% of trials with context-appropriate choices) in 3xTg AD mice infused with a vehicle ($n = 3$) or Fasudil and Lonafarnib ($n = 4$) in the Squiracle context. Error bars denote ± 1 SD, unpaired two-tailed t -test, n.s.: non-significant. Abbreviations: Aβ, amyloid-β; dSub, dorsal subiculum; iAβ, intraneuronal Aβ; t-tau, total tau; p-tau, phosphorylated tau.

t -test) and p-tau levels ($t_{10} = 2.24$, $p < 0.05$, unpaired two-tailed t -test). Combinatorial treatment moderately reduced CSF Aβ₄₀₋₄₂ levels (n.s.).

We then examined context-dependent spatial memory (Supplementary Figure S6) in 3xTg AD mice at 4-months-of-age, the same age as when cognitive deficits usually begin in this

model (Billings et al., 2005), after vehicle and drug infusions. Mice were trained to search for buried food rewards in two different contexts, one square and one circle (more details can be found in (Julian et al., 2015)). Animals infused with drugs initially searched in context-appropriate reward locations slightly more often than those infused with a vehicle. (n.s.;

Figure 3E). We further examined contextual memory recall in environments with progressive morphs of boundary geometry, increasing the number of boundary walls from most square-like to most circle-like. Compared to animals infused with a vehicle, drug infused mice searched more often in context-consistent reward locations ($\chi^2 = 69.17$, $p < 0.0001$; Pearson's Chi-squared test; Figure 3F). Furthermore, when contextual memory was tested in an ambiguous half-square half-circle context (the "Squirrel"), mice infused with drugs were slightly more likely to dig at a location previously associated with either the square or circle, compared to locations not associated with any context, and compared to control animals infused with a vehicle (n.s.; Figure 3G). Thus, combinatorial drug treatment led to an improvement of cognitive deficits usually associated with canonical AD.

Discussion

In this study we repurposed two FDA-approved drugs, Fasudil and Lonafarnib, both targeting independent biochemical cascades that halted the development of AD pathology in 3xTg AD mice. Treatment with Fasudil reduced early intraneuronal A β , the number and size of amyloid plaques in dSub, and CSF A β_{40-42} and p-tau levels. Lonafarnib infusions, on the other hand, did not affect intraneuronal A β but rather reduced early non-fibrillar forms of tau after overexpression in LEC layer II. Treatment with Lonafarnib also reduced the number of amyloid plaques, but unexpectedly increased their size in dSub, and only effectively decreased CSF A β_{40} and t-tau levels. Both drugs affected dense-core, rather than diffuse, amyloid plaques, and the former is associated with microglial activation, neurodegeneration, and cognitive decline in AD patients (Knowles et al., 1999; DeTure and Dickson, 2019). We found that novel combinatorial administration of these drugs effectively reduced early intraneuronal A β in younger mice, led to reduced CSF A β_{40} and p- and t-tau levels, and improved context-dependent spatial memory. This type of pattern completion is thought to depend on the normal function of the hippocampus (Pilly et al., 2018; Hainmueller and Bartos, 2020), a region that is compromised during early phases of AD.

Our results following Fasudil infusions are in line with previous reports of its efficacy in reducing A β levels (Tang and Liou, 2007; Herskowitz et al., 2013; Elliott et al., 2018; Sellers et al., 2018). Similarly, our findings after Lonafarnib treatment coincide with previous results of its efficacy to reduce AD-related neuropathology (Hernandez et al., 2019). Our findings of larger amyloid plaques following Lonafarnib treatment may be explained by reports of diminished levels of regulatory proteins in the autophagic system in older ages (Nixon and Yang, 2011; Menzies et al., 2017), which may lead to increased sequestration of nearby

A β peptides by amyloid plaques. Conversely, this finding could be due to an increase in intracellular digestion, resulting in a larger expansion of amyloid plaques (D'Andrea et al., 2001).

The efficacy of the novel combinatorial treatment of both drugs presented here aligns with several previous findings. A β has not only been shown to activate Wnt-PCP signaling through Dkk1 (Bafico et al., 2001; Sellers et al., 2018), but also to increase mTOR activity in 3xTg AD mice brain regions with high levels of intraneuronal A β (Caccamo et al., 2010; Caccamo et al., 2011). Activation of Wnt-PCP also leads to induction of GSK-3 β which contributes to the formation of tau pathology (Moon et al., 2004), and which has been found to suppress autophagy via mTOR complex 1 (mTORC1) and lysosomes (Azoulay-Alfaguter et al., 2015). Thus, regulating the tightly-linked Wnt and mTOR pathways (Yu et al., 2007) at early stages of AD has beneficial therapeutic effects in AD mouse models.

Limitations of the study

There are potential limitations of this study that should be considered while interpreting our results. We found that CSF t-tau levels generally increased in the first few days of microdialysis sampling, with lower, but still elevated levels at the end of drug treatment. This is consistent with CSF t-tau concentrations increasing in the first few days following injury (i.e., probe implantation in our experiments), then reduction over time (Neselius et al., 2012). However, we have previously shown that long-term implantation of our microdialysis probes does not lead to observable neuroinflammation in 3xTg AD mice (Bjorkli et al., 2021). In addition, intracerebral microdialysis is an invasive technique, so it is currently only used in patients requiring neurocritical care, neurosurgery, or brain biopsy (Marklund et al., 2009). A leaky BBB has often been found to precede amyloid plaque formation in AD patients (Zenaro et al., 2017) and 3xTg AD mice (Ujije et al., 2003), and could therefore affect drug penetration in our mice. Moreover, in our study and most preclinical translational AD research, there is an increased focus on familial rather than sporadic forms of AD. This limitation, however, should not detract from the value of the current study and other studies using transgenic models, as the continuums of sporadic and familial forms of AD are very similar, except for age-of-onset (Holmes and Lovestone, 2002).

Conclusion and future directions

In this study, we repurposed, Fasudil and Lonafarnib, targeting synaptic formation and autophagic pathways respectively, to test their therapeutic potential for attenuating AD-related pathology. We show that combinatorial treatment with both drugs was effective at reducing intraneuronal A β and led to improved cognitive performance in mice. Importantly, based on our own

characterization of 3xTg AD mice, we demonstrate potential timepoints for when it would be beneficial during the disease continuum to target Wnt and autophagic pathways to attenuate AD pathology. Targeting Wnt during early and late stages of the disease effectively reduced A β , whereas targeting mTOR did not affect A β levels at early stages of AD. Overexpression of tau in LEC layer II was effectively reduced by Lonafarnib at early stages, but treatment led to an increase in size of amyloid plaques at later stages of AD. Combinatorial treatment of both drugs when 3xTg AD mice start to display cognitive impairments not only reduced intraneuronal A β , but also attenuated context-dependent spatial memory deficits. Therefore, future studies should aim for longitudinal combinatorial treatment starting before observable cognitive deficits, while examining the effect on AD pathophysiology at later stages of the disease. Taken together, our findings lend support to the application of Wnt and mTOR regulation to attenuate AD pathology at various therapeutic timepoints in preclinical models.

Data availability statement

The original contributions presented in the study are included in the article/Supplementary Material, further inquiries can be directed to the corresponding author.

Ethics statement

The animal study was reviewed and approved by Norwegian Animal Research Authority and is in accordance with the Norwegian Animal Welfare Act §§ 1-28, the Norwegian Regulations of Animal Research §§ 1-26, and the European Convention for the Protection of Vertebrate Animals used for Experimental and Other Scientific Purposes (FOTS ID 21061).

Author contributions

Conceptualization: CB and IS; Methodology: CB, JBJ, AS, and IS; Investigation: CB and MH; Visualization: CB and MH; Funding acquisition: CB, AS, and IS; Project administration: CB, AS, and IS; Supervision: AS, IS, and CB; Writing—original draft: CB; Writing—review and editing: CB, MH, JBJ, AS, and IS.

References

- Avruch, J., Hara, K., Lin, Y., Liu, M., Long, X., Ortiz-Vega, S., et al. (2006). Insulin and amino-acid regulation of mTOR signaling and kinase activity through the Rheb GTPase. *Oncogene* 25 (48), 6361–6372. doi:10.1038/sj.onc.1209882
- Azoulay-Alfaguter, I., Elya, R., Avrahami, L., Katz, A., and Eldar-Finkelman, H. (2015). Combined regulation of mTORC1 and lysosomal acidification by GSK-3 suppresses autophagy and contributes to cancer cell growth. *Oncogene* 34 (35), 4613–4623. doi:10.1038/onc.2014.390
- Bafico, A., Liu, G., Yaniv, A., Gazit, A., and Aaronson, S. A. (2001). Novel mechanism of Wnt signalling inhibition mediated by Dickkopf-1 interaction with LRP6/Arrow. *Nat. Cell Biol.* 3 (7), 683–686. doi:10.1038/35083081
- Baixaui, F., López-Otin, C., and Mittelbrunn, M. (2014). Exosomes and autophagy: Coordinated mechanisms for the maintenance of cellular fitness. *Front. Immunol.* 5, 403. doi:10.3389/fimmu.2014.00403

Funding

This work was funded by the liaison Committee for Education, Research, and Innovation in Central Norway (Samarbeidsorganet HMN-NTNU) grant number 2018/42794. Joint Research Committee (Felles Forskningsutvalg—St. Olav's Hospital HF and the Faculty of Medicine, NTNU) grant number 2019/26157.

Acknowledgments

The authors would like to give special thanks to Claire Louet and the lab of Trude Helen Flo at CEMIR, the Norwegian University of Science and Technology (Trondheim, Norway) for assistance in proteomic analyses of CSF samples. We would also like to thank Nora Cecilie Ebbesen for allowing us to reproduce the schematic for the context-dependent spatial memory task. We also thank the late Dr. Peter Davies for providing the MC1 antibody for these studies.

Conflict of interest

The authors declare that the research was conducted in the absence of any commercial or financial relationships that could be construed as a potential conflict of interest.

Publisher's note

All claims expressed in this article are solely those of the authors and do not necessarily represent those of their affiliated organizations, or those of the publisher, the editors and the reviewers. Any product that may be evaluated in this article, or claim that may be made by its manufacturer, is not guaranteed or endorsed by the publisher.

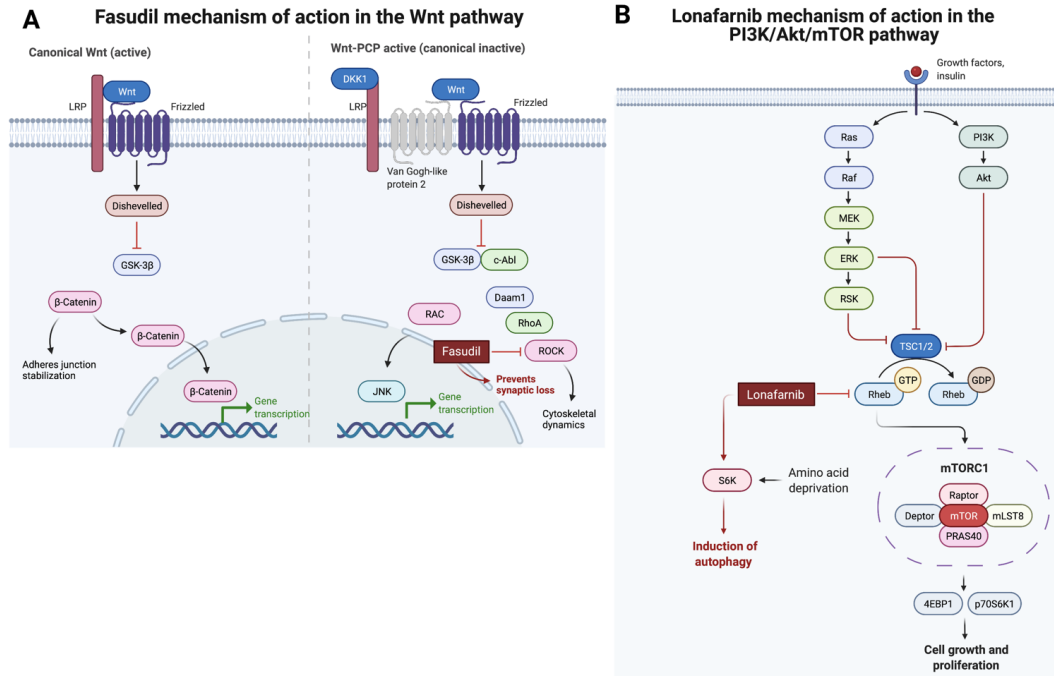
Supplementary material

The Supplementary Material for this article can be found online at: <https://www.frontiersin.org/articles/10.3389/fphar.2022.913971/full#supplementary-material>

- Berg, S., Kutra, D., Kroeger, T., Straehle, C. N., Kausler, B. X., Haubold, C., et al. (2019). Ilastik: Interactive machine learning for (bio)image analysis. *Nat. Methods* 16 (12), 1226–1232. doi:10.1038/s41592-019-0582-9
- Billings, L. M., Oddo, S., Green, K. N., McGaugh, J. L., and LaFerla, F. M. (2005). Intraneuronal β tau causes the onset of early Alzheimer's disease-related cognitive deficits in transgenic mice. *Neuron* 45 (5), 675–688. doi:10.1016/j.neuron.2005.01.040
- Bjorkli, C. (2019). *IHC AD neuropathology protocol*. Berkeley, CA: protocols.io. Available at: <https://protocols.io/view/ihc-ad-neuropathology-protocol-btbmnik6>.
- Bjorkli, C., and Lagartos-Donate, M. J. (2022). *Gallys-silver stain*. Berkeley, CA: protocols.io. doi:10.17504/protocols.io.b44cqysw
- Bjorkli, C., Louet, C., Flo, T. H., Hemler, M., Sandvig, A., Sandvig, I., et al. (2021). *In vivo* microdialysis in mice captures changes in Alzheimer's disease cerebrospinal fluid biomarkers consistent with developing pathology. *J. Alzheimers Dis.* 84 (4), 1781–1794. doi:10.3233/jad-210715
- Bjorkli, C. (2021). *Microdialysis guide cannula implantation surgery*. Berkeley, CA: protocols.io. doi:10.17504/protocols.io.bszzxf7n
- Bjorkli, C. (2022). *Peroxidase/DAB protocol*. Berkeley, CA: protocols.io. doi:10.17504/protocols.io.b44fqtyn
- Bjorkli, C., Sandvig, A., and Sandvig, I. (2020). Bridging the gap between fluid biomarkers for Alzheimer's disease, model systems, and patients. *Front. Aging Neurosci.* 12, 272. doi:10.3389/fnagi.2020.00272
- Blevins, J. E., Stanley, B. G., and Reidelberger, R. D. (2002). DMSO as a vehicle for central injections: Tests with feeding elicited by norepinephrine injected into the paraventricular nucleus. *Pharmacol. Biochem. Behav.* 71 (1), 277–282. doi:10.1016/S0091-3057(01)00659-1
- Braak, H., and Braak, E. (1991). Neuropathological staging of Alzheimer-related changes. *Acta Neuropathol.* 82 (4), 239–259. doi:10.1007/BF00308809
- Buchhave, P., Minthon, L., Zetterberg, H., Wallin, A. K., Blennow, K., Hansson, O., et al. (2012). Cerebrospinal fluid levels of beta-amyloid 1–42, but not of tau, are fully changed already 5 to 10 years before the onset of Alzheimer dementia. *Arch. Gen. Psychiatry* 69 (1), 98–106. doi:10.1001/archgenpsychiatry.2011.155
- Caccamo, A., Majumder, S., Richardson, A., Strong, R., and Oddo, S. (2010). Molecular interplay between mammalian target of rapamycin (mTOR), amyloid-beta, and tau: Effects on cognitive impairments. *J. Biol. Chem.* 285 (17), 13107–13120. doi:10.1074/jbc.M110.100420
- Caccamo, A., Maldonado, M. A., Majumder, S., Medina, D. X., Holbein, W., Magri, A., et al. (2011). Naturally secreted amyloid-beta increases mammalian target of rapamycin (mTOR) activity via a PRA540-mediated mechanism. *J. Biol. Chem.* 286 (11), 8924–8932. doi:10.1074/jbc.M110.180638
- Cohen, J. (1992). A power primer. *Psychol. Bull.* 112 (1), 155–159. doi:10.1037/0033-2909.112.1.155
- D'Andrea, M. R., and Nagele, R. G. (2002). MAP-2 immunolabeling can distinguish diffuse from dense-core amyloid plaques in brains with Alzheimer's disease. *Biotech. Histochem.* 77 (2), 95–103. doi:10.1080/bih.77.2.95.103
- D'Andrea, M. R., Nagele, R. G., Wang, H. Y., Peterson, P. A., and Lee, D. H. (2001). Evidence that neurones accumulating amyloid can undergo lysis to form amyloid plaques in Alzheimer's disease. *Histopathology* 38 (2), 120–134. doi:10.1046/j.1365-2559.2001.01082.x
- De Strooper, B., and Karran, E. (2016). The cellular phase of Alzheimer's disease. *Cell* 164 (4), 603–615. doi:10.1016/j.cell.2015.12.056
- Deguchi, Y. (2002). Application of *in vivo* brain microdialysis to the study of blood-brain barrier transport of drugs. *Drug Metab. Pharmacokinet.* 17 (5), 395–407. doi:10.2133/dmpk.17.395
- DeTure, M. A., and Dickson, D. W. (2019). The neuropathological diagnosis of Alzheimer's disease. *Mol. Neurodegener.* 14 (1), 32. doi:10.1186/s13024-019-0333-5
- Elliott, C., Rojo, A. I., Ribe, E., Broadstock, M., Xia, W., Morin, P., et al. (2018). A role for APP in Wnt signalling links synapse loss with β -amyloid production. *Transl. Psychiatry* 8 (1), 179. doi:10.1038/s41398-018-0231-6
- Ethell, I. M., and Pasquale, E. B. (2005). Molecular mechanisms of dendritic spine development and remodeling. *Prog. Neurobiol.* 75 (3), 161–205. doi:10.1016/j.neurobio.2005.02.003
- Forlenza, O. V., de Paula, V. J., Machado-Vieira, R., Diniz, B. S., and Gattaz, W. F. (2012). Does lithium prevent Alzheimer's disease? *Drugs Aging* 29 (5), 335–342. doi:10.2165/11599180-000000000-00000
- Gauthier, S., Albert, M., Fox, N., Goedert, M., Kivipelto, M., Mestre-Ferrandiz, J., et al. (2016). Why has therapy development for dementia failed in the last two decades? *Alzheimers Dement.* 12 (1), 60–64. doi:10.1016/j.jalz.2015.12.003
- Gu, Q.-F., Yu, J.-Z., Wu, H., Li, Y.-H., Liu, C.-Y., Feng, L., et al. (2018). Therapeutic effect of Rho kinase inhibitor FSD-C10 in a mouse model of Alzheimer's disease. *Exp. Ther. Med.* 16 (5), 3929–3938. doi:10.3892/etm.2018.6701
- Hainmueller, T., and Bartos, M. (2020). Dentate gyrus circuits for encoding, retrieval and discrimination of episodic memories. *Nat. Rev. Neurosci.* 21 (3), 153–168. doi:10.1038/s41583-019-0260-z
- Hamano, T., Shirafuji, N., Yen, S. H., Yoshida, H., Kanaan, N. M., Hayashi, K., et al. (2020). Rho-kinase ROCK inhibitors reduce oligomeric tau protein. *Neurobiol. Aging* 89, 41–54. doi:10.1016/j.neurobiolaging.2019.12.009
- Hanger, D. P., Hughes, K., Woodgett, J. R., Brion, J. P., and Anderton, B. H. (1992). Glycogen synthase kinase-3 induces Alzheimer's disease-like phosphorylation of tau: Generation of paired helical filament epitopes and neuronal localization of the kinase. *Neurosci. Lett.* 147 (1), 58–62. doi:10.1016/0304-3940(92)90774-2
- Hernandez, I., Luna, G., Rauch, J. N., Reis, S. A., Giroux, M., Karch, C. M., et al. (2019). A farnesyltransferase inhibitor activates lysosomes and reduces tau pathology in mice with tauopathy. *Sci. Transl. Med.* 11 (485), eaat3005. doi:10.1126/scitranslmed.aat3005
- Herskowitz, J. H., Feng, Y., Mattheyses, A. L., Hales, C. M., Higginbotham, L. A., Duong, D. M., et al. (2013). Pharmacologic inhibition of ROCK2 suppresses amyloid- β production in an Alzheimer's disease mouse model. *J. Neurosci.* 33 (49), 19086. doi:10.1523/JNEUROSCI.2508-13.2013
- Holmes, C., and Lovestone, S. (2002). The clinical phenotype of familial and sporadic late onset Alzheimer's disease. *Int. J. Geriatr. Psychiatry* 17 (2), 146–149. doi:10.1002/gps.540
- Inoki, K., Li, Y., Xu, T., and Guan, K. L. (2003). Rheb GTPase is a direct target of TSC2 GAP activity and regulates mTOR signaling. *Genes Dev.* 17 (15), 1829–1834. doi:10.1101/gad.1110003
- Javonillo, D. I., Tran, K. M., Phan, J., Hingco, E., Kramár, E. A., da Cunha, C., et al. (2022). Systematic phenotyping and characterization of the 3xTg-AD mouse model of Alzheimer's disease. *Front. Neurosci.* 15, 785276. doi:10.3389/fnins.2021.785276
- Julian, J. B., and Doeller, C. F. (2021). Remapping and realignment in the human hippocampal formation predict context-dependent spatial behavior. *Nat. Neurosci.* 24 (6), 863–872. doi:10.1038/s41593-021-00835-3
- Julian, J. B., Keinath, A. T., Muzzio, I. A., and Epstein, R. A. (2015). Place recognition and heading retrieval are mediated by dissociable cognitive systems in mice. *Proc. Natl. Acad. Sci. U. S. A.* 112 (20), 6503–6508. doi:10.1073/pnas.1424194112
- Killick, R., Ribe, E. M., Al-Shawi, R., Malik, B., Hooper, C., Fernandes, C., et al. (2014). Clusterin regulates β -amyloid toxicity via Dickkopf-1-driven induction of the wnt-PCP-JNK pathway. *Mol. Psychiatry* 19 (1), 88–98. doi:10.1038/mp.2012.163
- Knowles, R. B., Wyart, C., Buldyrev, S. V., Cruz, L., Urbanc, B., Hasselmo, M. E., et al. (1999). Plaque-induced neurite abnormalities: Implications for disruption of neural networks in Alzheimer's disease. *Proc. Natl. Acad. Sci. U. S. A.* 96 (9), 5274–5279. doi:10.1073/pnas.96.9.5274
- Liu, D., Pitta, M., Jiang, H., Lee, J. H., Zhang, G., Chen, X., et al. (2013). Nicotinamide forestalls pathology and cognitive decline in Alzheimer mice: Evidence for improved neuronal bioenergetics and autophagy procession. *Neurobiol. Aging* 34 (6), 1564–1580. doi:10.1016/j.neurobiolaging.2012.11.020
- Liu, J., and Li, L. (2019). Targeting autophagy for the treatment of Alzheimer's disease: Challenges and opportunities. *Front. Mol. Neurosci.* 12 (203). doi:10.3389/fmnl.2019.00203
- Majumder, S., Richardson, A., Strong, R., and Oddo, S. (2011). Inducing autophagy by rapamycin before, but not after, the formation of plaques and tangles ameliorates cognitive deficits. *PLoS One* 6 (9), e25416. doi:10.1371/journal.pone.0025416
- Marklund, N., Blennow, K., Zetterberg, H., Ronne-Engstrom, E., Enblad, P., Hillered, L., et al. (2009). Monitoring of brain interstitial total tau and beta amyloid proteins by microdialysis in patients with traumatic brain injury. *J. Neurosurg.* 110 (6), 1227–1237. doi:10.3171/2008.9.JNS08584
- Masel, J. (2011). Genetic drift. *Curr. Biol.* 21 (20), R837–R838. doi:10.1016/j.cub.2011.08.007
- Menzies, F. M., Fleming, A., Caricasole, A., Bento, C. F., Andrews, S. P., Ashkenazi, A., et al. (2017). Autophagy and neurodegeneration: Pathogenic mechanisms and therapeutic opportunities. *Neuron* 93 (5), 1015–1034. doi:10.1016/j.neuron.2017.01.022
- Moon, R. T., Kohn, A. D., De Ferrari, G. V., and Kaykas, A. (2004). WNT and beta-catenin signalling: Diseases and therapies. *Nat. Rev. Genet.* 5 (9), 691–701. doi:10.1038/nrg1427
- Mueed, Z., Tandon, P., Maurya, S. K., Deval, R., Kamal, M. A., Poddar, N. K., et al. (2019). Tau and mTOR: The hotspots for multifarious diseases in Alzheimer's development. *Front. Neurosci.* 12, 1017. doi:10.3389/fnins.2018.01017
- Mufson, E. J., Ikonovic, M. D., Counts, S. E., Perez, S. E., Malek-Ahmadi, M., Scheff, S. W., et al. (2016). Molecular and cellular pathophysiology of preclinical Alzheimer's disease. *Behav. Brain Res.* 311, 54–69. doi:10.1016/j.bbr.2016.05.030

- Neselius, S., Brisby, H., Theodorsson, A., Blennow, K., Zetterberg, H., Marcusson, J., et al. (2012). CSF-biomarkers in olympic boxing: Diagnosis and effects of repetitive head trauma. *PLoS ONE* 7 (4), e33606. doi:10.1371/journal.pone.0033606
- Nixon, R. A., and Yang, D. S. (2011). Autophagy failure in Alzheimer's disease—locating the primary defect. *Neurobiol. Dis.* 43 (1), 38–45. doi:10.1016/j.nbd.2011.01.021
- Oddo, S., Caccamo, A., Shepherd, J. D., Murphy, M. P., Golde, T. E., Kaye, R., et al. (2003). Triple-transgenic model of Alzheimer's disease with plaques and tangles: Intracellular Abeta and synaptic dysfunction. *Neuron* 39 (3), 409–421. doi:10.1016/s0896-6273(03)00434-3
- Pan, J., and Yeung, S. C. (2005). Recent advances in understanding the antineoplastic mechanisms of farnesyltransferase inhibitors. *Cancer Res.* 65 (20), 9109–9112. doi:10.1158/0008-5472.Can-05-2635
- Pardridge, W. M. (2005). The blood-brain barrier: Bottleneck in brain drug development. *NeuroRx* 2 (1), 3–14. doi:10.1602/neuroRx.2.1.3
- Paxinos, G., and Franklin, K. B. (2004). *The mouse brain in stereotaxic coordinates*. Houston, TX: Gulf Professional Publishing.
- Pilly, P. K., Howard, M. D., and Bhattacharyya, R. (2018). Modeling contextual modulation of memory associations in the Hippocampus. *Front. Hum. Neurosci.* 12, 442. doi:10.3389/fnhum.2018.00442
- Porquet, D., Griñán-Ferré, C., Ferrer, I., Camins, A., Sanfeliu, C., Del Valle, J., et al. (2014). Neuroprotective role of trans-resveratrol in a murine model of familial Alzheimer's disease. *J. Alzheimers Dis.* 42 (4), 1209–1220. doi:10.3233/jad-140444
- Schaeffer, V., Lavenir, I., Ozcelik, S., Tolnay, M., Winkler, D. T., Goedert, M., et al. (2012). Stimulation of autophagy reduces neurodegeneration in a mouse model of human tauopathy. *Brain* 135 (Pt 7), 2169–2177. doi:10.1093/brain/aw143
- Schratt, G. (2009). microRNAs at the synapse. *Nat. Rev. Neurosci.* 10 (12), 842–849. doi:10.1038/nrn2763
- Sellers, K. J., Elliott, C., Jackson, J., Ghosh, A., Ribe, E., Rojo, A. I., et al. (2018). Amyloid β synaptotoxicity is Wnt-PCP dependent and blocked by fasudil. *Alzheimers Dement.* 14 (3), 306–317. doi:10.1016/j.jalz.2017.09.008
- Siman, R., Cocca, R., and Dong, Y. (2015). The mTOR inhibitor rapamycin mitigates perforant pathway neurodegeneration and synapse loss in a mouse model of early-stage alzheimer-type tauopathy. *PLoS One* 10 (11), e0142340. doi:10.1371/journal.pone.0142340
- Snider, B. J., Fagan, A. M., Roe, C., Shah, A. R., Grant, E. A., Xiong, C., et al. (2009). Cerebrospinal fluid biomarkers and rate of cognitive decline in very mild dementia of the Alzheimer type. *Arch. Neurol.* 66 (5), 638–645. doi:10.1001/archneurol.2009.55
- Song, G., Li, Y., Lin, L., and Cao, Y. (2015). Anti-autophagic and anti-apoptotic effects of memantine in a SH-SY5Y cell model of Alzheimer's disease via mammalian target of rapamycin-dependent and -independent pathways. *Mol. Med. Rep.* 12 (5), 7615–7622. doi:10.3892/mmr.2015.4382
- Szymczak, A. L., Workman, C. J., Wang, Y., Vignali, K. M., Dilioglou, S., Vanin, E. F., et al. (2004). Correction of multi-gene deficiency *in vivo* using a single 'self-cleaving' 2A peptide-based retroviral vector. *Nat. Biotechnol.* 22 (5), 589–594. doi:10.1038/nbt957
- Tang, B. L., and Liou, Y. C. (2007). Novel modulators of amyloid-beta precursor protein processing. *J. Neurochem.* 100 (2), 314–323. doi:10.1111/j.1471-4159.2006.04215.x
- Thal, D. R., Rub, U., Orantes, M., and Braak, H. (2002). Phases of A beta-deposition in the human brain and its relevance for the development of AD. *Neurology* 58 (12), 1791–1800. doi:10.1212/wnl.58.12.1791
- Ujije, M., Dickstein, D. L., Carlow, D. A., and Jefferies, W. A. (2003). Blood-brain barrier permeability precedes senile plaque formation in an Alzheimer disease model. *Microcirculation* 10 (6), 463–470. doi:10.1038/sj.mn.7800212
- Wegmann, S., Bennett, R. E., Delorme, L., Robbins, A. B., Hu, M., MacKenzie, D., et al. (2019). Experimental evidence for the age dependence of tau protein spread in the brain. *Sci. Adv.* 5 (6), eaaw6404. doi:10.1126/sciadv.aaw6404
- Yan, Q., Matheson, C., Sun, J., Radeke, M. J., Feinstein, S. C., Miller, J. A., et al. (1994). Distribution of intracerebral ventricularly administered neurotrophins in rat brain and its correlation with trk receptor expression. *Exp. Neurol.* 127 (1), 23–36. doi:10.1006/exnr.1994.1076
- Yu, A., Rual, J. F., Tamai, K., Harada, Y., Vidal, M., He, X., et al. (2007). Association of Dishevelled with the clathrin AP-2 adaptor is required for Frizzled endocytosis and planar cell polarity signaling. *Dev. Cell* 12 (1), 129–141. doi:10.1016/j.devcel.2006.10.015
- Yuan, C., Gao, J., Guo, J., Bai, L., Marshall, C., Cai, Z., et al. (2014). Dimethyl sulfoxide damages mitochondrial integrity and membrane potential in cultured astrocytes. *PLoS one* 9 (9), e107447. doi:10.1371/journal.pone.0107447
- Zeldovich, L. (2017). Genetic drift: The ghost in the genome. *Lab. Anim.* 46 (6), 255–257. doi:10.1038/labana.1275
- Zenaro, E., Piacentino, G., and Constantini, G. (2017). The blood-brain barrier in Alzheimer's disease. *Neurobiol. Dis.* 107, 41–56. doi:10.1016/j.nbd.2016.07.007
- Zhang, L., Wang, L., Wang, R., Gao, Y., Che, H., Pan, Y., et al. (2017). Evaluating the effectiveness of GTM-1, rapamycin, and carbamazepine on autophagy and alzheimer disease. *Med. Sci. Monit.* 23, 801–808. doi:10.12659/msm.898679

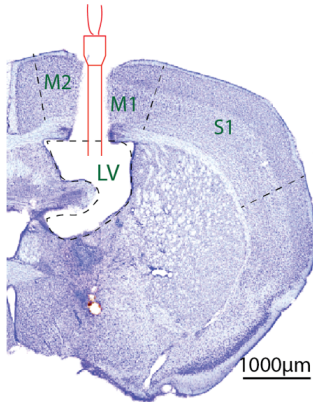
Supplementary Material



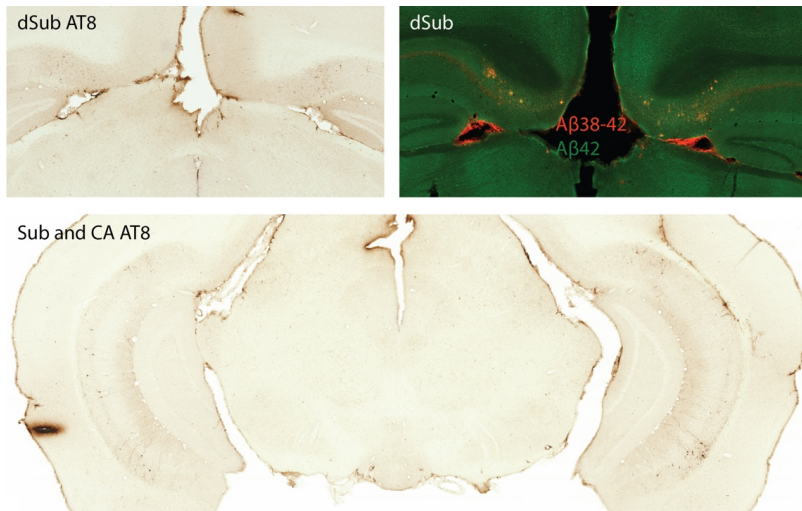
Supplementary Figure 1. Molecular action of Fasudil and Lonafarnib in the Wnt-PCP and PI3K/Akt/mTOR pathway, respectively. (A) Schematic of the canonical Wnt and Wnt-PCP pathways. A β has been shown to activate the Wnt-PCP pathway through the ability of A β to induce Dkk1. Dkk1 then prevents the binding interaction between LRP6 and frizzled, activating Wnt-PCP signaling and blocking canonical Wnt- β -catenin activity. In the Wnt-PCP pathway, the two arms diverge below disheveled, acting via Daam1/RhoA/ROCK to regulate cytoskeletal dynamics and JNK/c-Jun to regulate gene transcription. Along the same arm of Wnt-PCP signaling acting via Daam1/RhoA/ROCK, binding of a Wnt receptor to frizzled causes disheveled to inhibit the activity of GSK-3 β . The ROCK inhibitor Fasudil inhibits the arm of the Wnt-PCP pathway that promotes the retraction of dendritic spines and synapses through Daam1/RhoA/ROCK. Figure adapted from Sellers et al.¹. Abbreviations; Daam1: disheveled associated activator of morphogenesis 1; Dkk1: Dickkopf-1; GSK-3 β : glycogen synthase kinase-3 β ; JNK: c-Jun N-terminal kinase; LRP: low-density lipoprotein receptor-related protein; PCP: planar cell polarity; RhoA: Ras homolog family member A; ROCK: Rho-associated coiled-coil containing protein kinase; Wnt: Wingless-related integration site. (B) Schematic of the PI3K/Akt/mTOR pathway. Activation of mTOR results in activation of downstream components (i.e., 4EBP1 and p70S6K1). Lonafarnib works as a farnesyltransferase

¹ Sellers, K.J., Elliott, C., Jackson, J., Ghosh, A., Ribe, E., Rojo, A.I., et al. (2018). Amyloid β synaptotoxicity is Wnt-PCP dependent and blocked by fasudil. *Alzheimers Dement* 14(3), 306-317. doi: 10.1016/j.jalz.2017.09.008.

(farnesylation is a posttranslational modification of proteins) inhibitor which acts as an autophagic inducer by inhibiting mTOR. The mechanisms of action involve Rheb and the PI3K/Akt/mTOR pathway. Rheb acts downstream of TSC1/TSC2 and upstream of mTOR to regulate cell growth and activates S6 kinase 1 during amino acid deprivation via mTOR. Abbreviations; mTOR: mammalian target of rapamycin; Rheb: Ras homologue enriched in brain; PI3K: phosphatidylinositide 3-kinase; Akt: protein kinase B; TSC1/2: tuberous sclerosis complex 1/2. Figure created with biorender.com.

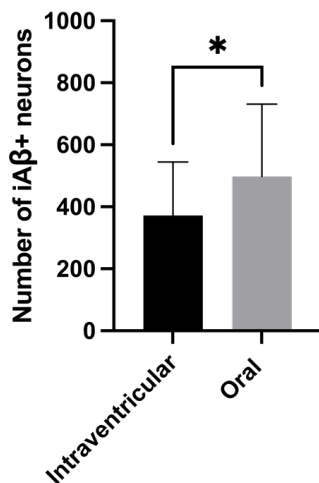


Supplementary Figure 2. Verification of microdialysis guide cannula implantation in the lateral ventricle. The microdialysis probe was successfully implanted in LV along the rostrocaudal axis in all animals ($n = 32$). Stereotaxic coordinates: A/P: -0.1mm , M/L: $+1.2\text{mm}$, D/V: -2.75mm . Delineations based on Paxinos & Franklin². Abbreviations; LV: lateral ventricle; M1: primary motor cortex; M2: secondary motor cortex; S1: primary somatosensory cortex.

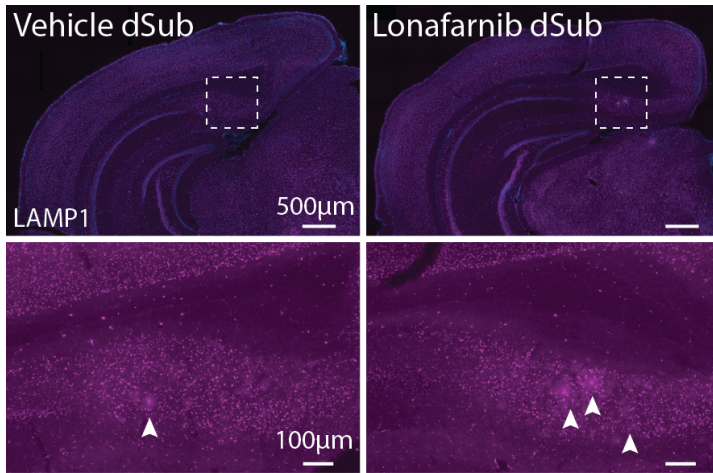


² Paxinos, G., and Franklin, K.B. (2004). *The mouse brain in stereotaxic coordinates*. Gulf Professional Publishing.

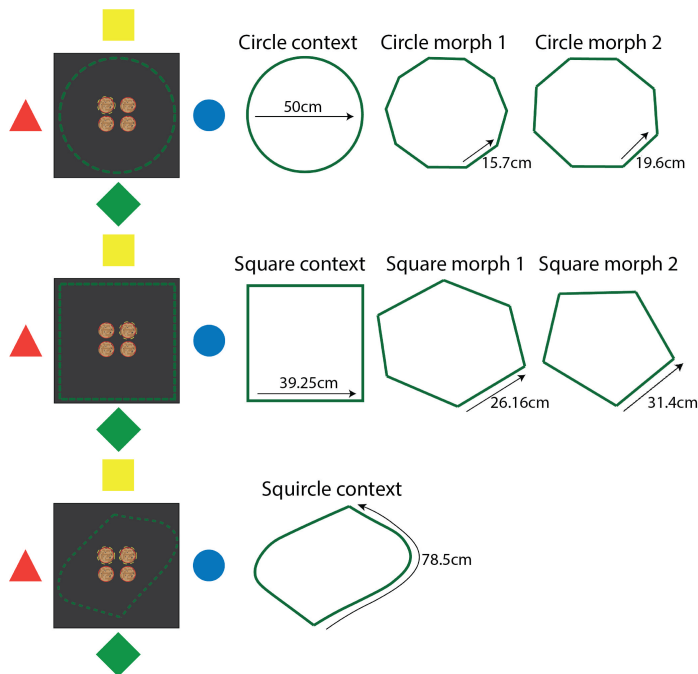
Supplementary Figure 3. No lateralization of neuropathology in 3xTg AD mice. Hyperphosphorylated pathological tau (AT8; brown) in an 18-month-old, and A β_{38-42} (McSA1; red) and A β_{42} (IBL A β_{42} ; green) in a 17-month-old 3xTg AD mouse (n = 2). Abbreviations; dSub: dorsal subiculum; Sub: subiculum; CA: cornu ammonis.



Supplementary Figure 4. The effect of intraventricular and oral administration of Fasudil and Lonafarnib. Mean number of A β + neurons in dSub of 3xTg AD mice after infusions of Lonafarnib and Fasudil via intraventricular microdialysis (n = 4) or oral administration (n = 3). Intra-neuronal A β in dSub was quantified from at least 7 brain sections for each animal using Ilastik. Error bars denote ± 1 SD, unpaired two-tailed t-test, * p < 0.05.). Abbreviations; iA β : intra-neuronal amyloid- β .

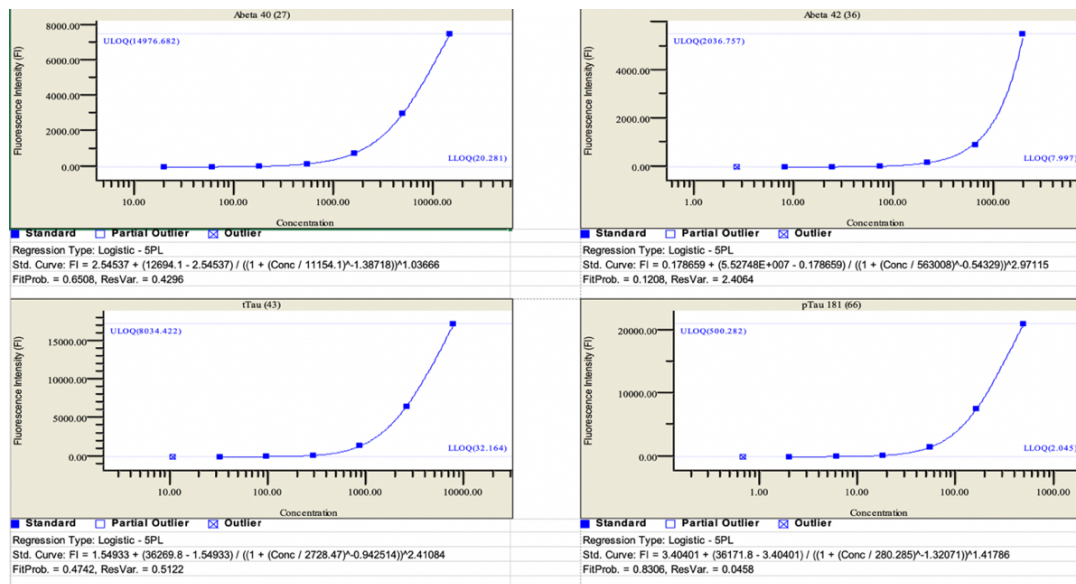


Supplementary Figure 5. LAMP1 (lysosomal marker; purple) immunoreactivity (arrowheads) in dSub in 14-month-old 3xTg AD mice receiving infusions of a vehicle (n = 2) or Lonafarnib (n = 4). Abbreviations; dSub: dorsal subiculum; LAMP1: lysosomal associated membrane protein 1.

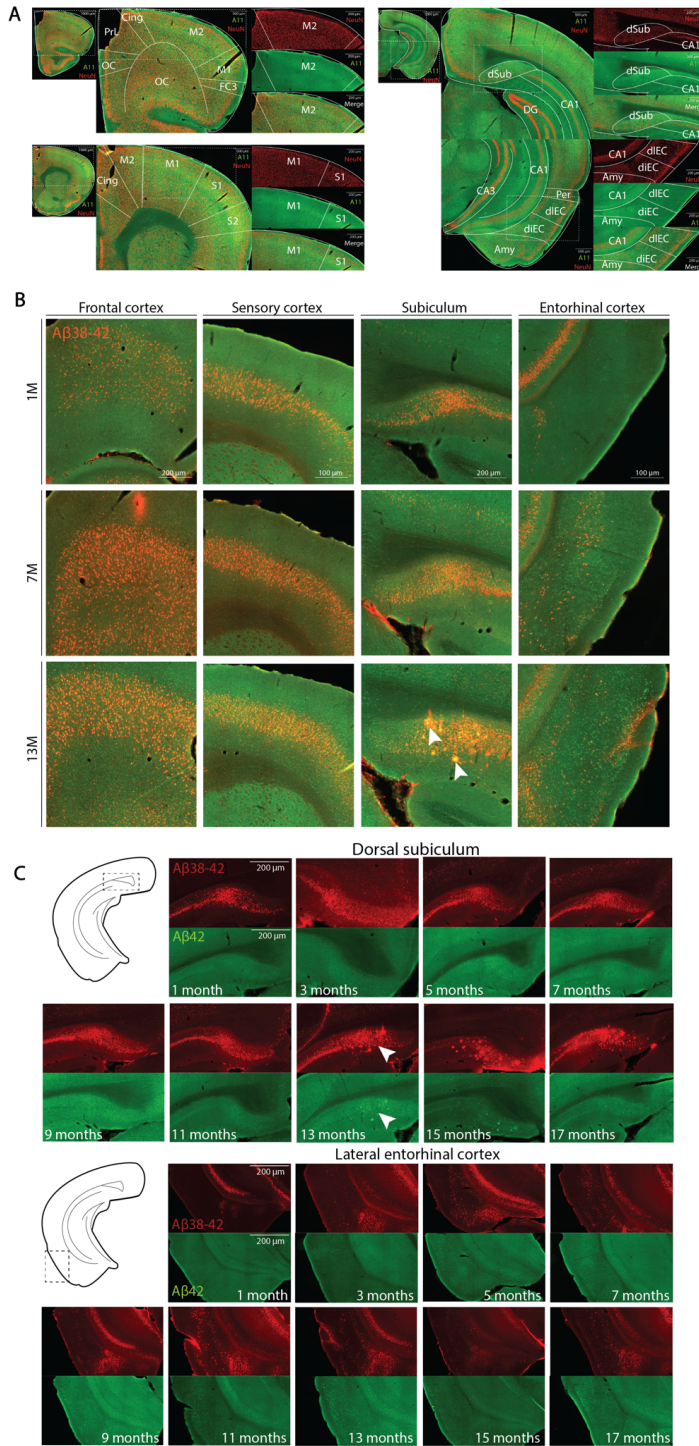


Supplementary Figure 6. Context-dependent spatial memory task design. Mice were initially taught to associate a specific reward location in a square and a circle context. The reward was buried in one of four cups with ginger-scented bedding. A trial was assessed as correct if the mice dug in the

reward location associated with each chamber. If they passed the training phase (66.6% correct digging), their contextual memory performance was tested in morph chambers: decagon (circle morph 1), octagon (circle morph 2), hexagon (square morph 1), and a pentagon (square morph 2). Mice were tested in morph chambers for 4 days, with 8 sessions a day. If they were able to complete the morph testing, they were tested in a Squire chamber on the fifth day. Since the Squire equally resembles a square and a circle context, a trial was considered correct if the mouse dug either of the reward locations attributable to the square- or circle context. Figure adapted by permission from Nora Cecilie Ebbesen.

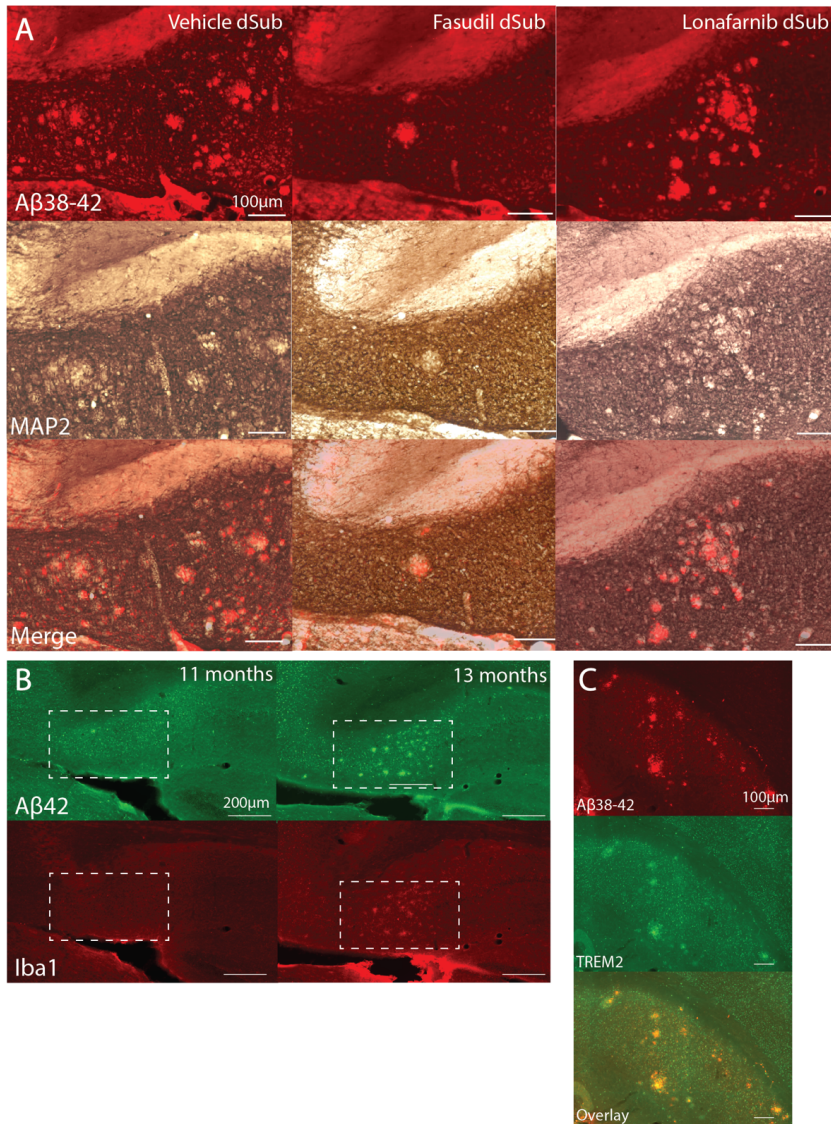


Supplementary Figure 7. LLOQ levels of CSF proteins. Lower limit of quantification (LLOQ) for A β ₄₀, A β ₄₂, t-tau, and p-tau from standard curves. Abbreviations; A β : amyloid- β ; t-tau: total tau; p-tau: phosphorylated tau.



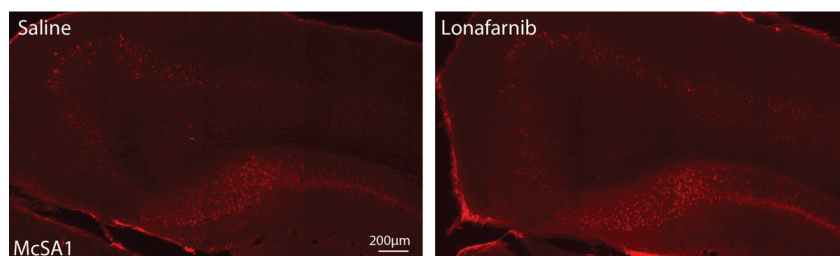
Supplementary Figure 8. Characterization of A β in the brain of our 3xTg AD mouse colony. (A) A11 (oligomeric A β specific; green) and NeuN (nuclei specific; red) immunoreactivity in the 3xTg AD mouse model at 1-month-of-age. At this age, there is little-to-none A11 immunoreactivity in frontal and sensory areas of the brain (left), as well as in the hippocampal and parahippocampal region (right). (B) A β_{38-42} immunoreactivity in frontal cortex, sensory cortex, Sub, and EC in the 3xTg AD mouse model at 1, 7 and 13 months of age. A β_{38-42} (McSA1; red) and A β_{42} (IBL A β_{42} ; green) immunoreactivity in the 3xTg AD mouse model. Amyloid plaques immunoreactive to A β_{38-42} (McSA1 antibody) are first apparent at 13 months of age in subiculum. (C) A β_{38-42} immunoreactivity in the 3xTg AD mouse model at various ages in the dSub and LEC. A β_{38-42} (McSA1; red) and A β_{42} (IBL A β_{42} ; green) immunoreactivity in the 3xTg AD mouse model. According to the ABC scoring system, diffuse amyloid plaques is scored in the cerebral cortex, hippocampus, striatum, midbrain, brainstem, and cerebellum according to protocols established by Thal et al.³ resulting in a Thal phase 0-5, which is translated into the NIA-AA score of A0-A3. Amyloid plaques immunoreactive to A β_{38-42} (McSA1 antibody) are first apparent at 13 months of age in dSub, whereas plaques immunoreactive to A β_{42} (IBL A β_{42} antibody) are first apparent at 15 months of age in dSub. Abbreviations; S1: primary somatosensory cortex; S2: secondary somatosensory cortex; Olf: olfactory area; OC: orbital cortex; PrL: prelimbic cortex; Cing: cingulate cortex; M1: primary motor cortex; M2: secondary motor cortex; FC3: frontal cortex area 3; Ins: insular cortex; CA1-3: cornu ammonis field 1-3; Amy: amygdala; diEC: dorsal intermediate entorhinal cortex; dLEC: dorsolateral entorhinal cortex; dSub: dorsal subiculum; PER: perirhinal cortex. A β : amyloid- β ; Sub: subiculum; LEC: lateral entorhinal cortex.

³ Thal, D.R., Rub, U., Orantes, M., and Braak, H. (2002). Phases of A beta-deposition in the human brain and its relevance for the development of AD. *Neurology* 58(12), 1791-1800. doi: 10.1212/wnl.58.12.1791.

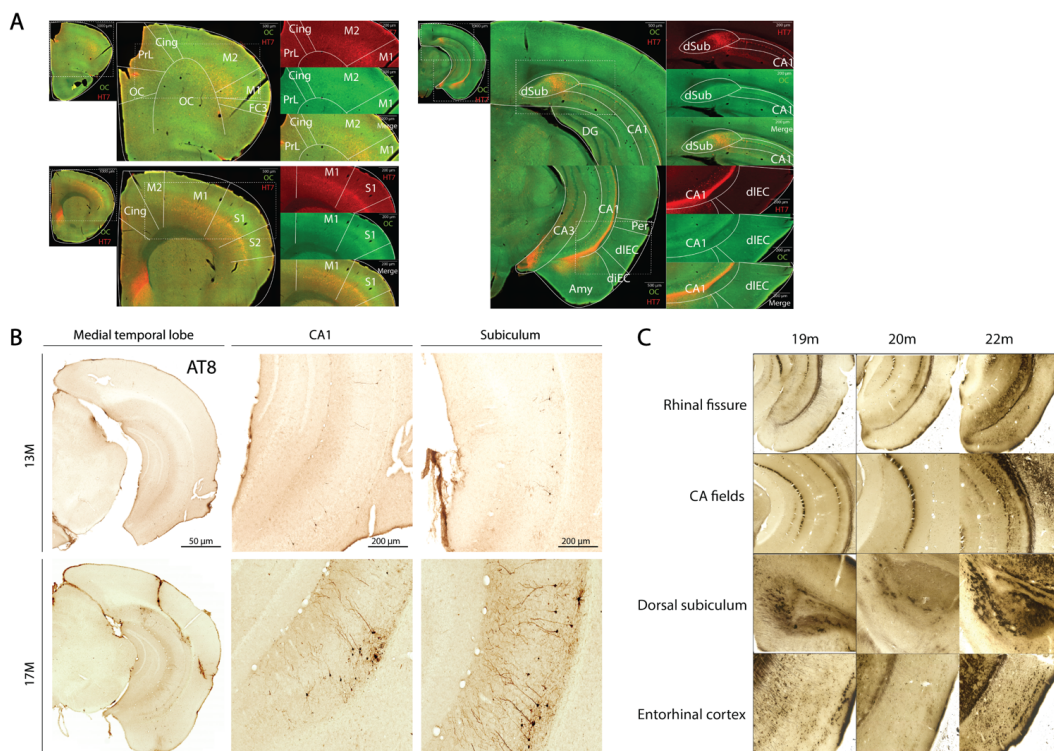


Supplementary Figure 9. Dense-core amyloid plaques after Fasudil and Lonafarnib infusions, and depiction of associated microglial activation surrounding dense-core amyloid plaques. (A) $A\beta_{38-42}$ (red; McSA1) staining for amyloid plaques (top panel) and microtubule-associated protein 2 (middle panel; brown; MAP2). McSA1 and the absence of MAP2 staining colocalized (bottom panel), confirming previous research indicating that MAP2 processes are absent within dense-core amyloid plaques. **(B)** $A\beta_{42}$ (IBL $A\beta_{42}$; green) and Iba1 (microglial marker; red) immunoreactivity in dSub at 11- and 13-months-of-age in the 3xTg AD mouse model. **(C)** $A\beta_{38-42}$ (McSA1; red) and TREM2 (microglial receptor; green) immunoreactivity in dSub at 13-months-of-age. Abbreviations; $A\beta$:

amyloid- β ; dSub: dorsal subiculum; Iba1: Ionized calcium-binding adapter molecule 1; TREM2: triggering receptor expressed on myeloid cells 2.

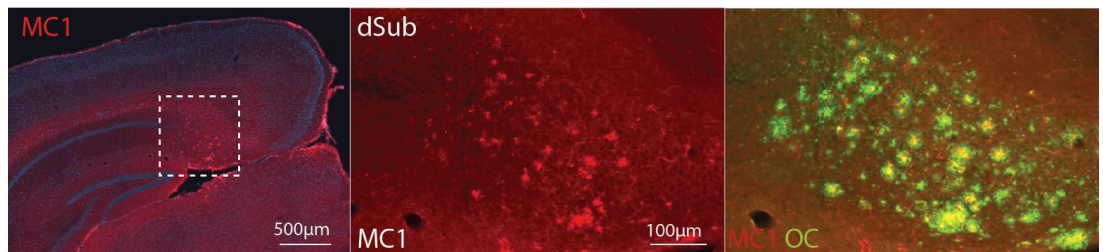


Supplementary Figure 10. Intracellular A β in dSub after Lonafarnib infusions. Lonafarnib did not affect the number of intracellular A β_{38-42} -positive neurons (McSA1; red) in dSub in 6-month-old 3xTg AD mice (n = 2).



Supplementary Figure 11. Characterization of tau in the brain of our 3xTg AD mouse colony. (A) MAPT (HT7; red) and fibrillar A β (OC; green) immunoreactivity in the entire brain at 1-month-of-age in 3xTg AD mice. (B) AT8 (detects phosphorylated tau proteins at serine 202 and threonine 205 residues; DAB) immunoreactivity in the 3xTg AD mouse at 13- and 17-months (M)-of-age. An ABC score for NFTs is determined in the trans-entorhinal area, CA, fronto-parietal cortex, and primary

visual cortex to generate a Braak stage⁴, which is translated into the NIA-AA score of B0-B3. Most existing mouse models do not generate NFTs, so the National Institutes of Health (NIH) have developed a modified B score for p-tau pathology, including distribution of cytoplasmic neuronal tau such as pre-tangles and threads. (C) Gallyas-silver staining in the 3xTg AD mouse at 19-, 20- and 22-months (m)-of-age. Abbreviations; S1: primary somatosensory cortex; S2: secondary somatosensory cortex; Olf: olfactory area; OC: orbital cortex; PrL: prelimbic cortex; Cing: cingulate cortex; M1: primary motor cortex; M2: secondary motor cortex; FC3: frontal cortex area 3; Ins: insular cortex; CA1: cornu ammonis field 1; CA2: cornu ammonis field 2; CA3: cornu ammonis field 3; Amy: amygdala; diEC: dorsal intermediate entorhinal cortex; dIEC: dorsolateral entorhinal cortex; dSub: dorsal subiculum; PER: perirhinal cortex.



Supplementary Figure 12. MC1+ amyloid plaques in 3xTg AD mice. Conformation-specific tau (MC1; red) and fibrillar A β (OC; green) immunoreactivity in dSub at 13-months-of-age. Abbreviations; dSub: dorsal subiculum.

Supplementary Table 1: Key resources

| Reagent type (species) or resource | Designation | Information | Identifiers/reference |
|---|---------------------------------------|--|---|
| Strain, strain background (<i>Mus musculus</i>) | 3xTg AD | B6;129-Psen1 ^{tm1Mpm} Tg(APP ^{Swe} ,tauP301L)1Lfa/Mmjax | MMRRC Strain #034830-JAX; RRID: MMRRC_034830-MU; PMID: 12895417 |
| Strain, strain background (<i>Mus musculus</i>) | B6129 | B6129SF2/J | Strain #:101045; RRID:IMSR_JAX:101045 |
| Genetic reagent (virus) | AAV-CBA-GFP-2A-P301L-Tau (serotype 8) | Viral Vector Core at Kavli Institute for Systems Neuroscience; contact Dr Raveendran, rajeevkumar.r.nair@ntnu.no | Gifted by Bradley Hyman's lab, Harvard Medical School; PMID: 31249873 |

⁴ Braak, H., and Braak, E. (1991). Neuropathological staging of Alzheimer-related changes. *Acta Neuropathol* 82(4), 239-259.

| | | | |
|----------|---|--|--|
| Antibody | Mouse anti-A β (McSA1)* | Targets the N-terminal amino acids 1-12 of human A β | MediMabs Cat# MM-0015-1P, RRID:AB_1807985 |
| Antibody | Anti-A β ₄₂ (rabbit polyclonal)* | A β ₄₂ (pre-oligomers) | Tecan (IBL) Cat# JP28051, RRID:AB_2341462 |
| Antibody | Anti-oligomer A11 (rabbit polyclonal) | Soluble A β ₄₀ /oligomeric A β ₄₂ (prefibrils) | Thermo Fisher Scientific Cat# AHB0052, RRID:AB_2536236 |
| Antibody | Anti-amyloid fibrils OC (rabbit polyclonal)* | Amyloid fibrils/fibrillar oligomers (protofibrils) | Millipore Cat# AB2286, RRID:AB_1977024 |
| Antibody | Anti-Iba1 (mouse monoclonal) | Ionized calcium binding adaptor molecule 1 (Iba1) | Abcam Cat# ab15690, RRID:AB_2224403 |
| Antibody | Anti-TREM2 (rabbit monoclonal) | TREM2 receptor | Thermo Fisher Scientific Cat# MA5-30971, RRID:AB_2786636 |
| Antibody | Anti-MAP2 (rabbit monoclonal) | Microtubule-associated protein 2 | Abcam Cat# ab183830, RRID:AB_2895301; PMID: 12083391 |
| Antibody | Anti-LAMP1 (rabbit polyclonal) | Lysosomal associated membrane protein 1 | Sigma-Aldrich Cat# L1418, RRID:AB_477157 |
| Antibody | Anti-phospho-tau AT8 (mouse monoclonal) | Tau phosphorylated at serine 202 and threonine 205 | Thermo Fisher Scientific Cat# MN1020, RRID:AB_223647 |
| Antibody | Anti-tau HT7 (mouse monoclonal) | Recognized tau ₁₅₉₋₁₆₃ and does not cross-react with murine tau | Thermo Fisher Scientific Cat# MN1000, RRID:AB_2314654; PMID: 1729400 |
| Antibody | Anti-tau MC1 (mouse monoclonal) | Conformation specific, detects misfolded tau relevant to tauopathy | Gifted by Peter Davies, Department of Pathology, Albert Einstein College of Medicine |
| Antibody | Anti-NeuN (rabbit monoclonal) | Neuronal labelling | Abcam Cat# ab177487, RRID:AB_2532109 |
| Antibody | Goat anti-mouse IgG (AF 657) | Secondary antibody | Thermo Fisher Scientific Cat# A-21235, RRID:AB_2535804 |
| Antibody | Goat anti-mouse IgG (AF 546) | Secondary antibody | Thermo Fisher Scientific Cat# A-11030, RRID:AB_2534089 |
| Antibody | Goat anti-mouse IgG (AF 488) | Secondary antibody | Thermo Fisher Scientific Cat# A28175, RRID:AB_2536161 |
| Antibody | Goat anti-rabbit IgG (AF 488) | Secondary antibody | Molecular Probes Cat# A-11008, RRID:AB_143165 |

| | | | |
|-------------------------|---|--|--|
| Antibody | Goat anti-rabbit IgG (AF 546) | Secondary antibody | Thermo Fisher Scientific Cat# A-11035, RRID:AB_2534093 |
| Chemical compound, drug | Fasudil | Rho kinase inhibitor; Selleck Chemicals | Cat# S1573; PMID: 29055813 |
| Chemical compound, drug | Lonafarnib | Farnesyltransferase inhibitor with antitumor activity; Cayman Chemical | Cat# CAY11746-1 mg; PMID: 30918111 |
| Chemical compound, drug | DAPI (4',6-Diamidino-2-Phenylindole, Dihydrochloride) | Nuclear and chromosome counterstain | Thermo Fisher Scientific Cat# D1306, RRID:AB_2629482 |
| Chemical compound, drug | Nissl (cresyl violet) | RNA labelling | Bjorkli 2019 doi: https://protocols.io/view/ihc-ad-neuropathology-protocol-btbmnik6 . |
| Chemical compound, drug | Gallyas-silver staining | Modified silver impregnation of NFTs | Bjorkli & Lagartos-Donate 2022 doi: dx.doi.org/10.17504/protocols.io.b44cqysw . |
| Chemical compound, drug | DAB | Chromogen for detecting antibodies | Bjorkli 2022 doi: dx.doi.org/10.17504/protocols.io.b44fqytn . |
| Software | GraphPad Prism, version 9 | Statistics and data visualization software | |
| Software | Zeiss ZEN lite | Microscope software | |
| Software | Ilastik | Cell counting software | PMID: 31570887 |
| Software | ANY-maze – Stoelting Co. | Video tracking software | |

* Labels amyloid plaques

Supplementary Table 2: Sample size for experimental conditions

| Experimental condition | 4 months-old | 6 months-old | 14 months-old |
|--------------------------------|----------------|--------------|---------------|
| Fasudil treatment (n) | | 6 | 4 |
| Lonafarnib treatment (n) | | 4* | 2 |
| Combinatorial treatment (n) | 6 ⁺ | | |
| Saline (vehicle) treatment (n) | 5 ⁺ | 6* | 2 |

* 2 of these animals were injected with AAV-tau

⁺ 3-4 of these animals underwent behavioral testing

Supplementary Table 3: Characterization summary for our 3xTg AD mouse colony

| Neuropathological marker | Previous characterizations^{5,6,7} | Our characterization |
|---------------------------------|--|--|
| Early intraneuronal A β | Present in CA1, amygdala and neocortex at 4 months-of-age ^{5,6} | Present in frontal and sensory cortex, hippocampus, and parts of the cerebellum at 1 month-of-age (Supplementary Fig. 8) |
| Amyloid plaques | Present in frontal cortex at 6 months-of-age ^{5,6} | Present in dorsal subiculum at 13 months-of-age (Supplementary Fig. 8B, C). Presents as dense-core amyloid plaques with surrounding reactive microglia (Supplementary Fig. 9) and MC1 co-labelling (Supplementary Fig. 12) |
| Early intraneuronal tau | Present in hippocampus and amygdala at 1 month-of-age ⁷ | Present in frontal and sensory cortex, and hippocampus at 1 month-of-age. Early intraneuronal tau decreased with aging (Supplementary Fig. 11A) |
| Pre-tangles | Present in CA1 at 12-15 months-of-age ^{5,6} | Present in CA1 and caudal subiculum at 13 months-of-age (Supplementary Fig. 11B) |
| Neurofibrillary tangles | Present in CA1 at 18 months-of-age ^{5,6} | Present in dorsal subiculum, CA1 and entorhinal cortex at 18 months-of-age, and present in entire brain parenchyma by 22 months-of-age (Supplementary Fig. 11C) |

⁵ Oddo, S., Caccamo, A., Shepherd, J.D., Murphy, M.P., Golde, T.E., Kaye, R., et al. (2003). Triple-Transgenic Model of Alzheimer's Disease with Plaques and Tangles. *Neuron* 39(3), 409-421.

⁶ Billings, L.M., Oddo, S., Green, K.N., McGaugh, J.L., and LaFerla, F.M. (2005). Intraneuronal Abeta causes the onset of early Alzheimer's disease-related cognitive deficits in transgenic mice. *Ibid.*45(5), 675-688. doi: 10.1016/j.neuron.2005.01.040.

⁷ Oh, K.-J., Perez, S.E., Lagalwar, S., Vana, L., Binder, L., and Mufson, E.J. (2010). Staging of Alzheimer's pathology in triple transgenic mice: a light and electron microscopic analysis. *International journal of Alzheimer's disease* 2010, 780102. doi: 10.4061/2010/780102.

Paper IV

Bjørkli, Christiana; Nair, Rajeevkumar R.; Witter, Menno P; Sandvig, Axel; Sandvig, Ioanna.
Overexpression of human tau in lateral entorhinal cortex layer II of 3xTg AD mice leads to tau deposition and a shift in perforant path terminals in the dentate gyrus.

This paper is not yet published and is therefore not included.

Paper V

Manipulation of neuronal activity in the entorhinal-hippocampal circuit affects intraneuronal amyloid- β levels

Christiana Bjorkli^{1,2*}, Nora C Ebbesen^{1,2}, Joshua B. Julian³, Menno P Witter^{4,5}, Axel Sandvig^{1,2,6,7}, Ioanna Sandvig^{1,2}

¹ Department of Neuromedicine and Movement Science, Faculty of Medicine and Health Sciences, Norwegian University of Science and Technology, Trondheim, Norway.

² Department of Neurology, St. Olav's Hospital, Trondheim, Norway.

³ Princeton Neuroscience Institute, Princeton University, Princeton, NJ, USA.

⁴ Kavli Institute for Systems Neuroscience and Centre for Neural Computation, Faculty of Medicine, Norwegian University of Science and Technology, Trondheim, Norway.

⁵ K.G. Jebsen Centre for Alzheimer's Disease, Trondheim, Norway.

⁶ Department of Clinical Neurosciences, Division of Neuro, Head and Neck, Umeå University Hospital, Sweden.

⁷ Department of Community Medicine and Rehabilitation, Umeå University, Sweden.

Running head: Manipulating the EC-HPC circuit affects intraneuronal A β

Number of pages: 17

Word count: 5329 (including all figure legends, and excluding references)

Number of figures: 3 main figures + 3 supplementary figures (1 supplementary table)

Keywords: Inhibitory DREADDs, Activity-dependent pathology, Entorhinal-Hippocampal circuit, Context-dependent memory, Amyloid-beta

Abstract

One of the neuropathological hallmarks of Alzheimer's disease (AD) is the accumulation of amyloid- β ($A\beta$) plaques, which is preceded by intraneuronal build-up of toxic, aggregated $A\beta$ during disease progression. $A\beta$ plaques are first deposited in the neocortex before appearing in the medial temporal lobe, and tau pathology with subsequent neurodegeneration in the latter anatomical region causes early memory impairments in patients. Current research suggests that early intraneuronal $A\beta$ build-up may begin in superficial layers of lateral entorhinal cortex (LEC). To examine whether manipulation of neuronal activity of LEC layer II neurons affected intraneuronal $A\beta$ levels in LEC and in downstream perforant path terminals in the hippocampus (HPC), we used a chemogenetic approach to selectively and chronically silence superficial LEC neurons in young and aged 3xTg AD mice and monitored its effect on intraneuronal $A\beta$ levels in LEC and HPC. Chronic chemogenetic silencing of LEC neurons led to reduced early intraneuronal $A\beta$ in LEC and in projection terminals in the HPC, compared with controls. Early intraneuronal $A\beta$ levels in the downstream HPC correlated with activity levels in superficial layers of LEC, with the subiculum being the earliest subregion involved, and our findings give evidence to early AD neuropathology originating in select neuronal populations.

1. Introduction

Alzheimer's disease (AD) constitutes most dementia cases, and knowledge is still lacking regarding the underlying factors that lead to the disease. The accumulation of hyperphosphorylated, misfolded tau proteins into neurofibrillary tangles (NFTs), coupled with deposition of amyloid-beta ($A\beta$) into extracellular plaques, are the two hallmark pathological features of AD in the brain [1-4]. The pathophysiology of AD is marked by slowly progressing abiotrophic neurodegeneration, which begins in the medial temporal lobes (MTLs), a region known to be critical for learning and memory [5, 6]. The MTLs comprise the hippocampus (HPC) along with the surrounding hippocampal region, including the entorhinal cortex (EC) that serves as the primary interface for HPC-neocortex circuits [5, 7, 8].

AD neuropathology follows a hierarchical deposition pattern in anatomically and functionally connected brain regions [3, 4]. In patients, the lateral EC (LEC) is an early region of neuronal loss [9] and likely the brain area from where AD pathology invades other brain regions [10, 11]. Neurons in the superficial layers of LEC form synapses via the perforant pathway with all hippocampal subregions, including the dentate gyrus (DG), cornu ammonis 1 and 3, and subiculum (Sub). The encoding of various forms of memory [12, 13], but particularly contextual memory [14], requires an intact EC-HPC circuit. It has remained elusive where toxic intraneuronal $A\beta$ originates in the brain, but current research suggests that this build-up may occur in superficial layers of EC during early stages of AD [11, 15, 16].

The presence of soluble, oligomeric intraneuronal $A\beta$ is considered more neurotoxic compared to the later-developed $A\beta$ plaques during progression of AD [17-26]. Since the EC-HPC circuit is affected [27-29], and intraneuronal $A\beta$ is present in EC during early stages of the

disease, changes originating in EC could affect neuropathological development in downstream perforant path terminals [30-34]. In this study we chronically silenced neuronal activity of LEC layer II neurons of young and aged 3xTg AD mice, by locally expressing inhibitory designer receptors exclusively activated by designer drugs (DREADDs) in these neurons. We subsequently activated the DREADDs by local infusions of the novel ligand deschloroclozapine (DCZ) and examined its effect on early intraneuronal A β build-up in LEC layer II and downstream HPC by immunolabelling.

2. Methods

2.1. Animals

3xTg AD mice (MMRRC Strain # 034830-JAX; RRID: MMRRC_034830-MU; $n = 27$) and control B6129 mice (Strain # 101045; RRID: IMSR_JAX:101045; $n = 17$) were included in these experiments. 3xTg AD mice contain human transgenes for amyloid precursor protein (*APP*) bearing the Swedish mutation, presenilin-1 (*PSEN1*) containing an M146V mutation, and microtubule-associated protein tau (*MAPT*) containing an P301L mutation. The donating investigators of the 3xTg AD mouse model has previously communicated to Jackson Laboratories that male transgenic mice may not exhibit all phenotypic traits of AD [35]. Therefore, only female mice were included in these experiments. All housing and breeding of animals was approved by the Norwegian Animal Research Authority and is in accordance with the Norwegian Animal Welfare Act §§ 1-28, the Norwegian Regulations of Animal Research §§ 1-26, and the European Convention for the Protection of Vertebrate Animals used for Experimental and Other Scientific Purposes (FOTS ID 21061). The animals were kept on a 12h light/dark cycle under standard laboratory conditions (19-22 °C, 50-60 % humidity), and had free access to food and water.

2.2. Stereotactic viral injections

Mice were anaesthetized with isoflurane (4% induction and 1-3% maintenance, IsoFlo vet., Abbott Laboratories, Chicago IL, USA) and oxygen (0.3 - 0.4 %) in an induction chamber before being transferred to a stereotaxic frame (David Kopf Instruments, California, USA) and placed on a temperature-controlled heating pad (40.5 – 41 °C). Mice were administered analgesics (Temgesic, Invidor UK, Slough, Great Britain [0.05-0.09 mg/kg], and Metacam, Boehringer Ingelheim Vetmedica, Copenhagen, Denmark [0.05-0.15 mg/kg]) and a local anesthetic (Marcain, Aspen Pharma, Ballerup, Denmark [0.03-0.18 mg/kg]) subcutaneously, and an incision was made to expose the skull. To horizontally align the skull, the ventral distance down to the stereotaxic landmarks bregma and lambda were assessed, and the medial-lateral alignment of the skull was examined by comparing the ventral distance down to the stereotaxic landmarks ± 1 mm laterally from the midline of the brain. A craniotomy was made at 0.5 mm anterior to lambda and ~ 4 mm lateral (dependent on animal weight) to the midline. A Hamilton microsyringe (Neuros 32-gauge syringe, 5 μ l, Hamilton company, Nevada, USA) was lowered vertically into the brain to a depth ~ 3.6 mm (dependent on animal weight) from the surface, and 500-1000 nl of viruses was injected using a microinjector (Nanoliter 2010,

World Precision Instruments Inc., USA). We used the following adeno-associated viruses (AAVs) for injections: AAV8 human M4 muscarinic (hM4) inhibitory DREADDs (hM4D_i)-mCherry (referred to as 'AAV-hM4D_i' hereafter) and AAV8 mCherry (referred to as 'AAV-mCherry' hereafter), both with the calcium/calmodulin-dependent protein kinase (CaMKII) promoter to drive expression of the DREADD in excitatory cells only). AAVs were generated by Dr. Nair at the Viral Vector Core Facility, at the Kavli Institute for Systems Neuroscience, Trondheim, Norway. AAV-mCherry was injected into the contralateral hemisphere of the one injected with AAV-hM4D_i in a portion of the mice ($n = 14$). The microsyringe was kept in place for 10 minutes prior to and after the injection, to minimize potential upward leakage of the viral solution. Metacam was given within 24 hours post-surgery. Animals were implanted with osmotic minipumps 6-7 days following injections.

2.3. Activation of inhibitory designer receptors

An Alzet osmotic minipump (model 1004, flow rate: 0.11 μ l/hour, Durect Corporation, California, USA) was primed with 100 μ l DCZ (MedChemExpress, USA) [36] at a dosage of 100 μ g/kg (or with sterile saline for controls), at 38°C in sterile saline for 48 hours prior to implantation.

Following the same procedure as the viral injection surgery up until the target coordinate was derived, mice were implanted with minipumps subcutaneously on the flank, slightly posterior to the scapulae. A hemostat was inserted into the incision to make a pocket for the minipump large enough to allow free movement of the animal (approximately 1 cm longer than the minipump). For the implantation of the intracranial cannula attached to the minipump (Durect Corporation, California, USA) a craniotomy was made at 0.1 mm posterior to bregma and 1.2 mm lateral to the midline to target the lateral ventricle. The intraventricular cannula was lowered into the brain to a depth 2.75 mm from the surface of the brain, attached to the skull using superglue and dental cement (Dentalon Plus, Cliniclands AB, Trelleborg, Sweden), while the catheter and minipump was secured under the skin with sutures. Analgesics were repeated within 24 hours post-surgery.

2.4. Context-dependent spatial memory testing

To confirm functional silencing of LEC layer II, we examined context-dependent spatial memory (**Supplementary Fig. 1**) in mice with intraventricular infusions of DCZ or saline. The basic training and testing protocol is also described in [37]. But in brief, disoriented mice were initially trained to dig for buried food rewards (Weetos choco, Nestlé S.A., Vevey, Switzerland) in two different chambers, one with square boundaries (4 x 29.25 cm) and one with circle boundaries (157 cm circumference). All chambers were built out of rectangular Legos (2 x 1 cm; Lego A/S, Billund, Denmark), and were 15 cm tall. Rewards were buried under odor-scented bedding in cups embedded in the chamber floors; the odor-masked bedding consisted of 1 g of ground fresh ginger for every 100 g of bedding. Each chamber was surrounded by the same distal cues for orientation. There were four possible reward locations

in each chamber, and the rewarded location differed between the square- and circle-chamber relative to the common reference frame provided by the distal cues. The training phase consisted of four training trials per chamber per day for 2 days, with successive trials alternated across chambers (8 trials total in the square chamber and 8 trials total in the circle chamber). If a given mouse achieved 66.6% correct performance during training, contextual memory was then tested in 4 testing sessions across 4 days, with 8 trials per session. Four 3xTg AD mice with silenced LEC were unable to complete the training phase and were therefore excluded from further analyses. During each testing session, the first two trials consisted of spatial memory being tested in the square- and circle-chamber with rewards. In trials 3-6, spatial memory was tested in four chambers with morphed boundary geometry, which continuously ranged from most-square-like to most-circle-like: a pentagon (5 x 31.4 cm), a hexagon (6 x 26.16 cm), an octagon (8 x 19.6 cm), and a decagon (10 x 15.7 cm). During the final 2 trials of each testing session (trials 7-8), the animals were again tested in the square and circle chambers with rewards. The order of the square-, circle- and morphed-chambers across trials in each session was randomized but was the same for each animal on a given day's session.

Dig locations and time spent in these locations were calculated using ANY-maze video tracking system (Stoelting Europe) via an overhead, centrally located camera (DMK 22AUC03 USB 2.0 monochrome industrial camera, The imaging Source Europe, Germany). Animals had access to water ad libitum but were maintained at 90-95 % of their free-feed weight to increase task motivation.

2.5. Tissue processing

Animals were sacrificed after neuronal silencing and/or behavioral testing. The animals were subjected to a novel object (Duplo Lego) 90 min prior to perfusions [38]. Mice were administered a lethal dose of sodium pentobarbital and transcardially perfused with Ringer's solution followed by paraformaldehyde (PFA, 4 %, Merck Millipore, Darmstadt, Germany) in 125 mM phosphate buffer (PB). Brains were extracted and fixed for a minimum of 24 hours in PFA at 4 °C and transferred to a 2 % dimethyl sulfoxide solution (VWR International, Radnor, PA, USA) prepared in PB for at least 24 hours at 4 °C. Brains were sectioned coronally at 40 µm on a freezing sliding-microtome, and an incision was made in the contralateral hemisphere of the one injected with the experimental virus to mark the control hemisphere.

2.6. Immunohistochemical processing

Immunolabeling for A β , reelin, mCherry, hM4 and cFos was conducted on tissue from all animals. See [39-42] for detailed protocols, and **Supplementary Table 1** for details regarding the antibodies used. Sections were scanned using a Mirax-midi slide scanner (objective 20X, NA 0.8; Carl Zeiss Microscopy, Oberkochen, Germany), using either reflected fluorescence (for sections stained with a fluorophore) or transmitted white light (for sections stained with Cresyl violet) as the light source.

2.7. Quantification of cFos+ and amyloid- β + neurons

Series of sections were chosen randomly and coded to ensure blinding to the investigators. The number of cells containing cFos and intraneuronal A β in LEC and HPC were estimated with Ilastik [43] using the Density Cell Counting workflow. LEC and HPC was delineated using cytoarchitectonic features in sections stained with Nissl, based on The Paxinos & Franklin Mouse Brain Atlas [44]. The regions constituting the human MTLs are equivalent to the hippocampal region in rodents, consisting of the HPC (CA1-3, DG, and Sub) and the adjacent perirhinal, entorhinal, and parahippocampal cortices [45]. The same surface area and rostrocaudal levels of each brain region was selected, and at least 4 brain sections containing infused hemispheres were used for quantification. Damaged regions of brain sections were excluded from analyses to avoid false-positive antibody expression.

2.8. Statistics

Effect size (Cohen's D) was calculated based on initial experiments between animals injected with experimental and control viruses and the resulting difference in LEC layer II cFos+ cells. Based on each group consisting of at least 4 animals, a large effect size of 1.57 was calculated [46]. Most of the dataset displayed a normal distribution (Shapiro-Wilk test) and therefore two-tailed, unpaired t-tests were used to compare mean differences. For the minor parts of the dataset that was not normally distributed, nonparametric statistical tests were used to compare means (Mann-Whitney U). All reported statistics were based on two-tailed significance tests. Statistical comparisons of behavioral data across LEC-silenced and control mice were conducted based on trial-wise pooling of data across mice separately for each group. Behavioral performance in the morphed environments of the contextual memory task was calculated as follows: dig in square-consistent location = 1, dig in circle-consistent location = 0, dig in any other location = 0.5. Context-consistency of reward locations was determined relative to the common reference frame defined by the distal cues shared across all contexts. We then assessed whether performance in the morphed environments was associated with more context-appropriate choices for control animals treated with a vehicle compared to LEC-silenced animals. All statistical tests and graphs were made in Prism 9 (GraphPad Software Inc., CA, USA).

3. Results

3.1. Verification of chronic neuronal silencing of lateral entorhinal cortex layer II at the molecular and functional level

We first verified neuronal silencing following injections of AAV-hM4D_i in LEC layer II and intraventricular DCZ infusions for 2-3 weeks (**Fig. 1A, B; Supplementary Fig. 2A**). Our injections were limited to reelin-expressing principal neurons in LEC layer II (**Supplementary Fig. 2B**). Moreover, hM4 receptor labelling was present in LEC layer II neurons infected with AAV-hM4D_i, but not when infected with the control virus AAV-mCherry (**Supplementary Fig. 2C**). hM4 receptor labelling was also not present in LEC layer II neurons infected with AAV-hM4D_i after saline infusions (**Supplementary Fig. 2D**). After injections of AAV-hM4D_i, we

observed reduced cFos expression in LEC layer II of 3xTg AD mice after DCZ (but not saline) infusions ($t = 19.43$, $p < .05$, unpaired two-tailed t-test; **Fig. 1C-E**).

To confirm functional silencing of LEC layer II, we examined context-dependent spatial memory (**Supplementary Fig. 1**). Mice were trained to dig for buried food rewards in two different contexts, one square and one circle. Mice with silenced LEC initially searched in context-appropriate reward locations less often than controls ($p < .05$; Fischer's exact test; **Fig. 1F**). To confirm that this spatial memory impairment was due to disrupted contextual processing, we further examined contextual memory recall in environments with progressive morphs of boundary geometry, increasing the number of boundary walls from most square-like to most circle-like. This type of pattern completion dependent behavior is thought to depend on the normal function of the HPC [47, 48]. Compared to controls, mice infused with DCZ searched less often in context-consistent reward locations ($\chi^2 = 24.13$, $p < 10^{-5}$; Pearson's Chi-squared test; **Fig. 1G**). These effects are unlikely to be explained by domain general search behavior, as response latency and movement speed did not differ between DCZ mice and controls (data not shown). Thus, silencing of LEC layer II neurons led to behavioral changes associated with a dysfunctional EC-HPC circuitry [27-29].

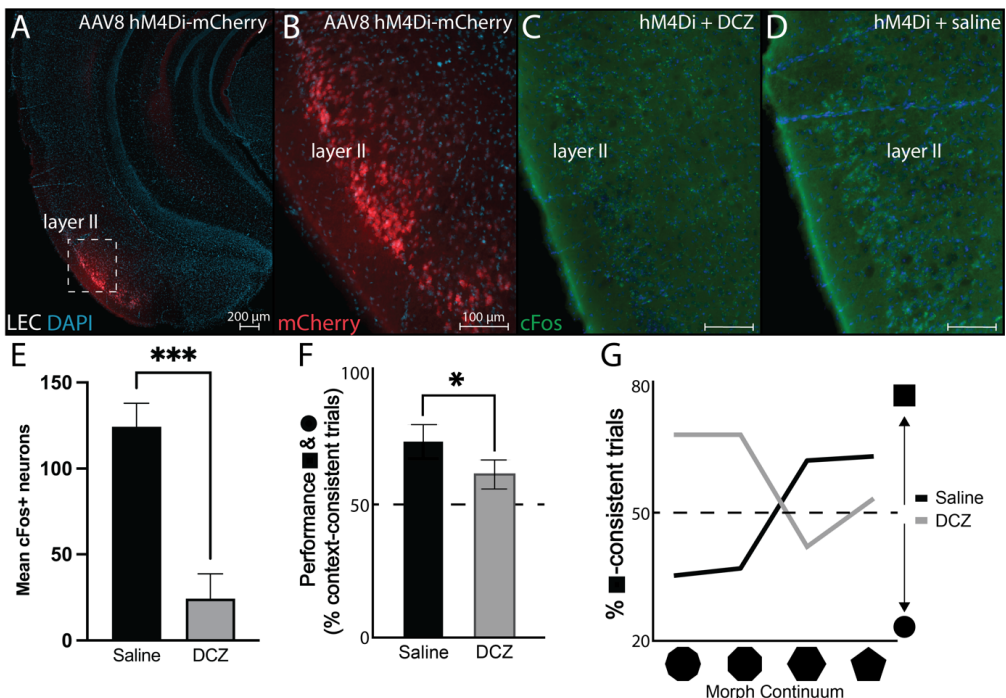


Figure 1. Chronic silencing of LEC layer II attenuates neuronal activity. **A)** AAV-hM4Di_i (mCherry; red) injection location in LEC layer II of 3xTg AD mice. **B)** Higher magnification mCherry⁺ (red) LEC layer II neurons in 3xTg AD mice. **C)** cFos⁺ (green) LEC layer neurons following AAV-hM4Di_i injections in LEC layer II and intraventricular infusions of DCZ for 2 weeks in 3xTg AD mice. **D)** cFos⁺ (green) LEC layer neurons following injections in LEC layer II and intraventricular infusions of saline for 2 weeks in 3xTg AD mice. **E)** Mean cFos⁺ LEC layer II neurons in infused and non-infused hemispheres (<4 brain sections) after AAV-hM4Di_i injections and DCZ ($n = 25$) or saline

($n = 9$) intraventricular infusions. **F**) Mean behavioral performance (% of trials with context-appropriate choices) in 3xTg AD mice with hM4D_i in LEC layer II and DCZ ($n = 2$) or saline ($n = 2$) infusions in the square and the circle contexts. **G**) Percentage of trials with square context-consistent dig in 3xTg AD mice with hM4D_i in LEC layer II and DCZ ($n = 2$) or saline ($n = 2$) infusions in each of the four morphed environments, ranging from most circle-like to most square-like in boundary geometry shape. Abbreviations; AAV: adeno-associated virus; hM4D_i: human M4 muscarinic (hM4) inhibitory DREADDs; LEC: lateral entorhinal cortex; DCZ: deschloroclozapine. Error bars denote ± 1 SD in panel E, and ± 1 SEM in panels F-G; * $p < .05$, *** $p < .001$.

3.2. Chronic neuronal silencing of lateral entorhinal cortex layer II lowered intraneuronal amyloid- β levels

Principal cells in LEC layer II can be distinguished from nearby neuronal populations based on their expression of the extracellular matrix glycoprotein reelin (**Fig. 2A**) [7]. Here we observed that reelin was expressed more in dorsal compared to ventral portions of LEC layer II ($t = 9.43$, $p < .001$, unpaired two-tailed t-test; **Fig. 2A, D**). Previous research suggests a link between reelin+ LEC layer II neurons and the build-up of toxic intraneuronal A β [10, 34], and we observed that intraneuronal A β colocalized with reelin, and was similarly more abundant in dorsal compared to ventral LEC layer II neurons ($t = 6.86$, $p < .0001$, unpaired two-tailed t-test; **Fig. 2B, C, E**). Therefore, we next examined whether LEC layer II neuronal silencing affected intraneuronal A β build-up in the same population of neurons. We observed less intraneuronal A β in LEC layer II neurons infected with AAV-hM4D_i and infused with DCZ than when infused with saline ($t = 3.52$, $p < .01$, unpaired two-tailed t-test; **Fig. 2F-H**), but no change in reelin levels of these same neurons (**Supplementary Fig. 3A**). Within 3xTg AD mice with silenced LEC layer II, we observed reduced intraneuronal A β in LEC layer II neurons to a greater degree in the hemisphere injected with AAV-hM4D_i compared to the contralateral non-injected/injected with AAV-mCherry hemisphere (**Supplementary Fig. 3B**).

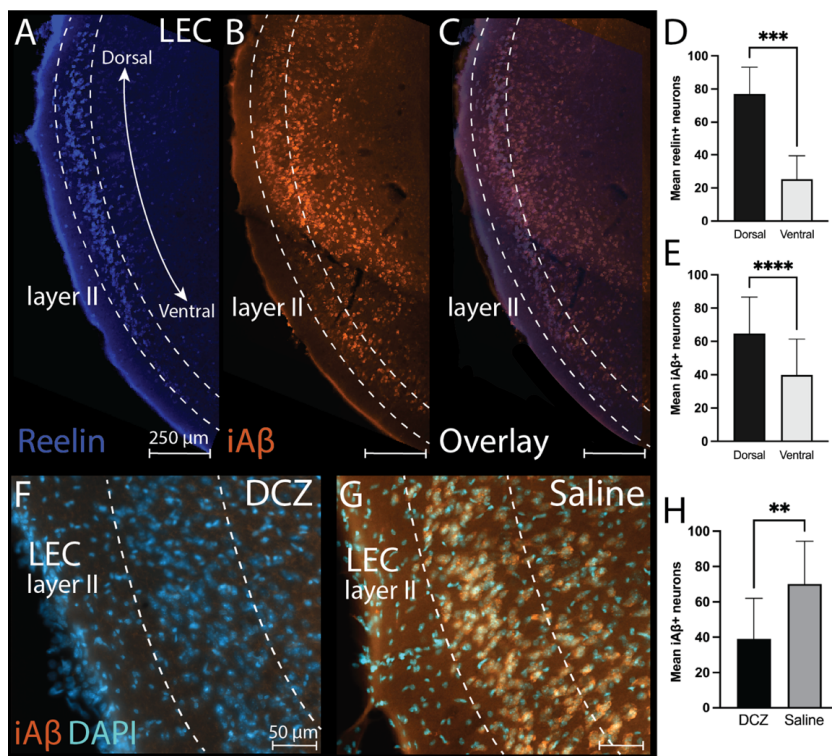


Figure 2. Targeted silencing of reelin-expressing LEC layer II results in reduced intraneuronal A β levels. **A)** Expression of reelin (blue) in the dorsal-ventral gradient of LEC layer II neurons. **B)** Expression of intraneuronal A β (McSA1 antibody; orange) in the dorsal-ventral gradient of LEC layer II neurons. **C)** Co-expression of reelin (blue) and intraneuronal A β (orange) in the dorsal-ventral gradient of LEC layer II neurons. **D)** Bar graph displaying mean reelin+ LEC layer II neurons in dorsal and ventral LEC layer II (<4 brain sections). **E)** Bar graph displaying mean intraneuronal A β + LEC layer II neurons in dorsal and ventral LEC layer II (<4 brain sections). **F)** Expression of intraneuronal A β (orange) in LEC layer II hM4D_i-infected neurons following DCZ infusions ($n = 25$). **G)** Expression of intraneuronal A β (orange) in LEC layer II hM4D_i-infected neurons following saline infusions ($n = 9$). **H)** Bar graph displaying mean intraneuronal A β + LEC layer II neurons in infused and non-infused hemispheres (<4 brain sections) after injections of AAV-hM4D_i and DCZ ($n = 25$) or saline ($n = 9$) intraventricular infusions. Abbreviations; LEC: lateral entorhinal cortex; iA β : intraneuronal amyloid- β ; DCZ: deschloroclozapine. Error bars denote ± 1 SD; ** $p < .01$, *** $p < .001$, **** $p < .0001$.

3.3. Chronic silencing of lateral entorhinal cortex layer II lowered intraneuronal amyloid- β levels in hippocampal terminal fields

We next tested whether chronic LEC layer II neuronal silencing reduced early intraneuronal A β presence in its projection terminals in HPC, specifically in those subregions of the HPC known to exhibit A β pathology in patients (i.e., dSub, CA1 and Sub) [4]. Chronic LEC layer II neuronal silencing reduced intraneuronal A β in projection terminals in the HPC broadly ($t = 2.87$, $p < .01$, unpaired two-tailed t-test; **Fig. 3A-E**). As expected, injections of AAV-hM4D_i into LEC layer II followed by saline infusions did not cause a reduction of intraneuronal A β in the HPC (n.s.; **Fig. 3F-J**). We also found no change in intraneuronal A β levels in downstream HPC when the length of inhibition was 2 or 3 weeks (n.s.; **Supplementary Fig. 3C**). Within HPC of

young 3xTg AD mice (2-months-old), intraneuronal A β was reduced in all subregions after LEC layer II silencing, with the greatest reduction observed in ventral Sub ($t = 3.99$, $p < .01$, unpaired two-tailed t-test; **Fig. 3D, K**). In older 3xTg AD mice (4- and 6-months-old), intraneuronal A β was reduced in all subregions after silencing, but CA1 (4-months-old: $t = 2.72$, $p < .05$, unpaired two-tailed t-test; **Fig. 3A-C**) and dorsal Sub (4-months-old: $t = 2.67$, $p < .05$; 6-months-old: $t = 3.08$, $p < .05$, unpaired two-tailed t-tests; **Fig. 3A-C**) displayed greater reduction (**Fig. 3L, M**).

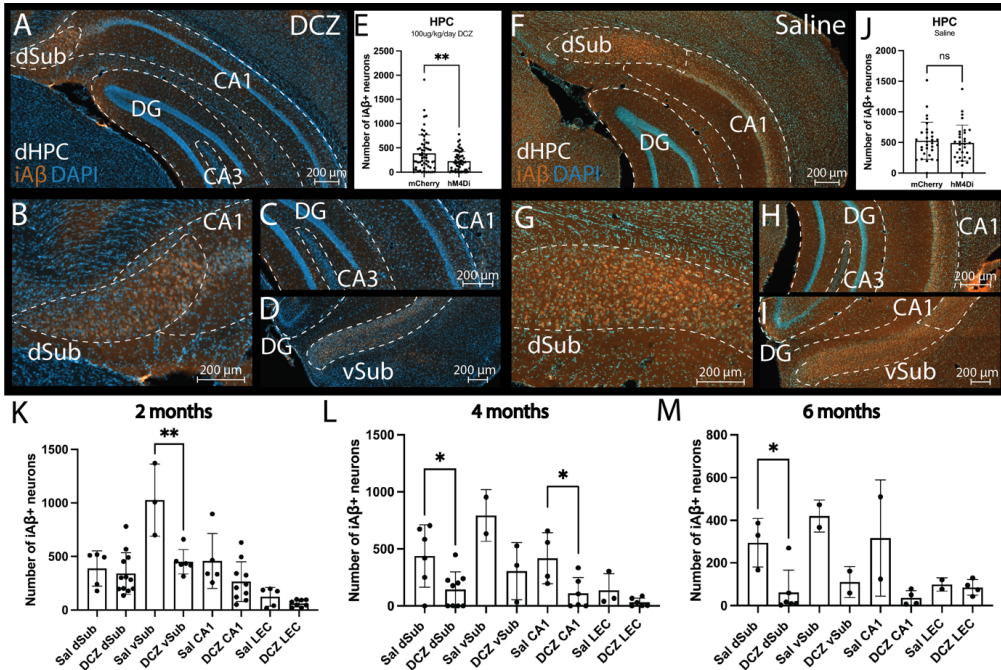


Figure 3. Reduced expression of intraneuronal A β in downstream HPC following LEC layer II neuronal silencing.

A) Macro-view of the expression of intraneuronal A β (McSA1 antibody; orange) in the dorsal HPC of 3xTg AD mice with silenced LEC layer II and DCZ infusions. **B)** Higher magnification view of intraneuronal A β expression (orange) in dorsal Sub and CA1 of 3xTg AD mice with silenced LEC layer II and DCZ infusions. **C)** Higher magnification view of intraneuronal A β expression (orange) in CA1/3 and DG of 3xTg AD mice with silenced LEC layer II and DCZ infusions. **D)** Higher magnification view of intraneuronal A β expression (orange) in ventral Sub of 3xTg AD mice with silenced LEC layer II and DCZ infusions. **E)** Box plots showing mean intraneuronal A β + neurons in HPC following injections of either AAV-hm4Di ($n = 25$) or AAV8 mCherry ($n = 8$) with DCZ infusions. Each dot represents a brain section containing the hippocampal subregions, and sections spanned the same rostro-caudal level for both AAV-hm4Di and AAV-mCherry injections. **F)** Macro-view of the expression of intraneuronal A β (McSA1 antibody; orange) in the dorsal HPC of 3xTg AD mice with LEC layer II AAV-hm4Di injections and saline infusions. **G)** Higher magnification view of intraneuronal A β expression (orange) in dorsal Sub of 3xTg AD mice with LEC layer II AAV-hm4Di injections and saline infusions. **H)** Higher magnification view of intraneuronal A β expression (orange) in CA1/3 and DG of 3xTg AD mice with LEC layer II AAV-hm4Di injections and saline infusions. **I)** Higher magnification view of intraneuronal A β expression (orange) in CA1 and ventral Sub of 3xTg AD mice with LEC layer II AAV-hm4Di injections and saline infusions. **J)** Box plots showing mean intraneuronal A β + neurons in HPC following injections of either AAV-hm4Di ($n = 9$) or AAV8 mCherry ($n = 6$) with saline infusions. Each dot represents a brain section containing the hippocampal subregions, and sections

spanned the same rostro-caudal level for both AAV-hM4D_i and AAV-mCherry injections. **K)** Box plots showing mean intraneuronal A β ⁺ neurons in hippocampal subregions (dSub, vSub, CA1) and LEC in 2-month-old 3xTg AD mice after AAV-hM4D_i injections and DCZ ($n = 8$) or saline ($n = 2$) infusions. **L)** Box plots showing mean intraneuronal A β ⁺ neurons in hippocampal subregions (dSub, vSub, CA1) and LEC in 4-month-old 3xTg AD mice after AAV-hM4D_i injections and DCZ ($n = 11$) or saline ($n = 3$) infusions. **M)** Box plots showing mean intraneuronal A β ⁺ neurons in hippocampal subregions (dSub, vSub, CA1) and LEC in 6-month-old 3xTg AD mice after AAV-hM4D_i injections and DCZ ($n = 5$) or saline ($n = 2$) infusions. Abbreviations; dSub: dorsal subiculum; DG: dentate gyrus; CA: cornu ammonis; iA β : intraneuronal amyloid- β ; dHPC: dorsal hippocampus; DCZ: deschloroclozapine; hM4D_i: human M4 muscarinic (hM4) inhibitory DREADDs; vSub: ventral subiculum; LEC: lateral entorhinal cortex; sal: saline. Error bars denote ± 1 SD; ** $p < .01$; * $p < .05$; ns: non-significant.

4. Discussion

To examine whether intraneuronal A β build-up correlated with neuronal activity levels, we silenced LEC layer II neuronal activity in 3xTg AD mice. This was done by targeted AAV-hM4D_i injections into LEC layer II followed by intraventricular infusions of the novel DREADD ligand DCZ. We opted to use DCZ rather than the conventionally used clozapine N-oxide (CNO) ligand, since the former ligand does not convert to clozapine and has a higher affinity to DREADDs [36]. Neuronal silencing caused context-dependent spatial memory deficits, indicating a functional role of LEC layer II neurons in cognitive functions known to be impaired early during AD progression in patients. Moreover, chronic inhibition of LEC layer II caused a reduction of intraneuronal A β levels within LEC neurons. Critically, chronic LEC layer II neuronal silencing also caused a reduction of intraneuronal A β levels in the subregions CA1 and Sub of the HPC, suggesting that activity levels in LEC affected intraneuronal A β in projections terminals in the HPC. The first subregion of the HPC that displayed reduced intraneuronal A β levels after neuronal silencing was the Sub. Together, these results suggest that intraneuronal A β build-up in LEC layer II and its perforant path terminals is regulated by neuronal activity.

It has previously been suggested that toxic intraneuronal A β build-up can appear in multiple brain regions simultaneously, before it encompasses the majority of association cortex [3, 4, 49, 50]. Alternatively, toxic A β may propagate in a cell-to-cell manner, consistent with the observation that the protein is found intracellularly [17, 51, 52]. However, neuroimaging and autopsy studies of AD patients have not pinpointed a precise anatomical origin of intraneuronal A β build-up. Animal studies have begun to shed light on the potential origin of early intraneuronal A β build-up in the brain. Specifically, it has been shown that *APP* mutations, of which can cause increased A β production [53], can be transported anterogradely via perforant path projections from superficial layers of EC to DG in rats [54], resulting in high levels of soluble A β peptides and plaque deposits in DG [55]. Recent findings suggest that lowered levels of reelin in LEC layer II principal neurons led to reduced intraneuronal A β in these neurons, as well as in projection terminals in the HPC [10]. This is in line with our current findings, which provide evidence of activity-dependent changes in intraneuronal A β build-up in the EC-HPC circuit.

In AD patients, extracellular A β plaques are usually first deposited in the neocortex, before appearing in MTL regions, such as the EC and the HPC [4]. In our experiments we did not observe intraneuronal A β in the DG of 3xTg AD mice, and this contrasts with reports from the traditional perforant path projections between LEC layer II and the molecular/granular cell layers of the DG [56]. However, the DG is usually spared for neuropathological deposits in experimental models and patients until very late stages of AD [4, 24, 35, 57]. This provides an explanation as to why manipulation of activity levels in LEC layer II did not affect intraneuronal A β in the DG of 3xTg AD mice. Our findings of intraneuronal A β in CA1 can be explained by direct projections between LEC layer II and CA1, which bypasses the DG [58], the vulnerability of the EC-CA1 circuitry to neurodegeneration during AD [59, 60], or the first presentation of A β plaques appearing in CA1 of unmanipulated 3xTg AD mice [24].

Since aging is the major risk factor for developing sporadic AD, the disease pathology may be linked to the degradation of cellular clearance systems [11, 61, 62]. In line with this, previous reports suggest that deficits in the autophagic pathway are associated with AD progression and lead to an increase in intraneuronal A β aggregates [63, 64]. We observed lowered intraneuronal A β levels after LEC layer II neuronal silencing even in very young 3xTg AD mice, and this could also be explained by hyperactivity in this brain region early in the disease progression [65]. Neuronal hyperactivity in the HPC has been shown to induce A β pathology in mouse models [66, 67] and patients [68] with AD. In our experiments, the Sub was the first hippocampal subregion to display changes in intraneuronal A β after chronic LEC layer II silencing. The Sub is of high interest in the field, as it acts as a gateway between the neocortex and HPC [69, 70] and is affected early by A β pathology [71, 72]. Moreover, previous work has shown that lesions to the Sub resulted in reduced spreading of A β to interconnected regions in mice. However, the phasing of hippocampal subfield involvement in toxic intraneuronal A β build-up needs to be investigated further. In summary, we show that early intraneuronal A β levels in the LEC and HPC correlated with activity levels, and our findings give evidence to early AD neuropathology originating in select neuronal populations.

5. References

1. Weller, J. and A. Budson, *Current understanding of Alzheimer's disease diagnosis and treatment*. F1000Res, 2018. **7**.
2. Lane, C.A., J. Hardy, and J.M. Schott, *Alzheimer's disease*. Eur J Neurol, 2018. **25**(1): p. 59-70.
3. Braak, H. and E. Braak, *Neuropathological staging of Alzheimer-related changes*. Acta Neuropathol, 1991. **82**(4): p. 239-59.
4. Thal, D.R., et al., *Phases of A beta-deposition in the human brain and its relevance for the development of AD*. Neurology, 2002. **58**(12): p. 1791-800.
5. Gallagher, M. and M.T. Koh, *Episodic memory on the path to Alzheimer's disease*. Curr Opin Neurobiol, 2011. **21**(6): p. 929-34.
6. Scoville, W.B. and M. B., *Loss of recent memory after bilateral hippocampal lesions*. J Neurol, 1957. **20**: p. 11-21.

7. Witter, M.P., et al., *Architecture of the Entorhinal Cortex A Review of Entorhinal Anatomy in Rodents with Some Comparative Notes*. Front Syst Neurosci, 2017. **11**: p. 46.
8. Burwell, R.D., *The parahippocampal region: corticocortical connectivity*. Ann N Y Acad Sci, 2000. **911**: p. 25-42.
9. Gomez-Isla, T., et al., *Profound loss of layer II entorhinal cortex neurons occurs in very mild Alzheimer's disease*. J Neurosci, 1996. **16**(14): p. 4491-500.
10. Kobre-Flatmoen, A., et al., *Lowering levels of reelin in entorhinal cortex layer II neurons results in lowered levels of intracellular amyloid- β* . bioRxiv, 2022: p. 2022.01.28.478143.
11. Kobre-Flatmoen, A., et al., *Re-emphasizing early Alzheimer's disease pathology starting in select entorhinal neurons, with a special focus on mitophagy*. Ageing Res Rev, 2021. **67**: p. 101307.
12. Squire, L.R., C.E. Stark, and R.E. Clark, *The medial temporal lobe*. Annu Rev Neurosci, 2004. **27**: p. 279-306.
13. Eichenbaum, H. and P.A. Lipton, *Towards a functional organization of the medial temporal lobe memory system: role of the parahippocampal and medial entorhinal cortical areas*. Hippocampus, 2008. **18**(12): p. 1314-24.
14. Marks, W.D., et al., *Neuronal Ensembles Organize Activity to Generate Contextual Memory*. Front Behav Neurosci, 2022. **16**.
15. Heggland, I., P. Kvellø, and M.P. Witter, *Electrophysiological Characterization of Networks and Single Cells in the Hippocampal Region of a Transgenic Rat Model of Alzheimer's Disease*. eNeuro, 2019. **6**(1).
16. Kobre-Flatmoen, A., A. Nagelhus, and M.P. Witter, *Reelin-immunoreactive neurons in entorhinal cortex layer II selectively express intracellular amyloid in early Alzheimer's disease*. Neurobiol Dis, 2016. **93**: p. 172-183.
17. D'Andrea, M.R., et al., *Evidence that neurones accumulating amyloid can undergo lysis to form amyloid plaques in Alzheimer's disease*. Histopathology, 2001. **38**(2): p. 120-34.
18. Skovronsky, D.M., R.W. Doms, and V.M. Lee, *Detection of a novel intraneuronal pool of insoluble amyloid beta protein that accumulates with time in culture*. J Cell Biol, 1998. **141**(4): p. 1031-1039.
19. Almeida, C.G., et al., *Beta-amyloid accumulation in APP mutant neurons reduces PSD-95 and GluR1 in synapses*. Neurobiol Dis, 2005. **20**(2): p. 187-98.
20. Casas, C., et al., *Massive CA1/2 neuronal loss with intraneuronal and N-terminal truncated A β 42 accumulation in a novel Alzheimer transgenic model*. Am J Pathol, 2004. **165**(4): p. 1289-300.
21. Moolman, D.L., et al., *Dendrite and dendritic spine alterations in Alzheimer models*. J Neurocytol, 2004. **33**(3): p. 377-87.
22. Mori, C., et al., *Intraneuronal A β 42 accumulation in Down syndrome brain*. Amyloid, 2002. **9**(2): p. 88-102.
23. Mucke, L., et al., *High-level neuronal expression of abeta 1-42 in wild-type human amyloid protein precursor transgenic mice: synaptotoxicity without plaque formation*. J Neurosci, 2000. **20**(11): p. 4050-8.
24. Oddo, S., et al., *Triple-Transgenic Model of Alzheimer's Disease with Plaques and Tangles*. Neuron, 2003. **39**(3): p. 409-421.

25. Spires, T.L., et al., *Dendritic spine abnormalities in amyloid precursor protein transgenic mice demonstrated by gene transfer and intravital multiphoton microscopy*. J Neurosci, 2005. **25**(31): p. 7278-87.
26. Takahashi, R.H., et al., *Intraneuronal Alzheimer abeta42 accumulates in multivesicular bodies and is associated with synaptic pathology*. Am J Pathol, 2002. **161**(5): p. 1869-79.
27. Hunt, L.A., A.E. Brown, and I.P. Gilman, *Drivers with dementia and outcomes of becoming lost while driving*. Am J Occup Ther, 2010. **64**(2): p. 225-32.
28. Hampel, H., et al., *Alzheimer's disease biomarker-guided diagnostic workflow using the added value of six combined cerebrospinal fluid candidates: Abeta1-42, total-tau, phosphorylated-tau, NFL, neurogranin, and YKL-40*. Alzheimers Dement, 2018. **14**(4): p. 492-501.
29. Palop, J.J. and L. Mucke, *Network abnormalities and interneuron dysfunction in Alzheimer disease*. Nat Rev Neurosci, 2016. **17**(12): p. 777-792.
30. Maass, A., et al., *Entorhinal Tau Pathology, Episodic Memory Decline, and Neurodegeneration in Aging*. J Neurosci, 2018. **38**(3): p. 530.
31. Pettigrew, C., et al., *Progressive medial temporal lobe atrophy during preclinical Alzheimer's disease*. Neuroimage Clin, 2017. **16**: p. 439-446.
32. Sanchez, J.S., et al., *The cortical origin and initial spread of medial temporal tauopathy in Alzheimer's disease assessed with positron emission tomography*. Sci Transl Med, 2021. **13**(577).
33. Angulo, S.L., et al., *Tau and amyloid-related pathologies in the entorhinal cortex have divergent effects in the hippocampal circuit*. Neurobiol Dis, 2017. **108**: p. 261-276.
34. Kobro-Flatmoen, A., A. Nagelhus, and M.P. Witter, *Reelin-immunoreactive neurons in entorhinal cortex layer II selectively express intracellular amyloid in early Alzheimer's disease*. Neurobiology of Disease, 2016. **93**: p. 172-183.
35. Billings, L.M., et al., *Intraneuronal Abeta causes the onset of early Alzheimer's disease-related cognitive deficits in transgenic mice*. Neuron, 2005. **45**(5): p. 675-88.
36. Nagai, Y., et al., *Deschloroclozapine, a potent and selective chemogenetic actuator enables rapid neuronal and behavioral modulations in mice and monkeys*. Nat Neurosci, 2020. **23**(9): p. 1157-1167.
37. Julian, J.B., et al., *Place recognition and heading retrieval are mediated by dissociable cognitive systems in mice*. Proc Natl Acad Sci U S A, 2015. **112**(20): p. 6503-8.
38. Bernstein, H.L., et al., *Novelty and Novel Objects Increase c-Fos Immunoreactivity in Mossy Cells in the Mouse Dentate Gyrus*. Neural Plasticity, 2019. **2019**: p. 1815371.
39. Bjorkli, C., *IHC AD neuropathology protocol* protocols.io, 2019.
40. Bjorkli, C., K. Hovde, and B. Monterotti, *Nissl (Cresyl Violet) staining*. protocols.io 2019.
41. Bjorkli, C., *Peroxidase/DAB protocol*. protocols.io, 2022.
42. Bjorkli, C. and M.J. Lagartos-Donate, *Gallyas-silver stain*. protocols.io, 2022.
43. Berg, S., et al., *ilastik: interactive machine learning for (bio)image analysis*. Nat Methods, 2019. **16**(12): p. 1226-1232.
44. Paxinos, G. and K.B. Franklin, *The mouse brain in stereotaxic coordinates*. 2nd ed. 2004: Gulf Professional Publishing.
45. Witter, M. and D.G. Amaral, *Hippocampal Formation*, in *The Rat Nervous System*. 2004, Elsevier Inc.
46. Cohen, J., *A power primer*. Psychol Bull, 1992. **112**(1): p. 155-9.

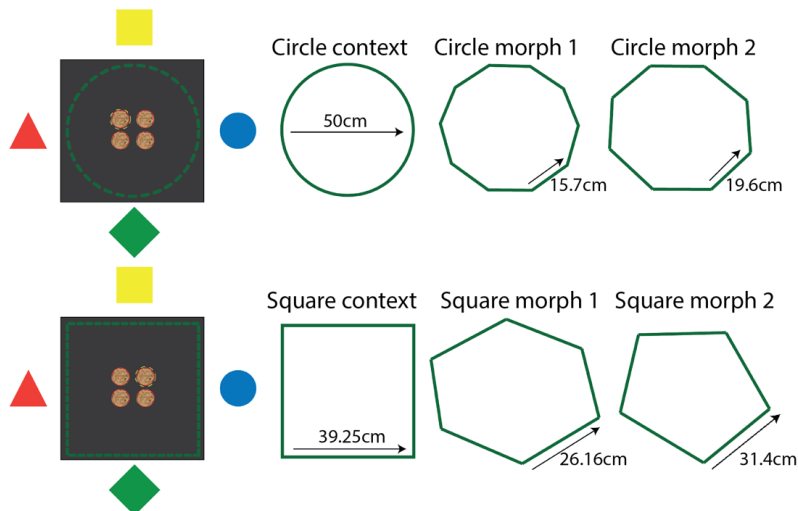
47. Hainmueller, T. and M. Bartos, *Dentate gyrus circuits for encoding, retrieval and discrimination of episodic memories*. *Nat Rev Neurosci*, 2020. **21**(3): p. 153-168.
48. Pilly, P.K., M.D. Howard, and R. Bhattacharyya, *Modeling Contextual Modulation of Memory Associations in the Hippocampus*. *Front Hum Neurosci*, 2018. **12**: p. 442-442.
49. Palmqvist, S., et al., *Earliest accumulation of β -amyloid occurs within the default-mode network and concurrently affects brain connectivity*. *Nat Commun*, 2017. **8**(1): p. 1214.
50. Whittington, A., D.J. Sharp, and R.N. Gunn, *Spatiotemporal Distribution of β -Amyloid in Alzheimer Disease Is the Result of Heterogeneous Regional Carrying Capacities*. *J Nucl Med*, 2018. **59**(5): p. 822-827.
51. Gouras, G.K., et al., *Intraneuronal A β 42 accumulation in human brain*. *Am J Pathol*, 2000. **156**(1): p. 15-20.
52. LaFerla, F.M., K.N. Green, and S. Oddo, *Intracellular amyloid-beta in Alzheimer's disease*. *Nat Rev Neurosci*, 2007. **8**(7): p. 499-509.
53. Selkoe, D.J. and J. Hardy, *The amyloid hypothesis of Alzheimer's disease at 25 years*. *EMBO Mol Med*, 2016. **8**(6): p. 595-608.
54. Buxbaum, J.D., et al., *Alzheimer amyloid protein precursor in the rat hippocampus: transport and processing through the perforant path*. *J Neurosci*, 1998. **18**(23): p. 9629-37.
55. Harris, J.A., et al., *Transsynaptic progression of amyloid- β -induced neuronal dysfunction within the entorhinal-hippocampal network*. *Neuron*, 2010. **68**(3): p. 428-41.
56. Witter, M.P., *The perforant path: projections from the entorhinal cortex to the dentate gyrus*. *Prog Brain Res*, 2007: p. 43-61.
57. Oh, K.-J., et al., *Staging of Alzheimer's Pathology in Triple Transgenic Mice: A Light and Electron Microscopic Analysis*. *International Journal of Alzheimer's Disease*, 2010. **2010**: p. 780102.
58. Witter, M.P., et al., *Entorhinal projections to the hippocampal CA1 region in the rat: an underestimated pathway*. *Neurosci Lett*, 1988. **85**(2): p. 193-8.
59. Furcila, D., J. DeFelipe, and L. Alonso-Nanclares, *A Study of Amyloid- β and Phosphotau in Plaques and Neurons in the Hippocampus of Alzheimer's Disease Patients*. *J Alzheimers Dis*, 2018. **64**(2): p. 417-435.
60. Yang, X., et al., *A novel mechanism of memory loss in Alzheimer's disease mice via the degeneration of entorhinal-CA1 synapses*. *Mol Psychiatry*, 2018. **23**(2): p. 199-210.
61. Fang, E.F., et al., *Mitophagy inhibits amyloid-beta and tau pathology and reverses cognitive deficits in models of Alzheimer's disease*. *Nat Neurosci*, 2019. **22**(3): p. 401-412.
62. Villeda, S.A., et al., *The ageing systemic milieu negatively regulates neurogenesis and cognitive function*. *Nature*, 2011. **477**(7362): p. 90-94.
63. Agholme, L., et al., *Amyloid- β secretion, generation, and lysosomal sequestration in response to proteasome inhibition: involvement of autophagy*. *J Alzheimers Dis*, 2012. **31**(2): p. 343-58.
64. Zheng, L., et al., *Macroautophagy-generated increase of lysosomal amyloid β -protein mediates oxidant-induced apoptosis of cultured neuroblastoma cells*. *Autophagy*, 2011. **7**(12): p. 1528-45.
65. Xu, W., et al., *Early hyperactivity in lateral entorhinal cortex is associated with elevated levels of A β PP metabolites in the Tg2576 mouse model of Alzheimer's disease*. *Exp Neurol*, 2015. **264**: p. 82-91.

66. Yamamoto, K., et al., *Chronic optogenetic activation augments $\alpha\beta$ pathology in a mouse model of Alzheimer disease*. *Cell Rep*, 2015. **11**(6): p. 859-865.
67. Busche, M.A., et al., *Critical role of soluble amyloid- β for early hippocampal hyperactivity in a mouse model of Alzheimer's disease*. *Proc Natl Acad Sci U S A*, 2012. **109**(22): p. 8740-5.
68. Leal, S.L., et al., *Hippocampal activation is associated with longitudinal amyloid accumulation and cognitive decline*. *eLife*, 2017. **6**: p. e22978.
69. O'Mara, S.M., et al., *The subiculum: a review of form, physiology and function*. *Prog Neurobiol*, 2001. **64**(2): p. 129-55.
70. Witter, M.P., et al., *Cortico-hippocampal communication by way of parallel parahippocampal-subicular pathways*. *Hippocampus*, 2000. **10**(4): p. 398-410.
71. Davies, D.C., A.C. Wilmott, and D.M.A. Mann, *Senile plaques are concentrated in the subicular region of the hippocampal formation in Alzheimer's disease*. *Neurosci Lett*, 1988. **94**(1): p. 228-233.
72. Schönheit, B., R. Zarski, and T.G. Ohm, *Spatial and temporal relationships between plaques and tangles in Alzheimer-pathology*. *Neurobiol Aging*, 2004. **25**(6): p. 697-711.

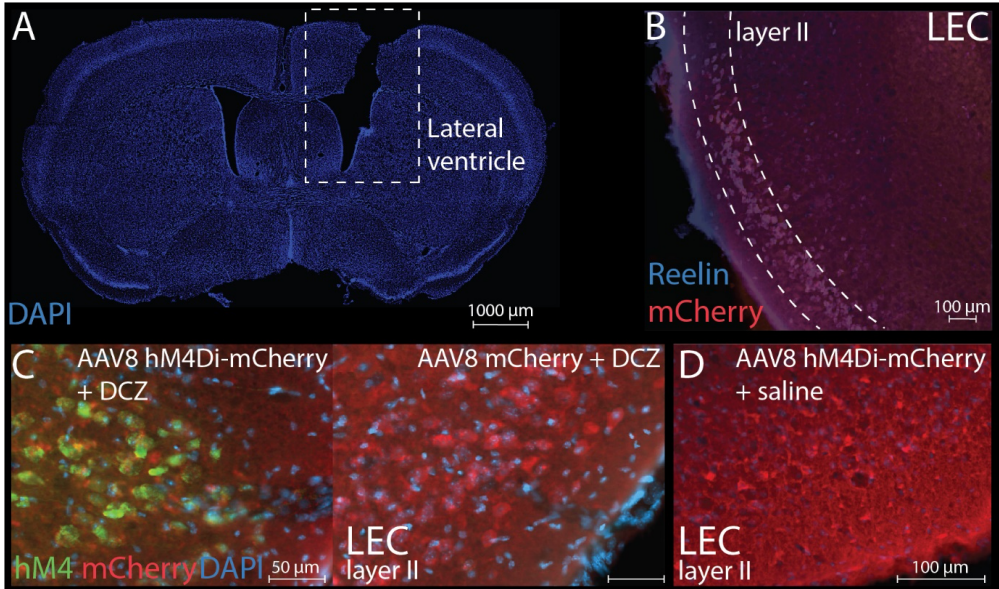
6. Acknowledgments

The authors would like to thank Dr. Rajeevkumar R. Nair for generating the viral vectors used in these experiments.

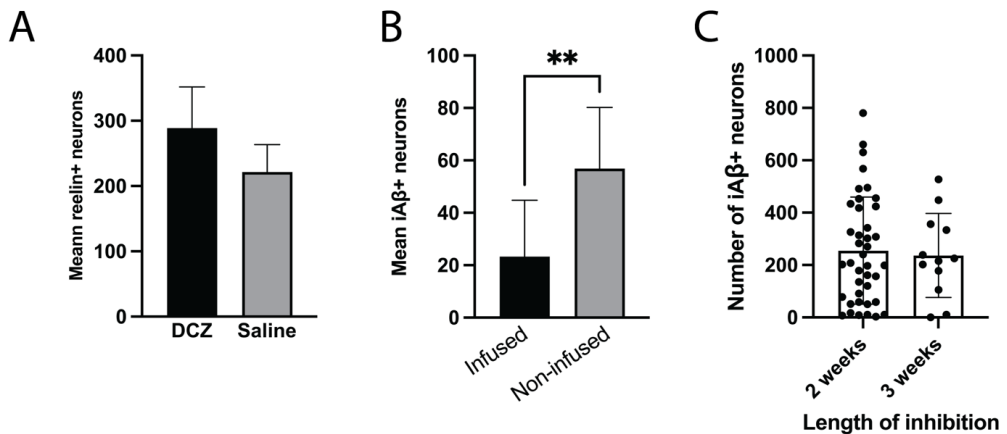
7. Supplementary material



Supplementary Figure 1. Context-dependent spatial memory task design. Mice were initially taught to associate a specific reward location in a square- and a circle-chamber. The reward was buried in one of four cups with ginger-scented bedding. A trial was assessed as correct if the mice dug in the reward location associated with each chamber. If they passed the training phase (66.6% correct digging), their contextual memory performance was tested in the following morph chambers: a decagon (circle morph 1), an octagon (circle morph 2), a hexagon (square morph 1), and a pentagon (square morph 2). Mice were tested in the morph chambers for 4 days, with 8 sessions a day.



Supplementary Figure 2. Verification of intraventricular cannula implantation and AAV-hM4Di injections in LEC layer II. **A)** Intracranial cannula implantation site in the lateral ventricle of a 3xTg AD mouse visualized by DAPI nucleic staining (blue). The intracranial cannula was connected to an osmotic minipump via a catheter that allowed for the continuous and controlled infusion of either DCZ or saline for 2-3 weeks. **B)** Co-labelling of reelin (marker for principal fan cells) and mCherry following AAV-hM4Di injections into LEC layer II. **C) Left:** Expression of hM4 receptors (green) and mCherry (red) after AAV-hM4Di injections in LEC layer II and DCZ infusions. **Right:** Lack of hM4 receptor expression (green), but not mCherry (red) after AAV-mCherry injections in LEC layer II and DCZ infusions. **D)** Lack of hM4 receptor expression (green) after AAV-hM4Di injections (mCherry; red) in LEC layer II and saline infusions. Abbreviations; LEC: lateral entorhinal cortex; hM4Di: modified inhibitory human muscarinic G-protein coupled receptor 4; hM4: human M4 muscarinic (hM4) inhibitory DREADDs; DCZ: deschloroclozapine.



Supplementary Figure 3. Supplementary effects of LEC layer II neuronal silencing in 3xTg AD mice. **A)** Bar graph displaying mean intraneuronal reelin levels in LEC layer II neurons (<4 brain sections) after AAV-hM4Di injections and DCZ ($n = 2$) and saline ($n = 2$) infusions. **B)** Bar graph displaying mean intraneuronal Aβ+ LEC layer II neurons in infused and non-infused hemispheres (<4 brain sections) after AAV-hM4Di injections and DCZ ($n = 25$) infusions ($t = 5.24$, $p < .01$, unpaired two-tailed t-test). **C)** Box plots showing mean intraneuronal Aβ+ LEC layer

II neurons after AAV-hM4D injections and DCZ infusions for 2 ($n = 21$) or 3 ($n = 4$) weeks. Each dot represents a brain section containing the hippocampal subregions, and sections spanned the same rostro-caudal level for both AAV-hM4D; and AAV-mCherry injections. Abbreviations; iA β : intraneuronal amyloid- β ; DCZ: deschloroclozapine. Error bars denote ± 1 SEM in panel A, and ± 1 SD in panels B-C; **: $p < .01$.

Supplementary Table 1: Antibodies used in experiments

| Antibody | Target | Identifier |
|------------------------------|--|---|
| Mouse anti-A β (McSA1) | Targets the N-terminal amino acids 1–12 of human A β | MediMabs Cat# MM-0015-1P, RRID:AB_1807985 |
| Mouse anti-reelin | Targets the extracellular matrix glycoprotein reelin | Millipore Cat# MAB5364, RRID:AB_2179313 |
| Mouse anti-mCherry | Targets mCherry fluorescence | Clontech Cat# 632543 |
| Rabbit anti-hM4 | Targets human muscarinic receptor 4 | Abcam Cat# ab189432 |
| Rabbit anti-cFos | Targets the cFos immediate-early gene | Abcam Cat# ab208942, RRID:AB_2747772 |

ISBN 978-82-326-6552-5 (printed ver.)
ISBN 978-82-326-5894-7 (electronic ver.)
ISSN 1503-8181 (printed ver.)
ISSN 2703-8084 (online ver.)



NTNU

Norwegian University of
Science and Technology